

**PERFORMANCE, DEGRADATION, AND RELIABILITY OF SOLAR  
PHOTOVOLTAIC (PV) MODULE UNDER ENVIRONMENTAL  
FIELD CONDITIONS**

By

Samuel Maina Ngure

A Thesis Submitted to the School of Engineering, Department of Mechanical,  
Production and Energy Engineering, in Partial Fulfilment of the Requirements for the  
Award of Doctor of Philosophy Degree in Energy Studies

Moi University

2023

## DECLARATION

### Declaration by the Candidate

This is my original work and has not been presented for a degree in any other University. No part of this thesis may be reproduced without the prior written permission of the author and/or Moi University.

Sign: \_\_\_\_\_ Date: \_\_\_\_\_

**Samuel Maina Ngure**

**ENG/DES/03/19**

### Declaration by the Supervisors

This thesis has been submitted with our approval as University supervisors.

Sign: \_\_\_\_\_ Date: \_\_\_\_\_

**Prof. Augustine B. Makokha**

Department of Mechanical, Production and Energy Engineering, Moi University,  
Eldoret, Kenya

Sign: \_\_\_\_\_ Date: \_\_\_\_\_

**Prof. Edwin O. Ataro**

Faculty of Engineering and the Built Environment  
Technical University of Kenya, Nairobi, Kenya

Sign: \_\_\_\_\_ Date: \_\_\_\_\_

**Prof. Muyiwa S. Adaramola**

Faculty of Environmental Sciences and Natural Resource Management, Norwegian  
University of Life Sciences, Ås, Norway

**DEDICATION**

I dedicate this thesis to my Late parents Christopher Ngure Mwaniki and Esther Wakiine Ngure.

## ACKNOWLEDGMENT

I acknowledge my Creator, the Almighty God, who gave me the physical and mental strength to undertake and accomplish this work. The success of this work is attributed to several people who selflessly offered their support. First and foremost, I would like to express my sincere gratitude to my supervisors, Prof Augustine B. Makokha, Prof Edwin O. Ataro and Prof Muiyiwa S. Adaramola for their continuous and constructive criticism. Their inspiration, guidance and commitment to see me through this program will forever be appreciated. May our Almighty God give them power and good health to continue with the good work. Secondly, I would like to thank my family (Florence Wanjiru, Precious, Austin and MaryPraise), and friends for their love, support and patience as I carried out my study work. I will forever be indebted to all of you, may God bless you abundantly. Last but not least, I would like to thank Moi University for giving me the opportunity to pursue the study, Strathmore University and Makueni County community for availing equipment and facility to conduct the study and ACE-PTRE II for funding my academic and research work that enabled me to complete this work.

## ABSTRACT

Solar Photovoltaic (PV) system is one of the most promising renewable energy resources globally. However, its utilization has remained low in Kenya. This may be attributed to lack of pertinent knowledge of the potential, opportunities, environmental, and economic benefits of the technology. The PV performance, degradation, and reliability in the East African region have not been documented and little information is available in the literature. The main objective of this research was to determine the performance, degradation, and reliability of solar PV modules under environmental field conditions. The specific objectives were to; evaluate the technical and economic performance of PV modules, analyze the effects of soiling on the performance of PV modules, determine the reliability, degradation rates and mechanism of PV modules. The study area was in Makueni County (semi-arid region), Strathmore University solar PV power plant, and Moi University (tropical-savanna region). The methodology involved review of the historical data of PV power plant and collection of weather data from Kenya Meteorological Department weather station located 300 metres from the solar plant. Secondly, installation of weather station and six PV modules was done in Moi University to establish the effects of soiling. The analysis of the contaminants collected from the PV modules was done using sieves and analytical balance weighing machine. Finally, the measurement of I-V curves, thermal images and visual inspections was conducted on the PV modules installed for more than 1 year. This was done through the use of I-V curve tracer, Infrared camera and PV module check list tool developed by National Renewable Energy Laboratory. The results indicated a performance ratio of 68% and a discounted payback period of 13 years. The model developed indicated that an increase in solar irradiance and wind speed, and decrease in relative humidity, increases the power output. The degradation rates ranged from 0.99% to 1.15%, per annum, which was due to different types of PV cell technology, while degradation mechanisms were established as discoloration of encapsulating materials (36.84 %) in warm semi-arid region and browning of encapsulating material in tropical savanna as the predominant mode. The contaminant contained high percentage of fine particles of less than 0.06 mm in size which caused reduction of short-circuit current. The reliability of the different PV system installation configurations ranged from 35% to 82%, indicating a weighted mean of 67%, which was due to number of components, and connection schemes, majority of modules being polycrystalline. In conclusion the results obtained, provided clear evidence of the technical and economic viability of PV modules in the region as a source of energy. The study recommends parallel connections of components, and regular cleaning to maintain high performance and reliability, and reduction of degradation rates in the region.

## TABLE OF CONTENTS

DECLARATION .....	ii
DEDICATION .....	iii
ACKNOWLEDGMENT .....	iv
ABSTRACT .....	v
TABLE OF CONTENTS .....	vi
LIST OF TABLES .....	xii
LIST OF FIGURES .....	xiii
SYMBOLS, ABBREVIATIONS AND NOTATIONS .....	xvi
<b>CHAPTER 1 .....</b>	<b>1</b>
<b>INTRODUCTION.....</b>	<b>1</b>
1.1 Background of the Study .....	1
1.2 Energy Situation in Kenya and Solar PV Development .....	3
1.3 Problem Statement .....	6
1.4 Main Objective.....	7
1.5 Specific Objectives .....	7
1.6 Contribution and Significance of this Study .....	8
1.7 Thesis Structure .....	9
<b>CHAPTER 2.....</b>	<b>10</b>
<b>LITERATURE REVIEW .....</b>	<b>10</b>
2.0 Introduction.....	10
2.1 Technical and Economic Performance of Solar PV Modules .....	10
2.1.1 Comparison of Solar PV Performance Based on Measured and Simulated Data .....	10
2.1.2 Effect of Weather and Environmental Conditions on Solar PV Performance	12
2.1.3 Effects of Tilt Angles and Orientation on Solar PV Performance .....	14
2.1.4 Technical and Economics Performance of Solar PV Module System .....	15
2.1.5 Knowledge Gap and Contribution of the Study .....	20
2.2 Effects of Dust Accumulation on the Performance of Solar PV Module .....	21
2.2.1 Knowledge Gap and Contributions .....	25
2.3 Degradation Mechanism and Degradation Rates of Solar PV Modules.....	25
2.3.1 Knowledge Gap and Research Questions .....	30
2.4 Reliability and Failure Rates of Solar PV Modules.....	32

2.4.1 Knowledge Gap and Contributions .....	34
<b>CHAPTER THREE .....</b>	<b>36</b>
<b>RESEARCH METHODOLOGY .....</b>	<b>36</b>
3.0 Introduction.....	36
3.1 Technical and Economic Performance of PV Modules in Tropical Savanna Region .....	36
3.1.1 Installation Descriptions and Location.....	36
3.1.2 Measurement and Data Collection .....	40
3.2 Performance Indicators .....	40
3.2.1 Technical Performance Indicators.....	41
3.2.2 Total Energy Generated (kWh) .....	41
3.2.3 System Yields.....	41
3.2.4 Capacity Utilization Factor (CUF).....	42
3.2.5 System Efficiency ( $\eta$ ).....	43
3.2.6 Total Energy Losses .....	43
3.2.7 Performance Ratio.....	44
3.3 Economic Analysis .....	44
3.3.1 Levelized Cost of Energy (LCOE).....	45
3.3.2 Net Present Value (NPV) .....	46
3.3.3 Discounted Cash Flow ( $Ct$ ) .....	46
3.3.4 Discounted Payback period (DPP).....	47
3.3.5 Internal Rate of Return (IRR).....	47
3.4 Data Analysis .....	47
3.5 Effects of Dust Accumulation on the Performance of PV Modules .....	48
3.5.1 Study Area.....	48
3.5.2 Solar Modules Description.....	50
3.5.3 Measurements and Instrumentations .....	50
3.5.4 Soiling Ratio (SRatio) .....	52
3.6 Degradation Mechanism and Rates Analysis of PV Modules .....	54
3.6.1 Study Area.....	54
3.6.2 Description of Deployed Solar Modules .....	55
3.6.3 Measurements and Instrumentations .....	59
3.6.4 Normalization of the Data .....	60

3.6.5 Degradation Analysis .....	62
3.7 Reliability and Failure Rates of PV Modules .....	64
3.7.1 Study Area.....	65
3.7.2 Reliability Analysis .....	65
3.7.3 Configurations of Solar-PV Systems Installation Design in this Study.....	68
3.7.4 Configuration of Solar-PV Systems Installation for Domestic Use.....	68
3.7.5 Configuration of Solar-PV Pumping Systems .....	69
3.7.6 Configuration of Solar-PV Systems Installation for Grid-Interactive .....	70
3.7.7 Configuration of Solar-PV Systems Installation for Power Generation .....	71
3.8 Failure Rate .....	73
<b>CHAPTER 4.....</b>	<b>74</b>
<b>RESULTS AND DISCUSSION .....</b>	<b>74</b>
4.0 Introduction.....	74
4.1 Tech-Economic Performance of PV Modules .....	74
4.1.1 Sub-Objectives .....	74
4.2 Technical Performance Analysis .....	75
4.2.1 Reference Yield.....	75
4.2.2 Scenario 1: Orientation effect on System 1 (south) and 4 (west-east) directions .....	77
4.2.3 Scenario 2: Tilt Angle Effect on System 2, (18°), and 3, (11°).....	84
4.3 Estimation of Power Output (kW) using Environmental Parameters.....	95
4.4 Economic Analysis .....	101
4.5 Conclusions and Recommendations .....	103
<b>CHAPTER 5.....</b>	<b>105</b>
5.1 Effects of Dust Accumulation on the Performance of PV Modules .....	105
5.1.1 Sub-Objectives .....	105
5.2 Dust Accumulations.....	105
5.3 Effects of Dust Accumulation on the Performances of the PV modules.....	106
5.3.1 I-V and P-V curve of the monocrystalline solar PV module .....	106
5.3.2 I-V and P-V Curve of the Polycrystalline Solar PV Module .....	109
5.3.3 I-V and P-V Curve of the Silicon Amorphous Thin Technology Solar PV Module.....	111
5.4 Discussion.....	113



5.5 Conclusion and Recommendations.....	115
<b>CHAPTER 6.....</b>	<b>116</b>
6.1 Degradation Mechanism and Degradation Rates of PV Modules .....	116
6.2 Sub-Objectives.....	116
6.3 Degradation Mechanisms; Visually Observable Defects and Thermal Images... ..	116
6.4 Degradation Rates Analysis.....	119
6.4.1 Short-Circuit Current (Isc) Degradation Rates.....	120
6.4.2 Open-Circuit Voltage (Voc) Degradation Rates .....	122
6.4.3 Fill Factor (FF) Degradation Rates .....	123
6.4.4 Power Output Degradation rates .....	125
6.4.5 Efficiency .....	126
6.5 Degradation Rate Model of the PV Module in Warm Semi-Arid Climatic Conditions.....	127
6.6 Discussion.....	129
6.7 Conclusion and Recommendations.....	134
<b>CHAPTER 7.....</b>	<b>136</b>
7.0 Reliability and Failure Rates of PV Modules .....	136
7.1. Sub-Objectives.....	136
7.2 Failure Rates .....	136
7.3 Reliability Analysis.....	138
7.4 Mean Time To Failure (MTTF).....	142
7.5 Conclusion and Recommendations.....	143
<b>CHAPTER 8.....</b>	<b>145</b>
Conclusion and Recommendations.....	145
REFERENCES .....	148
APPENDICES .....	158
Appendix I: System 1 performance analysis (2015) .....	158
Appendix II: System 1 performance analysis (2016).....	158
Appendix III: System 1 performance analysis (2017) .....	159
Appendix IV: System 1 performance analysis (2018) .....	159
Appendix V: System 1 performance analysis (2019).....	160
Appendix VI: System 2 performance analysis (2015) .....	160
Appendix VII: System 2 performance analysis (2016).....	161

Appendix VIII: System 2 performance analysis (2017).....	161
Appendix IX: System 2 performance analysis (2018) .....	162
Appendix X: System 2 performance analysis (2019).....	162
Appendix XI: System 3 performance analysis (2015) .....	163
Appendix XII: System 3 performance analysis (2016).....	163
Appendix XIII: System 3 performance analysis (2017).....	164
Appendix XIV: System 3 performance analysis (2018) .....	164
Appendix XV: System 3 performance analysis (2019).....	165
Appendix XVI: System 4 performance analysis (2015) .....	165
Appendix XVII: System 4 performance analysis (2016).....	166
Appendix XVIII: System 4 performance analysis (2017).....	166
Appendix XIX: System 4 performance analysis (2018) .....	167
Appendix XX: System 4 performance analysis (2019).....	167
Appendix XXI: Statistical performance analysis of PV modules .....	168
Appendix XXII: Statistical performance analysis of PV modules.....	169
Appendix XXIII: Statistical performance analysis of PV modules .....	170
Appendix XXIV: Statistical performance analysis of PV modules .....	171
Appendix XXV: Economic analysis of solar PV power plant.....	172
Appendix XXVI: Silicon Amorphous thin technology data of the clean module	173
Appendix XXVII: Silicon Amorphous thin technology data of the unclean module .....	174
Appendix XXVIII: Polycrystalline data of the clean module .....	175
Appendix XXIX: Polycrystalline data of the unclean module.....	176
Appendix XXX: Monocrystalline data of the clean module.....	177
Appendix XXXI: Monocrystalline data of the unclean module .....	178
Appendix XXXII: Data of silicon amorphous thin technology solar PV module .	179
Appendix XXXIII: Degradation analysis of silicon amorphous thin technology ..	180
Appendix XXXIV: Data of polycrystalline solar PV module in warm semi-arid .	181
Appendix XXXV: Degradation analysis of p-Si PV modules in warm semi-arid.	182
Appendix XXXVI: Data of polycrystalline solar PV module in warm semi-arid .	183
Appendix XXXVII: Degradation analysis of p-Si PV modules in warm semi- arid.....	184
Appendix XXXVIII: Data of polycrystalline technology in tropical savanna.....	185

Appendix XXXIX: Data of polycrystalline technology in tropical savanna .....	186
Appendix XL: Degradation analysis of polycrystalline technology in tropical savanna .....	187
Appendix XLI: Data of polycrystalline technology in tropical savanna.....	188
Appendix XLII: Data of monocrystalline technology in tropical savanna .....	189
Appendix XLIII: Data of monocrystalline technology in tropical savanna .....	190
Appendix XLIV: Reliability analysis of PV module installation configurations .	191
Appendix XLV: Solar PV system checklist.....	192
Appendix XLVI: Turnitin Originality Report.....	197

## LIST OF TABLES

<b>Table 2.1:</b> Model Developed from Environmental Parameters to Predict Solar PV Performance .....	14
<b>Table 2.2:</b> Summary of Selected Studies on Solar PV Modules Performances.....	18
<b>Table 2.3:</b> Summary of Selected Studies on Solar PV Modules Performances.....	19
<b>Table 2.4:</b> Summary of PV Module Studies on the Degradation Analysis.....	31
<b>Table 3.1:</b> Inverter Specification .....	37
<b>Table 3.2:</b> Solar PV Module Specification.....	38
<b>Table 3.3:</b> Design Parameters of the Economic Modeling .....	45
<b>Table 3.4:</b> Weather Station Parameters Specification.....	49
<b>Table 3.5:</b> Selected Specifications of the PV Modules at STC Deployed in Moi University.....	50
<b>Table 3.6:</b> Specifications of the Weighing Machine .....	51
<b>Table 3.7:</b> Specifications of the Sieves .....	52
<b>Table 3.8:</b> Selected Specifications of the Modules at STC .....	58
<b>Table 3.9:</b> Technical Specifications of Tri-Ka and Trisen .....	59
<b>Table 4.1:</b> Weather Parameters .....	75
<b>Table 4.2:</b> Reference Yield ( $Y_R$ ), (kWh/kW-day).....	76
<b>Table 4.3:</b> System 1 Technical Performance Indicators.....	77
<b>Table 4.4:</b> System 4 Technical Performance Indicators.....	79
<b>Table 4.5:</b> System 2 Technical Performance Indicators.....	85
<b>Table 4.6:</b> System 3 Technical Performance Indicators .....	86
<b>Table 4.7:</b> Financial Indicators of Solar PV Systems .....	103
<b>Table 5.1:</b> Effects of Dust Accumulation on the Performance of m-Si PV Module.	107
<b>Table 5.2:</b> Effects of Dust Accumulation on the Performance of p-Si PV Module..	110
<b>Table 5.3:</b> Effects of Dust Accumulation on the Performance of a-Si PV Module..	112
<b>Table 6.1:</b> Annual Average Degradation Rates of PV Modules (%) .....	120
<b>Table 6.2:</b> Power Degradation Rates and Mechanism of Solar PV Modules .....	133

## LIST OF FIGURES

<b>Figure 1.1:</b> Contribution by Energy Sources as of December 2021 of Kenya. ....	4
<b>Figure 1.2:</b> Installed Solar PV Capacity in Kenya from 2011-2020.....	5
<b>Figure 3.1:</b> Aerial View of the PV Power Plant in Strathmore University.....	39
<b>Figure 3.2:</b> Schematic Diagram of Solar PV Power Plant.....	40
<b>Figure 3.3:</b> Test Bed Installation of Solar PV Modules and Weather Station in Moi University.....	49
<b>Figure 3.4:</b> (A) Sample of the Dust Collected (B) Analytical Balance Weighing Machine.....	53
<b>Figure 3.5:</b> Sample of Dust after Separation by Sieve Depending on the Particle Size .....	54
<b>Figure 3.6:</b> Köppen Climatic Map of Kenya Indicating the Location of Study Areas .....	55
<b>Figure 3.7:</b> Data Collection Using Tri-Ka, Trisen and Infrared Camera .....	56
<b>Figure 3.8:</b> Measured Solar Irradiance ( $W/m^2$ ) Versus Measured Isc (A). ....	60
<b>Figure 3.9:</b> Measured Solar Irradiance ( $W/m^2$ ) Versus Measured Voc (V) .....	61
<b>Figure 3.10:</b> PV System Design for Domestic Use.....	69
<b>Figure 3.11:</b> PV System Design for Water Pumping .....	70
<b>Figure 3.12:</b> PV System Design for Grid Interactive.....	71
<b>Figure 3.13:</b> PV System Design for Electrical Generation to Supply the Grid .....	72
<b>Figure 4.1:</b> Reference Yield (kWh/kW-day) in years .....	77
<b>Figure 4.2:</b> Energy Output (kWh) for the Two Systems.....	80
<b>Figure 4.4:</b> System Efficiency (%) in Years .....	82
<b>Figure 4.5:</b> Capacity Utilization Factor in Years .....	83
<b>Figure 4.6:</b> Trends of Average performance ratio (%) .....	84
<b>Figure 4.7:</b> Trends of Energy Output (kWh) for System 2 and 3 .....	87
<b>Figure 4.8:</b> Final Yields (kWh/kW-day) in Years .....	87
<b>Figure 4.9:</b> System Efficiency (%) in Years .....	88
<b>Figure 4.10:</b> Capacity Utilization Factor (CUF) in Years .....	89
<b>Figure 4.11:</b> Trends of Annual Average Performances Ratio (PR) (%) .....	90
<b>Figure 4.12:</b> Annual Average Energy Output (kWh) for the Four Systems .....	90
<b>Figure 4.13:</b> Trends in Power Output (kW) .....	91
<b>Figure 4.14:</b> Final Yield (kWh/kW-day) in Years .....	92

<b>Figure 4.15:</b> System Efficiency (%) in Years .....	92
<b>Figure 4.16:</b> Capacity Utilization Factor (CUF) in Years .....	93
<b>Figure 4.17:</b> Trends of Performance Ratio (PR), (%) in Years.....	94
<b>Figure 4.18:</b> Power Output when Ambient Temperature was held at (20.44°C).....	97
<b>Figure 4.19:</b> Power Output (W) when Ambient Temperature was held at (18.45°C )98	
<b>Figure 4.20:</b> Power Output (W) when Ambient Temperature held at (22.21°C ).....	99
<b>Figure 4.21:</b> Power Output (W) when Wind Speed (m/s) held at (3.17 m/s) .....	100
<b>Figure 4.22:</b> Power Output (W) when Wind Speed (M/S) was held at (2.77m/S) ..	100
<b>Figure 4.23:</b> Power Output (W) when Wind Speed (M/S) was held at (3.97 M/S)..	101
<b>Figure 5.1:</b> I-V Curve of Monocrystalline Solar PV Module.....	108
<b>Figure 5.2:</b> P-V curve of monocrystalline solar PV module.....	109
<b>Figure 5.3:</b> I-V curve of polycrystalline solar module.....	110
<b>Figure 5.4:</b> P-V Curve for Polycrystalline Solar PV Module .....	111
<b>Figure 5.5:</b> I-V Curve of Amorphous Solar PV Module .....	112
<b>Figure 5.6:</b> P-V Curve of Amorphous Solar PV Module .....	113
<b>Figure 6.1:</b> (a) EVA Discolouration (b) Uneven Heating of PV Module.....	117
<b>Figure 6.2:</b> (a) Snail Tracks (b) Brown Discolouration EVA Materials (c) Uneven Heating of PV Module (d) Shattered Glass of Solar Module .....	119
<b>Figure 6.3:</b> Isc Degradation per Year Versus the Type of Cell Technology .....	121
<b>Figure 6.4:</b> The Degradation Rates of Short Circuit Currents Versus the Number of Years .....	122
<b>Figure 6.5:</b> Types of Cell Technology Versus Voc Degradation Rates.....	123
<b>Figure 6.6:</b> Voc Degradation Rates of Polycrystalline PV Modules in Warm..... Semi-Arid Region .....	123
<b>Figure 6.7:</b> Type of module technology versus FF degradation rates per year .....	124
<b>Figure 6.8:</b> FF Degradation Rates of p-Si Modules in the Warm Semi-Arid Region .....	124
<b>Figure 6.9:</b> Type of Solar Module Technology Verses Power Degradation Rates... .....	125
<b>Figure 6.10:</b> Power Degradations Rates of p-Si Modules in A Warm Semi-Arid Region .....	126
<b>Figure 6.11:</b> Solar PV Modules Efficiency (%).....	127
<b>Figure 6.12:</b> PV Modules Efficiency (%) in Warm Semi-Arid Region versus Years .....	127

**Figure 6.13:** Degradation rates model for warm semi-arid climatic conditions: ..... 128

**Figure 6.14:** Actual and Predicted Values of Power Degradation Rates ..... 129

## SYMBOLS, ABBREVIATIONS AND NOTATIONS

A	Amperes
AC	Alternating Current
Am <sup>2</sup>	Array area
a-Si: $\mu$ c-Si:	Hydrogenerated amorphous silicon/ hydrogenerated microcrystalline silicon hetero-junction
a-Si:H	hydrogenerated single-junction amorphous silicon
AT	Ambient temperature
AVG IDR	Annual average short circuit degradation rate
AVG Isc DR	Annual Average Isc Degradation Rate
AVG P DR	Annual Average Power Degradation Rate
AVG P DR	Average Annual Power Degradation Rate
AVG Voc DR	Annual Average Voc Degradation Rate
AVG Voc DR	Average Voc Degradation Rate
CDF	Cumulative Distribution Function
CdTe	Cadmium telluride
CIS	Copper indium selenium
Co	Initial capital investment
COV	Coefficient of variability
CSD	Classical sessional decomposition
C <sub>t</sub>	Discounted cash flow
CUF	Capacity utilization factor
DC	Direct Current
Diff.	Difference
DPP	Discounted payback period
DR	Degradation rate
E <sub>AC</sub>	AC energy output
EPRA	Energy and Petroleum Regulatory Authority
EVA	Ethylene vinyl acetate
FF	Fill Factor
FiT	feed-in tariff
FMEA	Failure Modes and Effects Analysis



FTA	fault tree analysis
G	Irradiance
g/cm	gram per centimeter
GHI	Global horizontal irradiance
$G_M$	Measured irradiance
$G_o$	Reference irradiance.
GoK	Government of Kenya
$G_{STC}$	Irradiation at standard test conditions
$G_T$	Total in-plane solar irradiation
h	Hour
HT	In-plane radiation
HW	Holt-Winters seasonal model
IEA	International Energy Agency
IEC	International Electrotechnical Commission
$I_M$	Measured current
$I_{mp}$	Current at maximum power
$I_{nc}$	Inclination angle
IRENA	International Renewable Energy Agency
IRR	Internal rate of return
$I_{sc}$	short circuit current
$I_{sc DR}$	Annual $I_{sc}$ Degradation Rate
$I_t$	Discounted annual cash flow
I-V	current- voltage
K	Kelvin
KNBS	Kenya National Bureau of Statistics
kW	Kilowatt
kWh	Kilowatt hour
LCOE	Levelized cost of energy
LID	Light Induced Degradation
LLS	linear least-square
LOLP	loss of load probability

$L_T$	Total energy losses
M	Measured
m	Meters
MAD	Mean average deviation
MAPE	Mean percentage error
MCS	Monte Carlo Simulation
mg	milligrams
MHz	Megahertz
mm	Millimeters
Mod	Module
MOE	Ministry of Energy
m-Si	monocrystalline silicon
MTTF	Mean Time To Failure
MTX	Main Transformer
MW	Megawatts
MW <sub>p</sub>	Megawatt power
$\eta$	efficiency
NREL	National Renewable Energy Laboratory
O&M	operation and maintenance
$O_t$	Operation and maintenance cost
P	Predicted
Pa	Pascal
$P_{AC}$	AC output power
PCA	principal component analysis
PDF	probability density function
PDR	Annual Power Degradation Rate
PDR	Annual Power Degradation Rate
PID	potential induced degradation
$P_{max}$	Maximum power
PR	performance ratio
p-Si	polycrystalline

PU	Unit cost
PV	photovoltaic
P-V	power-voltage curves
PVGIS	Photovoltaic Geographical Information System
PVSyst	Photovoltaic System
PVwatts	PVwatts Calculator
r	Discount rate
RH	Relative humidity
RMSE	Root mean squared error
s	Second
SDGs	Sustainable Development Goals
SDU	solar PV system for domestic use
SGT	solar PV system for grid-interactive
SPG	solar PV system for electrical power generation to feed the grid
SPP	simple payback period
SPU	solar PV system for pumping water
STL	Seasonal and trend decomposition using Loess
T Isc DR	Total short circuit current Degradation Rate
T Isc DR	Total short circuit Degradation Rate
T P DR	Total Power Degradation Rate
T Voc DR	Total Voc Degradation Rate
T	Time
T <sub>c</sub>	Measured module temperature
T <sub>c</sub>	Module temperature
Tech.	Technology
Temp	Temperature
TLCC	Total life-cycle cost
TR	Total Reliability
TX	Transformer
US\$	United State dollar
UV	ultra violet

V	Volts
VDR	Annual open circuit voltage Degradation Rate
V <sub>mp</sub>	Voltage at maximum power
V <sub>oc</sub>	Open circuit voltage
V <sub>oc</sub> DR	Annual V <sub>oc</sub> Degradation Rate
V <sub>ocM</sub>	Measured voltage
W	Watts
Wh	Watt hour
W <sub>p</sub>	Watt power
WS	Wind speed
Y	Years
YF	Final yield
YR	Reference yield
$\beta$	Voltage temperature coefficient
$\sigma$	standard deviation
$\alpha$	Current temperature coefficient

## **CHAPTER 1**

### **INTRODUCTION**

#### **1.1 Background of the Study**

Non-renewable energy sources (mainly fossil-fuels – coal, gas, and crude-oil) can no longer satisfy growing energy demand in a sustainable way. These fuels also face many challenges, such as a rise in project costs, opposition to the development of fossil-fuel-based thermal plants due to their contribution to climate change and future uncertainty in the availability of these fuels as well as the unpredictability of fossil-fuel prices.

There had been increasing and growing interest in the development of renewable energy resource-based power systems. In addition, towards attainment of sustainable peace and prosperity for people and the planet, and thereby improving the conditions and standards of living of the global population, all United Nations Member states adopted 17 Sustainable Development Goals (SDGs) in year 2015 termed ‘The 2030 Agenda for Sustainable Development’.

At the heart of these 17 SDGs is Goal 7, which aims to ensure access to affordable, reliable, sustainable, and modern energy for all by year 2030. Attainment of this goal could have a direct impact on the achievement of some other SDGs, such as SDG 3 (Good health and well-being), SDG 8 (Economic growth), SDG 11 (Sustainable cities and communities), and SDG 13 (Climate Action).

Due to their existence of environmentally friendly, the development of renewable energy sources, which can be defined as energy resources that are ever available in a continuous supply, could play a significant role in the achievement of SDG 7. Furthermore, being ‘local’ energy resources, the development of renewable energy-

based energy systems could play a crucial role in improving national and regional energy security.

In addition to power generation issues, the cost of transmission and distribution of electrical energy is one of the major factors that affect decisions in the implementation of power plant projects. Hence, the development of decentralized power systems (in which power generating plants are located within the premises or in close proximity to the consumers) based on solar photovoltaic (PV) systems can reduce investment costs as well as transmission and distribution losses.

In Kenya and many developing countries, most communities in the semi-arid areas are sparsely populated and hence, it is expensive for those communities to be connected to utility-grid networks. Small to medium decentralized power systems therefore, could serve as better options for access to electricity. One of the renewable energy technologies that can overcome most of these challenges is solar photovoltaic (PV) technology. Solar PV technology can be used to generate electricity directly without additional mechanical and generating components.

Furthermore, solar PV technologies are scalable and allow users to install various size solar PV modules according to their needs and financial ability. Solar PV technologies have other advantages compared to other sources of renewable energy, such as short implementation period, availability, less visual and noise impacts if installed on building roofs, reduction of energy-food conflict issues, and transmission and distribution losses.

Despite these advantages and the availability of solar energy resources, the uptake of solar PV as the source of electrical energy in Africa is still low compared to other sources such as hydropower and thermal. According to International Energy Agency

(IEA) (2022), in the year 2019 only 0.87% of the electricity energy produced in Africa was from solar PV systems.

One of the major challenges of low uptake of solar PV in Kenya as a source of electrical energy is attributed to a lack of information on solar technology potential to generate electricity, potential opportunities (e.g., energy consumption savings), its performance, degradation and reliability under local climatic conditions, and the economic benefits (National Energy Policy, Kenya, 2018).

The other issue for low utilization of solar PV energy in Kenya is associated with a lack of sufficient data which can inform the economic viability and sustainability of different PV technologies (National Energy Policy, Kenya, 2018). In this regard therefore, a comprehensive study of solar PV performance, degradation and reliability under the Kenyan climate conditions is essential in availing necessary data on performance and economic benefits.

## **1.2 Energy Situation in Kenya and Solar PV Development**

Currently, the primary energy supply in Kenya is dominated by biomass resources, which in recent times accounted for 68%, while crude oil and electricity accounted for about 22% and 10%, respectively (Takase et al., 2021). According to Kenya National Bureau of Statistics (KNBS, 2022) the total cumulative installed electrical power capacity increased from 2,339.9 MW in 2017 to about 2,989.6 MW in 2021, at an average growth rate of 129.94 MW/year while the effective capacity increased from 2,264.4 MW in 2017 to about 2,857.6 MW in 2021 at an average growth rate of 4.49% per year.

Kenya is the leading country in East Africa, with an electricity access rate of 76.49%, in terms of household electricity connectivity (EPRA, 2022; Gakunga, 2021). Figure

1.1 shows the electricity generation by energy sources as of December 2019 in Kenya. As can be observed with a combined contribution of 85.9%, hydropower, thermal oil, and geothermal energy dominate electricity generation in Kenya.

In addition, renewable energy resources (hydro, geothermal, wind, cogeneration and solar) accounted for 77.3% of installed power capacity at the end of 2021 in Kenya. Additionally, the installed solar energy capacity was only 5.8% compared to total installed capacity which can be considered as low usage.

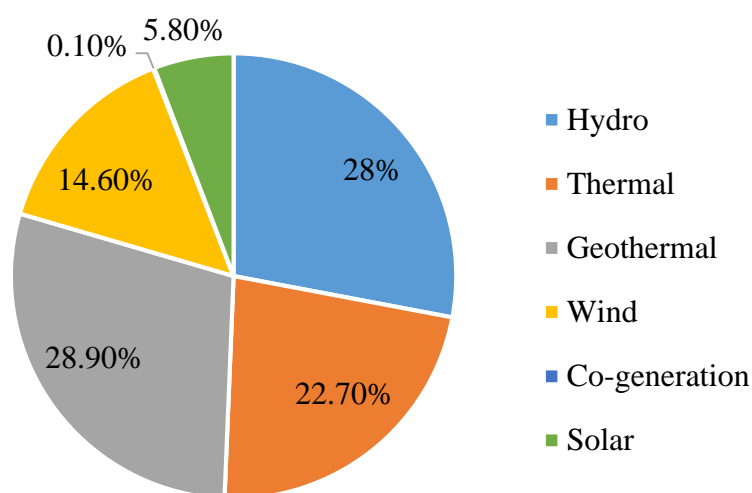


**Figure 1.1:** Contribution by Energy Sources as of December 2021 of Kenya.  
((Source: KNBS (2022))

Figure 1.2 shows the trend in development of solar PV capacity in Kenya from 2017 to 2020. It can be observed that solar PV installation capacity grew from about 2 MW in 2011 to about 106 MW in 2020. According to (KNBS, 2022) the installed solar energy capacity in Kenya was 172.5 MW by year 2021. It is expected that this trend will continue in future and hence, a proper understanding of environmental and operational conditions on solar PV installations in Kenya is of great interest.

The study of performance, degradation, reliability, and economic indicators of solar PV in the region will address the gap that exists in the open literature and accelerate its use.



This potential increase could be associated with more industries finding cleaner and alternative ways of generating electricity as well as users seeking alternative electricity sources due to unreliable and expensive grid connections of utility-supplied electricity.

In addition, it shows that before 2018, off-grid dominated solar PV installations in Kenya reached 97.4% in 2017. However, from 2018 to 2020, off-grid contribution dropped to 46.4% (or 49 MW out of 106 MW) relative to the total capacity. The drop on the off-grid contribution between 2018 to 2020, maybe due to accelerated grid connectivity in the country during the period.

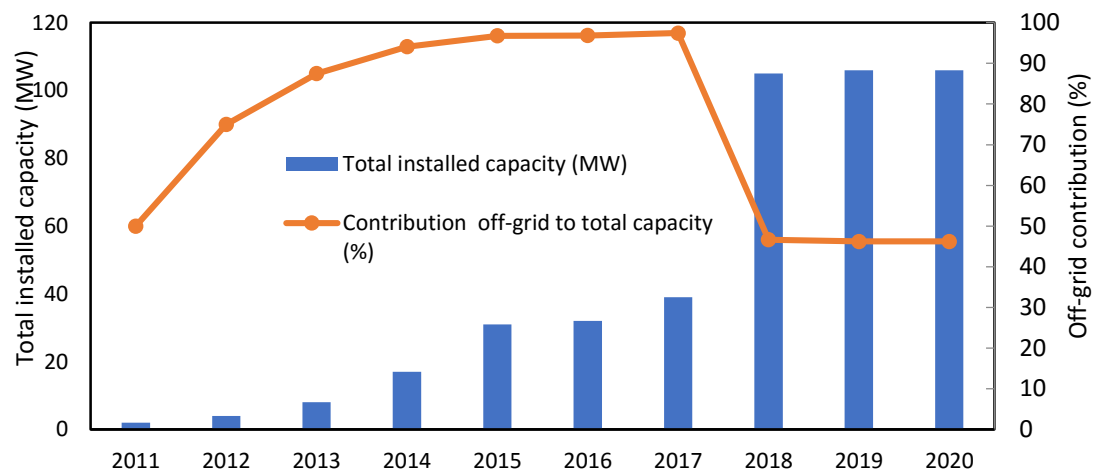


**Figure 1.2:** Installed Solar PV Capacity in Kenya from 2011-2020  
(Source: International Renewable Energy Agency (IRENA, 2022))

Electricity generation by solar photovoltaic (PV) technology can only be economical if the solar PV modules operate reliably for 25–30 years under field conditions. To ensure such levels of reliability, solar PV modules undergo stringent qualification tests developed as per international standards by International Electrotechnical Commission (IEC 61215-1-2-2021) and (IEC 61646-2008). These tests provide excellent information regarding module design, material, and process flaws which can lead to premature failure.

In addition to challenges discussed previously, another challenge in utilizing the solar PV system in Kenya is the proliferation of sub-standard solar modules and equipment (National Energy Policy, Kenya, 2018). This challenge and Kenya's harsh environmental conditions have contributed to infant failures and inefficiency of solar PV installations in the country. These failures can be assessed and quantified through evaluation of degradation rates and mechanism of installed solar PV modules.

Modules have to degrade at a rate of  $<1\%$  to work satisfactorily within warranty periods, which normally vary between 10 to 25 years. When solar PV modules are deployed in the field, they are affected by factors such as humidity, temperature, ultraviolet radiation, surface contamination (soiling) and mechanical stresses. These conditions have adverse impacts on various components of the solar PV modules, which include packing materials, adhesion, semiconductors, and metallization and hence, affect the performance of the modules.

According to literature, unfortunately, these degradation mechanisms as well as environmental conditions that influence these mechanisms are location specific and hence, different geographical regions (with different climatic conditions) have shown different module performance and degradation rates.

### **1.3 Problem Statement**

The performance, degradation and reliability of solar PV module electrical energy generation depend on environmental conditions of an area. Studies have indicated that environmental variables such as dust and air pollutants in the atmosphere cause a reduction in PV efficiency. The study of performance, degradation and reliability of solar PV modules are the best method to establish the potential for solar PV electrical energy generation in an area.

The performance, degradation and reliability of PV modules under outdoor conditions are found to be quite different from those determined under controlled laboratory conditions during qualification or certification testing. According to the literature environmental characteristics vary from location to location and hence generalized observations without investigation would have limited applicability.

The performance, degradation and reliability study of solar PV modules in Kenya had not been documented or little information is available in open literature. It was therefore important to assess accurately and precisely the performance, degradation and reliability of solar photovoltaic power plants. The findings of this study will provide useful information to government, interested individuals and organizations about actual performance, degradation and reliability of solar PV module systems in tropical savanna and semi-arid climatic conditions along the equatorial region.

#### **1.4 Main Objective**

The main objective of this study was to evaluate and analyze the performance, degradation and reliability of solar PV installation in Kenya.

#### **1.5 Specific Objectives**

- i) To evaluate the technical and economic performance of solar PV modules in tropical savanna semi-arid climatic conditions.
- ii) To analyze the effects of soiling on the performance of solar PV modules in tropical savanna climatic regions.
- iii) To evaluate the degradation mechanism and rates of solar PV modules in tropical savanna and warm semi-arid climatic conditions.
- iv) To determine the reliability and failure rates of solar PV modules in tropical savanna and semi-arid climatic conditions.

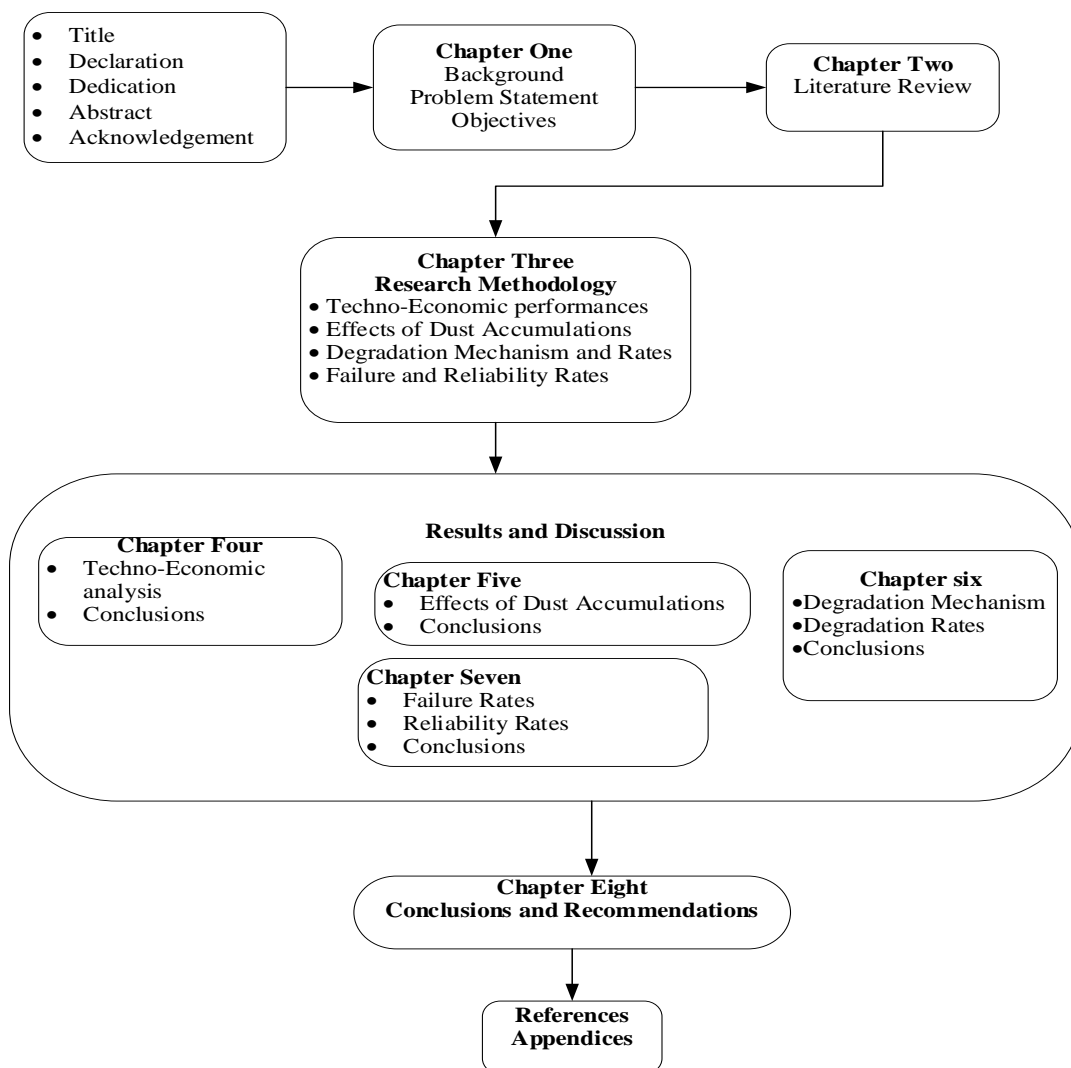
### **1.6 Contribution and Significance of this Study**

Government of Kenya in year 2018-2030 plans to; (1) Provide framework for connection of electricity generated from solar energy to national and isolated grids. (2) Support hybrid power generation systems involving solar and other energy sources to manage the effects caused by the intermittent nature and availability of solar energy. (3) Roll out installation of solar PV systems in all the remaining public facilities in the off-grid areas (National Energy Policy, Kenya, 2018).

For this to be effectively implemented, an in-depth study on the performance, degradation and reliability of solar PV systems need to be carried out. This will help to establish the measures required to maintain long term reliability and minimum connection rating of a solar PV system that can break even. In addition, the publications of reliability, degradation and performance of solar PV under Kenya climatic conditions will be done after completion of the work.

This will inform and address missing gap of the region, which can be used for design and establishment of the new solar power site for electrical energy generation while the data on soil distribution and accumulation can be used in the determination of soiling index and maintenance schedule required.

## 1.7 Thesis Structure



## **CHAPTER 2**

### **LITERATURE REVIEW**

#### **2.0 Introduction**

This chapter is divided into four sections. The first section discusses the technical and economic performance of PV modules. Under the technical performance, the study discusses, on the measured and simulated data, effects of weather and environmental conditions, tilt angle and orientation of installation design on PV modules. Finally, the economics performance of PV modules systems is deliberated.

Further section two addresses the effects of dust accumulations on the performance of PV modules. In addition, section three discusses the degradation mechanism and rates from different climatic conditions of PV modules. Finally, the study addressed the reliability and failure rates of PV modules on different installation design configurations.

#### **2.1 Technical and Economic Performance of Solar PV Modules**

The evaluation of technical and economic performance of solar PV modules in a specific climatic condition is an important study to be carried out. Such a study provides the missing data on the awareness on the potential, opportunity, and economic benefits offered by the PV technologies. The International Electrotechnical Commission (IEC) developed parameters to be used. These parameters are used to evaluate and compare the performance of different solar PV technologies in different climatic conditions.

##### **2.1.1 Comparison of Solar PV Performance Based on Measured and Simulated Data**

The performance of solar PV systems using both measured and simulated data yield different results as discussed in the subsequent literature. Thotakura (2020) reported

that, when compared with real-life performance, the software models underestimated the energy injected into the grid as follows: 5.33%, Photovoltaic Geographical Information System (PVGIS), 12.33%, PVwatts Calculator (PVwatts), and 30.64%, Photovoltaic System (PVSyst) in tropical wet and dry climates of India. This could be owed to the sources of the input data and the different methodologies of estimating the weather parameters for the different simulation tools. In a separate study, (Goel & Sharma, 2021) using measured data, PVSyst, and Helioscope software found that annual yield to be 9.2% and 14.75%, respectively higher than the measured value. It is conjectured that this is due to different sources of satellite data, (Meteonoum and ISHRAE).

Banda et al. (2019) reported a marginal difference between the measured and simulated performance ratio (PR) of 79.5% and 80%, respectively for a grid-connected solar PV power plant in Malawi. Ramanan et al. (2019) indicated uncertainty of measured and predicted values of 0.32% and 0.47% for polycrystalline (p-Si) and Copper indium selenium (CIS) systems, respectively. Vidal et al. (2020) indicated a simulated PR value of 85.5% and measured PR value as 89% with a discrepancy of 4%.

From the foregoing literature, it is clearly evident that simulation results do not always mimic the actual (measured) results. It can either overestimate or underestimate the actual performance. This can lead to wrong decisions on the system design, investment, and benefits associated with the utilization of the technology. However, the use of the actual data provides a good estimate and helps in the development of reliable models in actual performance, reliability, and economic benefit of the system of the climatic condition under consideration of the region.

### **2.1.2 Effect of Weather and Environmental Conditions on Solar PV Performance**

Many studies have investigated the effect of direct environmental variables on solar PV performance and developed models for predicting system performance. Sahouane et al. (2019) reported that the environmental parameters variation has a direct effect on the performance of both the energy conversion efficiency and the system losses. Al-Badi (2020) showed that high solar radiation and ambient temperature combined with low wind speed increase the module temperature and as a result increase the cell temperature loss. Similarly, (Arora et al., 2022) found that with the rise in ambient temperature the energy generated by solar PV modules decreases. The study also indicated that environmental conditions are the key factors affecting overall system performance.

In addition, the selection of the combination of environmental parameters greatly determines the accuracy of the model results. Ziane et al. (2021) indicated that preprocessing techniques can be a useful tool to identify crucial and important parameters, in order to construct a lightweight prediction model that depends on a lesser number of variables as possible. This saves time of computations and avoid overfitting the model.

AlSkaif et al. (2019) using principal component analysis (PCA) showed that relative humidity, visibility, temperature and cloud cover had the highest importance when selecting the PV system output power. Saad et al. (2022) used plane irradiance, precipitations, pressure and temperature as the environmental variables on the study of the impact of forecasting horizon and resolution on PV Power Prediction using Artificial Neural Networks. The study selected those variables based on availability and the literature findings.



Several studies in the literature have developed models to estimate the performance of solar PV modules in relation to environmental parameters as summarized in Table 2.1. Weather parameters can play a significant role in predicting the performance of a solar PV module in a specific region. From the literature, studies have used either one of the parameters to predict power output, efficiency, voltage, or current. This may not indicate good accuracy and validity of the predicted results.

The development of the model utilizing more than one parameter may therefore produce good accuracy. This study utilized three parameters to develop a model for predicting power out of solar PV power plants in tropical savanna regions. Parameters are selected based on the preprocessing technique, previous studies in the open literature, and the availability of data.

Most of the studies from literature have indicated the effects of solar irradiance, ambient temperature, and wind speed however, not much has been done on the effects of relative humidity (Gopi et al., 2021) on the performance of PV modules. Hence, this study further considered the combined effects of solar irradiance, ambient temperature, wind speed, and relative humidity on the performance of PV modules.

**Table 2.1:** Model Developed from Environmental Parameters to Predict Solar PV Performance

Author	Predictive Models	Findings/Observation
Ayadi et al. (2019)	$Y = 190 + 1500x$ , $R^2=0.765$ Y= Power output, x= Wind speed	An increase in wind speed increases power output
	$Y = 4472 - 15.31x$ , $R^2=0.5809$ Y=Power output, x= Relative humidity	An increase in relative humidity decreases power output
	$Y = 3125 - 67.19x$ , $R^2=0.8793$ Y=Power output, x= Ambient temperature	An increase in ambient temperature decreases power output
Salimi et al. (2020)	$P_{\text{clean}}=34.402-0.448T_{\text{air}}+0.1E_{\text{clean}}$ $R^2=0.8793$ , P=Power output, T= Ambient temperature, E=solar irradiation	Positive linear relationship
Njok & Ogbulezie (2019)	$EFF = -0.0206RH + 1.8011$ , $R^2=0.6557$ EFF=Efficiency= Relative humidity	Negative correlation
Gopi et al. (2021)	$E = 4897 - 2067G_{\text{POA}} + 768.9G_{\text{POA}}^2 - 54.84G_{\text{POA}}^3$ E=Energy generated, $G_{\text{POA}}$ = Irradiance	Irradiance increases energy generated increases

### 2.1.3 Effects of Tilt Angles and Orientation on Solar PV Performance

The performance of the solar PV module is affected by weather and meteorological conditions, efficiencies of the main components of the system, and their responses to environmental conditions as well as installation conditions (tilt angle and orientations) (Oloya et al., 2021). This study considers two scenarios, which are (1) systems with the same fixed tilt angle but different orientations and (2) systems with the same orientation but different tilt angles. All the installations considered in this study are made in the same location.

Seme et al. (2019) indicated that the performance of the photovoltaic system primarily depends on the proper inclination, azimuth angle shading, and snow barriers. The study

also indicated that PV systems installed in higher latitudes have lower final yields. Omar & Mahmoud (2018) indicated that fixed PV arrays should be tilted at the latitude of the location to capture the most solar energy. The study also indicated the optimum orientation of a PV module as the geographic true south. The study further used PVSYST software to compute the output power of a 1 kW peak PV system with different tilt angles. The results indicated that the system generated more energy with a tilt angle less than latitude and less energy with a tilt angle more than the latitude angle of the place.

To maximize the direct insolation received by PV modules, the tilt angle is usually the site's latitude and the modules are oriented towards the equator (Yu et al., 2019). However, in some set up other issues will arise due different interest like cost of the land. Installation of PV power plant on the roof will reduce the cost of land and competition with the land for farming. Single-axis tracking, dual-axis tracking, simple glass cover, hydrophobic glass cover, soiled glass, clean glass, partial shadow, use of phase-change material, computational fluid dynamic analysis, are the novel methods found in the literature for analysis and locating the optimum tilt angle (Yunus Khan et al., 2020). It can therefore, be indicated that the choice of optimal angle will also be affected by several factors which can be categorized as availability and cost of land, different uses of the land, and location of the PV power plant whether in rural or urban areas.

#### **2.1.4 Technical and Economics Performance of Solar PV Module System**

Technical analysis plays a critical role in presenting the relevant data for decision-making in the further improvement of design, installation, and commissioning, leading to better performance (Chawla & Tikkiwal, 2021; Martín-Martínez et al., 2019).

Studies had been conducted around the globe on PV modules technical and economic performance analysis using one year data such as (Alshare et al., 2020; Sreenath et al., 2021; Thotakura, 2020; Vidal et al., 2020). Martín-Martínez et al. (2019) reported that underestimating the complexity of a dual tracking system in the design phase underestimates operation and maintenance (O&M) which translates to underestimating the Levelized cost of energy (LCOE) of the plant. The study proposes further work on the longer time span in order to complete and extend performance analysis and confirm the trends observed. With more data, new mathematical models of PV could be developed to improve the accuracy of the PV power plants design.

Chawla & Tikkiwal (2021) indicated that the PV modules when arranged in variable-tilt will produce a higher yield annually. The study proposes an economic and environmental assessment of the proposed setup. Mensah et al. (2019) indicated the LCOE, discounted payback period (DPP), and simple payback period (SPP) of 2.5MW solar PV installed in Ghana as  $US\$0.2411/kWh$ , 14.95 years, and 8.34 years respectively.

Table 2.2 and 2.3 shows the summary of technical performances of PV modules from different regions. The table shows that those studies are regionally unbalanced while the PV module performance is location-specific. They indicate the studies conducted in Middle East, Asia, West Africa, Southern Africa, North Africa, Europe, and South America. Despite the usefulness of performance analysis of solar PV installations for stakeholders, much has not been done in literature as far as the study of solar PV module performance analysis in the East Africa region. This study, therefore, addresses the gap on the missing information on PR studies of the climatic conditions of East Africa region.

In addition, they show the technical performances parameters considered in the studies which includes reference yield, final yield, capacity utilization factor, efficiency and performance ratio. Further, they show the type of data used, either measured or simulated. Finally, they indicate cell technology of PV cells used.

**Table 2.2:** Summary of Selected Studies on Solar PV Modules Performances

Author	Cell Tech.	Measured (M) / Predicted (P)	Diff. (%)	YR (kWh /kW)	YF (kWh /kW)	CUF (%)	$\eta$ (%)	PR (%)	Region
Al-Badi (2020)		M		5.59	3.78	15	10.3	67	Middle east
Alshare et al. (2020)	P-Si	M	3.77	5.7	4.6	18.1	13	79.9	Middle east
		P		5.6	4.5	17.7	77		
Ramanan et al. (2019)	P-Si	M	0.47	5.35	4.20	17.79		78.48	India
	CIS	M			4.64	19.57	86.73		
	P-Si	P			4.21		78.85		
	CIS	P			4.66		87.26		
Arora et al. (2019)	P-Si	M	5 to 10	5.13	4.28	17.8	14.77	82.7	India
		P			4.70		14.16	85.6	
Thotakura et al. (2020)	P-Si	M			4.61	21.77		88	India
Martín-Martínez et al. (2019)	P-Si	M		7.87	6.68	27.84	10.94	84.86	Spain
		M		9.45	7.92	33.02	10.78	83.82	
		M		7.01	5.53	23.04	10.19	78.93	
		M		7.44	5.88	24.48	10.25	78.94	
		M		5.64	4.71	19.64	10.82	83.62	

**Table 2.3:** Summary of Selected Studies on Solar PV Modules Performances

Author	Cell Tech	Measured (M)/ Predicted (P)	Diff. (%)	YR (kWh /kW)	YF (kWh /kW)	CUF (%)	$\eta$ (%)	PR (%)	Region
El Hacen Jed et al. (2020)	M-a-Si	M			4.26			66	West Africa
Mensah et al. (2019)		M				16.2		70.6	West Africa
Daher et al. (2018)	P-Si	M	7.4	5.6	4.69	16.35	12.68	84	Djibouti
Banda et al. (2019)						17.7	14.6	79.5	Southern Africa
Sahouane et al. (2019)				6.2	4.4	18.58	10.99	71.89	North Africa
Necaibia et al. (2018)	M-Si	M		5.7-7.68	3.98-5.75	7.91	10.5-13.53	66.6-85.93	North Africa
Seme et al. (2019)					2.84	11.85		68.84	Europe
Vidal et al. (2020)		P			2.27	9.4		85.5	South America
		M			3.6	15.1		89	

In addition to the technical performance of solar PV installations, from an economic point of view and to assist in making informed-decisions, it is essential to know the financial value of generated electricity by the solar PV installations. This information could be helpful to assess the economic viability of the installation as well as to compare the cost of energy produced with global data and available local or national retail utility electricity prices or alternative sources of electricity. Hence, several studies have recommended that the economic performance of solar PV installations should be carried out along with technical assessment performance (Chawla & Tikkiwal, 2021; Seme et al., 2019).

#### **2.1.5 Knowledge Gap and Contribution of the Study**

From the literature it can be indicated that solar PV module performance depends on the climatic conditions of a specific region. The studies on the performance of solar PV modules had been carried out in different regions. These studies are regionally unbalanced and to the researcher's knowledge not much has been done (open literature) as far as the study of solar PV modules performance analysis in the East African regions.

Therefore, the goal of the study is to examine the technical and economic performance and develop the models of solar PV installations using long-term performance data, which can provide more data for better assessment of solar PV installation as well as investigate inter-annual variability in the installation's performance. The calculated economic indicators of the installations using the location's economic/financial parameters could provide useful information to policymakers and other interested



organizations to make the right decision in the formulation of policies, installation design, and improvement of the products.

## **2.2 Effects of Dust Accumulation on the Performance of Solar PV Module**

Olivares et al. (2020) determined the soiling impact on photovoltaic modules at the coastal area of the Atacama Desert. The study indicated the efficiency of the clean PV module and dirty PV module as 13.01% and 9.62% respectively. The study also indicated that the power behaved similarly as efficiency. Further, the study indicated that current was the most affected parameter due to soiling while the voltage of the two modules did show any significant variation. This can be associated with that the current is the flow of electronics, and are activated by light.

Alquthami & Menoufi (2019) investigated the impact of soiling on electrical parameters solar PV performance in two different locations. The study indicated that one location performed better than the other in terms of power output by 15%. The study recommended further work be carried out in order to examine the practical and real-time impact regarding each location, additionally, it recommended each PV module be tested and electrically characterized outdoors at its corresponding location.

Babatunde et al. (2018) did an analysis of the impact of dust on the performance of PV plants. The study found that when the cleaning procedure was implemented, an average of 2.5% variance in specific yield was recorded between the clean and unclean string system. The study recommended future work to analyze the effect of progressive accumulation of dust on daily, weekly, and monthly, and the effect of tilt angle on soiling.

Fraga et al. (2018) did an analysis of the effects on the performance of photovoltaic modules on a soccer stadium in Minas, Gerais, Brazil. The results showed that soiling

reduced peak power by approximately 13.7% and 6.5% and energy production by approximately 16.5% and 8% during dry periods and a period after rainfall respectively. The study concluded that only after manual cleaning the performance of the PV panels is fully restored. It recommended the importance of incorporating manual cleaning among the costs of a photovoltaic solar power plant and finding the economic optimum frequency to clean the modules.

Menoufi (2017) carried out a literature review on the studies on dust accumulation on the surface of photovoltaic panels. The study indicated that Asia as a continent has the most published articles in this field. According to the study, Africa was identified in previous research as one of the most dust accumulation zones in the world, but insignificant studies were noticed. The study recommended more studies should be directed towards the impact of dust accumulation on the performance of PV modules in Africa.

Sadat et al. (2021) indicated that by increasing the thickness of the accumulated dust on the PV panel from  $0.001 \text{ g/cm}^2$  to  $0.033 \text{ g/cm}^2$ , the open-circuit voltage dropped by 20.63 %, the short-circuit current decreased by 98.02 %, and the maximum electrical power was degraded by 98.13 %, while conversion efficiency reduced by 98.2%, which was a significant reduction in the solar cell efficiency. The study recommended an outdoor experiment to be performed at the site of installation to examine the impact of soiling from different perspectives and to assess the effect of other variables such as humidity and distribution of soiling on the PV performance and carry out an economic evaluation of the impact of soiling on the PV energy systems and developing optimal mitigation strategies.

Menoufi et al. (2017) investigated the effects of dust accumulation on photovoltaic panels in a case study at the East Bank of Nile (Egypt). The results indicated that the overall power output of the uncleaned solar PV module dropped by more than half compared to the regularly cleaned PV module. The study recommended further experiments within the same region putting into consideration different densities of accumulated dust throughout different intervals of time, and testing different PV technologies.

Ramli et al. (2016) conducted a study to investigate the effects of dust accumulation and weather conditions on PV power output in Surabaya, Indonesia. The results of the study indicated that dust accumulation after two weeks of exposure in dry seasons caused a drop of PV power output of 10.8%. The study recommended future work to be done on (1) monitoring and analysis of environmental effects (particularly dust accumulation and regional climatic parameters), on PV panel performance over long time periods. (2) An effective and efficient cleaning system and implementation procedure needs to be developed, based on accurate identification of dust deposition and weather conditions during the dry season.

Yadav et al. (2021) conducted a study of a preliminary investigation of dust deposition on solar cells. The results indicated that a solar cell incurs a 27% loss in voltage and 28% loss in current due to dust deposition on it. Cleaning of the panels was also seen as a remedy to this issue. A proper cleaning method needs to be established. The study further indicates that cleaning using brushes and wipers may cause scratches and add to the losses in the cell. The study proposed for more research to be done on the cleaning methods in order to optimize the power output of the solar cell.

Schill et al. (2015) investigated the impact of soiling on I-V curves and the efficiency of PV modules. The study indicated that the efficiency temporarily dropped by approximately 20%. The study also indicated that partial cleaning may cause partial shading and lead to hotspots. The study concluded that current-voltage (I-V) curve monitoring can be a useful tool for investigating the soiling impact.

Semaoui et al. (2020) conducted an experimental investigation of soiling impact on grid-connected PV power. The results indicated an average short circuit current reduction of around 8.79% with more than one month of outdoor exposure after cleaning in the summer period. Kagan et al. (2018) investigated the impact of non-uniform soiling on a PV system. The study indicated that there is a disconnect between soiling measurements based on the module short circuit current ( $I_{SC}$ ) measurements and maximum ( $P_{MAX}$ ) measurements. However, the results indicated a change in short current and a maximum power of 4.6% and 7.6% respectively between cleaned and uncleaned modules. The study recommended the measuring of actual module power output in order to accurately assess the soiling losses.

Kaundilya et al. (2018) conducted a study on the effects of soiling on crystalline and thin-film technology PV modules for the composite climate zone of India. The study established that an increase in the accumulation of dust results in the drop of short circuit current. It also found that the accumulation of dust was more on modules installed at tilt angles of  $16^\circ$  than at  $43^\circ$ . The study also observed that a drop in average photon energy was due to the change of transmissivity. It further observed that the dust effect on the PV module may be technology-specific and need to be quantified.

Dahlioui et al. (2019) investigated the impact of soiling on PV modules performance in semi-arid and hyper-arid climates in Morocco. The results indicated the average annual

soiling rate of 4% and energy production loss due to soiling of  $2Wh/W_p \cdot \text{day}$ . The study further proposed that in a semi-arid climate humid cleaning is required while in hyper-arid climate dry cleaning can be sufficient. The study recommended studies to be conducted on cleaning frequency and validation of soiling rate and energy production loss in several sites having different climatic conditions.

### **2.2.1 Knowledge Gap and Contributions**

From the literature, studies have recommended solar PV module to be tested in the installation sites to determine the effects of soiling on the power output. This is due to the fact that each location has a different type of soil and weather conditions. The type of soil and weather pattern will determine how it will be deposited and removed from the solar PV module, hence, its effects on the power output.

Studies have further indicated that, despite Africa being one of the most dust accumulation regions in the world, little information is available on the open literature. This study addressed this gap on the effects of soiling on the power output of solar PV modules in tropical savanna climatic conditions of Eastern Africa region. The data obtained can be used to determine frequency and procedure of cleaning solar PV module in order to optimally benefit from the PV systems.

Furthermore, the determination of the soiling ratio of the region can be used during the design, installation, technical and economic evaluation of solar PV systems in the region.

### **2.3 Degradation Mechanism and Degradation Rates of Solar PV Modules**

Degradation is the gradual deterioration of the characteristics of a component of a system that may affect its ability to operate within the limits of acceptability criteria, which is caused by the operating conditions. The PV module performance can be

degraded due to several factors such as: temperature, humidity, irradiation and mechanical shock. Each one of these various named factors may induce one or more types of module degradation such as corrosion, discoloration, delamination, breakage and cracking cells.

A Photovoltaic module degraded may continue to generate electricity from sunlight, even if its use is no longer optimal. However, the degraded state of the module can be more problematic when the degradation exceeds a critical threshold. Studies in the literature have indicated different forms of degradation and degradation rates for different climatic conditions.

Ndiaye et al. (2013) reported the main degradation modes of solar PV modules as corrosion, discolouration, delamination, hotspots, bubbles, and potential induced degradation (PID). Corrosion is usually caused by moisture ingress at the edges of the solar PV modules. It usually affects the metallic connections of solar PV cells hence increasing the leakage currents. It also affects the adhesion between cells and metallic frames. This can be prevented by properly sealing using gaskets of low diffusivity.

Delamination is the loss of adhesion between front glass and cells, between cells and encapsulating polymer. It also affects the back sheet and back encapsulating polymer. When the delamination occurs, it makes the module more susceptible to water ingress and affects the light from reaching the cells (Munoz et al., 2011). It usually causes power loss and corrosion of metallic parts. This usually occurs more in hot and humid climatic conditions.

Discoloration of solar PV modules is usually the degradation of encapsulating material, which changes color to brown or yellow. It affects the transmittance and hence degrades the short circuit current ( $I_{sc}$ ) of the solar PV module. This can cause the short circuit

current to degrade from 6% to 8% for partially discoloration solar PV module surface, and 10% to 13% for complete discoloration (Realini, et al., 2003.).

The main cause of discolouration of encapsulating materials of solar PV modules is ultraviolet rays combined with water under higher temperatures of 50°C (Oreški et al., 2009). Breakages and cracks of solar PV modules are caused by poor handling during packing, transportation, installation, and maintenance (Wohlgemuth & Kurtz, 2011). This may cause electrical shock and increase the probability of water ingress. It may also cause other forms of degradation such as delamination, corrosion, and discolouration which in turn degrades the power output of the solar PV module.

Silva et al. (2019) studied 48 solar photovoltaic modules under real operational conditions installed at the Research Laboratory of Power Electronics at the Federal University of Uberl in Brazil and found that discolouration of the encapsulating materials, snail tracks and hotspots at snail track sites as the main modes of degradation. They also observed that the visually observable damaged modules produced low power performances. They proposed more work to be done using the I-V curve tracer, thermo images, visual inspections, and the electroluminescence test of broken cells.

Quansah et al. (2020) carried out the degradation and longevity of solar photovoltaic modules analysis of recent field studies in Ghana whose landmass fall within latitude 5°N-11°N and longitude 3°W-1°E. They used PV module installations owned by government agencies, educational institutions, or private homes. The results indicate annual module performance degradation rates (peak power) of 0.8%-7%, 0.55%-2.07%, and 1.1%-2.4% for modules located in various climate sub categorizations. Visually observable defects were recorded in the humid climate with front-of-module and cell metallization being dominant.

Silvestre et al. (2016) studied the degradation of thin-film photovoltaic modules technologies, namely; hydrogenated single-junction amorphous silicon (a-Si: H), Hydrogenerated amorphous silicon/ hydrogenated microcrystalline silicon hetero-junction (a-Si:μc-Si:H), CIS, and Cadmium telluride (CdTe). The modules were deployed in Leganes, Spain, (Lat.: 40°19' N, long.:3°46' W, Altitude: 666 m). The PV modules were mounted on an equator-facing open rack with a tilt angle of 30°. The study results indicated that the CdTe module had the highest degradation rate of -4.45%/year, while the CIS module appeared to be most stable with a degradation rate of -1.04%/year. Understanding degradation would therefore be important for selecting the best PV technology for each specific climatic condition and for improving reliability and performance.

Atsu et al. (2020) studied the degradation rates and reliability of solar PV modules operated for twelve years under tropical climatic conditions in sub-Saharan Africa. The results indicated power output loss of between 34.5% (2.88% per year) to 41.4% (3.45% per year). The study further indicated Ethylene vinyl acetate (EVA) browning, cell interconnects, ribbons browning, and corrosion of solder bonds are visually observed degradation modes. This study also agreed with (Quansah et al., 2020) on the degradation of cell metallization which was done in different climatic regions. However, the power loss of the two studies was different and therefore the study of each climatic region should be done separately because performance in one region cannot always be replicated in other regions.

Malvoni et al. (2020) investigated the degradation rates of a 1MWp utility-scale photovoltaic system located in the tropical semi-arid climatic after 50 months of outdoor exposure. The study used various methods, which include the linear least-



square regression (LLS), the classical sessional decomposition (CSD), the Holt-Winters seasonal model (HW), and Seasonal and trend decomposition using Loess (STL). The results indicated degradation rates of 0.27% per year (LLS), 0.32% per year (CSD), 0.5% per year (HW) and 0.27% per year (STL). They found a difference when computing degradation rates by using different methods, which is associated with different climatic conditions and various periods. They proposed a standardized procedure to compare the degradation rates of various PV systems. This can be done by conducting various studies and selecting the methodology with the least errors.

Table 2.4 show a summary of some of the reported studies on performance and degradation of PV modules. Regions in Europe, America, West Africa, and North Africa have been covered in the open literature. It shows studies which have been conducted in West Africa, South America, North Africa, Asia, and Europe. In addition, it indicates the degradation rates and dominant degradation mechanisms established in those regions. Finally, it indicates the gap identified for future research.

These studies are regionally unbalanced and represent some regions while others remain unrepresented. To the researcher's knowledge, much has not been done (or reported in literature) as far as the studies on PV module degradation rates and mechanism in the East African region are concerned.

This study aims to address this gap by analyzing the degradation mechanisms and degradation rates of PV modules in two climatic conditions of the East African region. Different PV module technologies (amorphous silicon thin-film, monocrystalline and polycrystalline) are evaluated in the study. The study also introduces the concept of the degradation model to estimate the degradation rates of a specific climatic condition.

The model uses the degradation rates trends of the different solar modules deployed in different years in warm semi-arid climatic conditions.

### **2.3.1 Knowledge Gap and Research Questions**

Degradation studies on PV modules had been carried out from different climatic regions in the world. From the literature it is indicated that the degradation mechanism and rates of PV module differ from one region to another. Therefore, a study of degradation mechanism and rates from one region cannot represent all regions as it is region specific depending on the climatic conditions. The studies on the degradation analysis of PV was regionally unbalanced as presented in Tables 2.4. However, there is little information available in literature from Kenyan climatic regions. It was therefore important to assess accurately and precisely the degradation rates and mechanisms of PV modules for the region. This addressed the research and policy question of whether the PV modules deployed in the regions will perform as expected in warranties under climatic conditions of the regions under consideration in this study. Establishing the degradation mechanism and rates of a solar power plant is an essential factor in estimating the actual power generated for the whole lifespan. The understanding of the degradation mechanism of a specific region could therefore help PV module manufacturers, investors, government, and other stakeholders to make the informed decisions on potential economic benefits and viability of their installations.

**Table 2.4:** Summary of PV Module Studies on the Degradation Analysis

Author	Location	Results	Gap
Quansah et al. (2020)	Ghana	The results indicate annual module performance degradation rates (peak power) of 0.8%-7%, 0.55%-2.07%, and 1.1%-2.4% for modules located in various climate sub categorizations, cell metallization being dominants	The study proposes need to expand the number of modules studied
Silva et al. (2019)	Brazil	The study observed some forms of degradation such as discoloration of the encapsulating material, snail track, hot spots at snail track sites, hot spots randomly in some cells and near the metal frame on Kyocera manufactured modules.	For the proposed future work to include new tests of I-V curves, thermographic images, visual inspections and the electroluminescence test of broken cells.
Mohammed et al. (2016)	Algeria	An annual average power of degradation rate of PV modules of around 1.5%. while discoloration of encapsulant us the predominant modes of degradation.	It can be noted that environmental stressors are the causes of performance losses affecting electrical and financial of PV modules.
Malvoni et al. (2020)	India	Degradation rates of 0.27% per year (LLS), 0.32% per year (CSD), 0.5% per year (HW) and 0.27% per year (STL)	Proposed a standardized procedure to compare the degradation rates of various PV systems
Silvestre et al. (2016)	Spain	The results indicated that CdTe module had highest degradation rate of -4.45% /year while CIS module appeared to be most stable with a degradation rate of -1.04% /year.	Better understanding of degradation would be important for selecting the best PV technology for each specific climatic condition and for improving reliability and performance

#### **2.4 Reliability and Failure Rates of Solar PV Modules**

Nur'Aini et al. (2021) carried out the study on the reliability analysis and maintainability for the design of grid and hybrid solar power plant systems. The study utilized the fault tree analysis (FTA) methodology. The study indicated the reliability of on-grid and hybrid connection as 55.04%, and 98.38% respectively after 1 year of operation. It can be indicated that this study considered all the components being installed in series.

Aghdam & Abapour (2016) conducted a study on reliability and cost analysis of multistage boost converters connected to solar PV panels. The aim of the study was to evaluate the reliability of two-stage and three-stage interleaved converters in a PV generation system considering the cost. The study utilized Markov chain to derive models on reliability and Mean Time To Failure (*MTTF*). The results indicated that simultaneous operation was more reliable than redundant operation. It also indicated that the two-stage converter is more economical than the three-stage, and convectional converter in a life span of 15 years. This study considered the reliability of converters only.

Shahidirad et al. (2018) investigated the solar PV power plant structures based on Monte Carlo reliability and economic analysis. The aim of the study was to develop accurate models for reliability and stability of these plants. The study utilized the Monte Carlo simulations to derive the probability of system failure, partial failure and full generations. The results indicated that by increasing the number of branches the probability of 0% output power is unlikely. It also indicated that more branches reduce energy loss and increases energy generated by the system. It further showed that inverter failure was higher than other components. The study only considered a system

with one, two, and three branches while in practical situations there are plants with more than three branches.

Lillo-Bravo et al. (2018) conducted a study on the impact of energy losses due to failures on photovoltaic plant energy balance. The aim of the study was to estimate the failure rates grouped by components, and the relative impacts of failures on the PV plants energy balance through operation and maintenance follow-up data. A total of 15 PV plants were studied for a period of 15 months. The study indicated that failure rates greatly depend on the size and configuration of solar PV power plants. The study recommended thorough preventive maintenance in the PV modules to detect the different kinds of failure for a longer period of time.

Singh & Fernandez (2015) evaluated reliability of a solar PV system with and without battery storage. The aim of the study was to develop a model for solar PV systems considering variable behavior of solar resources and the outages due to hardware failure of a panel. The study utilized the Monte Carlo Simulation (MCS) in order to establish the loss of load probability (LOLP).

The results indicated a high value of LOLP when comparing between resource variation (radiation only) and hardware status of PV hardware. The reduction of performance of PV hardware can be due to effects of environmental field conditions which lead to degradation of the panels. The effects of environmental conditions can lead to solar PV hardware failure such as delamination of encapsulant material, partial cell disconnects, and hotspot. The study recommended the use of hardware status of solar PV modules for reliability analysis.

Baschel et al. (2018) investigated the impact of component reliability on large scale photovoltaic systems performance. The study utilized a dataset of failure rates of

systems operating from 3 to 5 years. The data was analyzed using Fault Tree analysis (FTA) and Failure Modes and Effects Analysis (FMEA). The results indicated that transformers and inverters issues contributed to 2/3 of the total energy loss of the solar PV system.

Yan et al. (2021) evaluated reliability of PV modules based on the exponential dispersion process. The aim of the study was to investigate the application of an exponential dispersion process in degradation modeling of solar PV modules. Using the stochastic process models the study indicated mean life time ranging from 6.78 years to 7.89 years. It can be indicated that the study investigated reliability, degradation rate, remaining useful life and the warranty time for the PV modules only.

#### **2.4.1 Knowledge Gap and Contributions**

The reliability of each system is an important factor to consider during design, installation, technical and economic evaluation phases. This enables the organization to have proper planning and prepare for any eventuality. The reliability of solar PV systems depend on various components which are connected in series and parallel. The design installation configuration can greatly determine the reliability and failure of the systems.

Majority of the studies in the literature had only considered one component in PV systems reliability analysis but have not considered the whole system. In addition to that majority of the studies had considered systems of PV modules connected in series only and using simulation. This study addresses this gap by collecting the data of the existing PV systems in the region. The data is used to determine the failure and degradation rates which were used to calculate reliabilities of various installation configurations.

The data on the failure rates and reliability of different installations configurations and components could provide useful information to installation designers and other interested organizations to make the right decision in the installation design and improvement of the products.

## **CHAPTER THREE**

### **RESEARCH METHODOLOGY**

#### **3.0 Introduction**

Chapter three is divided into four sections. Section one deals with the technical and economic performance of PV modules tropical savanna climatic conditions. The section starts with the descriptions of the study area, installation configurations, measurement and data collection procedure. In addition, it indicates the parameters and performance indicators used to establish the technical and economic performances of PV modules. Section two presents the materials and methods used to analyze the effects of dust accumulation on the performance of PV modules in tropical savanna climatic conditions. Further, section three covers the study area, equipment and procedure employed to determine the degradation mechanism and rates of PV modules installed in tropical savanna and warm semi-arid climatic conditions. Finally, section four present the methodology used to determine the reliability and failure rates of PV modules in tropical savanna and semi-arid climatic conditions.

#### **3.1 Technical and Economic Performance of PV Modules in Tropical Savanna Region**

##### **3.1.1 Installation Descriptions and Location**

This study was conducted on four solar PV installations (each had an installed capacity of 20 kW), which are located at Strathmore University, Nairobi, Kenya (Latitude:  $1^{\circ}17'$ , Longitude  $36^{\circ}49'$ , and Attitude: 1691.8 m). This site of Strathmore University was classified under tropical savanna climate according to the Köppen climatic map. The meteorological data were collected from the weather station at the Kenya meteorological department, (Wilson airport) which was located within 300 meters from the of Strathmore University's solar PV power plant. According to the data available,



Strathmore University receives an average ambient temperature, relative humidity, and rainfall of 18.8°C, 64.5%, and 49.17mm respectively.

The solar PV systems were installed in June 2014 and comprised 2,400 PV modules with each module having a rated peak power of 250W, which amounted to 600kW and they were arranged into 30 systems. Each system consisted of 80 modules, which were arranged into 2 parallel strings and each string consisted of 40 modules connected in series. Each system is connected to the grid through a 17kW SMA sunny box DC-AC inverter. Each system supplied power to each building and the surplus was supplied to the grid. The PV modules were installed on selected buildings' rooftops and these buildings had different orientations relative to the compass south and had different pitch angles, hence the PV modules were installed at different tilt angles and orientations.

Table 3.1 shows the technical specifications of the 3-phase inverter used. It indicates that the inverter output voltage, power, maximum input dc voltage, current, efficiency, and warranty.

**Table 3.1:** Inverter Specification

<b>Model</b>	<b>Se 17K SolarEdge</b>
Phase	3
Output voltage	415V
Output power	17kW
Maximum input voltage(dc)	1000V
Maximum input current(dc)	23A
Efficiency	98%
Warranty	12 years

**Source:** solaredge.com

Table 3.2 shows the selected technical specifications of the polycrystalline solar PV modules installed. It shows the PV module  $V_{MP}$ ,  $I_{MP}$ ,  $V_{OC}$ ,  $I_{SC}$ , maximum power, and fill factor. In addition, it indicates NOCT, temperature coefficient of power, voltage, and current. Finally, it shows the weight and dimensions of the PV module.

**Table 3.2:** Solar PV Module Specification

<b>Model</b>	<b>JKM250 PP-60</b>
Cell	Polycrystalline
Voltage at maximum power ( $V_{mp}$ ) Volts (V)	30.5
Current at maximum power ( $I_{mp}$ ) (A)	8.2
Open circuit voltage ( $V_{oc}$ ) (V)	37.7
Short circuit current ( $I_{sc}$ ) Amperes(A)	8.85
Maximum power ( $P_{max}$ ) Watts (W)	250
Fill Factor (FF)	0.75
Normal operating cell temperature (NOCT)	45°C
Temperature (Temp.) Coefficient of $I_{sc}$	0.06%/Kelvin (K)
Temp. Coefficient of Power	-0.41%/K
Temp. Coefficient of Voltage	-0.117V/K
Weight	18.5kg
Dimensions (mm)	1,650×992×40

**Source:** Jinko solar module nameplate

The PV power plant consisted of 30 array systems with different installations design depending on the orientations and tilt angles. For the analysis of this study the PV module power plant system was grouped according to the orientation and tilt angles and two scenarios were developed. Using the simple random technique 4 of the 30 arrays were selected randomly.

Figure 3.1 shows the aerial view of the solar PV systems installation in Strathmore University Power Plant in four different buildings. Figure 3.1 (A) shows the PV module

system installed oriented East to West with a tilt angle of  $18^\circ$  and labeled System 1. Figure 3.1 (B) shows the system installed oriented to South with a tilt angle of  $18^\circ$  and labeled System 2. Figure 3.1 (C) shows the system installed oriented to South, with tilt angle of  $11^\circ$  and labeled System 3. Figure 3.1 (D) shows the system installed oriented to East to West with tilt angle of  $18^\circ$  and labeled System 4.

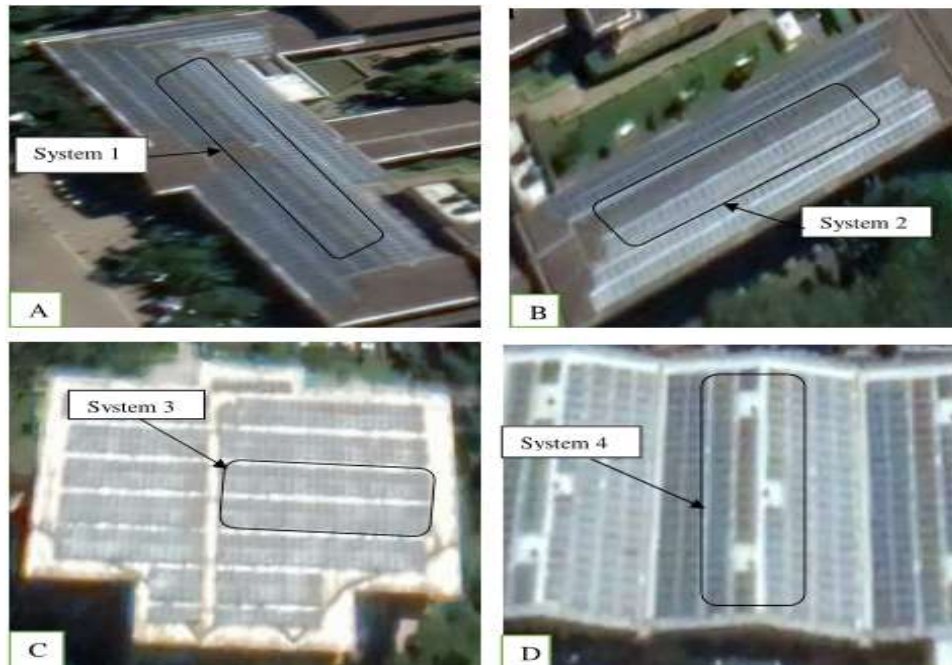


**Figure 3.1:** Aerial View of the PV Power Plant in Strathmore University

The first scenario examined the effects of orientations on the system performance, one oriented East to West, and the second oriented South represented in this study as System One and Four respectively, with same tilt angle. The second scenario examined the effects of different tilt angles on system performance with the same orientations, one tilted at an angle of  $18^\circ$  and the other at  $11^\circ$ , represented in this study as System Two and Three respectively.

Figure 3.2 indicates the schematic diagram of the solar PV power plant. The system shows that solar PV modules connected in series were 40 using a single string. The combination of two strings adding to the total number of modules 80 connected in parallel then connected to a 3-phase inverter. The inverter was designed to supply

energy to the building and the excess supplied to the grids. All the 30 systems had the same configurations as shown in Figure 3.2.

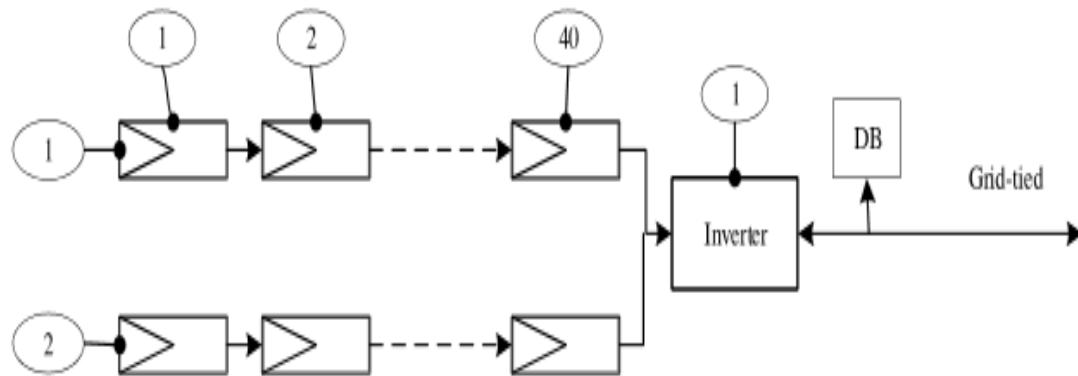


**Figure 3.1:** Schematic Diagram of Solar PV Power Plant

### 3.1.2 Measurement and Data Collection

The data was acquired through the data acquisition module of the inverter and collected by the Solar Edge software monitoring system since June 2014 and is still ongoing. The collected data included voltages, current, power, and energy of each installation system averaged at an interval of 1 hour where daily, weekly, monthly, and yearly collected parameters were derived.

The results presented in this study consisted of the data recorded between January 1<sup>st</sup>, 2015, to December 31<sup>st</sup>, 2019. The environmental parameters of solar irradiance, relative humidity, ambient temperature, and wind speed were used.

### 3.2 Performance Indicators

Conventionally, the performance monitoring of PV modules/ systems in real operating conditions is studied as per guidelines of international standard IEC 61724 provided by the International Electrotechnical Commission (IEC), which is based on the technical indicators. The economic viability of solar PV installation was assessed using a set of financial indicators.

### 3.2.1 Technical Performance Indicators

Technical performance of a solar PV system was evaluated using the performance indicators. The performance indicators were used to compare the performance of any system with similar installations irrespective of the location and installed capacity. The technical performance indicators include total energy generated, systems yield, capacity utilization factor, system efficiency, total energy loss, and performance ratio.

### 3.2.2 Total Energy Generated (kWh)

Total energy output (kWh) of a system is the power output (kW) over a given period of time (hourly, daily, monthly, and annually). In this study it indicates the amount of alternating current (AC) power produced by the system. The total energy output (kWh) was determined in monthly and annually terms as indicated in Equation 3.1 as presented by (Alshare et al., 2020).

$$E_{AC} = \sum_{t=1}^N E_{AC,t} \quad 3.1$$

Where  $E_{AC}$  is the AC energy output at time  $t$ , and  $N$  is the total duration of time.  $N$  represent hours, days, months, and years.

### 3.2.3 System Yields

System yields indicated the actual array operation relative to its rated capacity. System yields parameters defined by IEC are array yield, final yield, and reference yield. According to (Quansah et al., 2017) the most important technical performance indices are final energy output, final yield, and performance ratio. The overall performance of the grid-tied PV system can be evaluated using the three indicators and performance of different solar PV installations can be compared. This study considered ac power only which is commonly used in the region therefore, array yield was not considered.

Final yield ( $Y_F$ ) is the energy output from the inverter (AC energy) normalized by the PV system rated capacity. It indicated the number of hours per day the PV system operated at its rated power in order to produce the same amount of energy as was recorded. Alternatively, this represented the equivalent number of hours a PV system generated the rated power output after DC to AC conversion. It was computed using Equation 3.2 as presented by (Chawla & Tikkiwal, 2021);

$$Y_F = \frac{E_{AC}}{PV_{rated}} \quad 3.2$$

The reference yield ( $Y_R$ ) is the ratio of the total in-plane solar radiation to the array reference irradiance. It is a measure of the theoretical energy available at a specific location over a specified period of time. It represents the number of peak hours per day or the solar radiation (Sharma & Chandel, 2013). The reference yield was calculated using Equation 3.3 as presented by (Chawla & Tikkiwal, 2021) where  $H_T$  is the in-plane radiation and  $G_O$  is the reference irradiance.

$$Y_R = \frac{H_T}{G_O} \quad 3.3$$

where  $H_T$  is the total in-plane radiation and  $G_O$  is the array reference irradiance ( $1\text{kW}/\text{m}^2$ ).

#### **3.2.4 Capacity Utilization Factor (CUF)**

Capacity utilization factor (CUF) is the ratio of AC energy (kWh) generated by the solar PV system over a given period of time (daily, monthly, year) to the energy output (kWh) that would have been generated if the system were operated at full capacity for the entire period. It indicates the number of hours the system will operate at its fully rated capacity per day/month/annual. It can also be defined as the ratio of the actual annual energy output to the amount of energy the system would produce if it works at full rated power for 24 h/day for a year (365 days).

CUF can be used to estimate the power output that the system will generate in a particular climatic condition. It can also be used to estimate the economic viability of a solar PV power plant project. The annual CUF of the solar PV system was calculated using Equation 3.4 as presented by (Malvoni et al., 2020);

$$\text{CUF} = \frac{Y_F}{24 \times 365} = \frac{\text{PR} \times Y_R}{8760} \quad 3.4$$

### 3.2.5 System Efficiency ( $\eta$ )

There are several factors that can affect the efficiency of solar modules. Saleem & Rashid (2016) indicated direction, angle, temperature, shade and load on the PV module as some of the factors. The change of direction and angle of the PV module will cause change in short circuit current hence reduction of power output and efficiency. The increase of temperature will increase current and reduce voltage translating to overall reduction of the power output, hence reduction in efficiency (Saleem & Rashid, 2016).

Therefore, the efficiency of a solar PV module depends on the power input and how much of it will be generated. The power input to the PV module will be determined by the available solar irradiance. Hence, efficiency of the PV module system was given by inverter AC output power ( $P_{AC}(W)$ ) divided by the Total in-plane solar irradiation ( $G_T W/m^2$ ) multiplied by total PV array area ( $A_a m^2$ ) and was determined using Equation 3.5 as presented by (Malvoni et al., 2020):

$$\eta_{\text{system}} = \frac{P_{AC}}{G_T A_a} \times 100\% \quad 3.5$$

### 3.2.6 Total Energy Losses

Total energy losses ( $L_T$ ) of the PV plant (combining PV losses due to irradiance level, array temperature, quality of the module, wiring losses, mismatch and inverter losses,

etc.) represent the difference between the reference yield ( $Y_R$ ), and the Final yield ( $Y_F$ ), and it was calculated using Equation 3.6 as presented by (Adaramola & Vågnes, 2015);

$$L_T = Y_R - Y_F \quad 3.6$$

### 3.2.7 Performance Ratio

Performance ratio is the ratio of final energy yield ( $Y_F$ ) divided by reference yield ( $Y_R$ ). It allows the comparison of different PV systems independent of geographical location, tilt angle, orientation, and power plant capacity. It was determined as indicated by (Chawla & Tikkiwal, 2021) in Equation 3.7:

$$PR = \frac{Y_F}{Y_R} \times 100\% \quad 3.7$$

### 3.3 Economic Analysis

The aim of the economic analysis was to calculate the costs and the benefits of investment and quantify through financial indicators the economic convenience of the PV systems project in the region. The discounted cash flows generated from the investment had been projected for a period of 20 years, equal to the period in which the feed-in tariff (FiT) was granted by the Government of Kenya (GoK). The financial indicators used for economic analysis in this study were net present value (NPV), the discounted payback period (DPP), the Levelized cost of energy (LCOE), and internal rate of return (IRR).

The costs and expenses had been presented in terms of dollars for easier comparison with others studies in the globe. The Strathmore University solar PV power plant project was fully funded through a soft loan at a rate of 4.1% per annum (Da Silva, 2017).



Table 3.3 presents data used in carrying out the economic analysis of this study as provided through discussions and availed documents. The table indicates the lifetime, degradation rate, and discount rate as 20 years, 1.15% annually, and 4.1% annually respectively of the PV module power plant. In addition, it shows the project investment cost, feed-in tariff, and annual operation and maintenance cost.

**Table 3.3:** Design Parameters of the Economic Modeling

Parameters	Data	References
Lifetime, n (years)	20	Ministry of Energy, Kenya (2012)
Degradation rate (DR)	1.15%	(Ngure et al., 2022)
Discount rate (r) (%)	4.1%	Da Silva (2017)
Project investment cost	US \$ 1,200,000	Strathmore University (discussion with the engineer)
A feed-in tariff (FiT)	US\$0.12	Ministry of Energy, Kenya (2012)
Operation and maintenance cost per year ( $O_t$ )	US\$2,500	Strathmore University

### 3.3.1 Levelized Cost of Energy (LCOE)

Levelized cost of energy (LCOE) is the ratio of the total life-cycle cost of the installation to discounted produced energy over its economic life. It was calculated using Equation 3.8 as presented by (Behar et al., 2021):

$$LCOE = \frac{TLCC}{\sum_{t=0}^n E_{AC}} \quad 3.8$$

Where  $E_{AC}$ , is energy produced and TLCC is the total life-cycle cost.

Equation 3.9 was used to determine the energy generated for a period of 20 years using the effects of degradation rates

$$E_{AC,n} = E_{AC,n-1}(1 - D_R) \quad 3.9$$

Where  $D_R$  is degradation rate

Total life-cycle cost (TLCC) represents the costs incurred over the economic life of the solar PV installation, and it was calculated using the initial capital investment and annual operation and maintenance cost ( $O_t$ ).

### 3.3.2 Net Present Value (NPV)

Net present value (NPV) determines the feasibility of the solar PV power plant project. A positive NPV indicates an economically feasible project while a negative NPV indicates an economically infeasible project. It was calculated using Equations 3.10 as indicated by (Behar et al., 2021):

$$NPV = -C_o + \sum_{t=0}^n \frac{C_t}{(1+r)^t} \quad 3.10$$

Where  $C_o$  is initial capital investment,  $C_t$  is the discounted cash flow in the year;  $t$  is the cash flow time;  $n$  is the lifespan of the project  $r$  is the discount rate.

### 3.3.3 Discounted Cash Flow ( $C_t$ )

Discounted annual cash flow was obtained from the difference between the annual inflows and annual outflows using Equation 3.11 as presented by (Tudisca et al., 2013) where  $I_t$  is the discounted annual cash flow and  $O_t$  is the operation and maintenance (O&M) cost.

$$C_t = I_t - O_t \quad 3.11$$

The discounted annual cash flow was calculated using Equation 3.12 as presented by (Tudisca et al., 2013):

$$I_t = E_{AC1} * FiT + E_{AC2} P_U \quad 3.12$$

Where  $E_{AC1}$  is the electrical energy feed to the grid, which was taken as 80%;  $E_{AC2}$  is the electrical energy consumed by the owner and 20% supplied on the national grid according to (Munene, 2019) and discussions held with the engineer in-charge of the

project.  $FiT$  was the feed-in tariff rate taken as US\$0.12/kWh with an annual increment rate of 20% (Energy, 2012), and  $P_U$  was the unit cost of the electrical energy in Kenya which varied from US\$0.18/kWh to US\$0.26/kWh during this period. The energy consumed by the owner was considered as saving.

### 3.3.4 Discounted Payback period (DPP)

Discounted payback period (DPP) is the number of years required so that the cumulative discounted cash flow equals the initial investment. The DPP was established using Equation 3.13 as presented by (Oloya et al., 2021).

$$DPP = \sum_{t=0}^n \frac{C_t}{(1+r)^t} = C_o \quad 3.13$$

### 3.3.5 Internal Rate of Return (IRR)

Internal rate of return (IRR) is the discount rate at which the discounted benefits are equal to the discounted costs. It can also be defined as determining a value of NPV equals zero. An investment is convenient if its IRR is higher than a predetermined reference discount rate. The IRR was determined using Equation 3.14 as illustrated by (Behar et al., 2021).

$$NPV = -C_o + \sum_{t=0}^n \frac{C_t}{(1+r)^t} = 0 \quad 3.14$$

## 3.4 Data Analysis

MATLAB was used during the model development and simulation phase. The model developed used power output as output variable, while wind speed, relative humidity, solar irradiance, and ambient temperature were used as input variables. Previous studies in the open literature and the availability of data informed the decision of the selection of the four weather parameters. The study used correlation of different variables with power output for feature selection. The preprocessing techniques of each individual

simulation were carried out and using coefficient of correlation the best combination of variables was selected. To assess the performance of the developed model Root Mean Squared Error (RMSE), Mean Average Deviation (MAD), Mean Absolute Error (MAE), and Mean Percentage Error (MAPE) were used.

### **3.5 Effects of Dust Accumulation on the Performance of PV Modules**

#### **3.5.1 Study Area**

The study was conducted in Moi University, Main Campus, Kenya (latitude 0.284, Longitude 35.28 and altitude 2,100 m). The Uasin Gishu County is classified as a tropical savanna climatic condition according to the Köppen climatic map. The monthly average ambient temperature, humidity and rainfall of Moi University, Main campus, Eldoret was 16.20 °C, 76.86%, and 60.48mm respectively.

The environmental parameters were collected using the weather station installed in the site. Figure 3.3 presents the test bed of six PV modules and weather station installed on a rooftop of the gate building of Technology Block, School of Engineering, Moi University at a fixed angle tilted at 10° facing south. The tilt angle was chosen based on models developed by (Elhab et al.,2012; Khoo et al., 2014) because the PV modules were installed near the equator. It shows two PV modules each of monocrystalline, polycrystalline, silicon amorphous thin technology and a weather station.

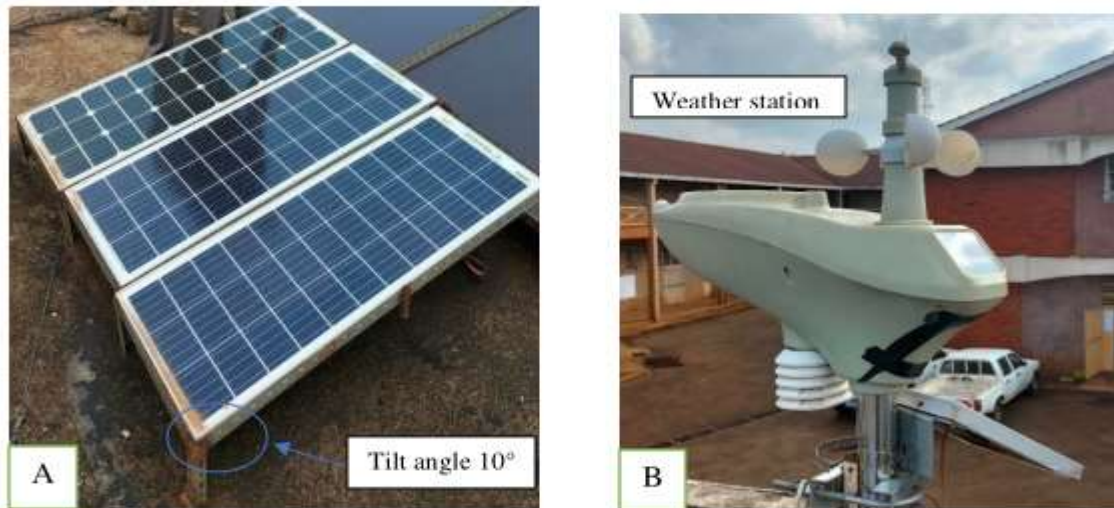


**Figure 3.3:** Test Bed Installation of Solar PV Modules and Weather Station in Moi University

Table 3.4 shows the specification of the weather station parameters. It indicates the measured outdoor parameters as temperature, relative humidity, rain volume, and wind speed with an accuracy of  $\pm 1^\circ\text{C}$ ,  $\pm 5\%$ ,  $\pm 10\%$ , and  $\pm 1\text{m/s}$  respectively. While the indoor environmental parameters measured are temperature, humidity, and air pressure with an accuracy of  $\pm 1^\circ\text{C}$ ,  $\pm 5\%$ , and  $\pm 3\text{hpa}$  respectively.

**Table 3.4:** Weather Station Parameters Specification

Outdoor parameters			
Parameter	Range	Accuracy	Resolution
Temperature	$-40 \sim +60^\circ\text{C}$	$\pm 1^\circ\text{C}$	$0.1^\circ\text{C}$
Humidity	$1\% \sim 99\%$	$\pm 5\%$	
Rain volume	$0 - 9999 \text{ mm}$	$\pm 10\%$	$0.3\text{mm}$
Wind speed	$0-50 \text{ m/s}$	$\pm 1\text{m/s}$	
Wind direction	$0 \text{ to } 359 \text{ degrees}$		
Light	$0-200\text{k Lux}$	$\pm 15\%$	
Indoor parameters			
Temperature	$0^\circ\text{C}--60^\circ\text{C}$	$\pm 1^\circ\text{C}$	$0.1^\circ\text{C}$
Humidity	$10\% \sim 99\%$	$\pm 5\%$	$1\%$
Air Pressure	$300-1100\text{hPa}$	$\pm 3\text{hpa}$	$0.1\text{hPa}$
<b>Transmission distance:</b>	<b>Max. 100</b>	<b>Frequency:</b>	<b>433 MHz</b>
	<b>metre</b>		

**Source:** Catalog

### 3.5.2 Solar Modules Description

Table 3.5 shows the selected technical specifications of the solar PV modules investigated in this study. It indicates three types of PV module models, type of cell technology, power rating and NOCT. In addition, it shows  $I_{SC}$ ,  $V_{OC}$ ,  $V_{MP}$ , and  $I_{MP}$ . Further it indicates weight and dimension of PV modules. The modules specifications were obtained from the nameplates provided at the back of the module provided by the manufacturer.

The solar modules encountered in this study were from three different manufacturers and technologies. The maximum power rating of the modules was 100W per module. The solar PV modules comprised 6 modules of three different technologies namely 2 monocrystalline, 2 polycrystalline, and 2 silicon amorphous thin technologies. The three technologies were selected because they were widely used in the region.

**Table 3.5:** Selected Specifications of the PV Modules at STC Deployed in Moi University

Type	SUNGEN	SUNNYPEX	SOLAR MAX
Model	SG-HN100-GG LV	SUN-100-36P	DG-P 100W
Cell technology	a-Si	p-Si	m-Si
V <sub>mp</sub> (V)	35.0	18	18
I <sub>mp</sub> (A)	2.86	5.55	5.56
V <sub>oc</sub> (V)	46.0	21.24	21.24
I <sub>sc</sub> (A)	3.48	5.90	6.12
P (W)	100	100	100
NOCT	40.28°C	-40/+85°C	
Weight (Kg)	26	9.0	
Dimension (mm)	1400×1100×7	1390×540×30	

**Source:** Manufacturer's nameplate, all technical data at STC

### 3.5.3 Measurements and Instrumentations

Ambient temperature, humidity, and wind speed were collected using an installed weather station. The weather station collected data at an interval of 3 minutes and stored

at a data logger. Two modules were available for each technology. One of the modules of each pair was manually cleaned using water and detergent before taking measurements whereas the other was left to naturally clean and accumulate dust.

The dust accumulation losses could be directly determined by comparing the electrical output of the soiled to the cleaned module as presented by (Fernández-Solas et al., 2022). The dust accumulated from each cleaned module was collected every month for a period of 1 year using a test tube and taken to the Kenyatta University, Civil laboratory for measurement. The soil parameters measured were the diameter and the mass. The mass was measured using an Analytical electronic balance 3 decimal machine. Table 3.6 shows specifications of Analytical electronic balance 3 decimal machine used. It shows the capacity, maximum, and minimum mass as 220g, 220g, and 200gm respectively. In addition, it indicates the readability of 1mg.

**Table 3.6:** Specifications of the Weighing Machine

<b>Model</b>	<b>BSM 220.3 Electronic balance</b>
NO.	A101821008880
Capacity	220g
Maximum	220g
Minimum	200gm
Readability	1mg
e=10d=10gm	

Source: Equipment nameplate

Table 3.7 shows specifications of the Sieves used. It indicates that the first Sieve has aperture opening of 0.075mm and the diameter of 200mm. Second Sieve has aperture opening of 0.075mm and the diameter of 200mm. The diameter was measured using Sieves whose specifications are shown in Table 3.7.

**Table 3.7: Specifications of the Sieves**

<b>Sieve 1</b>	
Model No.	213203/1
Aperture opening	0.075mm
Diameter	200mm
ISO: 3310-1:2106	
<b>Sieve 2</b>	
Model No.	213203/1
Aperture opening	0.075mm
Diameter	200mm
ISO: 3310-1:2106	

The outdoor characterization was based on the collection of 50 I-V curves measured on 3 consecutive clear-sky days within 4 hours after manually cleaning the PV modules for a period of 4 months. The I-V curves and weather parameters were measured using Tri-ka and Trisen. The specification of Tri-ka and Trisen are indicated in Table 3.9 in section 3.6.3. The Tri-ka was set that only I-V curves that had been measured with a  $G_{POA} > 500W/m^2$  and with a variation of  $G_{POA} < 0.5\%$  during the I-V swap were considered. The electrical characteristics parameters ( $P_{MAX}$ ,  $I_{sc}$ , and  $V_{oc}$ ) were then extracted from each of the selected I-V curves and translated to STC using Equations 16 and 17 in Section 3.5.7

#### **3.5.4 Soiling Ratio (SRatio)**

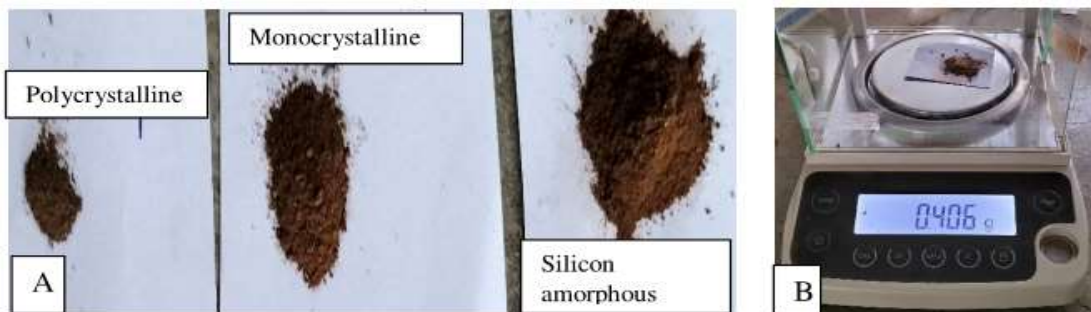
One of the common metrics used to indicate the effects of the dust accumulation on solar PV modules is the soiling ratio (SRatio). The IEC 61724-1 (International Electromechanical Commission, 2017) defined the SRatio as the ratio of the actual electrical output of a PV array under given soiling conditions, to the output expressed if the solar PV module was clean and free of soiling as presented in Equation 3.15. SRatio is a dimensionless parameter that varies between 1 (no soiling condition) to 0.



$$\text{SRatio} = \frac{Z_{\text{soil}}}{Z_{\text{clean}}} \quad 3.15$$

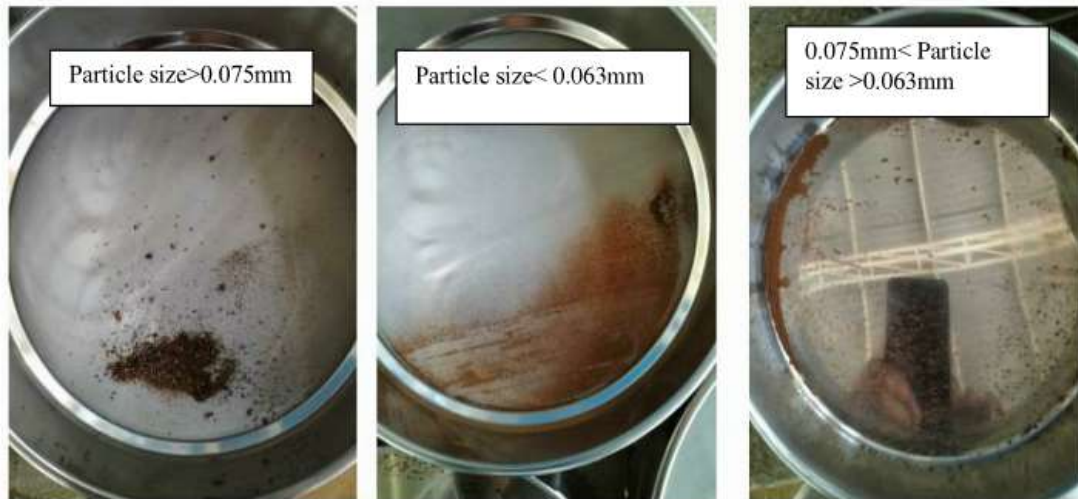
where  $Z_{\text{soil}}$  is the electrical output parameter measured from outdoor soiling conditions and  $Z_{\text{clean}}$  is an electrical output measured under clean condition of the referenced solar PV module.

Figure 3.4 (A) shows the sample of the soil collected while Figure 3.4 (B) indicates the dust being measured. Figure 3.4 (A) shows that more dust accumulated on the silicon amorphous thin technology PV module than polycrystalline and monocrystalline. In addition, it indicates monocrystalline PV module accumulated more dust than polycrystalline PV module. Figure 3.4 (B) indicates dust sample being measured using Analytical balance weighing machine.



**Figure 3.4:**(A) Sample of the Dust Collected (B) Analytical Balance Weighing Machine

Figure 3.5 shows the dust accumulated particles after separation using Sieve 1 and 2 which indicates the proportion of each particle size. The figure indicates that dust accumulation with large diameter and small diameter was dominant in the sample collected.



**Figure 3.5:** Sample of Dust after Separation by Sieve Depending on the Particle Size

The electrical output parameter considered in this study were short-circuit current ( $I_{sc}$ ), current at maximum power point ( $I_{mp}$ ), open circuit voltage ( $V_{OC}$ ), voltage at maximum power point ( $V_{MP}$ ), and maximum power point ( $P_{max}$ ) from both the soiled module or cell and the reference clean module or cell, under the same operating conditions.

### 3.6 Degradation Mechanism and Rates Analysis of PV Modules

#### 3.6.1 Study Area

The study was conducted in Makindu, Makueni County, (latitude -2.28, Longitude 37.82 and altitude 1,070 m) and Strathmore University solar PV power plant, Nairobi, Kenya (Latitude:  $1^{\circ}17'$ , Longitude  $36^{\circ}49'$ , and Attitude: 1691.8 m), in Kenya. Makueni County is classified as a warm semi-arid region while Nairobi County is classified as tropical savanna climatic condition. This classification is based on the Köppen climate map of Kenya as indicated in Figure 3.6.

The monthly average ambient temperature, humidity, and rainfall of Makindu, Makueni County, Kenya were  $22.8^{\circ}\text{C}$ , 62.33% and 47.33mm respectively, ([www.climatic-data.org](http://www.climatic-data.org)). Strathmore University, Nairobi, Kenya on the other hand, records a monthly

average ambient temperature, humidity, and rainfall of 18.8°C, 64.5% and 49.17mm respectively, according to Kenya Meteorological Department data.

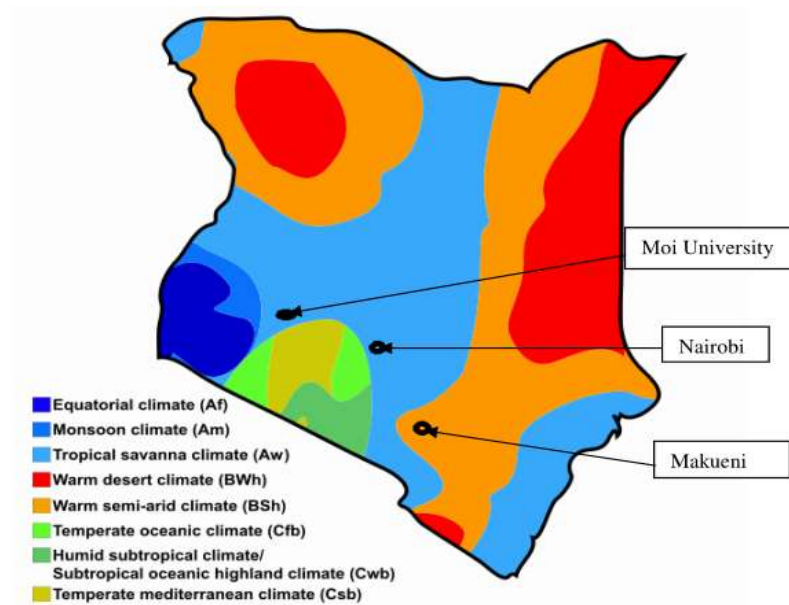


**Figure 3.6:** Köppen Climatic Map of Kenya Indicating the Location of Study Areas  
Licensed; [Creative Commons Attribution-Share Alike 4.0 International](https://creativecommons.org/licenses/by-sa/4.0/)

### 3.6.2 Description of Deployed Solar Modules

Depending on their uses and solar cell technology, the studied modules were classified into four categories, as summarized below:

The first category consisted of 12 polycrystalline units rated at 250W connected in series totaling 1.5 kW and 12 silicon amorphous thin-film technology units rated at 100W connected in series totaling 1.2 kW. These modules were used for pumping the water from boreholes during the day only and were not connected to any energy storage system. The second category consisted of 8 modules. These modules are owned by different clients and used for domestic lighting and powering electronic gadgets. They were connected to charge controllers, inverters, and batteries.

The third category consisted of a sample of 16 polycrystalline modules rated at 250W each in Strathmore University solar PV power plant. They were used for supplying power to the University and the excess supplied to the national grid. These modules were connected to the grid via hybrid inverters. The final category consisted of six monocrystalline nodules. These modules were installed in a test bed at Strathmore University. They were used for study purposes and were not connected to any load. The modules were in open circuit conditions.

Figure 3.7 (A) shows data collection at warm semi-arid climatic conditions using both Tri-ka and Trisen. Tri-ka is directly connected to solar PV module on open circuit mode. Tri-ka collect data on electrical parameters which include open circuit voltage, short circuit current, power output, voltage and current at maximum power point. Trisen is placed at the same tilt angle as PV module and placed adjacent to each other. It communicates with the Tri-ka and collects the data on temperature and irradiation. Figure 3.7 (B) shows the data collection in the warm semi-arid climatic conditions using Infrared camera.

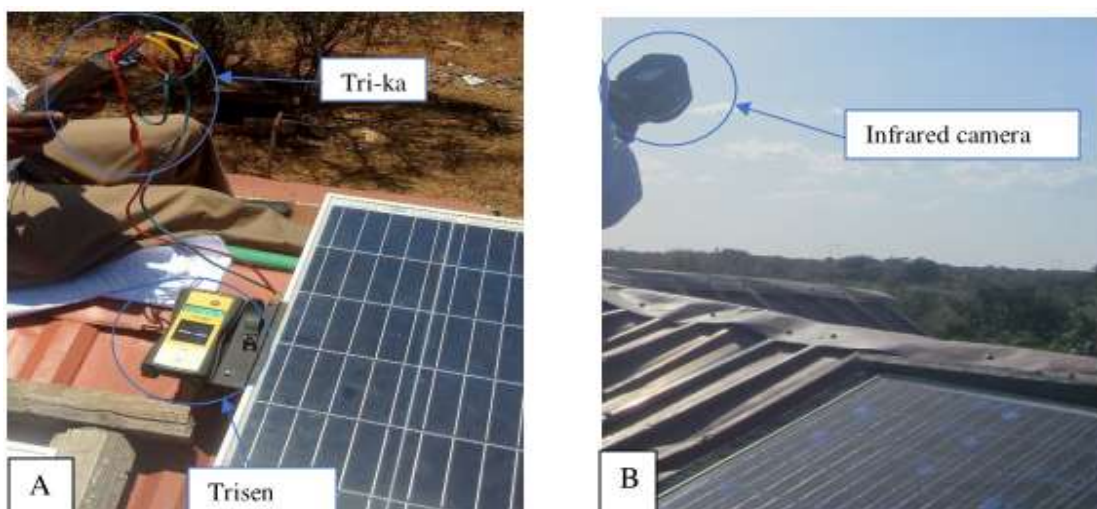


**Figure 3.7:** Data Collection Using Tri-Ka, Trisen and Infrared Camera

Table 3.8 shows selected technical specifications, year of deployment, and the number of solar PV modules installations examined in this study. The solar modules encountered in this study were from different manufacturers and solar cell technology. The panels were deployed at different times from 2013 to 2018. It also indicates the types of cell technology deployed in the regions that were under consideration in this study.

It indicates that 12 PV modules were amorphous silicon thin technology, 35 PV modules were polycrystalline, and 6 PV modules were monocrystalline. In addition, it indicates the use of the PV modules installed in both the climatic conditions which includes domestic use, water pumping, training models and grid-interactive system.

The maximum power rating of the modules ranged from 30W to 250W. The module specifications were obtained from the nameplates provided at the back side of the PV module provided by the manufacturer, while modules' deployment dates were obtained from institutional records, owners and engineers/technicians who designed and installed the systems.

**Table 3.8:** Selected Specifications of the Modules at STC

Type	Grundfos	Jinko	American solar	Chloride Solar	Ubbink	Schott solar	Premier	Barefoot	Ubbink	Davis & Shirtliff
Model	Gf100tf	JKM250PP-60	As-6p30-250w	Asl100-18-P		D-55122	PSS 1230	160-30-0003-1		YL85P-17b2/3
Year	2014	2014	2014	2018	2016	2014	2014	2018	2018	2013
N	12	16	12	2	1	6	1	1	1	1
Cell	Thin	Poly	Poly	Poly	Poly	Mono	Poly	Poly	Poly	Poly
Vmp(V)	70	30.5	30.3	18	18	36.4	17.2	18	18	17.5
Imp(A)	1.43	8.2	8.26	5.56	7.9	5.22	1.75	1.67	4.4	4.86
Voc(V)	96	37.7	38	21.24	21.6	45.2	22	20.88	21.6	22
Isc(A)	1.7	8.85	8.76	5.99	8.8	5.46	1.9	1.74	5.2	5.36
P(W)	100	250	250	100	140	190	30	30	80	85
FF	0.61	0.75	0.75	0.79	0.74	0.77	0.72	0.83	0.71	0.72
$\eta$ (%)	-	15.31	15.4	14.9	17.8	14.5	14.9	14.9	17.8	14.3
USE	P-W	G	P-W	H	H	T	H	H	H	H

Definition of symbols: P-W for water pump, G-Grid tie, H-Sand alone domestic use, T-Training purpose

### 3.6.3 Measurements and Instrumentations

Table 3.9 shows the technical characteristics of the Tri-ka and Trisen, which were used to measure the electrical and weather parameters respectively, in this study. The electrical characteristics, which were measured, were short circuit current ( $I_{SC}$ ), open-circuit voltage ( $V_{OC}$ ), power ( $P$ ), maximum power point current ( $I_{MP}$ ), maximum power point voltage ( $V_{MP}$ ), and fill factor ( $FF$ ).

The Trisen, which accompanied Tri-ka, was used to measure the temperature and irradiance during I-V curve measurements. During the measurement, the Tri-ka and Trisen are kept in constant communication. To reduce the impact of angle-of-incidence effects of irradiance, measurements were conducted between 10 am and 2 pm local time (East African time).

**Table 3.9:** Technical Specifications of Tri-Ka and Trisen

Specification	Tri-ka	Trisen
Voltage measuring range	1.0-1000V (<math>\pm 1\%</math>) ( $U_{OC} > 50$ )	N.A.
Current measuring range	0.1-15.0A (<math>\pm 1\%</math>)	N.A.
Ambient temperature	0-50° c	0-60° c
Admissible relative humidity	<math>< 80\%</math> RH	<math>< 80\%</math> RH
Temperature measuring range	N.A.	0-100° C ( $\pm 3\%$ to a black body)
Irradiation measuring range	N.A.	100-1200W/m <sup>2</sup> $\pm 5\%$

In addition, an infrared camera was used to get the thermal images of the studied modules. The thermal imaging was used to check those defects that cannot be identified using visual inspections. It was used to check the cracks and hotspots in the solar PV modules. Furthermore, the National Renewable Energy Laboratory (NREL) tool was used as a guide to collect data on the visual inspection. The visual data collected

includes burn marks, bubbles, cracks, delamination, wire connection, connectors, junction box, frames, water ingress, discoloration, and snail trails. It took approximately 15 to 20 minutes to conduct a full visual inspection for a single module.

### 3.6.4 Normalization of the Data

The electrical data measured using the I-V curve tracer was under field environmental conditions. Therefore, the data requirements were to be translated into standard test conditions (temperature 25° C, irradiation at 1000W/m<sup>2</sup>, and 1.5 air mass), which was then used for comparison between the measured data and the standard test conditions data. The actual cell temperature was measured using Trisen.

Figure 3.8 indicates the relationship between measured solar irradiance (W/m<sup>2</sup>) and measured short circuit current,  $I_{sc}(A)$ . It indicates a linear relationship. The regression equation on the graph indicates a good positive coefficient of correlation  $R^2=0.9531$  between measured irradiance and measured short circuit current. Therefore, when translating measured short-circuit current value into STC, a component to account for different solar irradiance should be taken into consideration as depicted by Equation (1) in this study.

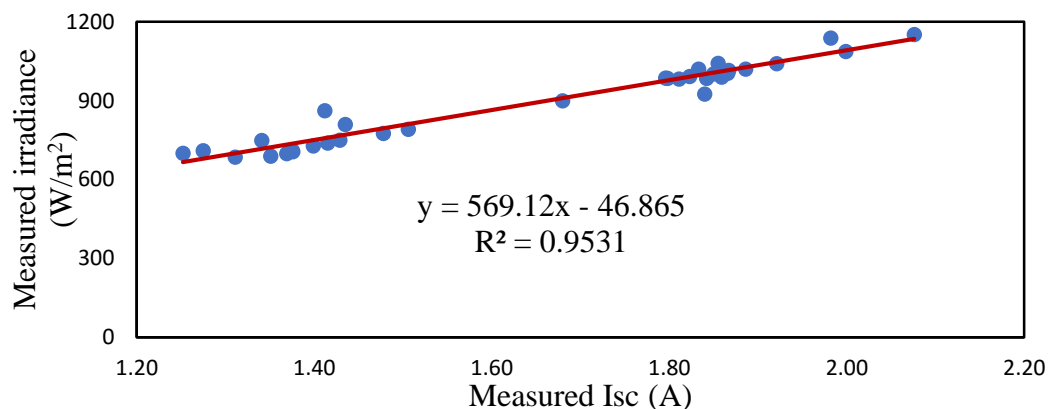


**Figure 3.8:** Measured Solar Irradiance (W/m<sup>2</sup>) Versus Measured Isc (A).



It was noted that measured current is directly proportional to measured irradiance. Therefore, the translation of the current into STC equivalent considering the effects of irradiance can be obtained using Equation 3.16 as presented by (Kahoul et al., 2014).

$$I_{SC} = I_M \left( \frac{G_{STC}}{G_M} \right) (1 + \alpha(T_C - 25)) \quad 3.16$$

where  $I_{SC}$  is the translated current value (A),  $I_M$  is the measured current value (A),  $G_M$  is the measured irradiance ( $W/m^2$ ) value,  $\alpha$ , is the current temperature coefficient ( $/^{\circ}C$ ),  $T_C$  is the measured cell temperature ( $^{\circ}C$ ) and  $G_{STC}$  is the irradiation at standard test conditions (STC).

Figure 3.9 indicates the relationship between measured solar irradiance ( $W/m^2$ ) and open circuit voltage. The figure indicates that when the solar irradiance decreases the open circuit voltage increases. When translating the open-circuit voltage into STC value therefore, a ratio of measured irradiance divided by irradiance at STC should be included in the Equation (17).

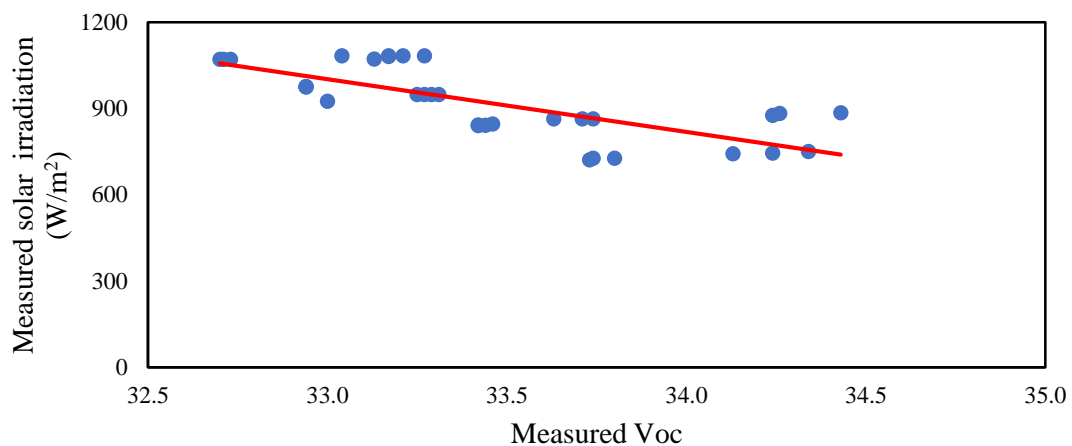


**Figure 3.9:** Measured Solar Irradiance ( $W/m^2$ ) Versus Measured Voc (V)

The translation of the measured voltage into the STC equivalent was done using Equation 3.17 as shown by (Afonso et al., 2015). This study modified the equation to indicate the effect of irradiance as shown in Figure 11.

$$V_{OC} = V_{OCM} \left[ \beta \times \frac{G_M}{G_{STC}} \times (T_c - 25) \right] \quad 3.17$$

where  $V_{OC}$  was the translated voltage to STC and  $V_{OCM}$  was the measured voltage at field environmental conditions (volts) and  $\beta$ , was the voltage temperature coefficient.

The maximum power ( $P_{MAX}$ ) used was calculated using Equation 3.18 as presented by (Afonso et al., 2015):

$$P_{MAX2} = (I_{sc} \times V_{oc} \times FF) (W) \quad 3.18$$

Where FF is the Fill Factor and W is the watts.

The efficiency of solar PV panels indicated the rate at which received power was converted into useful power. The solar PV power conversion efficiency was determined using Equation 3.19 as illustrated;

$$\eta = \frac{P_{max}}{P_{in}} = \frac{I_{mp} \times V_{mp}}{\text{Incident solar radiation} \times \text{Area of solar PV module}} \quad 3.19$$

### 3.6.5 Degradation Analysis

The degradation rates of the solar modules in warm semi-arid and tropical climatic conditions were determined using the following Equations 5, 6, 7, 8, 9, 10, 11, and 12 as presented by (Bouaichi et al., 2017):

The short-circuit current degradation rate was used to determine the rate at which the PV module current, under field environmental conditions, had degraded for the entire period of deployment. The short-circuit current degradation rate was determined using Equation 3.20:

$$DRI_{sc} = \left( 1 - \frac{I_{SC(CAL)}}{I_{SC(STC)}} \right) \times 100 \quad 3.20$$

Where  $DRI_{SC}$  was the short circuit degradation rate,  $I_{SC(CAL)}$  was the translated short circuit current  $I_{SC(STC)}$  is the short circuit current at standard test conditions.

The annual short-circuit current degradation rate was used to determine the rate at which the PV module current under field environmental conditions degraded annually.

The short-circuit current degradation rate per year was calculated using Equation 3.21:

$$\% DRI_{scyear} = DRI_{sc} Y \times 100 \quad 3.21$$

where  $DRI_{SCyear}$  was the short circuit current degradation rate per year, and  $Y$  was the number of years of deployment of solar PV modules.

The open-circuit voltage degradation rate was used to determine the rate at which the PV module current, under field environmental conditions, had degraded for the entire period of deployment. The open-circuit voltage degradation rate per year was calculated using Equation 3.22:

$$DRV_{oc} = \left( 1 - \frac{V_{oc(CAL)}}{V_{oc(STC)}} \right) \times 100 \quad 3.22$$

where  $DRV_{OC}$  was the open-circuit voltage degradation rate,  $V_{OC(CAL)}$  was the translated open-circuit voltage, and  $V_{OC(STC)}$  was the open-circuit voltage at standard test conditions. Hence the open-circuit voltage degradation rate per year was determined using Equation 3.23:

$$\% DRV_{ocyear} = DRV_{oc} Y \times 100 \quad 3.23$$

where  $DRV_{OCyear}$  was the open-circuit voltage degradation rate.

The fill factor (FF) degradation rate was used to determine the rate at which the PV module current, under field environmental conditions, had degraded for the entire

period of deployment. The fill factor degradation rate was determined using Equation 3.24:

$$DRFF = \left(1 - \frac{FF_{cal}}{FF_{STC}}\right) \quad 3.24$$

where  $DRFF$  was the fill factor degradation rate,  $FF_{CAL}$  was the translated fill factor and  $FF_{STC}$  was fill factor at standard test conditions and the fill factor degradation rate per year was determined using Equation 3.25:

$$\% DRFF_{year} = DRFFY \times 100 \quad 3.25$$

where  $DRFF$  was the fill factor degradation rate.

The power output degradation rate was used to determine the rate at which the PV module power output, under field environmental conditions, had degraded for the entire period of deployment. The power output degradation rate was determined using Equation 3.26:

$$DRP = \left(1 - \frac{P_{cal}}{P_{STC}}\right) \quad 3.26$$

where  $DRP$  was power degradation rate,  $P_{CAL}$  was the translated power output and  $P_{STC}$  was the reference power at standard test conditions, and the power degradation rate per year was determined using Equation 3.27.

$$\% DRP_{year} = DRPY \quad 3.27$$

where  $DRP$  was the power degradation rate.

### **3.7 Reliability and Failure Rates of PV Modules**

Reliability is the probability that a product performs its intended function without failure under specified conditions for a specified period. It contains three important elements: intended function, specified period of time, and specified conditions Yang (2007). Therefore, this study was conducted to check the reliability of solar PV systems

in 3 climatic conditions of the East African region. The study involved establishing different installation design configuration, failure rates of components, replacement of the components and time taken to replace those components.

### 3.7.1 Study Area

The study was conducted in Makindu, Makueni County, whose location is indicated in section 4.2, Strathmore University solar PV power plant, Nairobi County, whose location is indicated in section 3.2 and Garrissa solar PV power plant, Garrissa County in Kenya. Makueni County is classified as a warm semi-arid region while Nairobi County is classified as tropical savanna climatic condition. Garrissa County is classified as having hot semi-arid climatic conditions. This classification is based on the Köppen climate map of Kenya. Kenya has high insolation rates with an average of 5-7 peak sunshine hours and receives average daily insolation of 4-6 kWh/m<sup>2</sup>.

### 3.7.2 Reliability Analysis

Reliability is the probability of a component performing its functions without failure. The reliability function indicates that a system will perform its function without failure in a given time ( $t$ ). Reliability can be written as a function of time as presented by (Sayed et al., 2019) in Equation 3.28.

$$R(T) = P(T > t) \quad 3.28$$

The cumulative distribution function (CDF), denoted as  $F(t)$ , represents the unreliability of the system. Since the total reliability of the system must be equal to 1. Then the *CDF* can be defined as indicated by (Sayed et al., 2019) in Equation 3.29.

$$F(t) = 1 - R(t) \quad 3.29$$

The probability density function (*PDF*), denoted as  $f(t)$ , indicates the distribution of the failure over the entire time range. The density function can be expressed as indicated by (Sayed et al., 2019) in Equation 3.30 and 3.31.

$$R(t) = \int_t^{\infty} f(t)dt \quad 3.30$$

$$F(t) = \int_{-\infty}^t f(t)dt \quad 3.31$$

The mean time to failure (*MTTF*) for the sub-systems, which indicates the expected life for the sub-system, represents the most common method for specifying reliability of non-repairable items like solar PV modules. It was calculated using Equation 3.32 as presented by (Sayed et al., 2019).

$$MTTF = \int_0^{\infty} t \times f(t)dt = \int_0^{\infty} R(t)dt \quad 3.32$$

The solar PV power plant systems are complex systems which consist of several sub-systems. These subsystems can be connected in series, parallel or combination of series and parallel. In series connection the failure of one subsystem led to the total failure of the system. While in parallel connection the failure of one subsystem may not lead to total failure hence, all the subsystem must fail in order to cause the total failure of the system.

Using Boolean techniques, the reliability performance for a non-repairable system for example solar PV module having  $n$  subsystems connected in series was calculated using Equation 3.33 as applied by (Sayed et al., 2019).

$$R_{\text{sub assembly}} = \prod_{i=1}^n R_i \quad 3.33$$

Where,  $R_i$  is the reliability of the sub-assembly  $i$ . For an exponential distribution, the total assembly reliability becomes Equation 34 as used by (Sayed et al., 2019).

$$R_{\text{subsystem,TOT}} = 1 - e^{-m_i \lambda_i t} \quad 3.34$$

Where,  $m_i$ , was the total number of the sub systems  $i$ , and  $\lambda_i$ , was the failure rate of sub-system  $i$ .

If the system contains  $n$ , modules in series and  $m$ , modules in parallel then reliability was established using Equation 3.35 as presented by (Sayed et al., 2019);

$$R_{\text{array}} = 1 - (1 - e^{-(m \times n \times \lambda \times t)}) \quad 3.35$$

The reliability of batteries  $R_B$ , with failure rate of  $\lambda_B$ , was established using Equation 3.36 as modified from (Sayed et al., 2019);

$$R_B = e^{\lambda_B \times t} \quad 3.36$$

The reliability of charge controller  $R_C$ , with failure rate of  $\lambda_C$ , was established using Equation 3.37 as modified from (Sayed et al., 2019);

$$R_C = e^{\lambda_C \times t} \quad 3.37$$

The reliability of inverter  $R_i$ , with failure rate of  $\lambda_i$ , was established using Equation 3.38, as modified from (Sayed et al., 2019), for the system with central inverter configurations.

$$R_i = e^{\lambda_i \times t} \quad 3.38$$

The reliability of inverter  $R_i$ , with failure rate of  $\lambda_i$ , was established using Equation 3.39, as modified from (Sayed et al., 2019), for the system with string inverter configurations.

$$R_i = 1 - (1 - e^{-(m \times \lambda_i \times t)}) \quad 3.39$$

Where  $m$  was the number of parallel strings.

Hence, the total system reliability for a configuration with central inverter and modules connected in a combination of series-parallel, connected to battery, charge controller

and inverters was determined using Equation 3.40 as modified from (Sayed et al., 2019);

$$R_{SYS} = 1 - (1 - e^{-n \times \lambda_m \times t_m}) \times (e^{-(\lambda_C \times \lambda_B \times \lambda_i) \times t}) \quad 3.40$$

After obtaining the reliability equations of the four different configurations, the probability distribution functions (pdf) of the systems were developed using Equation 3.41.

$$\text{pdf} = f(t) = \frac{\Delta}{\Delta t} R(t) \quad 3.41$$

Finally, the average useful life span *MTTF* of the system was established using Equation 3.42 (Ghosh, 2012).

$$MTTF = \int_0^{\infty} R(t) \Delta t \quad 3.42$$

### 3.7.3 Configurations of Solar-PV Systems Installation Design in this Study

The use of the solar PV generated in the study area was classified into four types. They include domestic use (SDU), pumping water (SPU), grid-interactive (SGT), and solar PV system for electrical power generation to feed the grid (SPG). Four types of installation design configuration systems were therefore identified and their reliability functions developed. It should be indicated that each system consists of all the following components or some of them. The components include a solar PV module, a charge controller, a battery, and an inverter. The two types of system configurations that were encountered were systems with central and string inverter configurations.

### 3.7.4 Configuration of Solar-PV Systems Installation for Domestic Use

The majority of solar PV systems that were identified in Makueni County consisted of the solar PV module either one or two, an inverter, a charge controller, and one battery



system. Where two or three solar PV modules were installed, they were connected in series. Figure 3.10 shows the system configurations for domestic use.

The systems components were connected in series apart from the battery which was designed so that it provides power in the absence of solar. This indicates that the system is designed to operate during the day and for a few hours during the night depending on the size of the battery. It indicates that if the PV module, inverter, and charge controller of one of components fails, the whole system will not function. However, if the battery fails the system can function during the day.

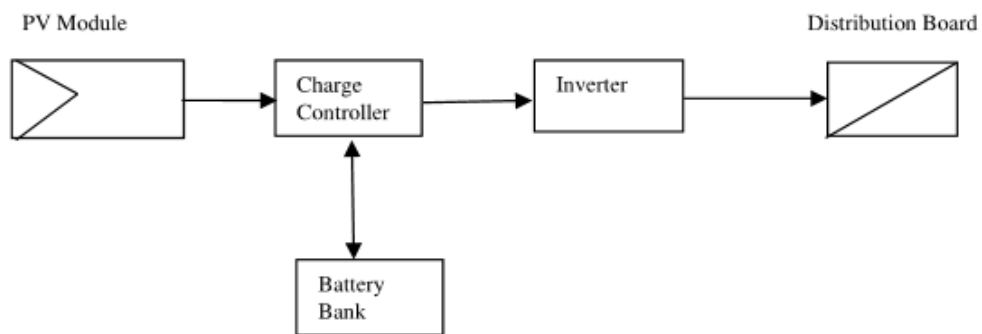


**Figure 3.10:** PV System Design for Domestic Use

The system reliability was taken to follow the exponential distribution as indicated in Equation 3.43 as modified from (Sayed et al., 2019).

$$R_{SYS} = 1 - ((1 - e^{-(\lambda_m \times t)}) \times (e^{-(\lambda_c + \lambda_B + \lambda_i) \times t})) \quad 3.43$$

Where  $R_{SYS}$  was the total system reliability,  $\lambda_m$  was the solar PV module failure rate,  $\lambda_B$  was the battery failure rate,  $\lambda_c$  was the charge controller failure rate,  $\lambda_i$  was the inverter failure rate.

### 3.7.5 Configuration of Solar-PV Pumping Systems

These systems consisted of 12 solar PV modules, inverters, protection systems, and the water pump. Figure 3.11 shows the schematic diagram of the installation configuration systems. It indicates that PV modules are connected in series and connected series to

inverters, protection systems, and the pump. This indicates that the system is designed to operate during the day. It also indicates that if one of the components fails the whole system will not function.

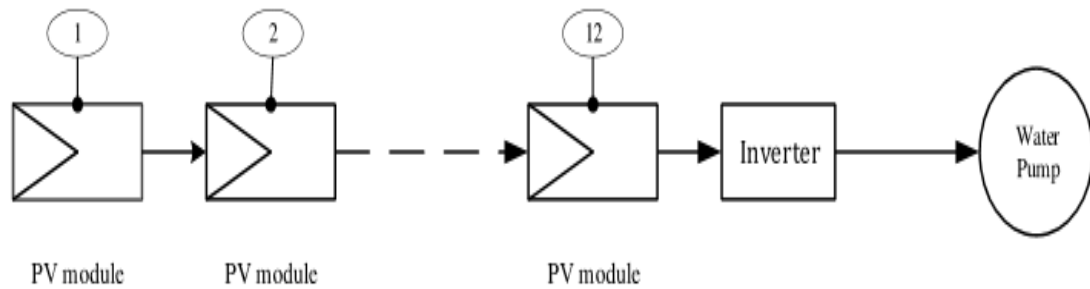


**Figure 3.11:** PV System Design for Water Pumping

The system reliability was established by multiplying the reliability of each component in the system as indicated in Equation 3.44 as modified from (Sayed et al., 2019).

$$R_{SYS} = [1 - ((1 - e^{-(n \times \lambda_m \times t)}) \times e^{-\lambda_i \times t})] \quad 3.44$$

Where  $R_{SYS}$  was the total system reliability,  $\lambda_m$  was the solar PV module failure rate,  $\lambda_i$  was the inverter failure rate,  $n$  was the number of solar PV modules connected in series, and  $t$ , was the time taken for the failure to occur in hours per year.

### 3.7.6 Configuration of Solar-PV Systems Installation for Grid-Interactive

The system consisted of 2,400 polycrystalline PV modules installed in 6 different buildings. 40 solar PV modules were connected in series to form 1 string. 2 strings were connected in parallel and connected to a hybrid inverter through the protection systems and to the grid. Figure 3.12 shows the system configurations.

It shows that if one string failed, the system continued in operation from the other parallel connection. The failure of one of the modules may not lead to the total failure of the system. However, the failure of any other components that were a hybrid inverter or protection system may lead to total failure of the system.

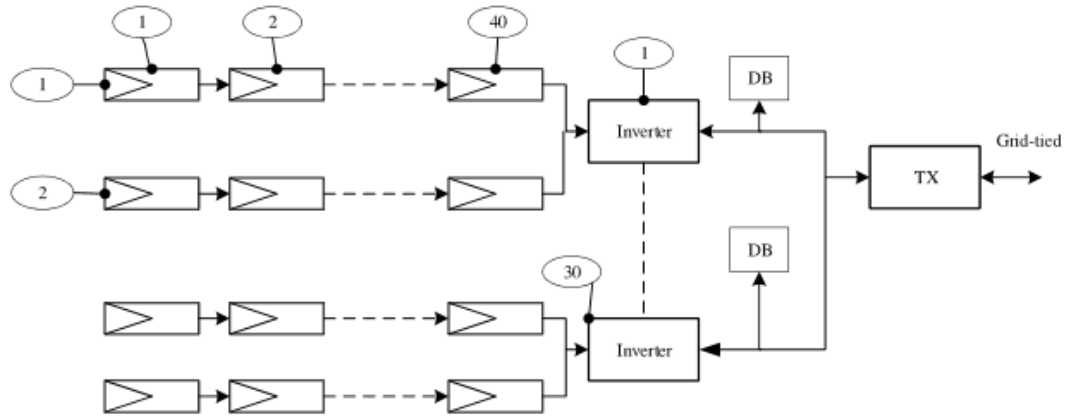


**Figure 3.12:** PV System Design for Grid Interactive

The sub-system reliability was established by applying Equation 3.45 as modified from (Sayed et al., 2019).

$$R_{SUB-SYS} = 1 - ((1 - e^{-(n \times \lambda_m \times t)}) \times (e^{-\lambda_i \times t})) \quad 3.45$$

Where  $R_{SUB-SYS}$  was the sub-system reliability,  $\lambda_m$  was the solar PV module failure rate,  $\lambda_i$  was the inverter failure rate,  $n$  was the number of solar PV modules connected in series, and  $t$ , was the time taken for the failure to occur in hours per year.

The total reliability of the system becomes as presented by Equation 3.46. Where  $K$  is the number of parallel sub-systems as modified from (Sayed et al., 2019).

$$R_{SYS} = 1 - [1 - R_{SUB-SYS}]^K \quad 3.46$$

### 3.7.7 Configuration of Solar-PV Systems Installation for Power Generation

The system consisted of 206,272 polycrystalline PV modules rated 265W, 1172 inverters rated 42kW, 33 step-up transformers rated 408V/33kV, 5 services cables, and one 33kV/132kV main step-up transformers which were connected to the grid. 206,272 solar PV modules were divided into 9,376 strings each consisted of 22 series connected solar PV modules. 8 strings were connected in parallel to 1 inverter. An

array of 36 inverters were connected in parallel to one 1 step-up transformer rated 480V/33kV.

Seven (7) transformers were then connected in parallel to 1 service cable which fed the busbar. 1 of service cable was connected to 5 step-up transformers and finally, the main step-up transformer rated 33kV/132kV was connected from the busbar to the grid. Figure 3.13 shows the part of system installation configurations.

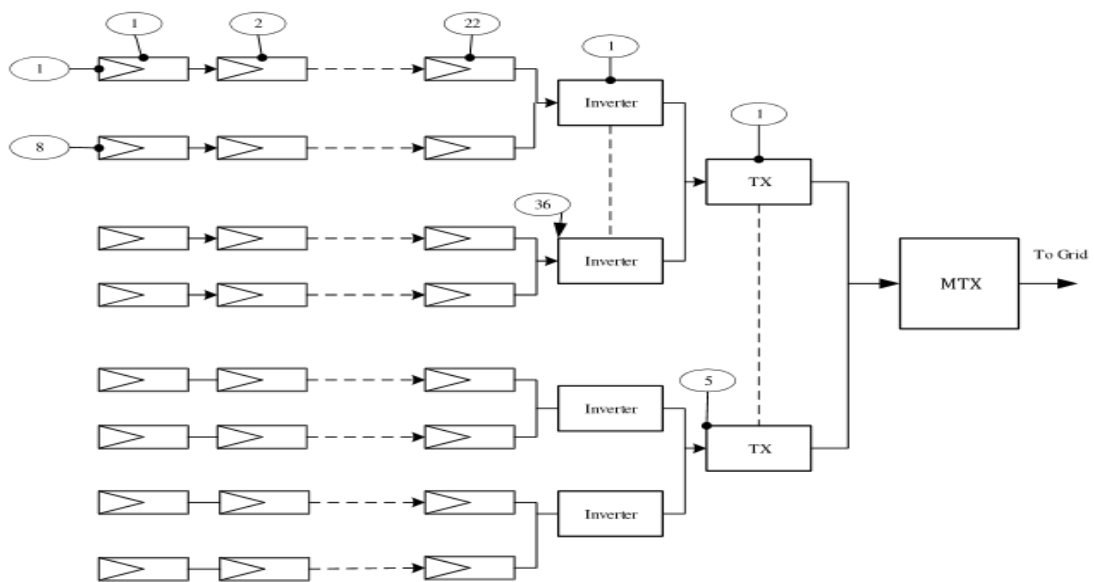


**Figure 3.13:** PV System Design for Electrical Generation to Supply the Grid

The reliability of this system was assumed to take exponential distribution. However, the failure of main transformers leads to total failure of the system. The system reliability was established by calculating series and parallel connections of each component in the system as indicated in Equation 3.47 as modified from (Sayed et al., 2019).

$$R_{SYS} = [1 - ((1 - e^{-n \times \lambda_m \times t})^a)] \times [1 - (1 - e^{-(n \times \lambda_i \times t)})^b] \times [1 - (1 - e^{-(n \times \lambda_{TX} \times t)})^c] \times [1 - (1 - e^{-(n \times \lambda_S \times t)})^d] \times e^{\lambda_{MT} \times t} \quad 3.47$$

Where  $R_{SYS}$  was the total system reliability,  $\lambda_m$ , was the solar PV module failure rate,  $\lambda_i$ , was the inverter failure rate,  $\lambda_{TX}$ , was the transformer failure rate,  $\lambda_S$ , was the service cable failure rate,  $\lambda_{MT}$  was the main transformer failure rate and  $t$  was the time taken for the failure to occur.

### **3.8 Failure Rate**

The failure rate was the anticipated number of times the item fails within a certain period. It was a calculated value that provides a measure of reliability for a product. This value was expressed as the failure in time, rate of failures per million hours. For example, if a component has a failure rate of two failures per million hours, it is anticipated that it fails twice in a one-million-hour period (Nur'Aini et al., 2021).

## **CHAPTER 4**

### **RESULTS AND DISCUSSION**

#### **4.0 Introduction**

Results and discussion are covered in chapter Four, Five, Six and Seven. Chapter four discuss the results of the technical and economic performance of PV modules in tropical savanna climatic conditions. In addition, two models have been developed using environmental parameters. Chapter five presents the results and discussion on the effects of dust accumulation on PV modules in tropical savanna climatic conditions. Chapter six covers the degradation mechanism and rates of PV modules installed in tropical savanna and warm semi-arid climatic regions. Finally, chapter seven present the reliability analysis and failure rates of PV modules in tropical and semi-arid climatic conditions.

#### **4.1 Tech-Economic Performance of PV Modules**

The results of technical and economic performances, as well as the model development, are presented in this chapter. The chapter begins with technical analysis, development of the model, economic analysis and conclusions. The workings are attached as appendices (I) to (XXV).

##### **4.1.1 Sub-Objectives**

- To evaluate the technical performance of solar PV systems in tropical savanna climatic conditions of the East African region.
- To develop a model to predict power output of solar PV systems using weather parameters in tropical savanna climatic conditions of the Kenya region.
- To determine the economic viability of solar PV systems in tropical savanna climatic conditions of the East African region.

## 4.2 Technical Performance Analysis

The parameters evaluated in this section include energy output, reference yield, final yield, system efficiency, capacity utilization factor, and performance ratio. Table 4.1 shows the average weather parameters of tropical savanna climatic conditions under consideration in this study. It indicates that lowest average global horizontal irradiance (GHI) was recorded in year 2019 at  $419.93\text{W/m}^2$  and the highest in year 2015 at  $462.35\text{W/m}^2$  with an average of  $439.19\text{W/m}^2$ . In addition, it indicates the annual average ambient temperature of  $20.49^\circ\text{C}$  and annual average wind speed of  $3.10\text{m/s}$ . The working of chapter four is presented in Appendix A to Y.

**Table 4.1:** Weather Parameters

<b>Year</b>	<b>Average Global horizontal irradiance (GHI), (W/m<sup>2</sup>)</b>	<b>Average Ambient temperature (AT), (°C)</b>	<b>Average Relative Humidity, (%)</b>	<b>Average Wind speed (WS), (m/s)</b>
<b>2015</b>	462.35	20.38	63	3.11
<b>2016</b>	430.42	20.29	61	3.54
<b>2017</b>	430.67	20.56	61	3.42
<b>2018</b>	452.60	19.91	68	2.34
<b>2019</b>	419.93	20.87	66	3.09
<b>AVG</b>	<b>439.19</b>	<b>20.40</b>	<b>64</b>	<b>3.10</b>

### 4.2.1 Reference Yield

Table 4.2 shows an annual average of reference yield determined for PV modules system installed in tropical savanna climatic condition. The table indicates that the minimum reference yield was determined in year 2016 as  $5.17\text{ kWh/kW-day}$  and maximum in year 2015 as  $5.54\text{ kWh/kW-day}$  with an annual average of  $5.33\text{ kWh/kW-day}$ .

**Table 4.2:** Reference Yield ( $Y_R$ ), (kWh/kW-day)

<b>Year</b>	<b>2015</b>	<b>2016</b>	<b>2017</b>	<b>2018</b>	<b>2019</b>	<b>AVG</b>
<b><math>Y_R</math>, (kWh/kW-day)</b>	5.54	5.17	5.28	5.43	5.22	<b>5.33</b>

Figure 4.1 presents the average daily annual reference yield ( $Y_R$ ) calculated for the installations' site for a period of 5 years. The results showed an average reference yield which varied from a maximum value of 5.54 kWh/kW-day (in year 2015) to a minimum value of 5.17 kWh/kW-day (in year 2016). The average daily annual reference yield ( $Y_R$ ) was determined as 5.28 kWh/kW-day with inter-annual coefficient of variability of 2.20%.

Similar results of 5.13 kWh/kW-day, 5.6 kWh/kW-day and 5.35 kWh/kW-day were obtained by (Arora et al., 2022; Daher et al., 2018) in northern India and tropical desert respectively. From Tables 2.2 and 2.3 the reference yield of different solar PV systems installed in different regions varied from 5.13 kWh/kW-day to 7.68 kWh/kW-day. Martín-Martínez et al. (2019) indicated the reference yield of 8 different solar plants which varied from 3.62 kWh/kW-day to 10.02 kWh/kW-day. Therefore, the values obtained in this study were within the values reported in other regions. The wide variation of the results indicated by (Martín-Martínez et al., 2019) may be associated with high weather variations in the region, where the study was carried out (winter to summer). However, this is not the case in the tropical regions, which experience a minimum weather variations pattern.



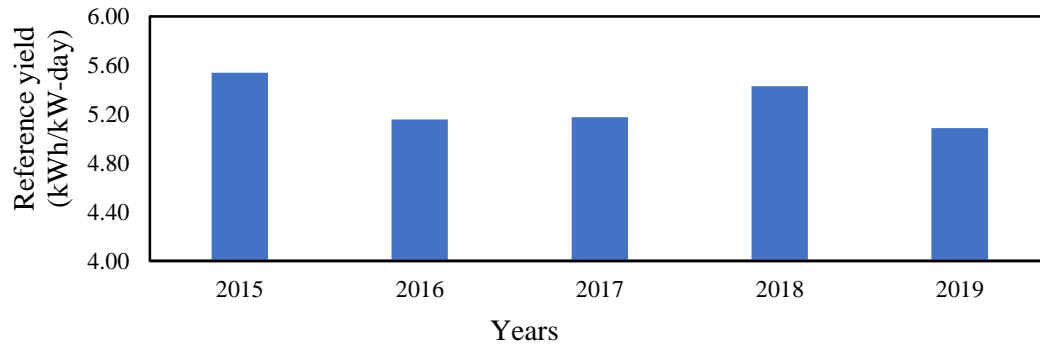


**Figure 4.1:** Reference Yield (kWh/kW-day) in years

#### 4.2.2 Scenario 1: Orientation effect on System 1 (south) and 4 (west-east) directions

Table 4.3 shows the technical performance indicators of System One which was installed at fixed angle of  $18^\circ$  and oriented south for a period of 5 years. The table indicates that the minimum final yield ( $Y_F$ ) was determined in year 2018 as 3.43 kWh/kW-day and a maximum of 3.80 kWh/kW-day in year 2015. An annual average final yield was established as 3.60 kWh/kW-day with a standard deviation of 0.09 and inter-annual coefficient of variability of 2.06%.

**Table 4.3:** System 1 Technical Performance Indicators

Year	YF (kWh/kW-day)	EAC (MWh)	PR, (%)	CUF, (%)	$\eta$ , (%)
<b>2015</b>	3.80	27.68	69	16	9.81
<b>2016</b>	3.44	25.19	67	14	9.67
<b>2017</b>	3.66	26.69	70	15	10.89
<b>2018</b>	3.43	24.94	64	14	9.35
<b>2019</b>	3.68	26.82	72	15	10.74
<b>MEAN</b>	3.60	26.31	69.4	15	10.10
<b><math>\sigma</math></b>	0.09	0.54	2.32	0.005	0.42
<b>COV.</b>	2.63	2.06	3.34	3.05	4.13

In addition, it indicates that System 1 generated an energy output of maximum of 27.68MWh, in the year 2015, and a minimum of 24.94MWh, in the year 2018. The annual average energy output (MWh) generated by system 1 was 26.31MWh with a

standard deviation of 0.54 and inter-annual coefficient of variability of 2.06%. Further, it shows an average performance ratio (PR) with a minimum of 64%, in the year 2018 and a maximum of 75%, in the year 2019. The annual average PR was determined as 69.4%, standard deviation of 2.32, with an inter-annual coefficient of variability of 3.34%. It also indicates an average CUF of system 1 at a maximum value of as 0.16, in the year 2015 and a minimum value of 0.14, in the years 2016 and 2018 .

The annual average CUF of system 1 was determined as 0.15 with standard deviation of 0.005 and an inter-annual coefficient of variability of 3.06%. Finally, it indicates an average system efficiency of system 1 as minimum of 9.35%, in the year 2018 and a maximum of 10.89% in the year 2017. The annual average efficiency of system 1 was established as 10.09% with a standard deviation of 0.43 and an inter-annual coefficient of variability of 4.13%.

Table 4.4 shows the technical performance indicators of System Four which was installed at fixed angle of 18° and oriented East-West for a period of 5 years. The table indicates that the minimum final yield ( $Y_F$ ) was determined in year 2016 as 3.38 kWh/kW-day and a maximum of 3.65 kWh/kW-day in year 2015. An annual average final yield was established as 3.46 kWh/kW-day with a standard deviation of 0.05 and inter-annual coefficient of variability of 1.51%.

In addition, it indicates that System Four generated an energy output of maximum of 26.57MWh, in the year 2015, and a minimum of 24.7MWh, in the year 2016. The annual average energy output (MWh) generated by system Four was 25.23MWh with a standard deviation of 0.38 and inter-annual coefficient of variability of 1.50%. Further, it shows an average performance ratio (PR) with a minimum of 64%, in the year 2018 and a maximum of 70%, in the year 2019. The annual average PR was

determined as 67.20%, standard deviation of 1.30, with an inter-annual coefficient of variability of 1.94%.

It also indicates an average CUF of System Four at a maximum value of as 0.15, in the year 2015 and a minimum value of 0.14, in the other years. The annual average CUF of System Four was determined as 0.145 with standard deviation of 0.002 and an inter-annual coefficient of variability of 1.59%. Finally, it indicates an average system efficiency of System Four as minimum of 9.18%, in the year 2018 and a maximum of 10.47% in the year 2017. The annual average efficiency of System Four was established as 9.78% with a standard deviation of 0.30 and an inter-annual coefficient of variability of 3.05%.

**Table 4.4:** System 4 Technical Performance Indicators

<b>Year</b>	<b>YF (kWh/kW-day)</b>	<b>EAC (MWh)</b>	<b>PR, (%)</b>	<b>CUF, (%)</b>	<b><math>\eta</math>, (%)</b>
<b>2015</b>	3.65	26.57	67	15	9.54
<b>2016</b>	3.38	24.70	66	14	9.57
<b>2017</b>	3.43	25.02	69	14	10.47
<b>2018</b>	3.41	24.83	64	14	9.18
<b>2019</b>	3.44	25.03	70	14	10.15
<b>MEAN</b>	3.46	25.23	67.20	14	9.78
<b><math>\sigma</math></b>	0.05	0.38	1.30	0.002	0.30
<b>COV.</b>	1.51	1.50	1.94	1.59	3.05

Figure 4.2 indicates the comparison of energy output (kWh) generated by the two systems for a period of 5 years from 2015 to 2019. The energy output (kWh) of systems 1 and 4 declined at a rate of 0.72%, per year, and 1.22% per year respectively. The minimum energy output was recorded on year 2016 and 2018. Similar results were obtained by (Oloya et al., 2021) who indicated high energy output in years 2017 and 2019 but low energy output in the year 2018 for a system installed near the equator.

System 1 indicated more energy output performances than System 4 which can be associated with good installation orientation. The high performance in the year 2015 can be associated with modules being newly installed, thus high radiation transmittance due to absence of dust accumulation and other degradation mechanisms, while low performance in 2018 can be associated with high relative humidity experienced during the year. The effects of relative humidity on the power output of solar PV modules have been demonstrated by the model presented in section 4.3 of this study. The lowest performance in 2016 compared to 2015 can be associated with the Light Induced Degradation (LID) which usually affects the module during its initial period of operation.

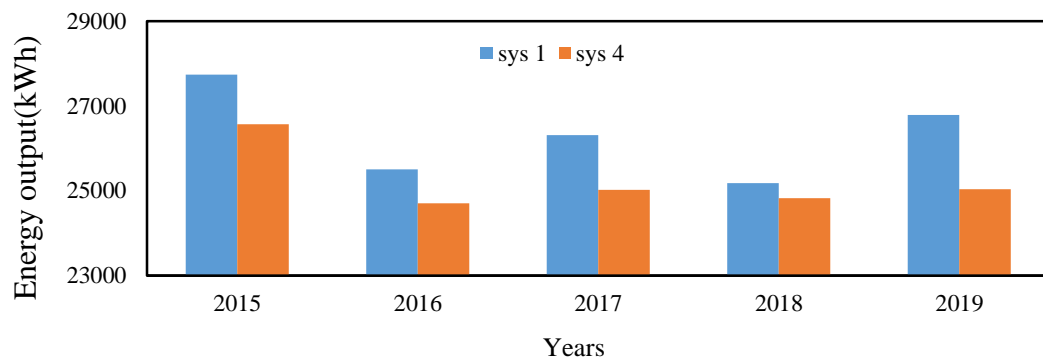


**Figure 4.2:** Energy Output (kWh) for the Two Systems

Figure 4.3 shows the comparison of final yield ( $Y_F$ ) for System 1 and System 4 for a period of 5 years. The  $Y_F$  (kWh/kW-day) of Systems 1 was observed to be better compared System 4. Year 2015 and 2019 recorded higher results than the overall annual average value. This can be associated with low relative humidity and high temperature recorded in year 2019 as indicated Table 4.1. The good performance of PV modules in year 2015 was associated with the environmental and PV modules conditions. Years 2018 and 2016 recorded  $Y_F$  below the annual average value.

Similar results of 3.78 kWh/kW-day, 3.98 kWh/kW-day and 3.99 kWh/kW-day were obtained by (Al-Badi, 2020; Necaibia et al., 2018; S. K. Yadav & Bajpai, 2018). From Tables 2.2 and 2.3 the final yield of different solar PV systems installed in different regions varied from 2.27 kWh/kW-day to 4.70 kWh/kW-day. Martín-Martínez et al. (2019) indicated the final yield of 8 different solar plants which varied from 2.04 kWh/kW-day to 7.92 kWh/kW-day.

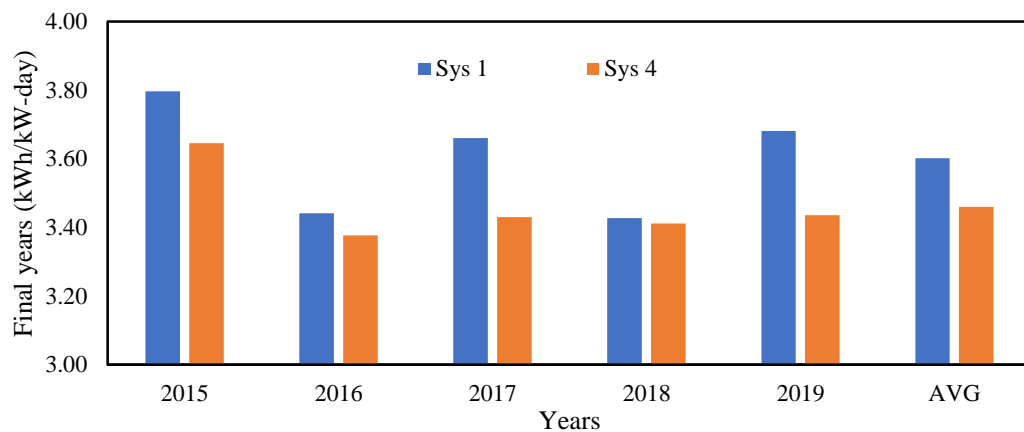


**Figure 4.3:** Final Yields (kWh-kW-day) in Years

Figure 4.4 shows the comparison of system efficiency for the two installations for a period of 5 years. The results indicate that System 1 recorded high average efficiency of 10.10%, compared to System 4 average efficiency of 9.78%. Year 2017 and 2019 recorded highest efficiency while year 2018 had the lowest efficiency. Low efficiency in years 2015 and 2016 with the Light Induced Degradation (LID) which usually affects the module during its initial period of operation.

From Table 2.2 and 2.3 the system efficiency of different solar PV systems installed in different regions varied from 10.3% to 14.77%. Martín-Martínez et al. (2019) indicated the efficiency of 8 different solar plants which varied from 8.40% to 11.98%. Therefore, the findings of this study were similar with the results obtained from other

regions which indicated low operating efficiency of module in real life climatic conditions.

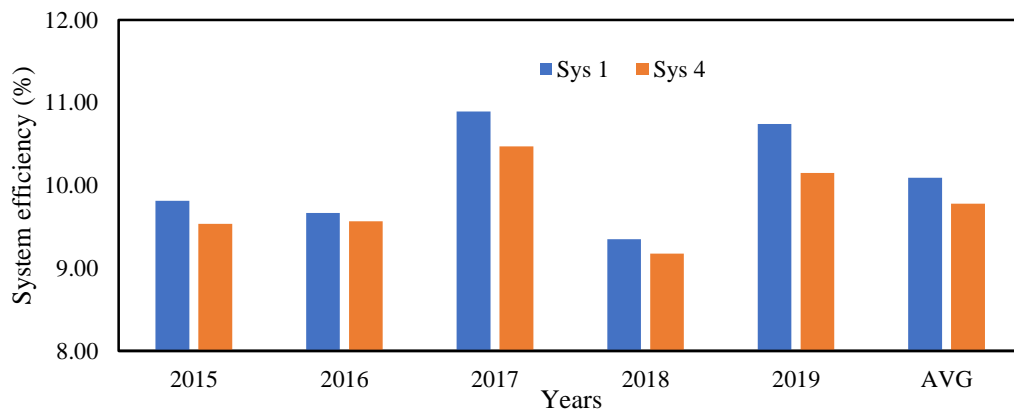


**Figure 4.4: System Efficiency (%) in Years**

Figure 4.5 shows the comparison of CUF for System 1 and System 4 for a period of 5 years. The results indicate an average CUF of System 1 as 15% and System 4 as 14%. CUF of System 1 was high in Years 2015, 2017 and 2019 which was associated with good orientation and environmental conditions. The orientation of the PV modules affected the number of hours the modules were exposed to the sunlight. The CUF of system 4 which had been installed at fixed angle of  $18^\circ$  and oriented east and west was maximum in the year 2015 at 0.15, and a minimum of 0.14, in the subsequent years.

Seme et al. (2019) found that CUF varied from 9.61% to 14.57% with an average of 11.85%. This implies that solar PV systems operated for an average of 2.84 hours per day in Slovenia which was lower than the average of 3.6 hours per day in tropical savanna climatic conditions in Kenya. From Tables 2.2 and 2.3 the CUF of different solar PV systems installed in different regions varied from 7.91% to 23.06%, which are within the range of results reported by previous studies in different locations such as (Shiva Kumar & Sudhakar, 2015), 17.68%; (KhareSaxena et al., 2021), 19.27%; (Sreenath et al., 2022), 16.5% to 18.8%; (Sreenath et al., 2021), 14.25% to 17.09%; and (Saxena et al., 2021), 19% to 21%. Martín-Martínez et al. (2019) calculated the CUF of

8 different solar plants which varied from 7.54% to 33.02%. Therefore, the results obtained in this study are similar to the results obtained from other regions.

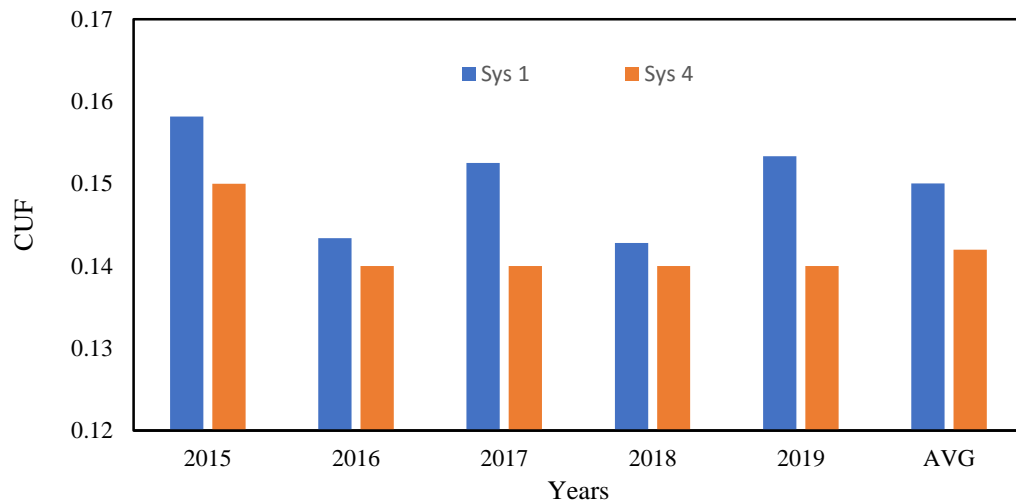


**Figure 4.5:** Capacity Utilization Factor in Years

Figure 4.6 shows the PR for the two installations for a period of 5 years. The results indicate an average PR of the System 1 was better than that of System 4 except year 2018 which recorded the same results. The highest PR was established in years 2017 and 2019 for both Systems. Low PR on year 2018 was associated with high humidity recorded during the year.

From the information presented in Table 2.2 and 2.3, it can be observed that the PR obtained from this study are similar to results reported by studies in different locations of different solar PV systems installed in different regions varied from 66% to 89%. (see for examples: (Shiva Kumar & Sudhakar, 2015), 86.12%; (KhareSaxena et al., 2021), 80.72%; (Sreenath et al., 2022), 75%; (Sreenath et al., 2021), 80%; (Saxena et al., 2021), 70% to 80% and (Martín-Martínez et al., 2019), 59.46% to 85.66%).

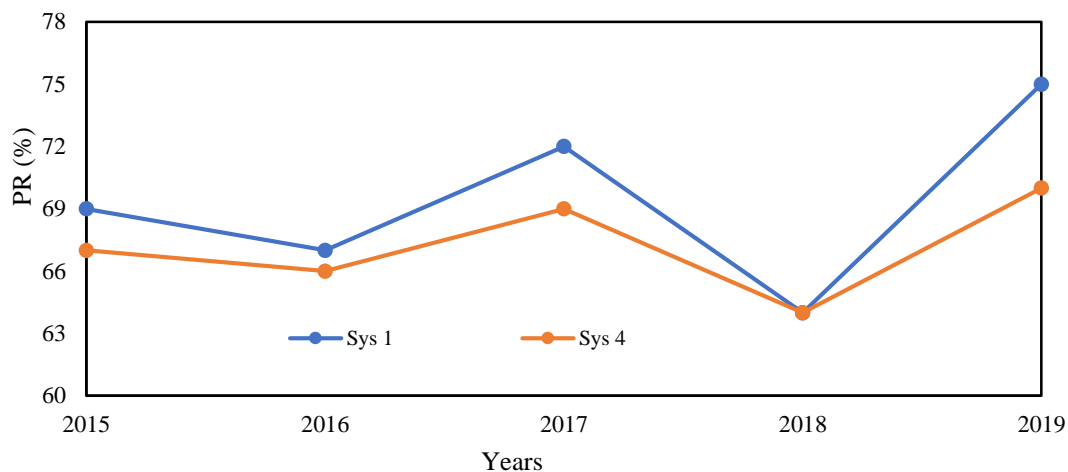


**Figure 4.6:** Trends of Average performance ratio (%)

#### 4.2.3 Scenario 2: Tilt Angle Effect on System 2, (18°), and 3, (11°)

Table 4.5 shows the technical performance indicators of System Two which was installed at tilt fixed angle of 18° and oriented South for a period of 5 years. The table indicates an annual average final yield was established as 3.61 kWh/kW-day with a standard deviation of 0.077 and inter-annual coefficient of variability of 2.13%.

In addition, it indicates the annual average energy output (MWh) generated by system Two was 26.27MWh with a standard deviation of 0.38 and inter-annual coefficient of variability of 2.58%. Further, it shows an average performance ratio (PR) established as 69.4%, standard deviation of 1.64, with an inter-annual coefficient of variability of 2.36%.

It also indicates an annual average CUF of system Two as 0.15 with standard deviation of 0.003 and an inter-annual coefficient of variability of 1.89%. Finally, it indicates the annual average efficiency of system Two was established as 10.22% with a standard deviation of 0.41 and an inter-annual coefficient of variability of 4.01%.



**Table 4.5:** System 2 Technical Performance Indicators

<b>Year</b>	<b>YF (kWh/kW-day)</b>	<b>EAC (MWh)</b>	<b>PR, (%)</b>	<b>CUF, (%)</b>	<b><math>\eta</math>, (%)</b>
<b>2015</b>	3.80	27.74	70	16	9.96
<b>2016</b>	3.48	25.51	68	15	9.87
<b>2017</b>	3.61	26.31	70	15	11
<b>2018</b>	3.46	26.18	65	14	9.38
<b>2019</b>	3.68	26.79	72	15	10.89
<b>MEAN</b>	3.61	26.27	69.4	15	10.22
<b><math>\sigma</math></b>	0.077	0.677	1.64	0.003	0.41
<b>COV.</b>	2.13	2.58	2.36	1.89	4.01

Table 4.6 shows the technical performance indicators of System Three which was installed at tilt fixed angle of  $11^\circ$  and oriented South for a period of 5 years. The table indicates an annual average final yield was established as 3.54kWh/kW-day with a standard deviation of 0.161 and inter-annual coefficient of variability of 4.55%. In addition, it indicates the annual average energy output (MWh) generated by system Three was 25.91MWh with a standard deviation of 1.123 and inter-annual coefficient of variability of 4.34%.

Further, it shows an average performance ratio (PR) established as 68.2%, standard deviation of 2.66, with an inter-annual coefficient of variability of 3.90%. It also indicates an annual average CUF of system Three as 15% with standard deviation of 0.007 and an inter-annual coefficient of variability of 4.97%. Finally, it indicates the annual average efficiency of System Three was established as 9.87% with a standard deviation of 0.48 and an inter-annual coefficient of variability of 4.86%.

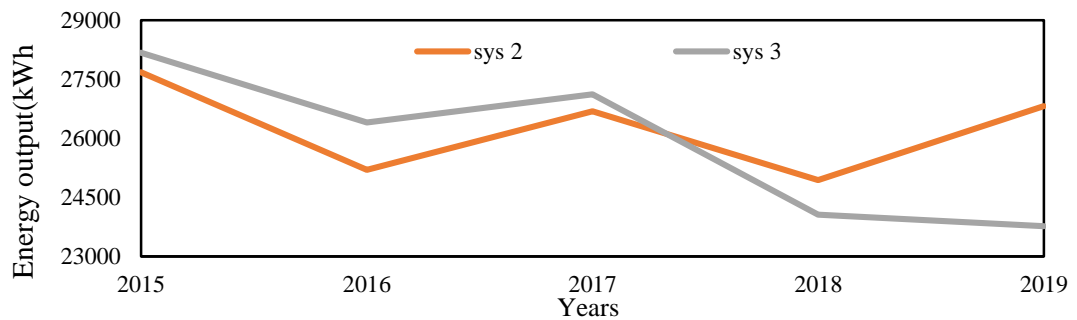
**Table 4.6:** System 3 Technical Performance Indicators

<b>Year</b>	<b>YF</b> <b>(kWh/kW-</b> <b>day)</b>	<b>EAC (MWh)</b>	<b>PR, (%)</b>	<b>CUF, (%)</b>	<b><math>\eta</math>, (%)</b>
<b>2015</b>	3.86	28.17	70	16	10.17
<b>2016</b>	3.61	26.40	70	15	10.22
<b>2017</b>	3.72	27.12	74	16	10.91
<b>2018</b>	3.31	24.06	62	14	8.43
<b>2019</b>	3.20	23.77	65	13	9.61
<b>MEAN</b>	3.54	25.91	68.2	15	9.87
<b><math>\sigma</math></b>	0.161	1.123	2.66	0.007	0.48
<b>COV.</b>	4.55	4.34	3.90	4.97	4.86

Figure 4.7 shows the comparison of energy output (kWh) generated by the two systems for a period of 5 years from the year 2015 to the year 2019. System 2 generated energy output (MWh) of maximum 27.68MWh, in the year 2015 and a minimum of 24.94MWh, in the year 2018. System 3 generated a maximum of 28.17MWh, in the year 2015 and a minimum of 23.32MWh in the year 2019. The energy output (kWh) of systems 2 and 3 declined at an annual average rate of 0.64%, and 1.74% respectively.

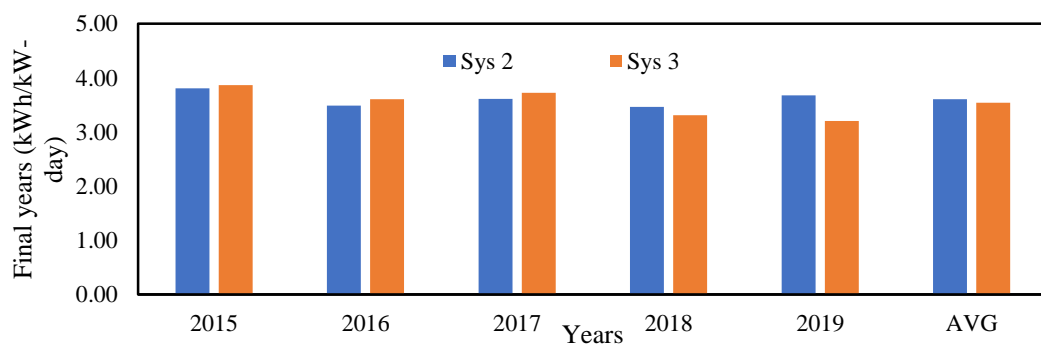
System 3 indicates good performances than system 4 between years 2015 to 2017 which can be associated with lower tilt angle. The site being near the equator low tilt angle will reduce partial shading of the system hence good performance. However, low tilt angle causes dust accumulation in lower side of module with time, hence creating partial shading or hotspots and eventually reduction in energy output as indicated by performance of system 4 in year 2018 and 2019. Regular manual cleaning was therefore required.

This study results shows that as tilt angle was increased the performances also increased as indicated by (Babatunde et al., 2018). However, it can also be indicated that the tilt angle will also be affected by sun altitude angle of the location.



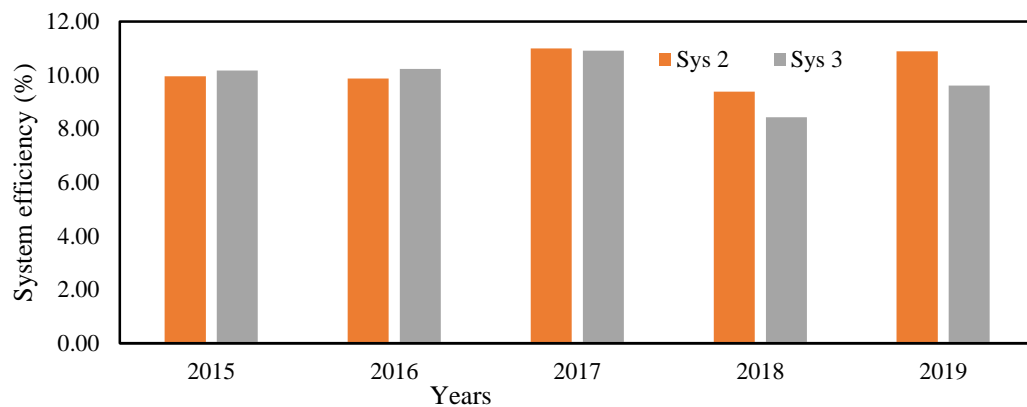
**Figure 4.7:** Trends of Energy Output (kWh) for System 2 and 3

Figure 4.8 shows the average final yield of the system 2 which had been installed at fixed angle of  $18^\circ$  and oriented south, indicated a maximum of 3.80 kWh/kW-day, in the year 2015, and a minimum of 3.46 kWh/kW-day, in the year 2018. The average daily final yield of the system 3 which was installed at fixed angle of  $11^\circ$  and oriented south, was calculated as maximum of 3.86 kWh/kW-day, in the year 2015, and minimum of 3.20 kWh/kW-day, in the year 2019. Ashwini et al. (2016) conducted simulation of fixed tilt angles of  $13^\circ$ ,  $22^\circ$ , and  $30^\circ$ , which indicated the final yield (kWh/kW-day) as 4.24, 3.92, and 4.27 respectively hence the highest tilt angle indicated the high performance.



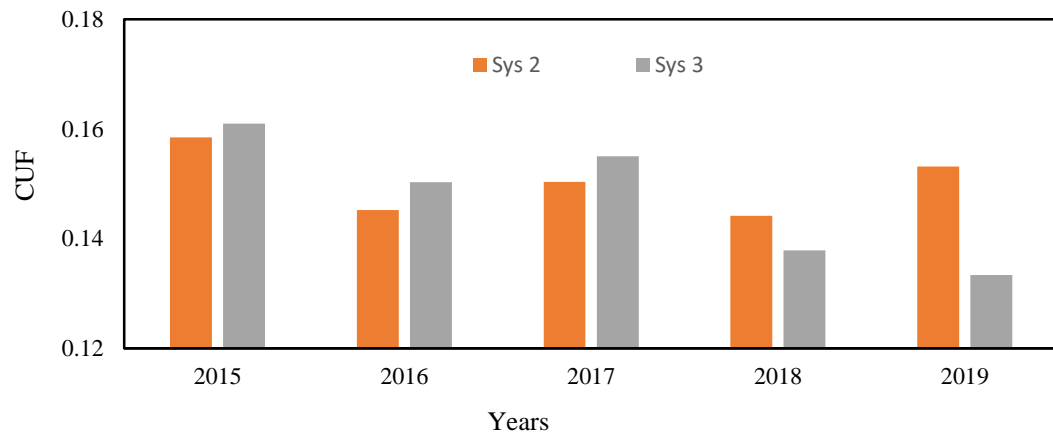
**Figure 4.8:** Final Yields (kWh/kW-day) in Years

Figure 4.9 shows the yearly average system efficiency (%) of the system 2 which had been installed at fixed angle of  $18^\circ$  and oriented south as a maximum of 11%, in the year 2017, and a minimum of 9.38%, in the year 2018. The annual average system efficiency (%) of system 3 which was installed at fixed angle of  $11^\circ$  and oriented south was calculated as a maximum of 10.91%, in the year 2017 and a minimum of 8.43%, in the year 2018.



**Figure 4.9:** System Efficiency (%) in Years

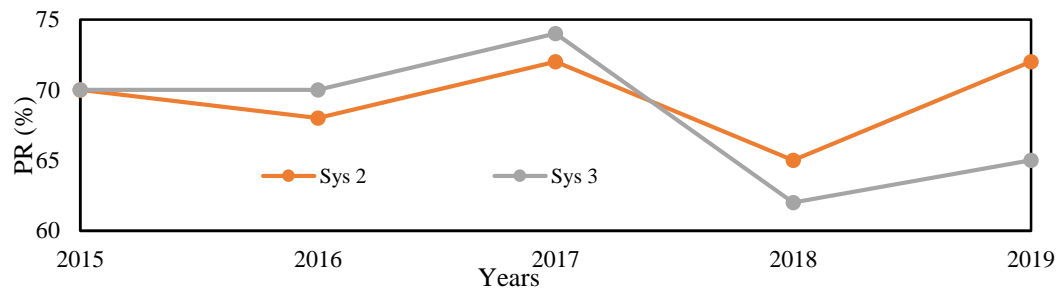
Figure 4.10 shows the yearly average CUF of the system 2 which had been installed at a fixed angle of  $18^\circ$  and oriented south as maximum of 0.16, in the year 2015 and a minimum of 0.14, in the year 2018. The CUF of system 3 which was installed at a fixed angle of  $11^\circ$  and oriented south was calculated as a maximum of 0.16, in the year 2015, and a minimum of 0.13, in the year 2019.



**Figure 4.10:** Capacity Utilization Factor (CUF) in Years

Figure 4.11 shows the average PR of system 2 which had been installed at a fixed angle of  $18^\circ$  and oriented south as a maximum of, 72%, in year 2019 and a minimum of 65%, in the year 2018. The PR of system 3 which was installed at fixed angle of  $11^\circ$  and oriented south was calculated as a maximum of 74%, in the year 2017 and a minimum of 62%, in the year 2018.

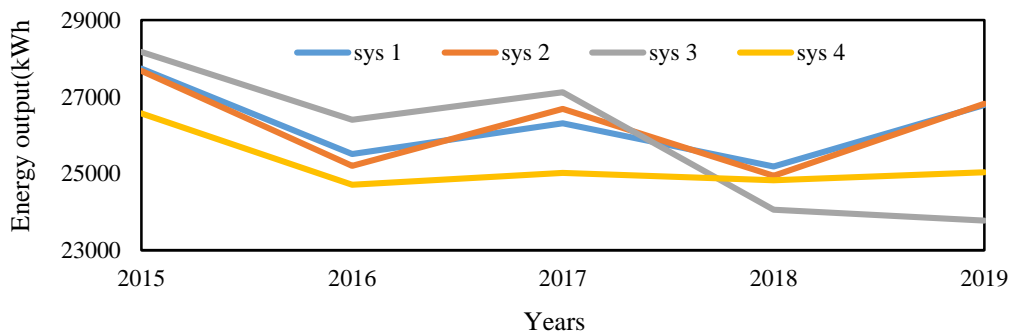
Ashwini et al. (2016) conducted a simulation of fixed tilt angles of  $13^\circ$ ,  $22^\circ$ , and  $30^\circ$ , which indicated the performance ratio (%) as 77.4, 76.83, and 77.4 respectively. Chawla & Tikkiwal (2021) simulated a solar PV system of fixed and variable tilt angles of Poly-Si in Barmer, Jodhpur, Jaisalmer, and Kalan Ghat in arid climatic conditions of India and indicated PR as 81.44%, 80.44%, 81.48% and 81.46% respectively in a fixed tilt angle and 80.44%, 79.17%, 81.43% and 79.41% for a variable tilt angle. This indicated that the results obtained from this study which varied from 62% to 72% were approximately the same as results from other regions.



**Figure 4.11:** Trends of Annual Average Performances Ratio (PR) (%)

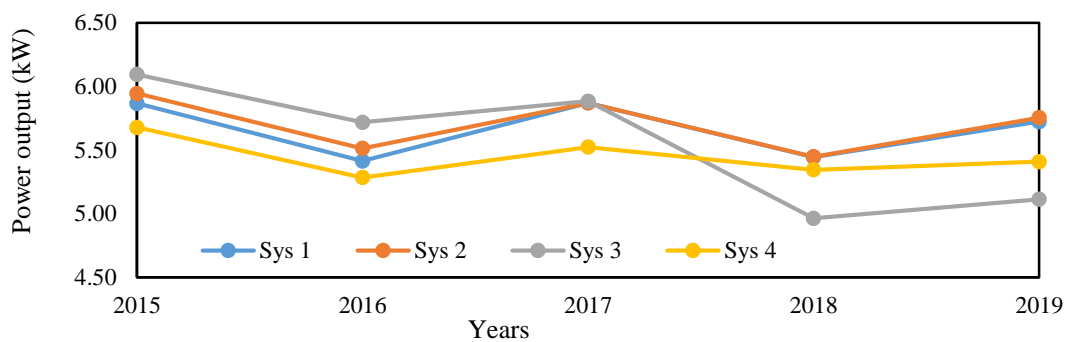
Figure 4.12 shows the overall average energy output (kWh) for the four systems for a period of 5 years from 2015 to 2019. The overall average energy output (kWh) for five years, for all systems was established as 27.5MWh, 25.5MWh, 26.3MWh, 24.8MWh, and 25.6MWh for years 2015, 2016, 2017, 2018, and 2019 respectively. The overall average energy output (kWh) for the four systems for a period of 5 years was established as 25.9MWh.

The average value presented 44.35% of the total energy output expected if the system operated for 8 hours a day for a whole year. The lowest energy output (kWh) was established in the year 2018 which presented 42.47% if the system was operated for 8 hours a day for a whole year. The highest energy output (kWh) was determined in the year 2015 which presented 47.09% if the system was operated for 8 hours a day for a whole year.



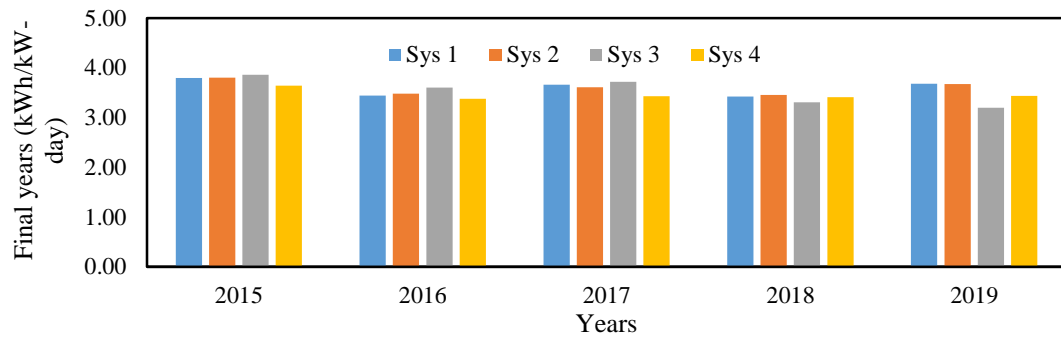
**Figure 4.12:** Annual Average Energy Output (kWh) for the Four Systems

Figure 4.13 shows the overall average power output (kW) for the four systems for a period of 5 years from 2015 to 2019. The annual average power output (kW) for five years, for system 1, 2, 3, and 4 was established as 5.66 kW, 5.71 kW, 5.55 kW, and 5.45kW respectively, from year 2015, to 2019. The overall annual average power output (kW) for the four systems for a period of 5 years was established as 5.59 kW. This indicated that the systems operated at 27.95%, of their full rated capacity of 20 kW.



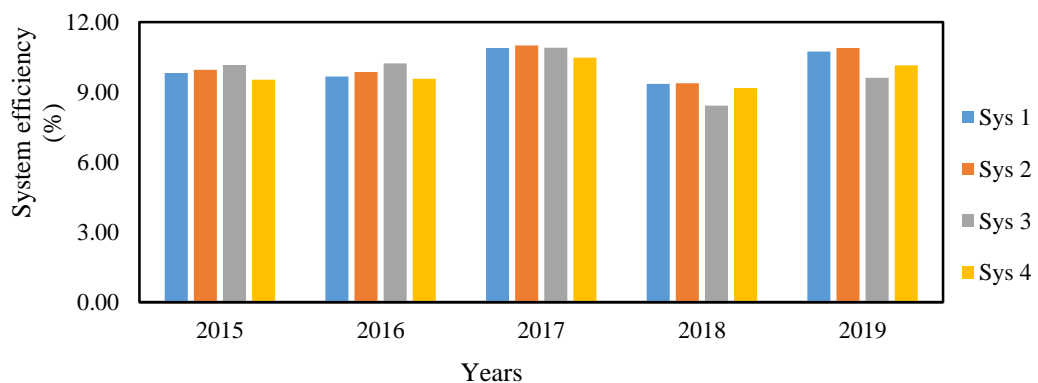
**Figure 4.13:** Trends in Power Output (kW)

Figure 4.14 shows the annual average final yield (kWh/kW-day) for the four systems for a period of 5 years. The annual average final yield (kWh/kW-day) for system 1, 2, 3, and 4 was established as 3.60 kWh/kW – day, 3.61kWh/kW – day, 3.54 kWh/kW – day, and 3.46 kWh/kW – day respectively for a period of five years, from 2015 to 2019. The overall average final yield (kWh/kW-day) for the four systems for a period of 5 years from year 2015 to 2019 was established as 3.55 kWh/kW – day.



**Figure 4.14:** Final Yield (kWh/kW-day) in Years

Figure 4.15 presents the results of annual average efficiency (%) for the four systems for a period of 5 years. The results show annual average efficiency (%), for system 1, 2, 3, and 4 as 10.09%, 10.22%, 9.87%, and 9.78% respectively for a period of five years, from 2015 to 2019. The overall annual average efficiency (%) for the four systems for a period of 5 years from year 2015 to 2019 was established as 10.00%. From Figure 4.15 it can be indicated that all the systems recorded high efficiency in 2017 and low efficiency in 2018.



**Figure 4.15:** System Efficiency (%) in Years

The overall average CUF for all four systems in 5 years was established as 0.15. The CUF of 0.15 implies that the solar PV power plant operated for 3.6 hours per day at its fully rated capacity. The country estimates solar insolation of 4-6 kWh/m<sup>2</sup>/day. The lowest CUF was obtained in the year 2017 in the month of June by systems 1 and 2



which was determined as 0.08. This implies that the system operated for 1.92 hours per day at its fully rated capacity.

The highest CUF was determined as 0.21 in the month of January by system 1 in 2017.

This implied that the system operated for 5.04 hours per day for its fully rated capacity.

From Figure 4.16 it can be indicated that all the systems recorded high CUF in 2015 and low CUF in 2018.

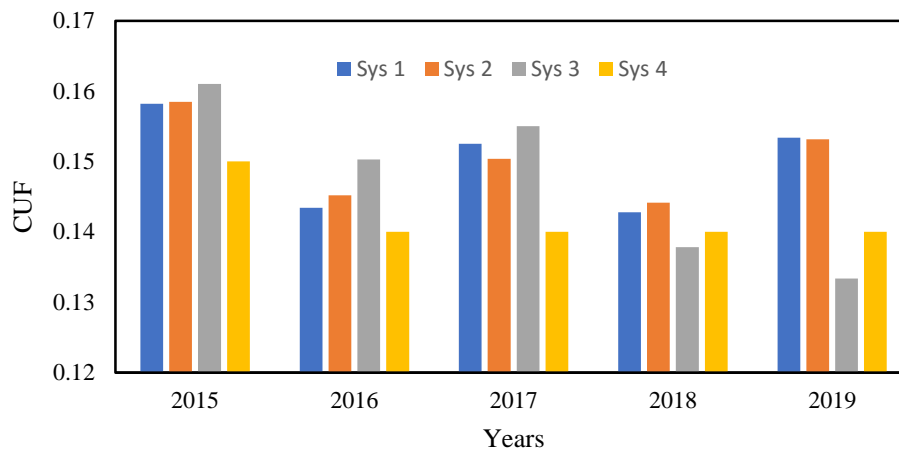


**Figure 4.16:** Capacity Utilization Factor (CUF) in Years

Figure 4.17 presents the results of annual average performance ratio (%) for the four systems for a period of 5 years. The overall average PR for the four systems for a period of 5 years was established as 69%. The lowest PR was determined in the month of March in the year 2018 where systems 1, 2, 3, and 4 were 44%, 44%, 43%, and 43% respectively. The highest was determined in the month of December 2017 by system 4 as 97%. The results indicated that solar PV power plants can generate power output throughout the year in the region.

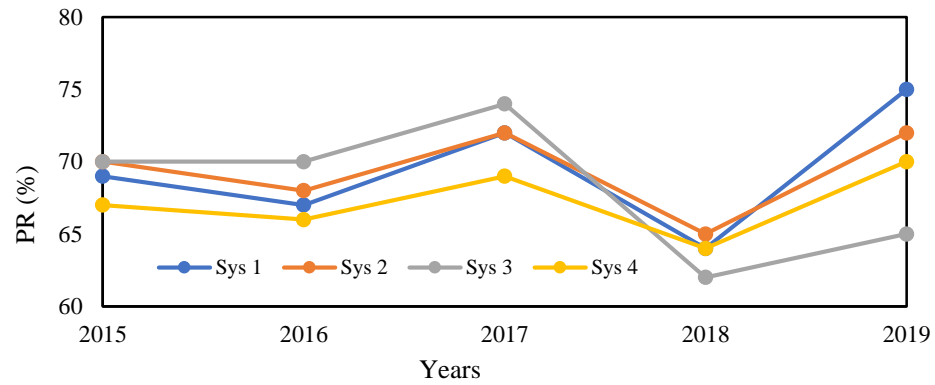


**Figure 4.17:** Trends of Performance Ratio (PR), (%) in Years

The first scenario investigated the effects of orientation against system performance. System 1 which was installed with a tilt angle of  $18^\circ$ , oriented south, indicated an average energy output, final yield, CUF, PR, and efficiency of 26.24MWh, 3.6kWh/kW, 0.15, 69.4% and 10.04%. While system 4 which was installed with a tilt angle of  $18^\circ$  oriented west and east indicated an average energy output, final yield, CUF, PR and efficiency of 25.2MWh, 3.46kWh/kW, 0.14, 67%, and 9.78%. System 1 indicated slightly better performance than system 4 due to the fact that it was better oriented in relation to the solar path.

The second scenario investigated the effects of tilt angle against system performance. The solar PV system 2, which was installed with a tilt angle of  $18^\circ$ , oriented south, indicated an average energy output, final yield, CUF, PR and efficiency of 26.3MWh, 3.61kWh/kW, 0.15, 69% and 10.22%. While the solar PV system 3, which was installed with a tilt angle of  $11^\circ$  oriented south indicated an average energy output, final yield, CUF, PR, and efficiency of 25.8MWh, 3.54kWh/kW, 0.15, 68%, and 9.87%.

The slightly lower results of system 3 compared to system 2 may be associated with lower tilt angle. The low tilt angle will allow accumulation of dust in the lower part of the module. The accumulation of dust will lead to formation of hotspots on module cells

and hence affects the generation of voltage and transmission current in the solar PV module.

### **4.3 Estimation of Power Output (kW) using Environmental Parameters**

The environmental parameters which include solar irradiance ( $\text{W}/\text{m}^2$ ), ambient temperature ( $^{\circ}\text{C}$ ) wind velocity ( $\text{m}/\text{s}$ ), and relative humidity were considered in this study. The use of a power output model to estimate power output can be a useful tool to predict the performance and economic viability of the solar PV power plant during the design, installation, and operation stages. The use of weather parameters as input variables in the prediction of the power output model can be useful due to the availability of the data from various weather stations and satellite data. Most of the models developed (Ayadi et al., 2019; Bhattacharya et al., 2014; Mensah et al., 2019; Njok & Ogbulezie, 2019; Salimi et al., 2020) had used a single parameter as input to predict the power output, efficiency, current, and voltage. Those models that use a single weather parameter as input indicate low coefficient of correlation. Therefore, the predicted value and actual value indicates large discrepancies.

To the best of the researcher's knowledge as indicated by various models in the literature, non-had considered the use of three parameters as input to the model. This study has developed two models using three weather parameters as input and power (watts) as output variable. One of the parameters was held constant depending on the average value of that day, month, or year.

This holding of one of the parameters constants which can be varied depending on the conditions, is useful to estimate power output at given weather conditions. The first model uses solar irradiance, wind speed and ambient temperature as input variables

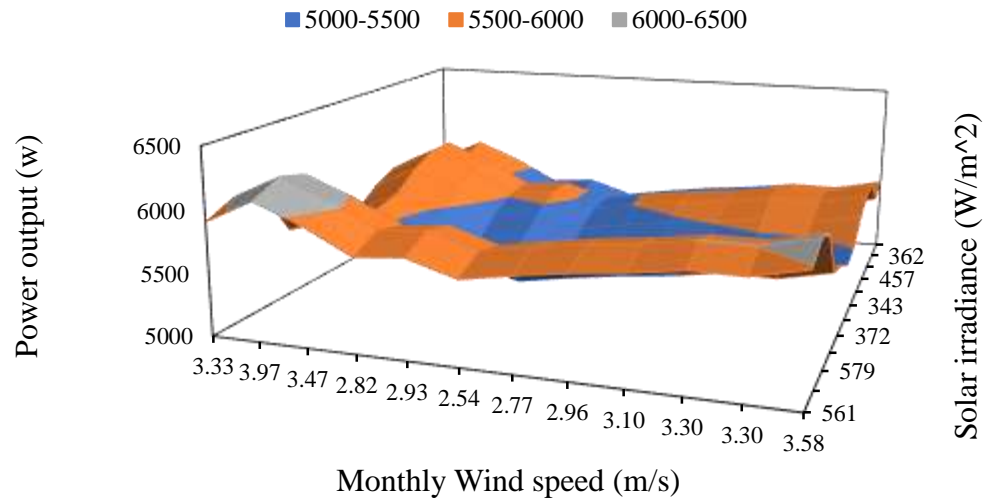
while the second model utilizes solar irradiance, relative humidity, and wind speed as the input to the model.

Figure 4.18 shows the relationship between the monthly average power output (W) of the solar PV power plant against the monthly solar irradiance ( $W/m^2$ ), wind speed (m/s), and holding an ambient temperature average value of  $20.44^\circ C$ . Figure 4.18 present the simulation results of equation 4.1, (with coefficient of correlation  $R^2 = 0.97$ ), developed for the final power output as function of solar irradiance, wind speed, and ambient temperature. The model was developed using MATLAB.

$$P_{ac}(W) = 2.2SI + 305.48WS + 423.72AT - 5001.65 \quad 4.1$$

where  $SI$  is the solar irradiance ( $W/m^2$ ),  $WS$  is the wind speed ( $m/s$ ) and  $AT$  is the ambient temperature ( $^\circ C$ ).

The model indicated the mean average deviation (MAD) of 237.81 between the measured and predicted values. In addition, the mean average percentage error (MAPE) was determined as 4.11%, MAE was established as 21.62, and RMSE was calculated as 286.35.



**Figure 4.18:** Power Output when Ambient Temperature was held at (20.44°C).

The results indicate that as the wind speed and solar irradiance increases the power output increases. It can also be noted that as the solar irradiance increases the wind speed increases and translates to increase of power output. The increase of wind speed provides cooling effects and removes dust on the solar cells. This partly helps to maintain the working temperature range and allows proper absorption of light by solar cells.

This translate to proper functionality and high power output. Ziane et al. (2021) indicated the RMSE values that ranged from 104.67 to 325.21 and MAE ranged from 47.39 to 167.84. In addition, (Gopi et al., 2021) developed different models and reported percentage variation between measured and predicted values as 3.76%,1.31%,7.61%, 7.29%, 9.76% and 12.56%.

Ayadi et al. (2019) developed a model to indicate the relationship between power output and wind speed with  $R^2 = 0.765$  and power output against temperature with  $R^2 = 0.8783$ . Bhattacharya et al. (2014) developed a model between efficiency and wind speed with  $R^2 = 0.4702$  and efficiency and ambient temperature with  $R^2 =$

0.9297. Salimi et al. (2020) developed a model between power output versus solar radiation and ambient temperature with  $R^2 = 0.92$ . Hammad et al. (2018) developed a model between effects of dust, temperature versus efficiency with  $R^2 = 0.877$ .

Mensah et al. (2019) developed a model for energy generated against solar radiation with  $R^2 = 0.8683$ . Njok & Ogbulezie (2019) developed models on current versus panel temperature with  $R^2 = 0.9393$  and efficiency versus ambient temperature with  $R^2 = 0.623$ . From the open literature available data it can be indicated that as the model variables were increased the good fit of the predicted to actual data is achieved. Therefore, by the use of more weather parameters the coefficient obtained from the obtained model indicates good accuracy and validity of the predicted results.

Holding ambient temperature at minimum value of  $18.45^\circ\text{C}$  indicated in Figure 4.19. When the ambient temperature is held at minimum as expected, the power output will be low and correspond to power output of May to August.

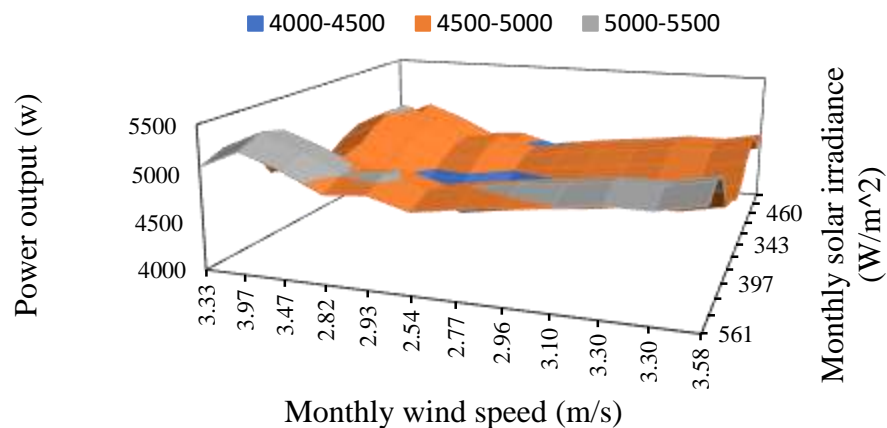


**Figure 4.19:** Power Output (W) when Ambient Temperature was held at ( $18.45^\circ\text{C}$ )

Holding ambient temperature at maximum value of  $22.21^\circ\text{C}$  results are indicated in Figure 4.20. The results indicated that power output of the system increased as the ambient temperature was held at average maximum value of  $22.21^\circ\text{C}$  of the tropical

savanna climatic region. It can be noted that the maximum ambient temperature recorded in the region is within polycrystalline cell operating temperature.

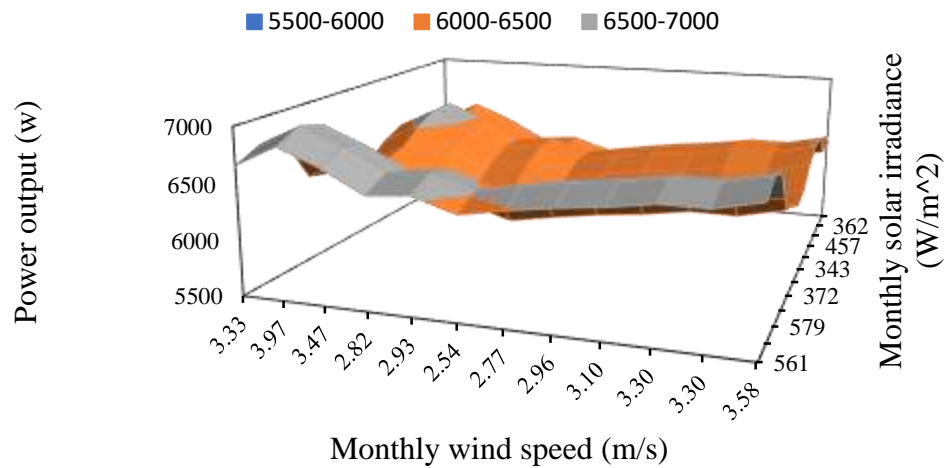


**Figure 4.20:** Power Output (W) when Ambient Temperature held at (22.21°C )

The second consideration was to develop a model using power output (W), solar irradiance ( $\text{W}/\text{m}^2$ ), relative humidity (%), and wind speed (m/s). Figure 4.21 shows the variation of power output with solar irradiance, relative humidity and holding wind speed at an average value of 3.17 m/s. The results were obtained from equation 4.2 with coefficient of correlation of  $R^2=0.91$ . where RH is relative humidity. Ayadi et al. (2019) developed a model of power output against relative humidity with  $R^2 = 0.5809$ . Njok & Ogbulezie (2019) developed two model between current versus relative humidity with  $R^2 = 0.6615$  and efficiency versus relative humidity with  $R^2 = 0.6557$ . The model indicated the mean average deviation (MAD) of 190.33 between the measured and predicted values. In addition, the mean average percentage error (MAPE) was determined as 3.59%, MAE was established as 17.3, and RMSE was calculated as 245.5. Therefore, by the use of more weather parameters the coefficient obtained from the model, indicates good accuracy and validity of the predicted results.

$$P_{ac} = (-2.01)SI + 919.57WS - 109.53RH + 10,543.01 \quad 4.2$$

The results indicate that as relative humidity decrease and solar irradiance increases the power output increases.

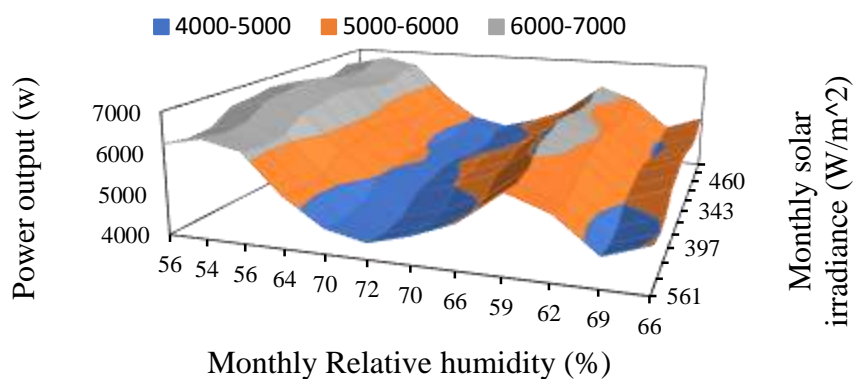


**Figure 4.21:** Power Output (W) when Wind Speed (m/s) held at (3.17 m/s)

It was also noted that when wind speed was held at a minimum annual average value of 2.77m/s the power output decreased as indicated in Figure 4.22. The average annual minimum and maximum are in reference to data obtained from the Kenya meteorological department of tropical savanna region.

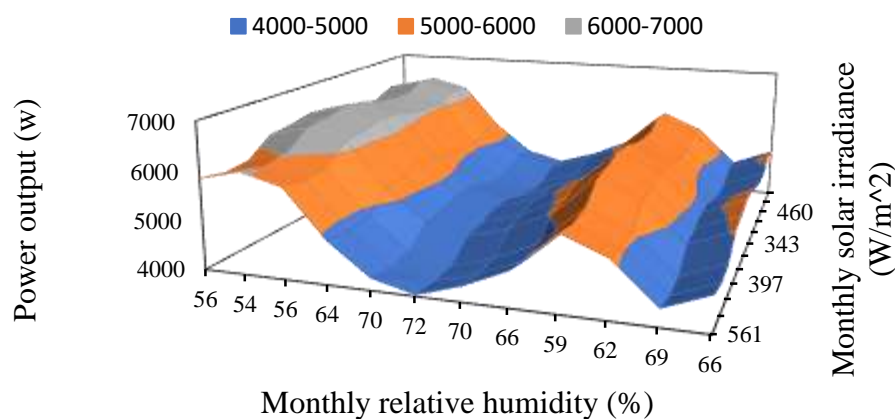


**Figure 4.22:** Power Output (W) when Wind Speed (M/S) was held at (2.77m/S).

When the wind speed was held at a maximum annual average value of 3.97 m/s the power output increases as relative humidity decreases and solar irradiance increases as indicated in Figure 4.23.



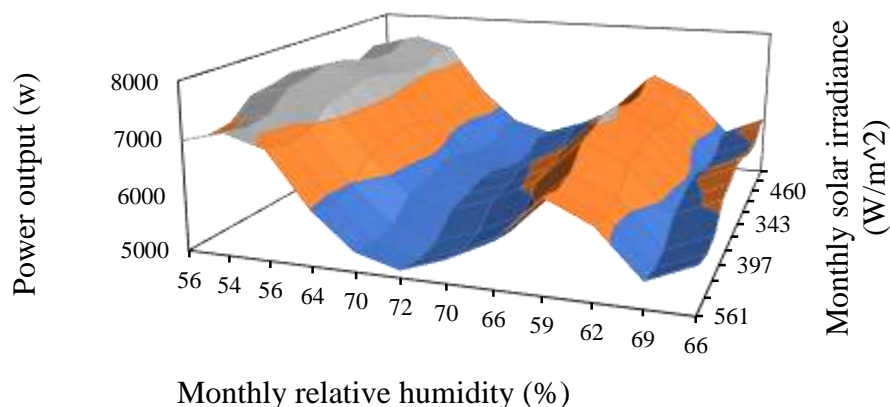


**Figure 4.23:** Power Output (W) when Wind Speed (M/S) was held at (3.97 M/S)

The increase of the relative humidity allows more adhesion of dust particles on the solar panel. This partly adhesion of dust particles blocks the sunlight from reaching the solar cells hence reduction in to power output.

#### 4.4 Economic Analysis

The financial indicators determined for economic analysis in this section are net present value (NPV), the discounted payback period (DPP), the simple payback period (SPP), the Levelized cost of energy (LCOE), and internal rate of return (IRR). The total project cost of 600kW was installed at *US\$1,200,000*. This amount was used to install 30 arrays. All the 30-array had identical parts, such as the number and types of modules, inverters, and other components. Therefore, this study assumed that each array cost was the same hence *US\$40,000* each. The project life span was taken as 20 years according to the FiT policy (Ministry of Energy, 2012). The LCOE of the project was established as *US\$0.1679/kWh* taking the loan repayment period as 7 years.

The financial indicators of the project were calculated as NPV of *US\$14,893*, IRR of 5.93%, DPP of 13 years and SPP of 9 years. Table 4.7 indicates the results of NPV, IRR, DPP and LCOE when the four systems were considered individually. The results indicate that NPV range from *US\$10,901* to *US\$14,468*, DPP ranged between 13 years

to 14 years, IRR ranged from 5.0% to 5.86% and LCOE ranged from *US\$0.1656* to *US\$0.1726*. The working excel sheet for the economic analysis is presented in Appendix (Y) for a period of 20 years.

Other studies have indicated the LCOE values of *US \$0.246 per kWh* by Adaramola (2015), Mensah et al. (2019) indicated a LCOE of *USA\$0.2411* and payback period (DPP) of 14.95 years. Yazdani & Yaghoubi (2021) indicated a LCOE of *US \$0.099/kWh* and DPP of 5.82 years, Alshare et al. (2020) indicated SPP of 4.32 years and IRR of 30.11%, Omar & Mahmoud (2018) indicated DPP (years) and IRR (%) of the three systems as 4.916 years, 4.926 years and 4.958 years and 25.1%, 25.1%, and 24.9%, respectively.

Sharma et al. (2016) indicated a DPP of 5.08 years for a solar photovoltaic System at the administration building. (KhareSaxena et al., 2021), reported a simple payback period of 5.9 years; (Saxena et al., 2021) reported a 5-6 years; and (Sreenath et al., 2021) reported a 7.9 years and LCOE of *US\$0.0102*. The LCOE values determined in this study, which are between *US\$0.1656* and *US\$0.1736*, are relatively lower than values reported by other studies (as indicated above). These values indicated a higher value of LCOE compared to this study which found a LCOE of between *US\$0.1656* and *US\$0.1736*. This may be associated with a high value of capacity utilization factor (CUF) in the region compared to Norway climatic conditions. However, the discounted payback period agrees with other studies of 13 years and 14 years. Table 4.7 shows a summary of the selected financial indicators of the four systems.

**Table 4.7:** Financial Indicators of Solar PV Systems

<b>Systems</b>	<b>NPV (US\$)</b>	<b>DPP (Year)</b>	<b>IRR (%)</b>	<b>LCOE (US\$/kWh)</b>
<b>System 1</b>	14,336	13	5.86	0.1658
<b>System 2</b>	14,468	13	5.23	0.1656
<b>System 3</b>	12,900	13	5.00	0.1687
<b>System 4</b>	10,901	14	5.20	0.1726

#### 4.5 Conclusions and Recommendations

The aim of the study was to examine the technical and economic performance and develop the models of solar PV installations using long-term performance data. This has provided more information for better assessment of solar PV installation in the region. The annual average energy output (kWh), power output (W), reference yields (kWh/kW – day,) final yields (kWh/kW – day), capacity utilization factor (CUF), system efficiency ( $\eta$ ) and PR(%) were established as 26043 kWh, 5594 W, 5.28 kWh/kW – day, 3.60 kWh/kW – day, 0.15, 10% and 68% respectively. The economic indicators of the system were established as LCOE of US\$0.1679/kWh, NPV of US\$14,893, DPP of 13 years, SPP of 9 years and IRR of 5.93%. This study has developed two models to estimate power output (watts) using 3 weather parameters as input variables. The results have indicated a high coefficient of determination ( $R^2$ ) obtained from the models developed which translate to good accuracy and validity of the predicted results. This study has established that when relative humidity increases, the power output of a solar PV system decreases. Increase in wind speed and ambient temperature will affect the power output of solar PV modules positively.

More models need to be developed in order to estimate the power output of solar PV systems which can help in design, installation and operation stages. Furthermore, the

study recommends development of methods to maintain optimum weather parameters operation conditions and the investigation of the effects of climatic change on the performance of solar PV modules. The study established that the solar PV system was more useful in terms of energy savings.

The solar PV module using polycrystalline technology can therefore be used as alternative sources of electrical energy and the project can be economically viable in tropical savanna climatic conditions. The results of this study were based on the cost of the year 2013 to the year 2014 during the design, installations, and commissioning of the project. The study recommends further investigation in order to establish LCOE using the cost reduction trends and effects in the improvement of the efficiency of the solar PV modules technology.

## CHAPTER 5

### 5.1 Effects of Dust Accumulation on the Performance of PV Modules

The results of the effects of dust accumulation of solar PV modules are presented in this chapter. The chapter begins with determination of the size and mass of the contaminants. Then the results of the I-V and power-voltage (P-V) curves are shown on both clean and dirty modules. Finally, the discussion, conclusion and recommendations are presented. The full workings of chapter five are attached as Appendix (XXVI) to (XXX). The objective of this chapter was to determine the effects of dust accumulations on performance of solar PV modules in tropical savanna climatic conditions of the East African region. This objective was achieved through the following sub-objectives as indicated in section 3.4.1.

#### 5.1.1 Sub-Objectives

- To determine the monthly mass of soil deposit on the solar PV module of monocrystalline, polycrystalline and silicon amorphous thin technology.
- To determine the size of soil particles of the dust accumulated on the solar PV modules.
- To establish the effects of dust accumulations on the performance of solar PV modules in tropical savanna climatic conditions of the East African region.

### 5.2 Dust Accumulations

The dust was collected for a period of one year. The annual mass of the collected accumulated dust was established as 1.385g, 0.406g and 0.44g for a-Si, m-Si, and p-Si modules respectively. This translated to monthly average mass of 0.115g, 0.406g and 0.44g for a-Si, m-Si, and p-Si modules respectively. The heavier amount of dust accumulated on the silicon amorphous thin technology solar PV module was due to the

larger surface area of the module as indicated in Table 3.5 compared to the other types of solar PV module investigated.

The average mass of the dust collected was determined as having a diameter greater than 0.075mm as 0.701gm accounting for 42.54%, a diameter less than 0.075mm but greater than 0.063mm as 0.254g accounting for 15.41%, and less than 0.063mm was 0.693gm accounting to 42.05%. This indicated that the type of dust accumulated contained a high percentage of finer soil particles. The smaller diameter of dust particles causes high loss performance solar PV module compared to the large size dust particles. For the same dust type, finer particles have a greater impact than coarse particles (Vidyanandan, 2017).

This can be associated with the greater ability of finer particles to reduce the inter-particle gap between them and hence blocking the light path more than that of large particles. Permanent soiling can easily occur with finer dust particles if humidity condensates and sticks dust to the surface particularly at the bottom of a tilted module. The study was done near the equator hence lesser tilt angle, together with high humidity experienced in the region resulted in dust sticking in the lower part of the solar PV module as shown in Figure 5.1. Regular manual cleaning on the solar PV module is therefore required.

### **5.3 Effects of Dust Accumulation on the Performances of the PV modules**

#### **5.3.1 I-V and P-V curve of the monocrystalline solar PV module**

Table 5.1 indicates the results of the monocrystalline module under the effects of dust accumulation and clean conditions in tropical savanna climatic conditions. Results under dust accumulated conditions were determined as average values of  $I_{SC}$ ,  $I_{MP}$ ,  $V_{MP}$ ,  $V_{OC}$  as 4.38A, 3.99A, 16.56V, and 21.10V respectively. The results under the cleaned

conditions were  $I_{sc}$ ,  $I_{mp}$ ,  $V_{mpp}$ , and  $V_{oc}$  as 5.28A, 4.85A, 16.30V, and 21.33V respectively. Soiling ratio was established for  $I_{SC}$ ,  $I_{MP}$ ,  $V_{MP}$ ,  $V_{OC}$  as 0.17, 0.18, 0.02, and 0.01 respectively. This implies that open-circuit voltage was not affected by the soiling of the module but short circuit current was more affected.

Further it indicates the results under soiled conditions for FF, Pmax, and efficiency as 16.56V, 0.72, 66.01W and 9.6% respectively. Results under clean conditions for FF, Pmax, and efficiency were indicated as 16.30V, 0.70, 78.96W, and 10.5% respectively. The soiling ratio on FF, Pmax, and efficiency was established as 0.03, 0.16 and 0.09.

**Table 5.1:** Effects of Dust Accumulation on the Performance of m-Si PV Module

<b>Parameter measured</b>	<b>Dust accumulated PV module</b>	<b>Cleaned PV module</b>	<b>Soiling ratio</b>
<b><math>I_{sc}</math> (A)</b>	4.38	5.28	0.17
<b><math>I_{MP}</math> (A)</b>	3.99	4.85	0.18
<b><math>V_{MP}</math> (A)</b>	16.30	16.56	0.02
<b><math>V_{oc}</math> (V)</b>	21.10	21.33	0.01
<b>FF (%)</b>	72	70	0.03
<b>P<sub>MAX</sub> (W)</b>	66.01	78.96	0.16
<b><math>\eta</math> (%)</b>	9.6	10.50	0.09

Figure 5.1 shows the I-V curves of the monocrystalline PV module under dust accumulated conditions and clean conditions. The figure indicates insignificant difference between open circuit voltage of clean and dust accumulated PV module. In addition, the figure indicates a significant difference between short circuit current under cleaned and dust accumulated PV module.

This was due to the fact that short circuit current depends on the light intensity. Therefore, the dust scattered the intensity of light reaching the surface of a solar cell

and hence reduction in the number of photons to generate electrons. This was contributed by the size of soil particles as indicated in section 5.2, the area and number of the solar PV cell covered by dust. The area and the number of the solar PV modules cells covered by the dust reduced the area exposed to the light sources.

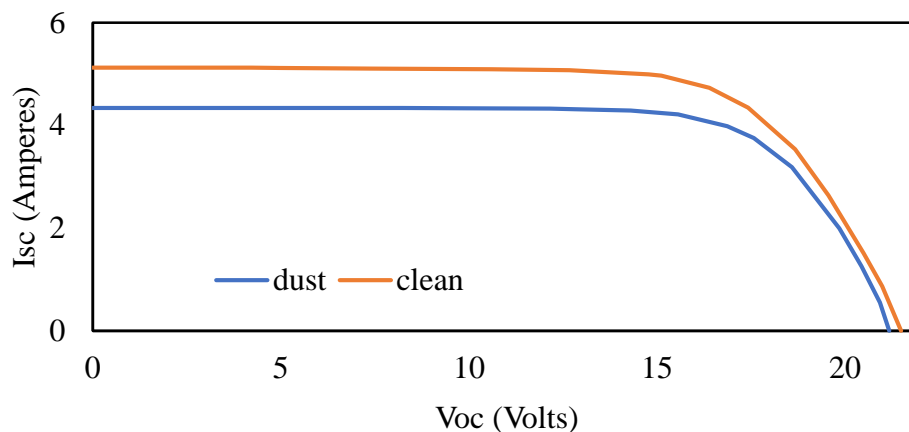


**Figure 5.1:** I-V Curve of Monocrystalline Solar PV Module

Figure 5.2 shows the V-P curves of the monocrystalline PV module under dust accumulated conditions and clean conditions. The figure indicates insignificant difference between open circuit voltage of clean and dust accumulated PV module. In addition, the figure indicates a significant difference between the maximum power point under cleaned and dust accumulated PV module.

It was therefore, soiling ratio of power loss of the monocrystalline PV module taken as 16%. This implied that the monocrystalline solar PV module which was not cleaned generated 16%, less power output compared to the cleaned one, due to dust accumulation in tropical savanna climatic conditions. The loss of power can be associated with the loss of current as discussed earlier.

The loss can also be associated with the type of soil which contains a high percentage of finer particles. The finer soil particles have more adhesion to the panel and requires



cleaning in order to remove it. It can also be associated with bird dropping which can eventually cause the hotspot on the module if it is not removed.

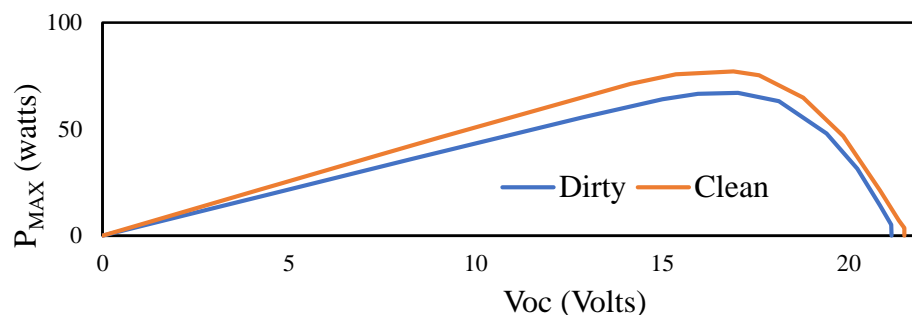


**Figure 5.2:** P-V curve of monocrystalline solar PV module

### 5.3.2 I-V and P-V Curve of the Polycrystalline Solar PV Module

Table 5.2 indicates the results of the polycrystalline module under the effects of soiling and clean conditions in tropical savanna climatic conditions. Results under soiled conditions indicated the average values of  $I_{sc}$ ,  $I_{mp}$ ,  $V_{mp}$ , and  $V_{oc}$  as 5.54A, 5.21A, 16.60V, and 21.04V respectively. The results obtained under the cleaned conditions were  $I_{sc}$ ,  $I_{mp}$ ,  $V_{mp}$ , and  $V_{oc}$  as 6.11A, 5.61A, 16.85V, and 21.45V respectively. Soiling ratio was established for  $I_{sc}$ ,  $I_{mp}$ ,  $V_{mp}$ ,  $V_{oc}$  as 0.09, 0.07, 0.01, and 0.02 respectively.

Further, it indicates the P-V curve of the polycrystalline solar PV module. Results under soiled conditions for the PV modules were FF, Pmax, and efficiency determined as 16.60V, 0.74, 86.48W, and 11.40% respectively. Results obtained under clean conditions for the PV module were FF, Pmax, and efficiency were determined as 16.85V, 0.72, 94.57W, and 12.6% respectively. Soiling ratio was established for FF, Pmax, and efficiency determined as 0.03, 0.09, and 0.09 respectively.

**Table 5.2:** Effects of Dust Accumulation on the Performance of p-Si PV Module

Parameter measured	Dust accumulated PV module	Cleaned PV module	Soiling ratio
$I_{sc}$ (A)	5.54	6.11	0.09
$I_{MP}$ (A)	5.21	5.61	0.07
$V_{MP}$ (A)	16.60	16.85	0.01
$V_{oc}$ (V)	21.04	21.45	0.02
FF (%)	74	72	0.03
P <sub>MAX</sub> (W)	86.48	94.57	0.09
$\eta$ (%)	11.40	12.60	0.09

Figure 5.3 shows the I-V curves of the polycrystalline PV module under dust accumulated conditions and clean conditions. The figure indicates insignificant difference between open circuit voltage of clean and dust accumulated PV module. In addition, the figure indicates a significant difference between short circuit current under cleaned and dust accumulated PV module.

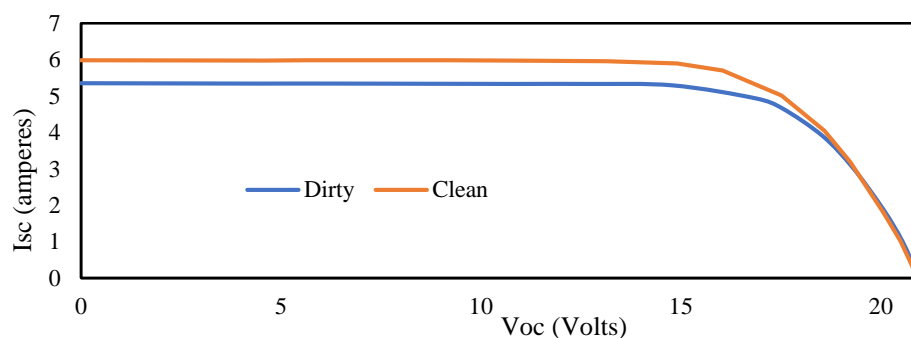
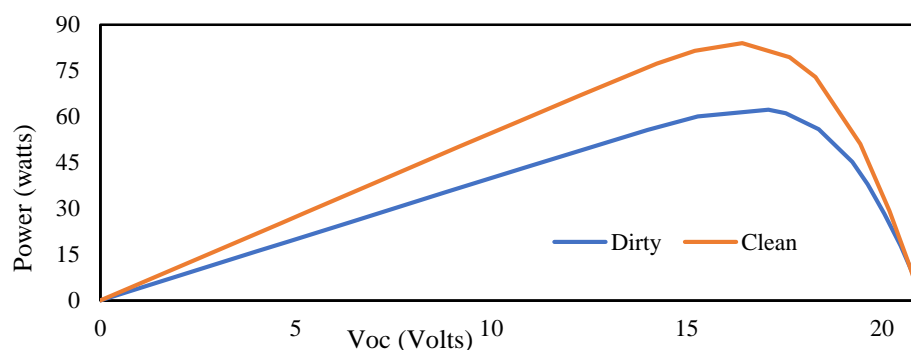
**Figure 5.3:** I-V curve of polycrystalline solar module

Figure 5.4 shows the P-V curves of the polycrystalline PV module under dust accumulated conditions and clean conditions. The figure indicates insignificant difference between open circuit voltage of clean and dust accumulated PV module. In addition, the figure indicates a significant difference between the maximum power point under cleaned and dust accumulated PV module.

This implies that if the polycrystalline solar PV module was left unattended it will lose 9% of power output due to dust accumulation in tropical savanna climatic conditions.

The loss of power can be associated with the loss of current and type of soil.



**Figure 5.4:** P-V Curve for Polycrystalline Solar PV Module

### 5.3.3 I-V and P-V Curve of the Silicon Amorphous Thin Technology Solar PV Module

Table 5.3 indicates the results of the silicon amorphous thin technology solar PV module under the effects of dust accumulation and clean conditions in tropical savanna climatic conditions. Results under soiled conditions were established for  $I_{sc}$ ,  $I_{mp}$ ,  $V_{mp}$ , and  $V_{oc}$  as 3.14A, 2.49A, 29.13V, and 40.19V respectively. The results obtained under the cleaned conditions were  $I_{sc}$ ,  $I_{mp}$ ,  $V_{mp}$ , and  $V_{oc}$  as 3.53A, 2.79A, 28.58V, and 39.81V respectively. Soiling ratio was established for  $I_{sc}$ ,  $I_{mp}$ ,  $V_{mp}$ ,  $V_{oc}$  as 0.11, 0.11, 0.02, and 0.01 respectively.

Further, it shows the results under dust accumulation conditions were established for FF,  $P_{max}$ , and efficiency as 0.58, 72.53W, and 4.5% respectively. Results obtained under clean conditions for FF,  $P_{max}$ , and efficiency were indicated as 0.57, 79.60W, and 5.2% respectively. Soiling ratio was established for FF,  $P_{max}$ , and efficiency determined as 0.02, 0.09, and 0.12 respectively.

**Table 5.3:** Effects of Dust Accumulation on the Performance of a-Si PV Module

Parameter measured	Dust accumulated PV module	Cleaned PV module	Soiling ratio
<b>I<sub>sc</sub> (A)</b>	3.14	3.53	0.11
<b>I<sub>MP</sub> (A)</b>	2.49	2.79	0.11
<b>V<sub>MP</sub> (A)</b>	29.13	28.58	0.02
<b>V<sub>oc</sub> (V)</b>	40.19	39.81	0.01
<b>FF (%)</b>	58.00	57.00	0.02
<b>P<sub>MAX</sub> (W)</b>	72.53	79.60	0.09
<b>η (%)</b>	4.50	5.20	0.12

Figure 5.5 shows the I-V curves of the silicon amorphous thin technology PV module under dust accumulated conditions and clean conditions. The figure indicates insignificant different between open circuit voltage of clean and dust accumulated PV module. In addition, the figure indicates a significant difference between short circuit current under cleaned and dust accumulated PV module. This implies that open-circuit voltage is not affected by the soiling of the module but short circuit current is more affected.

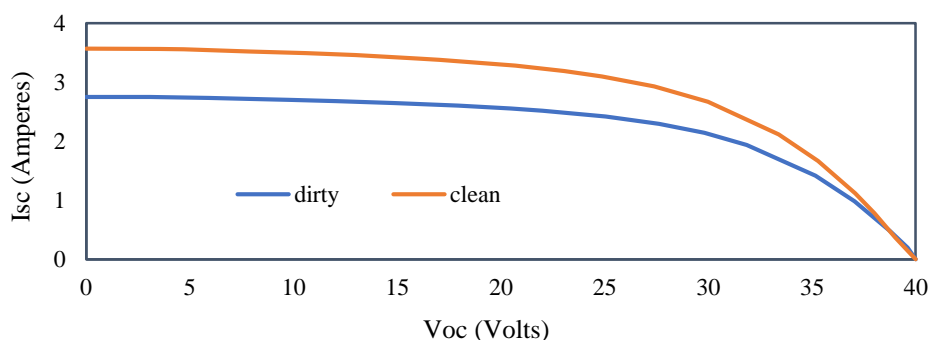
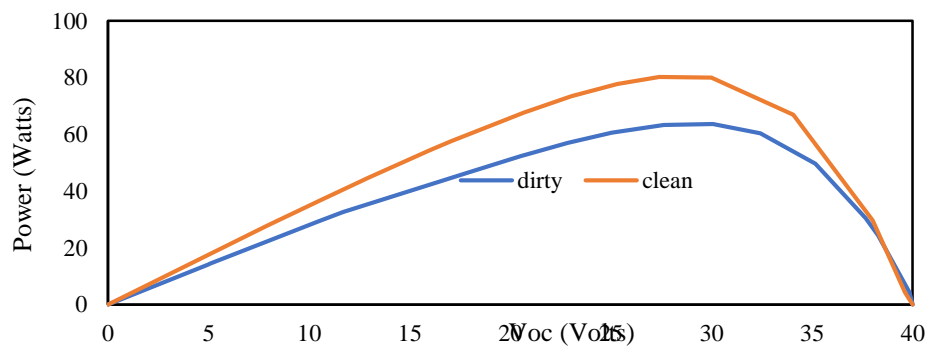
**Figure 5.5:** I-V Curve of Amorphous Solar PV Module

Figure 5.6 shows the V-P curves of the a-Si, PV module under dust accumulated conditions and clean conditions. The figure indicates insignificant different between  $V_{oc}$  of clean and dust accumulated PV module. In addition, the figure indicates a

significant difference between the maximum power point under cleaned and dust accumulated PV module. This implies that if the p-Si, PV module was left unattended it will lose 9% of power output due to dust accumulation in tropical savanna climatic conditions.



**Figure 5.6:** P-V Curve of Amorphous Solar PV Module

#### 5.4 Discussion

The short circuit current of the three solar cell technologies was much more reduced compared to open-circuit voltage. This observation was associated with the fact that short circuit current depends on the light intensity and the area of the exposure of the solar cell. Dust accumulation on the solar cell may cause shading hence reducing the area of exposure while it may also reduce the intensity of light reaching the solar cell. This was also associated with the high percentage of finer soil particles from the soil sample. This study agrees with other studies such as (Ali Sadat et al., 2021; Hachicha et al., 2019; Kagan et al., 2018; Kaundilya et al., 2018; Olivares et al., 2020; Semaoui et al., 2020; A. Yadav et al., 2021).

However, it can be indicated that the short circuit current soiling ratio loss of monocrystalline, polycrystalline, and amorphous silicon technology of 17%, 9%, and 11% was less than the results obtained by (Yadav et al., 2021) of 28% which was conducted in the laboratory. The results, however, indicate higher figures than the study

conducted by (Semaoui et al., 2020) which indicated 8.79%, and (Kagan et al., 2018) of 4.6%. This was associated with the duration of the exposure and type of soil.

The loss of the short circuit current led to the loss of power of the three solar cell technologies modules. This study concurs with other studies such as (Sadat et al., 2021; Alquthami & Menoufi, 2019; Fraga et al., 2018; Hachicha et al., 2019; Kagan et al., 2018; Menoufi et al., 2017; Olivares et al., 2020; Ramli et al., 2016; Semaoui et al., 2020; Ullah et al., 2020; A. Yadav et al., 2021) which indicated the loss of power due to dust accumulations effects was due current loss of PV modules. This study also found that the dust effects on the solar PV module may be technology-specific as observed by (Kaundilya et al., 2018). This study indicated that polycrystalline was less affected by soiling compared to amorphous silicon technology and monocrystalline which indicated more power loss. The high loss of m-Si compared to p-Si and a-Si, was associated with the single crystal structure whereby, when it was blocked it affected the functionality of the whole cell.

The study found that dust deposition on the solar PV module did not significantly affect the open circuit voltage of the three technologies which indicated a small difference of between 1% and 2%, for cleaned and uncleaned PV modules. This was associated with the fact that open-circuit voltage is not directly proportional to sunlight as the case of short-circuit current. However, the open-circuit voltage corresponds to the amount of forward bias on the solar cell due to the bias of the solar cell junction with light generated current. These results concur with (Rao et al., 2014) which indicated that soiling had insignificant effects on open circuit voltage.

## 5.5 Conclusion and Recommendations

The performance of solar PV modules is affected by the type, texture and soiling ratio in given climatic conditions. It was also affected by the type, material and size of the solar PV module technology. The soil in the tropical savanna region under investigation in this study was established to contain a high percentage of finer soil particles of less than 0.063mm. The finer particles have greater impact on the PV module, because they reduce inter-particle gap between them hence, blocking the light towards the solar cell.

The finer soil particles easily condensate and stick at the lower side of the solar PV module. This can lead to the creation of hotspots and cell disconnects on the PV modules. The hotspots will also negatively affect the operation and performances of the solar cell. Therefore, the study recommends regular cleaning of the modules in order to increase the power output and efficiency. The study established that open circuit voltage was less affected by accumulation of dust indicating a soiling ratio of between 0.01 and 0.02. The short circuit current was more negatively affected by soil accumulation indicating a soiling ratio of between 0.09 and 0.17.

The polycrystalline solar PV module was less affected by the accumulation of dust compared to monocrystalline and silicon amorphous thin technology. The power loss due to the accumulation of dust was established as 9%, 11% and 17% for polycrystalline, silicon amorphous thin technology and monocrystalline respectively. The study recommends further investigation in order to determine the soiling rate as this will enable the establishment of the cleaning frequency of the solar PV module in the region.

## CHAPTER 6

### 6.1 Degradation Mechanism and Degradation Rates of PV Modules

The results of the degradation analysis of soiling of solar PV modules are presented in this chapter. The chapter begins with the analysis of degradation mechanisms (visually observable defects and thermal images), and degradation rates analysis (short-circuit current, open-circuit voltage, fill factor, power, and efficiency). The degradation rates model of the solar PV module in warm semi-arid climatic conditions and discussion are then presented.

### 6.2 Sub-Objectives

- To determine the degradation mechanisms of solar PV modules in tropical savanna and warm semi-arid climatic conditions.
- To determine the degradation rates of solar PV modules in tropical savanna and warm semi-arid climatic conditions.
- To develop the degradation rates model of solar PV modules in warm semi-arid climatic conditions.

### 6.3 Degradation Mechanisms; Visually Observable Defects and Thermal Images

One of the objectives of this study was to identify the major degradation mechanism of the modules. Most of the modules examined did not indicate any visible degradation mechanism, and this was associated with the short period of deployment. However, few modules showed signs of degradation hence those modules were considered and analyzed individually. One of the major degradation mechanisms observed was EVA discolouration. It was observed that 7 (36.84%) out of the 19 solar modules polycrystalline in warm semi-arid climatic conditions indicated this defect. Figure 6.1 (a) indicates the Ubbink solar module (with a rated power of 140 W), which was of the



polycrystalline type deployed for 5 years in warm semi-arid climatic conditions, which indicated EVA discolouration degradation in all its 36 cells. Most of the cells indicated 75%-100% of the fraction affected by EVA discolouration degradation.

Figure 6.1 (b) indicates uneven heating of the same module showing hot spots areas. The module indicated dust accumulation near frames on all sides. The module did not indicate any other visible defects. It indicated a high short circuit degradation rate of between 8.50% per year. This implied that the module will not be able to operate at the expected warranty. The following issues were observed; poor installation which included roof mounting with no provision of air circulation, and was not properly grounded.

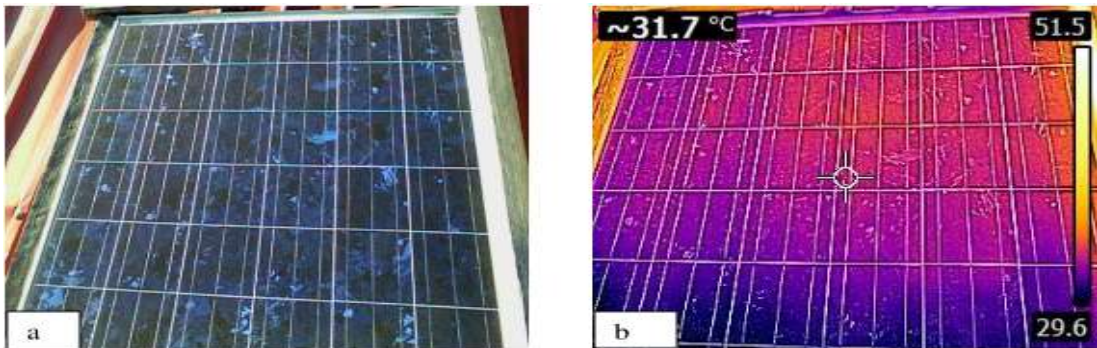


**Figure 6.1:** (a) EVA Discolouration (b) Uneven Heating of PV Module

The discolouration of EVA leads to the low transmissivity of light which leads to a decrease of short circuit current ( $I_{SC}$ ). The position of discolouration of EVA on a solar cell result in the degradation of  $I_{SC}$  because it reduces the current flowing through the solar cell. Therefore, it does not matter the position or the connection of the cells. However, discolouration does not affect the open-circuit voltage and fill factor. Rajput et al. (2016) presented power degradation rates of 7 modules which varied from 2.08% to 3.48% per year with an average of 2.60% per year due to the effects of EVA discolouration. The module studied in this work indicated a power degradation of 8.20% per year, which was more than the rates of the above study.

Figure 6.2 (a) indicates snail tracks in the Jinko solar polycrystalline module installed in tropical savanna. All the modules in the tropical savanna indicated these marks. Figure 6.2 (b) indicates the browning of EVA discolouration materials. All the Jinko solar modules in tropical savanna indicated browning of EVA discolouration materials. Figure 6.2 (c) indicates uneven heating of the solar module of Jinko in the tropical savanna region.

This indicated the presence of hot spots, especially in areas with snail tracks and EVA discolouration. The hotspots lead to disconnection of the solar cell thereby reducing the amount of current generated. Figure 6.2 (d) indicates the shuttered glass of the Jinko solar module in tropical savanna climatic conditions. The shuttered glass blocks solar cells from receiving the sunlight and tends to create hotspots. This led to high acceleration degradation of short circuit current and ingress of water into PV modules. This led to destruction of the EVA materials, solar cells and disconnect of the ribbons due to corrosions. Hence, power output reduction.

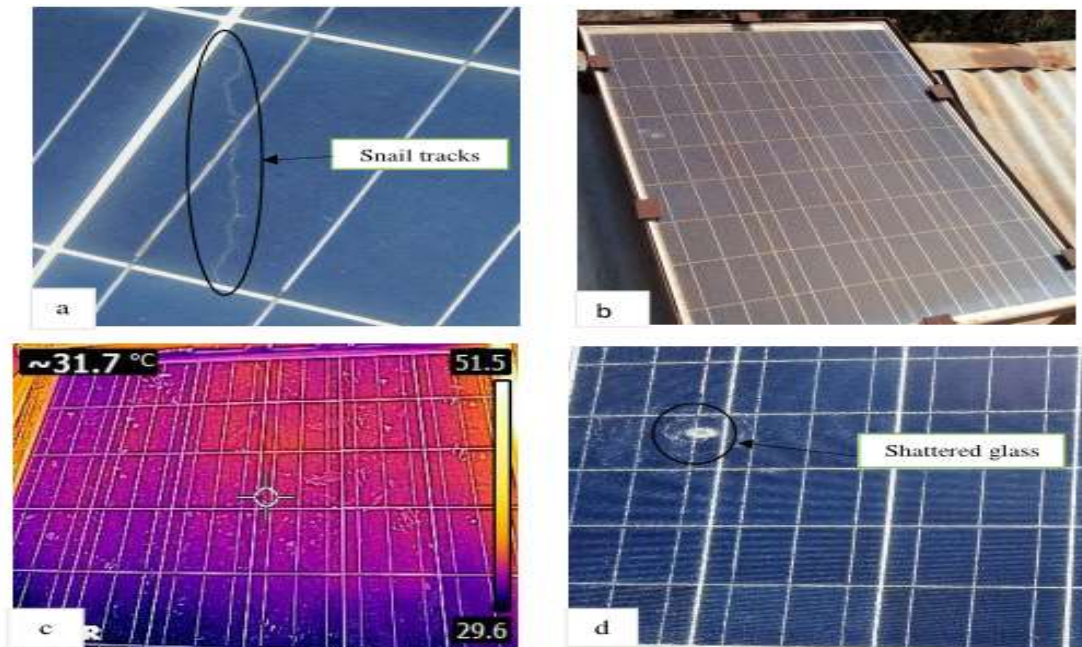


**Figure 6.2:** (a) Snail Tracks (b) Brown Discolouration EVA Materials (c) Uneven Heating of PV Module (d) Shattered Glass of Solar Module

It was determined that out of 5 (6.25%) modules 80 installed in the tropical savanna region suffered from glass shattering. The shattering of glass can allow ingress of water, dust, and current flush over. This current flush-over causes shock for anybody who comes into contact with it. It can be indicated that Grundfos amorphous silicon thin-film technology installed in warm semi-arid climatic conditions and Schott monocrystalline solar modules installed in tropical savanna climatic conditions did not indicate any sign of visible defects.

#### 6.4 Degradation Rates Analysis

The following electrical parameters are usually specified in any solar module templates at STC conditions. They include short circuit current ( $I_{SC}$ ), open-circuit voltage ( $V_{OC}$ ), maximum voltage ( $V_{MP}$ ), maximum current ( $I_{MP}$ ), maximum power ( $P_{MAX}$ ), and fill factor (FF). The change in the performance of these factors after exposure to field conditions indicates the degradation under effects of environmental conditions of a specific region. The different types of modules included polycrystalline from different

manufacturers, monocrystalline, and silicon amorphous thin technology as indicated in Table 3.5. The study was done in warm semi-arid areas and tropical savanna climatic conditions.

Table 6.1 presents the annual average degradation rates of PV modules in warm semi-arid and tropical savanna climatic conditions which have operated for a period of 6 years. The table shows that silicon amorphous thin technology (Grundfos) recorded high degradation rates on  $I_{SC}$ ,  $V_{OC}$ , and  $P_{MAX}$  of 1.84%, 0.75%, and 1.44%, respectively. In addition, it indicates that monocrystalline (Schott) recorded low degradation rates on  $I_{SC}$ ,  $V_{OC}$ , and  $P_{MAX}$  of 0.92%, 0.04%, and 0.99%, respectively. Finally, it indicates that silicon amorphous thin technology (Grundfos) recorded low degradation rate on FF of 0.51%.

**Table 6.1:** Annual Average Degradation Rates of PV Modules (%)

	Warm semi-arid climatic conditions		Tropical savanna climatic conditions	
	Amerisolar, (p-Si)	Grundfos, (a-Si)	Jinko, (p-Si)	Schott, (m-Si)
$I_{SC}$	1.03	1.84	1.05	0.92
$V_{OC}$	0.16	0.75	0.13	0.04
$P_{MAX}$	1.22	1.44	1.15	0.99
FF	0.93	0.51	2.04	0.76

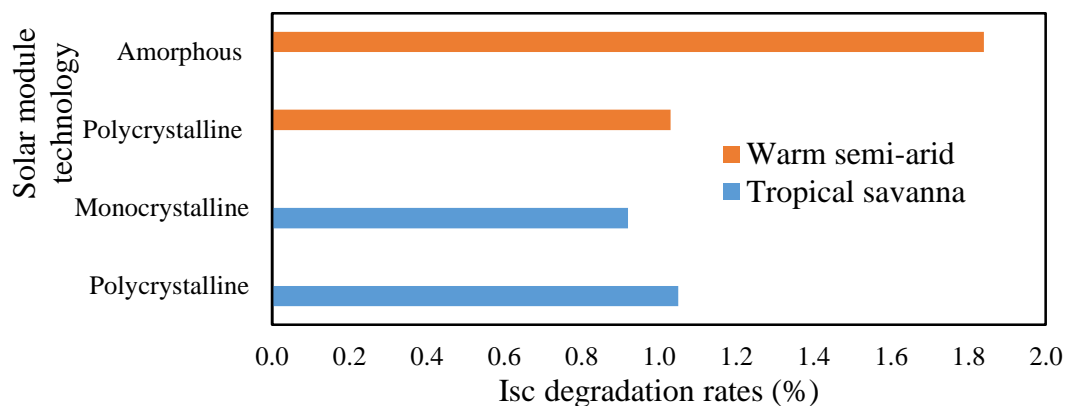
#### 6.4.1 Short-Circuit Current ( $I_{sc}$ ) Degradation Rates

Figure 6.3 shows the average short circuit current ( $I_{sc}$ ) degradation rates of 12 Amerisolar modules, 16 Jinko solar modules, 12 Grundfos modules, and 6 Schott solar modules. The Amerisolar and Jinko solar were of polycrystalline silicon cell technology, Grundfos was of silicon thin-film technology while Schott solar modules

were monocrystalline cell technology. Full details of module specifications are indicated in Table 3.8. All the modules had operated for 6 years.

The Amerisolar and Grundfos modules were operating in warm semi-arid climatic conditions while the Jinko solar and Schott modules were operating in tropical savanna climatic conditions. Results indicated the minimum short circuit current degradation rate of Amerisolar, Jinko solar, Grundfos, and Schott of 0.62%, 0.41%, 0.21%, and 0.4 % per year.

It also indicated the maximum  $I_{sc}$  degradation rates of Amerisolar, Jinko solar, Grundfos, and Schott of 1.38%, 1.51%, 4.27%, and 1.81% per year. Finally, the results indicated the average  $I_{sc}$  degradation rates of Amerisolar, Jinko solar, Grundfos, and Schott of 1.03%, 1.05%, 1.84%, and 0.92% per year.



**Figure 6.3:**  $I_{sc}$  Degradation per Year Versus the Type of Cell Technology

Figure 6.4 indicates the results of the  $I_{sc}$  which has operated for different periods in warm semi-arid climatic conditions. Results indicated  $I_{sc}$  degradation rates of 2.15%, 0.94%, 1.03%, 1.01%, and 0.45% per year for 3, 5, 6, 7, and 8 years outdoor installed modules, respectively. The mean of every solar module per year was calculated. Then the weighted mean was determined based on the number of solar PV modules.

The Isc degradation rate was established using the weighted average mean as 1.03% per year. It can be indicated that 4 of the remaining 7 modules were 3 years old and hence their high degradation rate was associated with potential induced degradation rate which occurs during the early period of deployment. The mounting option of the other 3 solar PV modules did not leave a good space for air circulation position and may have affected their performance.

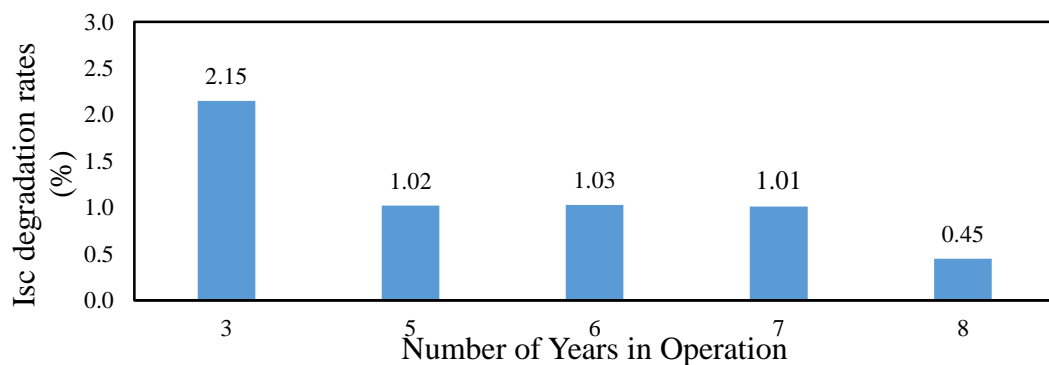


**Figure 6.4:** The Degradation Rates of Short Circuit Currents Versus the Number of Years

#### 6.4.2 Open-Circuit Voltage (Voc) Degradation Rates

Figure 6.5 shows the open-circuit voltage (Voc) average degradation rates of 12 Amerisolar modules, 16 Jinko solar modules, 12 Grundfos modules, and 6 Schott solar modules. The description and operation conditions of the modules are in Table 3.8. Results indicated the open-circuit voltage minimum degradation rate of Amerisolar, Jinko solar, Grundfos, and Schott of 0.13%, 0.10%, 0.02%, and 0.01 % per year.

It also indicated the *Voc* maximum degradation rates of Amerisolar, Jinko solar, Grundfos, and Schott of 0.19%, 0.15%, 1.04%, and 0.09% per year. Finally, the results indicated average *Voc* degradation rates of Amerisolar, Jinko solar, Grundfos, and Schott of 0.16%, 0.13%, 0.75%, and 0.04% per year.

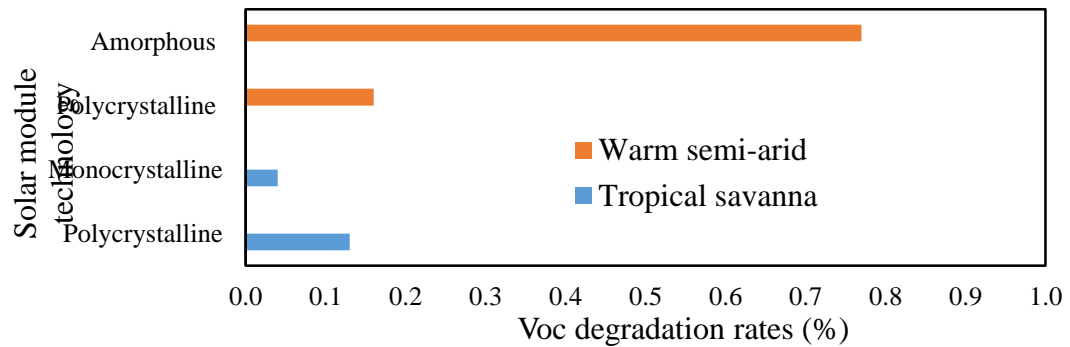


**Figure 6.5:** Types of Cell Technology Versus Voc Degradation Rates

Figure 6.6 indicates the results of the Voc which has operated for different periods in warm semi-arid climatic conditions. Results had indicated Voc degradation rates of 0.11%, 0.13%, 0.16%, 0.03%, and 0.08% per year for the solar PV modules which were deployed for 3, 5, 6, 7 and 8 years respectively. The Voc degradation rate was determined using the weighted mean as 0.23%. This implies that  $V_{OC}$  was less affected compared to  $I_{SC}$ .

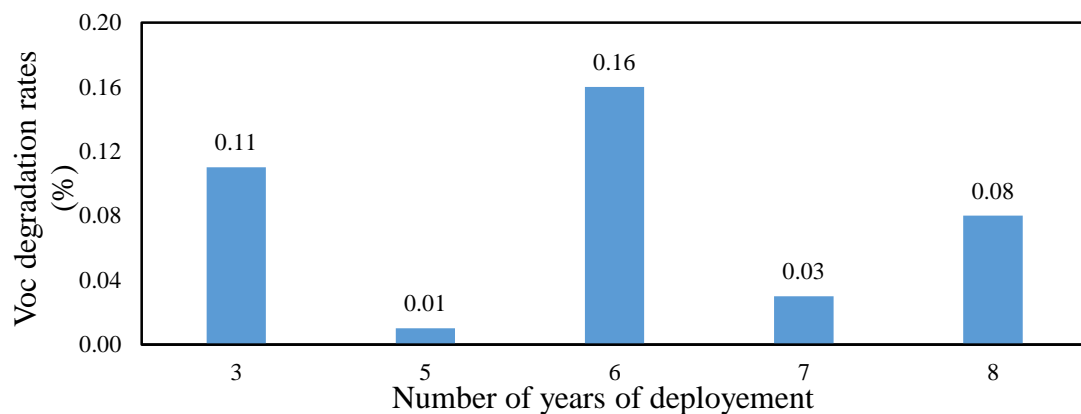


**Figure 6.6:** Voc Degradation Rates of Polycrystalline PV Modules in Warm Semi-Arid Region

#### 6.4.3 Fill Factor (FF) Degradation Rates

Figure 6.7 presents the fill factor (FF) average degradation rates of 12 Amerisolar modules, 16 Jinko solar modules, 12 Grundfos modules, and 6 Schott solar modules. The description and operation conditions of the modules are in Section 3.6.2 in Table

3.8. Results indicated the fill factor minimum degradation rate of Amerisolar, Jinko solar, Grundfos, and Schott of 0%, 1.11%, 0.09%, and 0.56 % per year.

It also indicated the fill factor (FF) maximum degradation rates of Amerisolar, Jinko solar, Grundfos, and Schott of 1.33%, 3.78%, 0.96%, and 0.87% per year. Finally, the results indicated average FF degradation rates of Amerisolar, Jinko solar, Grundfos, and Schott of 0.93%, 2.04%, 0.51%, and 0.76% per year.

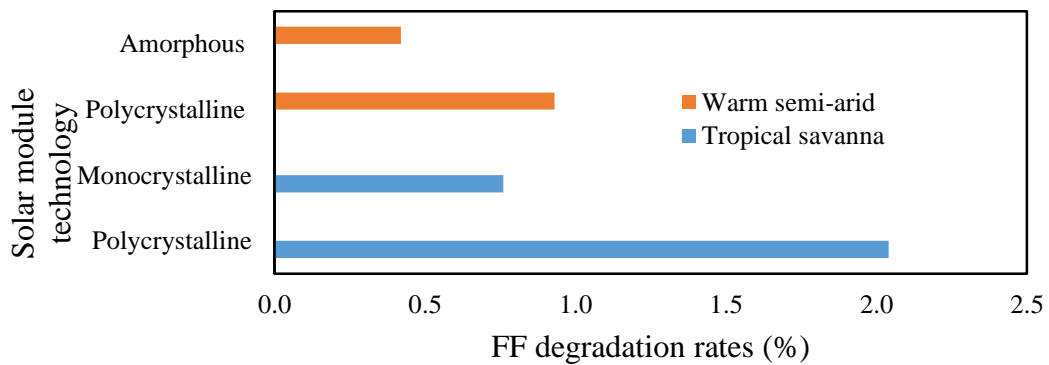


**Figure 6.7:** Type of module technology versus FF degradation rates per year

Figure 6.8 indicates the results of the fill factor (FF) which has operated for different periods in warm semi-arid climatic conditions. Results had indicated fill factor (FF) degradation rates of 2.32%, 2.25%, 0.93%, 2.98%, and 0.17% per year for the solar PV modules which were deployed 3, 5, 6, 7 and 8 years respectively. The weighted mean of fill factor (FF) degradation rate was established as 0.93%, per year.

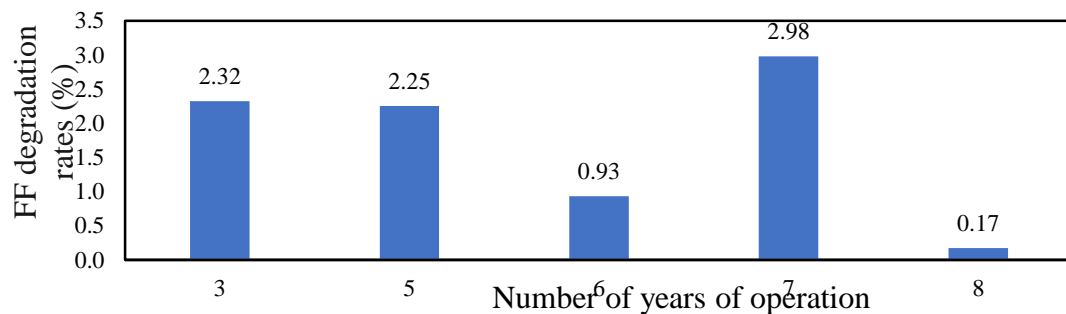


**Figure 6.8:** FF Degradation Rates of p-Si Modules in the Warm Semi-Arid Region



#### 6.4.4 Power Output Degradation rates

Figure 6.9 shows the power average degradation rates of 12 Amerisolar modules, 16 Jinko solar modules, 12 Grundfos modules, and 6 Schott solar modules. The description and operation conditions of the modules are in Section 3.6.2 and Table 3.8. Results indicated the power minimum degradation rate of Amerisolar, Jinko solar, Grundfos, and Schott of 0.8%, 0.50%, 0.34%, and 0.40% per year.

It also indicated the power maximum degradation rates of Amerisolar, Jinko solar, Grundfos, and Schott of 1.57%, 1.58%, 3.30%, and 1.81% per year. Finally, the results indicated an average power degradation rate of Amerisolar, Jinko solar, Grundfos, and Schott of 1.22%, 1.15%, 1.44%, and 0.99% per year.

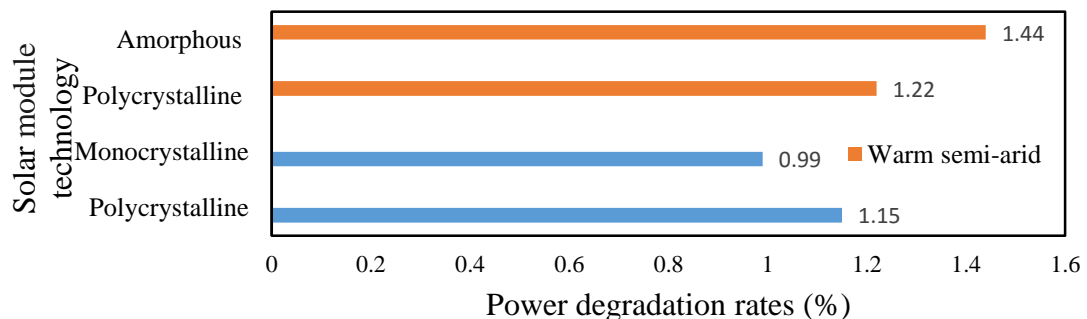


**Figure 6.9:** Type of Solar Module Technology Verses Power Degradation Rates

Figure 6.10 indicates the results of the power which has operated for different periods in warm semi-arid climatic conditions. Results had indicated power degradation rates of 2.16%, 1.81%, 1.22%, 1% and 0.54% per year for the solar PV modules that were deployed for 3, 5, 6, 7 and 8 years, respectively. The weighted mean of power degradation rate was determined as 1.22%.

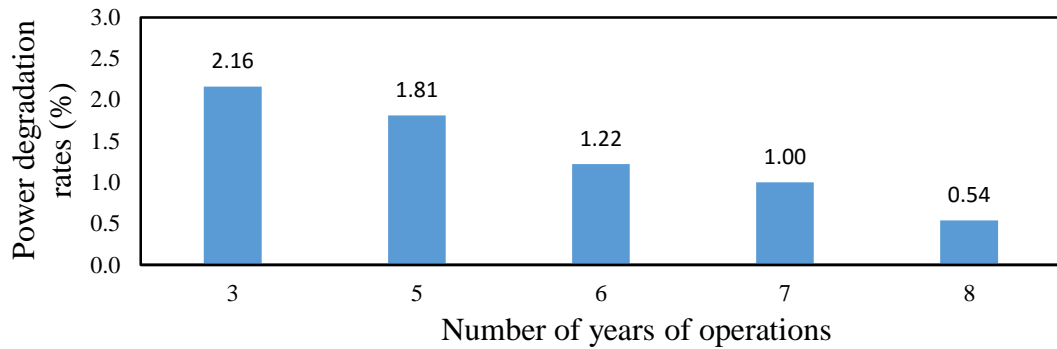


**Figure 6.10:** Power Degradations Rates of p-Si Modules in A Warm Semi-Arid Region

#### 6.4.5 Efficiency

Figure 6.11 shows the average efficiency of 12 Amerisolar modules, 16 Jinko solar modules, 12 Grundfos modules, and 6 Schott solar modules. Results indicated the minimum efficiency of Amerisolar, Jinko solar, Grundfos, and Schott of 10.99%, 9.45%, 6.57%, and 11.96 % per year. It also indicated the maximum efficiency of Amerisolar, Jinko solar, Grundfos, and Schott of 12.61%, 11.71%, 7.45%, and 13.60% per year.

Finally, the results indicated an average efficiency of Amerisolar, Jinko solar, Grundfos, and Schott of 11.71%, 10.71%, 6.96%, and 12.70% per year. As expected, the values were lower than efficiency at STC as indicated in Table 3.8. It can be reported that the monocrystalline indicated less difference between the efficiency at STC and real environmental climatic conditions operating efficiency value by 1.8%.

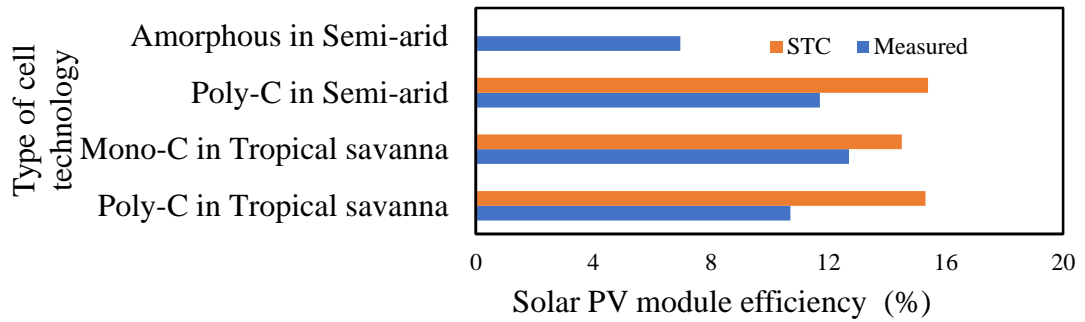


**Figure 6.11:** Solar PV Modules Efficiency (%).

Figure 6.12 indicates the efficiency of the modules installed in the warm semi-arid region. The results indicate that modules that were installed 3, 5, 6, 7 and 8 years recorded efficiency of 9.17%, 10.77%, 11.71% 7.63% and 9.16% respectively. These values were lower than efficiency at STC values as indicated in Table 3.8. The results indicated a difference of 5.73%, 7.03%, 3.69% 7.27%, and 5.14% for the modules that have been installed for 3, 5, 6, 7, and 8 years respectively.

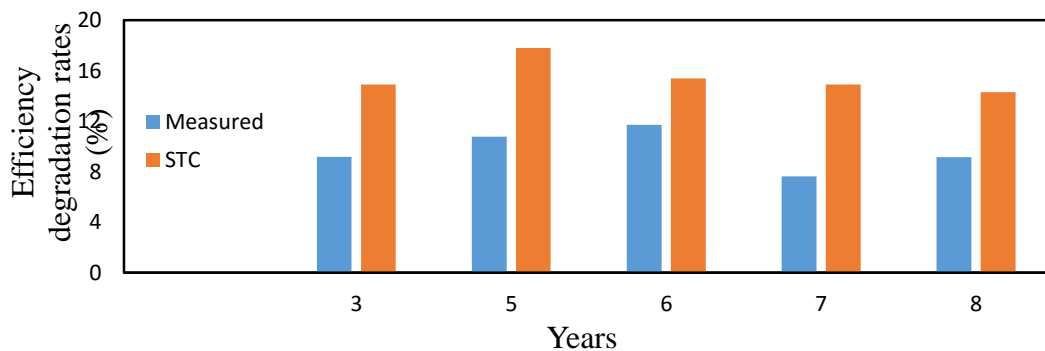


**Figure 6.12:** PV Modules Efficiency (%) in Warm Semi-Arid Region versus Years

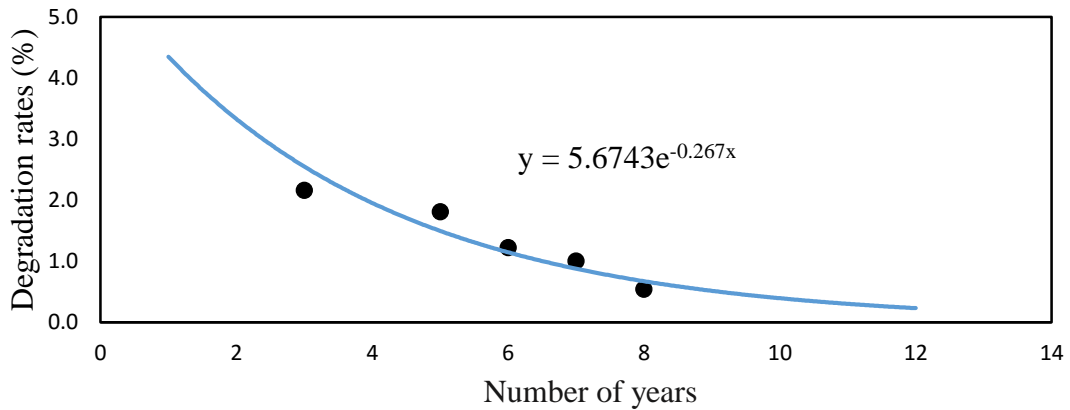
### 6.5 Degradation Rate Model of the PV Module in Warm Semi-Arid Climatic Conditions

Figure 6.13 shows the profile of power degradation rates of the solar module in warm semi-arid climatic conditions. A fitted model indicates an exponential relationship between degradation rate and of the number of years of deployments as indicated in Equation 6.1 with  $R^2 = 0.956$ .

$$y = 5.674e^{-0.267x}$$

6.1

where  $y$  is the predicted degradation rates and  $X$  is the number of years of deployment



**Figure 6.13:** Degradation rates model for warm semi-arid climatic conditions:

The developed expression (Equation 6.1) can be used to estimate the degradation rate at a specific year and cumulative degradation rate within a given period. Using this expression, the solar PV modules in the region could degrade at 0.23% in year 12 and 0.01% in year 25, for example. Overall, developed expression indicated that modules could produce 81.5% of their rated values after 25 years of operation and with an average degradation rate of 0.74% per year.

The model further indicates that the modules will degrade at higher rates during the initial periods of deployment. This can be due to light induced degradation (LID) and early fatality rates. The early fatality can be associated with poor handling of materials during transportation and installation phases. This can be further associated with unqualified staff or lack of manpower with ethical know how to handle the task. However, it can be indicated that the study was conducted for modules which had been installed for a period of between 3 years to 9 years. This is below 25 years warranty.

The study expects degradation to follow the bath-tub curve which indicates high degradation rate at initial period due to infant mortality phase, low degradation rate

during long useful life phase, and high degradation rate during wear out phase. Hence, the degradation from the study follows the same pattern.

Figure 6.14 presents a comparison of the measured and predicted values of the power degradation rates of solar PV in warm semi-arid climatic conditions. The predicted values compare closely with the measured values and therefore the model can be used to estimate the power degradation rates.

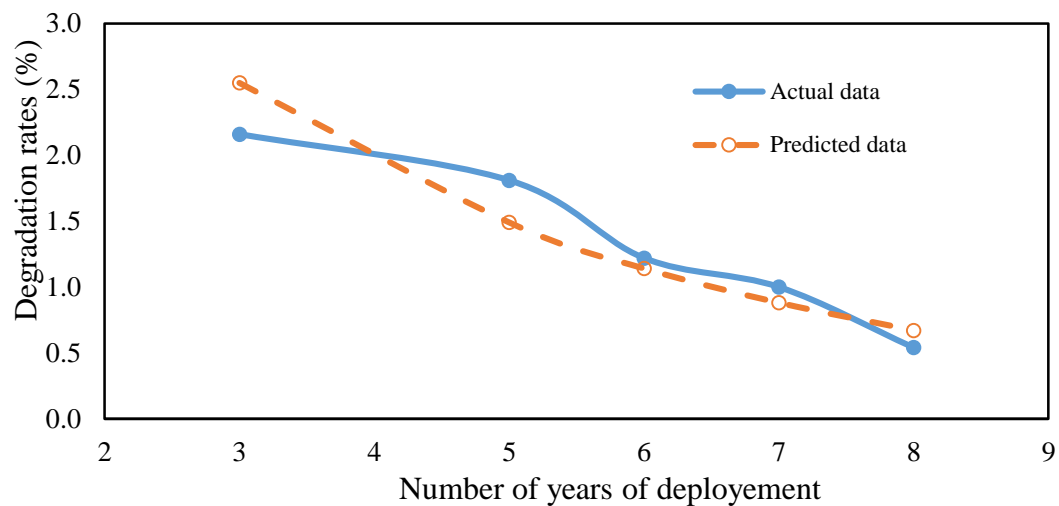


**Figure 6.14:** Actual and Predicted Values of Power Degradation Rates

## 6.6 Discussion

The study conducted by (Quansah et al., 2020) determined degradation rates of 3 climatic conditions namely humid region, sub-humid humid, and sub-humid dry climates in Ghana of  $I_{sc}$  as 1.1%, 0.49%, and 0.8%,  $V_{oc}$  as 0.4%, 0.18% and 0.3%,  $FF$  as 0.5%, 0.89% and 0.5% and  $P$  as 1.8%, 1.43%, and 1.5% respectively for both monocrystalline and polycrystalline. The study indicated front of module defects, delamination, and browning of encapsulant materials as the major defects in those climatic areas. Ndiaye et al. (2014) established degradation rates of modules that have been exposed for 3.4 and 4 years respectively for  $I_{sc}$  as 0.38% and 0.77%,  $V_{oc}$  as 0.03%

and 0.01%,  $FF$  as 0.94% and 2.36%, and  $P$  as 1.62%, and 2.96%, per year respectively for polycrystalline modules in the tropical environment.

Atsu et al. (2020) indicated degradation rates of  $I_{sc}$ ,  $V_{oc}$ ,  $FF$ , and  $P$  as 0.98%, 1.23%, 1.5%, and 3.19% per year respectively for a monocrystalline solar module that was installed in 2007 in tropical climatic conditions. Limmanee et al. (2016) determined power degradation rates of multi p – si, hetero – junction si, micromorph, and CIGS under tropical climatic conditions after 4 years of outdoor exposure. It indicated power degradation rates of *multi p – si*, *HIT*, micromorph, and *CIGS* as 1.2%, 1.3%, 1.8-6.1%, and 1.7% respectively.

Quansah & Adaramola (2018) indicated degradation rates of monocrystalline after 16 years of deployment for  $I_{sc}$ ,  $V_{oc}$ ,  $FF$ , and  $P$  as 0.75%, 0.35%, 0.54%, and 1.54% respectively in the sub-humid dry region. The browning of encapsulant material and degraded junction box adhesive was indicated as the dominant degradation mechanism. Sadat et al. (2021) determined the annual power degradation rate of the monocrystalline solar module in Adrar, Algeria Sahara after long exposure as 1.5%. The study also indicated delamination, burn marks, and discoloration of encapsulant as degradation mechanisms, and the latter being the predominant mode.

Silvestre et al. (2016) conducted a study of degradation of thin-film photovoltaic modules technologies. The study indicated the degradation rates of *a – si:H*, *CIS*, *CdTe*, and micromorph as 2.28%, 1.04%, 4.55%, and 2.72% respectively. Sharma et al. (2014) determined power degradation rates of –si, m – c – si, and *HIT* as 5.7%, 0.51%, and 0.31% respectively in a composite climatic area after 28 months of exposure. The study identified the soiling of glass as the mode of degradation mechanism in all modules and oxidation of silver front grid metallization fingers and

anti-reflective coating in monocrystalline silicon (*m-c - si*). Presented in Table 2.4 are selected studies of power degradation rates and mechanisms of solar PV modules in different regions and climatic conditions.

The results obtained in this study indicate lower power degradation rates for East Africa regions except results of Asia composite climatic conditions. This could be attributable to favorable operating module temperature which varied from 38°C to 48.7°C with a mean of 43°C in tropical savanna and 31.3°C to 56.7°C with a mean of 45.31°C in a warm semi-arid region. These values are close to the NOCT value of 45°C. The discolouration and browning of encapsulating materials are identified as the predominant degradation mechanism mode in most of the climatic conditions. This study has revealed that all the technologies will meet the warranty expectation on both climatic conditions considered in the East African region. Table 6.2 presents a summary of the selected studies of power degradation rates and mechanism of solar PV modules from different climatic conditions and regions.

Table 6.2 shows the summary of the previous studies on the dominant degradation mechanisms of various PV modules in different regions. It shows the dominant degradation mechanisms reported from various regions as delamination, browning of encapsulant materials, cell interconnects ribbons browning, corrosion, soiling of glass, burn marks, and degraded junction box. This is similar with the results obtained from this study which indicates browning and discoloration of encapsulant material as dominant mode of degradation mechanism of tropical savanna and warm semi-arid climatic conditions of Eastern Africa.

Table 6.2 also indicates the degradation rates of solar PV modules in different regions of the world. It indicates that HIT PV module recorded the lowest degradation rate of

0.31% in composite climatic of Asia. In addition, it shows that Micromorph PV module recorded the highest degradation rate which varied from 1.8% to 6.1%, installed on the tropical climate of Far East. The same type of PV module recorded high degradation rate of 2.96% on tropical environment of West Africa.

This study established the degradation rates of polycrystalline PV module, as 1.15% and 1.22% for tropical savanna and warm semi-arid conditions respectively. In addition, it established the degradation rate of monocrystalline as 0.99% in tropical savanna. Finally, it established the degradation rates of silicon amorphous thin technology as 1.44% in warm semi-arid region of Eastern Africa. This shows similar results as presented from other regions.



**Table 6.2:** Power Degradation Rates and Mechanism of Solar PV Modules

References	Location	Climatic conditions	Power degradation rate per year (%)	Common degradation mechanisms
Quansah et al. (2020)	West Africa	Humid	1.8%	Delamination, Browning of encapsulant materials
		Sub-humid humid	1.43%	
		Sub-humid	1.5%	
Ndiaye et al. (2014)	West Africa	tropical environment	1.62%	Not indicated
			2.96%	
Atsu et al. (2020)	West Africa	Tropical climate	3.19%	EVA browning, cell interconnects ribbons browning and the corrosion
Limmanee et al. (2016)	Far East	Tropical climate	multi c – si 1.2%	Not indicated
			HIT 1.3%	
			Micromorph: 1.8-6.1%,	
			CIGS 1.7%	
Silvestre et al. (2016)	Europe	Continental climate condition	a – si: H 2.8%	Not indicated
			CIS 1.04%	
			CdTe 4.55%,	
			Micromorph 2.72%	
Sharma et al. (2014)	Asia	composite climatic	a – si 5.7%	Soiling of glass
			m – si 0.51%	
			HIT 0.31%	
Quansah & Adaramola (2018)	West Africa	sub-humid	m-Si 1.54%	Browning of encapsulant material Degraded junction box adhesive
Sadat et al. (2021)	North Africa	Sahara region	m-Si 1.5%	Delamination, Burn marks, Discoloration of encapsulant material
This study	East Africa	Tropical savanna	p-Si 1.15%	Browning of encapsulant material
			m-Si 0.99%	
		Warm semi-arid	p-Si 1.22%	Discolouration of encapsulant material
			a – Si 1.44%	None at the time of data inspection

## 6.7 Conclusion and Recommendations

This study presents the degradation rates, mechanism, and model for the solar PV module. The study covers two climatic conditions namely warm semi-arid and tropical savanna climatic conditions. The study establishes discoloration of encapsulant material at 36.84% for the solar PV module investigated as the predominant mode of degradation mechanism for polycrystalline modules in warm semi-arid climatic conditions. It also indicates browning of encapsulating materials as the predominant mode of degradation mechanism in tropical savanna for both polycrystalline and monocrystalline modules accounting for 100%. This indicated that all the PV modules in the tropical savanna region had this defect.

The study determined the degradation rates for various modules under two climatic conditions after 6 years of outdoor exposures as follows: Polycrystalline in warm semi-arid climatic conditions with  $I_{sc}$ ,  $V_{oc}$ , FF and  $P$  as 1.03%, 0.16%, 0.93% and 1.22% respectively; Polycrystalline in tropical savanna climatic conditions with  $I_{sc}$ ,  $V_{oc}$ , FF, and  $P$  as 1.05%, 0.13%, 2.04%, and 1.15% respectively; Monocrystalline in tropical savanna climatic conditions with  $I_{sc}$ ,  $V_{oc}$ , FF and  $P$  as 0.92%, 0.04%, 0.76% and 0.99% respectively, and lastly the Silicon amorphous thin-film technology in warm semi-arid climatic conditions with  $I_{sc}$ ,  $V_{oc}$ , FF, and  $P$  as 1.84%, 0.77%, 0.42%, and 1.44% respectively.

The study establishes that short circuit current and fill factor as the major contributor to power degradation rates. This can be associated with the degradation mechanism of encapsulant material. The degraded encapsulant material affects the transmittance of light reaching the cells hence degrading the short circuit current of the solar PV module.

A simple model was developed for predicting the degradation rates of solar PV modules for the first 12 years of exposure in warm semi-arid climatic conditions. This model can be used to estimate the performance of the solar PV modules as indicated by the warranty. The model indicates an exponential degradation rate of the modules. This implies that the modules will degrade at high rates during the first 5 years of exposure then the degradation rates will slow down to low rates. The study proposes more models to be developed in different climatic conditions for different technologies.

From the study it can be indicated that discoloration of encapsulant material was the dominant degradation mechanism in the region. This caused by the presence of water, ultraviolet rays, and higher temperatures of 50°C. The ingress of water into the PV modules maybe caused by breakages, cracks, substandard products, and poor handling of the materials. It is therefore recommended that stringent measures should be put in place on the solar PV products used and minimum qualifications for technicians handling the products. In additions, the study recommends future work to investigate the cause of breakages and cracks in the PV modules.

## CHAPTER 7

### 7.0 Reliability and Failure Rates of PV Modules

Reliability analysis of solar PV systems in tropical savanna and semi-arid regions of Eastern Africa was assumed to take exponential distribution as indicated in section 6.5. The four main installation configurations were considered and four parameters established. The parameters included failure rates of different components, reliability of the systems and MTTF. The main objective of this chapter was to establish the reliability of solar PV systems in the region. This main objective was achieved through the following sub-objectives as indicated in section 7.1.

#### 7.1. Sub-Objectives

- To identify the type of solar PV modules installation configuration systems in the region.
- To determine the failure rates of components of different solar PV module installation configurations in tropical savanna and semi-arid climatic conditions of Eastern Africa region.
- To determine the reliability of different solar PV module installation configurations in tropical savanna and semi-arid climatic conditions of Eastern Africa region.
- To determine the MTTF of components of different solar PV module installation configurations in tropical savanna and semi-arid climatic conditions of Eastern Africa region.

#### 7.2 Failure Rates

The failure rates of different components were determined from the data collected using the NREL tool as modified to accommodate the data for inverter, charge controller and transformers. The sample of the NREL tool used is indicated in Appendix (XLV). The failure of solar PV modules was determined using degradation rates as established in

section 6.3.4. The degradation rates of SDU, SPU and SGT were established as 1.22%, 1.33%, and 1.15%, respectively.

The failure rates of SPG components were however determined using data obtained from the site observation and discussion with the engineers. Table 7.1 indicates the average failure rates of components of four different installations design configurations for solar PV power plants systems. The table indicates that the failure rates of solar PV modules ranged from  $0.49 \times 10^{-6}$ , failures per year for *SPG*, to  $3.93 \times 10^{-6}$ , failures per year for *SDU*.

The failure rate for inverter ranged from  $0.19 \times 10^{-6}$ , failures per year for *SGT*, to  $8.058 \times 10^{-5}$ , failures per year for *SDU*. The failure rates per year for charge controller, transformer, main transformer and battery were established as  $9.21 \times 10^{-5}$ ,  $0.761 \times 10^{-6}$ ,  $9.132 \times 10^{-6}$ , and  $3.171 \times 10^{-5}$  respectively. The failure rates of different components may vary due to infant mortality during installation, warranty of the product, field environmental conditions such as wind which contributed to the majority of the failure rate of the solar PV modules of *SPG* and different numbers and sizes of power plants.

**Table 7.1:** Failure Rates of Components of Solar PV Power Plants

	SDU	SPU	SGT	SPG
Solar PV modules ( $\lambda$ )	$3.93 \times 10^{-6}$	$3.93 \times 10^{-6}$	$3.71 \times 10^{-6}$	$0.4 \times 10^{-6}$
Inverter ( $\lambda$ )	$8.058 \times 10^{-5}$	$0.537 \times 10^{-6}$	$0.19 \times 10^{-6}$	$2.75 \times 10^{-6}$
Charge controller ( $\lambda$ )	$9.21 \times 10^{-5}$			
Battery ( $\lambda$ )	$3.805 \times 10^{-5}$			
Transformer ( $\lambda$ )				$0.761 \times 10^{-6}$
Main Transformer ( $\lambda$ )				$9.132 \times 10^{-6}$

Nur'Aini et al. (2021) used probabilistic failure rate for a grid system as  $1.22 \times 10^{-3}$  failures per year. Baschel et al. (2018) used the failure rates for solar PV module and string inverter as 0.035, failures per  $10^{-6}h$ , and 15.1, failures per  $10^{-6}h$ . Lillo-Bravo et al. (2018) used a failure rate of solar PV plant as 0.00034081.

Sayed et al. (2019) used failures of different sizes of power plants for solar PV modules failure rates which ranged between  $0.02061 \times 10^{-6}$ , failures per year to  $0.51251 \times 10^{-6}$ , failures per year, inverter failure rates which ranged between  $0.125 \times 10^{-6}$ , failures per year to  $2.9999 \times 10^{-6}$ , failures per year, battery failure rates which ranged between  $4 \times 10^{-6}$ , failures per year to  $7.7 \times 10^{-6}$ , failures per year, and charge controller failure rates rate of  $0.01998 \times 10^{-6}$ , failures per year.

The various rates of the study by (Sayed et al., 2019) were due to different sizes of power plants. Failure rates ( $\lambda$ ) established in this study of various components of different installations design configurations were similar with the results obtained from other studies from different solar PV power systems plants. The different values of failure rate were associated with climatic conditions of the site like wind, number of components, and warranty of the components.

### **7.3 Reliability Analysis**

The reliability of different installation designs of solar PV systems was obtained using different failure rates as indicated in Table 7.1 and applying Equations 3.28 up to Equation 3.47. The results show that the reliability of solar PV systems declined at an exponential rate as shown in Figure 7.1. Table 7.2 shows the reliability of the four installation design configuration systems for a period of 25 years in tropical and semi-arid climatic conditions of Eastern Africa. The table shows that the solar installation system for domestic use (SDU), the solar installation system for water pumping (SPU),

the solar installation system for grid-tied (SGT), and the solar installation system for power generation (SPG), was 98%, 92%, 98% and 97% respectively during the first year of operations. The low reliability of SPG was associated with a high number of destructions of the PV modules by high-speed wind.

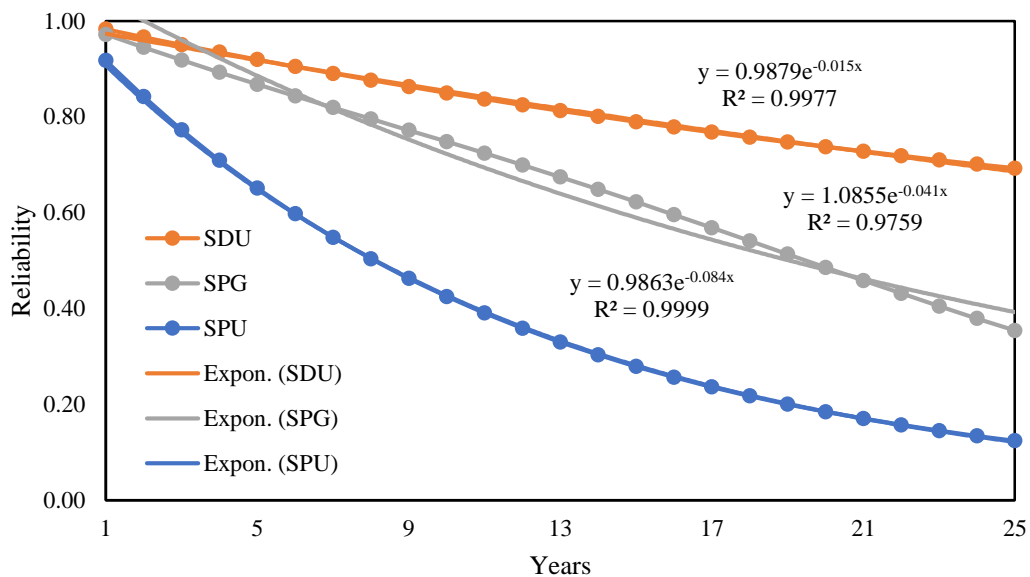


**Figure 7.1:** Reliability of Solar PV Modules with Different Installation Configurations

The reliabilities of the solar PV systems were established for SDU, SPU, SGT, and SPG at the 25<sup>th</sup> year of operation as 69%, 12%, 00%, and 35% respectively. The 00% of SGT from the 20<sup>th</sup> year to 25<sup>th</sup> year of deployment does not imply that the system will not be generating power but indicates that all the subsystems will not be working as expected. For instance, the solar PV modules which are supposed to be generating 80% of the rated power will be producing less than that figure.

The mean average reliabilities for the SDU, SPU, SGT, and SPG were established as 82%, 40%, 35%, and 67%, respectively for a period of 25 years. The workings are presented in the Appendix (RR). The low reliability on SGT system was associated with

the highest number of solar PV modules connected in series that was 40 modules compared to other system which had 1, 12, and 22 for SDU, SPU, and SPG respectively.

**Table 7.2:** Reliability of Solar PV Systems in Kenya

<b>YEARS</b>	<b>SDU (%)</b>	<b>SPU (%)</b>	<b>SGT (%)</b>	<b>SPG (%)</b>
<b>1</b>	98	92	98	97
<b>5</b>	92	65	91	87
<b>10</b>	85	42	38	75
<b>15</b>	79	28	04	62
<b>20</b>	74	18	00	49
<b>25</b>	69	12	00	35

Even though the SPG had a greater number of solar PV module connected in series per string compared to the SPU, it showed high reliability. This was associated with high number of strings connected in parallel per inverter which was eight (8) for SPG compared to only one (1) string for the SPU. It was therefore shown that the greater the number of components connected in parallel, the higher the reliability of the solar PV systems. This implies that increasing the rating of solar PV modules and reducing the number of PV modules connected in series will lead to an increase of the reliability of the system.

Nur'Aini et al. (2021) established the reliability of Grid and Hybrid solar power plants as 55.504% and 98.38% for a period of one year and 00% for both systems for a period of 20 years in Wonogiri Regency, Indonesia. Zini et al. (2011) established reliabilities for 7 different solar PV power plants of different sizes as 79.94%, 66.22%, 37.71%,



17.0%, 6.64%, 2.59% and 1.01% for 100kW, 200kW, 500kW, 1000kW, 1500kW, 2000kW, and 2500kW respectively for a period of one year.

The study further determined the reliability of 100kW and 200kW as 1.14% and 0.003% respectively and 00% for the other five solar PV power plants after 20 years of operation. From the study of (Zini et al., 2011) and this study, it can be indicated that as the number of series connected components increases, the reliability of the system decreases. Zini et al. (2011) studied systems with 437, 874, 2166, 4351, 6517, 8702 and 10868 numbers of solar modules.

Shahidirad et al. (2018) determined the probability of full generation of a system as 97.7% and indicated that a system with more parallel connected systems had more profit compared to a system with single or two branches. Those findings agreed with this study which indicated high reliability value of the *SPG* which had 8 strings connected to one inverter with a mean reliability of 67%, compared to *SGT* with two strings connected to one inverter with a mean reliability of 35%.

Baschel et al. (2018) established the system availability of 98.3% and 99.07% for the central inverter (*CI*) and string inverter (*SI*) respectively. This shows that when components are connected in parallel, the system reliability increases. The study also indicated that automatic identification of failures and dealing with them immediately would be considered good practice. The automation of solar PV power plants should therefore be included in design and installation stages to increase reliability.

Sayed et al. (2019) determined the sub-assemblies' reliability of the solar PV systems for a period of one of the operations for 7 power plants rated 100kW, 200kW, 500kW, 1000kW, 1500kW, 2000kW, and 2500kW as 71.81%, 54.5%, 23.88%, 7.59%, 1.92%, 0.48% and 0.12% respectively. The study also indicated reliabilities as 0.133% for

100kW, and 0.0005% for 200kW, while the rest of the 5 systems indicated a reliability of 00% after 20 years of operation.

Khalilnejad et al. (2016) indicated that the reliability of solar PV modules decrease from 0.99 to 0.81 for a period of 1 year. The current study findings therefore concur with other studies that the reliability is high at initial periods and decreases as time progresses as shown in Figure 59. This may be due to wear and tear of the equipment, exposure to the environment and life span of the components (warranty periods).

The other factors that contribute to reduction of reliability of the solar PV modules include accumulation of dust, formation of hotspots, cell disconnections and poor maintenance. Proper installation designs of the solar PV modules systems may increase the system reliability. This may include connections of more components in parallel compared to series connections.

#### **7.4 Mean Time To Failure (MTTF)**

The mean time to failure (MTTF) shows the time within which a component will operate without failure. The MTTF can also be used to determine the life span of various components. This study had established the MTTF of the SDU and SPU of the components installed in warm semi-arid climatic conditions of solar PV module, charge controller, inverter and battery as 29.04 years, 4 years, 3.5 years, and 3 years respectively.

The MTTF of the component installed in hot semi-arid climatic conditions for SPG were established for solar PV modules, inverter, transformer and main transformer as 28.84 years, 4.15 years, 15 years and 25 years respectively. Finally, the MTTF of the component for SGT installed in tropical savanna climatic conditions for solar PV module and inverter were 30.77 years and 5.26 years respectively.

Nur'Aini et al. (2021) presented the useful life solar panel to be between 20-25 years, inverter as 5-10 years, and battery less than 7 years. Sayed et al. (2019) indicated the expected lifetime of the PV modules without the encapsulation failures, converter, inverter, and storage systems as 43.73 years, 30.77 years, 8.3 years and 10.31 years respectively.

Aghdam & Abapour (2016) determined the *MTTF* of two-stage and three-stage interleaved boost converters as 9.8 years and 14.8 years respectively. The current study had determined the lifespan of solar PV modules to be between 28 years to 31 years. Other studies in the open literature have indicated life spans of between 20 years to 44 years for solar PV modules.

The manufacturer's warranty indicated a life span of 20 to 25 years for the module to produce 80% of their rated capacity. This is an indication that the solar PV modules can be a reliable source of electrical energy within the warranty period and beyond. Great care is however required during the installation stage to avoid infant mortality and also during the operation stage to reduce accelerated degradation.

## **7.5 Conclusion and Recommendations**

The study identified four different installation designs in the region for different uses which includes solar PV system for domestic use, solar PV system for pumping water, solar PV system for grid interactive, and solar PV system for power generation. The study established reliability of solar PV modules of SDU, SPU, SGT, and SPG, as 82%, 40%, 35%, and 67%, respectively. The *MTTF* of the system components indicated that those components will operate as expected as per the warranty. The warranties of the system components of solar PV modules, charger controllers, inverters, batteries, and

transformers were indicated as 25 years, 1 year, 5 to 10 years, and batteries as 3 years to 10 years respectively.

The study also established that reliability of solar PV systems increases when more components (inverters and PV modules) are connected in parallel compared to series connection. This is because if one component fails in series connection it affects the whole system. This can be achieved by increasing the rating of solar PV modules and reducing the number of components connected in series. The study recommends more studies to be carried out in the region to identify more installation designs and establish their failure rates, reliability and MTTF.

## CHAPTER 8

### Conclusion and Recommendations

The first objective of this study was to evaluate the technical and economic performance of solar PV modules in tropical savanna semi-arid climatic conditions. This has provided more data for better assessment of solar PV installation in the region. The results established capacity utilization factor (CUF), system efficiency ( $\eta$ ), and PR (%) as 0.15, 10% and 68% respectively. The economic indicators of the system were established as LCOE of US\$0.1679/kWh, DPP of 13 years, SPP of 9 years and IRR of 5.93%.

This study also developed two models to estimate power output (watts) using 3 weather parameters as input variables. The results have indicated a high coefficient of determination ( $R^2$ ) obtained from the models developed, which translates to good accuracy and validity of the predicted results. The study further established that the solar PV system was more useful in terms of energy savings. The solar PV module using polycrystalline technology can therefore be used as alternative sources of electrical energy and the project can be economically viable in tropical savanna climatic conditions in the region.

The study recommends further investigation in order to establish LCOE using the cost reduction trends and effects in the improvement of the efficiency of the solar PV modules technology. From the model developed the study recommends the investigation on the effects of phase change materials in the performance of the PV system.

The second objective of the study was to analyze the effects of soiling on the performance of solar PV modules in tropical savanna climatic regions. The results

showed that the soil under the study region contained high percentage of finer soil particles of less than 0.063mm. The finer particles have greater impact on the PV module, because they reduce inter-particle gap between them hence, blocking the light towards the solar cell. The study established that open circuit voltage was less affected by accumulation of dust indicating a soiling ratio of between 0.01 and 0.02. While the short circuit current was more negatively affected by soil accumulation indicating a soiling ratio of between 0.09 and 0.17.

The polycrystalline solar PV module was less affected by the accumulation of dust compared to monocrystalline and silicon amorphous thin technology. The power loss due to the accumulation of dust was established as 9%, 11% and 17% for polycrystalline, silicon amorphous thin technology and monocrystalline respectively. Regular cleaning is therefore required in order to increase the electrical power output in the region of PV systems. The study recommends further studies in order to establish the soiling rates, this will enable to establish the cleaning frequency of the solar PV module in the region.

The third objective of the study was to determine the degradation mechanism and rates of solar PV modules in tropical savanna and warm semi-arid climatic conditions. The study establishes discoloration of encapsulant material at 36.84% for the solar PV module investigated as the predominant mode of degradation mechanism for polycrystalline modules in warm semi-arid climatic conditions. It also indicates browning of encapsulating materials as the predominant mode of degradation mechanism in tropical savanna for both polycrystalline and monocrystalline modules accounting for 100%.

The study establishes short circuit current and fill factor as the major contributor to power degradation rates. This can be associated with the degradation mechanism of encapsulant material. The degraded encapsulant material affects the transmittance of light reaching the cells hence degrading the short circuit current of the solar PV module. The study established that the modules degrade exponentially. It was therefore established that majority of the modules will perfectly function as indicated in the warranties, however proper installation, operation, and maintenance is required.

The fourth objective of the study was to determine the reliability and failure rates of solar PV modules in tropical savanna and semi-arid climatic conditions. The study established reliability of solar PV modules of SDU, SPU, SGT, and SPG, as 82%, 40%, 35%, and 67%, respectively. The MTTF of the system components indicated that those components will operate as expected as per the warranty. The lifespan of the system components of solar PV modules was determined to range between 29 to 31 years, charger controllers 4 years, inverters ranged from 4 to 6 years, batteries 3 years, and transformers ranged between 15 to 25 years.

The study recommends that when more than one component parallel connections can be used to improve performance and reliability of the system. Finally, more studies to be carried out in the region to identify more installation designs and establish their failure rates, reliability and MTTF of different components.

## REFERENCES

- Adaramola, M. S., & Vågnes, E. E. T. (2015). Preliminary assessment of a small-scale rooftop PV-grid tied in Norwegian climatic conditions. *Energy Conversion and Management*, *90*, 458–465. <https://doi.org/10.1016/j.enconman.2014.11.028>
- Afonso, M. M. D., Carvalho, P. C. M., Antunes, F. L. M., & Hiluy Filho, J. J. (2015). Deterioration and performance evaluation of photovoltaic modules in a semi-arid climate. *Renewable Energy and Power Quality Journal*, 424–428. <https://doi.org/10.24084/repqj13.345>
- Aghdam, F. H., & Abapour, M. (2016). Reliability and Cost Analysis of Multistage Boost Converters Connected to PV Panels. *IEEE Journal of Photovoltaics*, *6*(4), 981–989. <https://doi.org/10.1109/JPHOTOV.2016.2566885>
- Al-Badi, A. (2020). Performance assessment of 20.4 kW eco-house grid-connected PV plant in Oman. *International Journal of Sustainable Engineering*, *13*(3), 230–241. <https://doi.org/10.1080/19397038.2019.1658824>
- Ali Sadat, S., Faraji, J., Nazififard, M., & Ketabi, A. (2021). The experimental analysis of dust deposition effect on solar photovoltaic panels in Iran's desert environment. *Sustainable Energy Technologies and Assessments*, *47*, 101542. <https://doi.org/10.1016/j.seta.2021.101542>
- Alquthami, T., & Menoufi, K. (2019). Soiling of Photovoltaic Modules: Comparing between Two Distinct Locations within the Framework of Developing the Photovoltaic Soiling Index (PVSI). *Sustainability*, *11*(17), 4697. <https://doi.org/10.3390/su11174697>
- Alshare, A., Tashtoush, B., Altarazi, S., & El-khalil, H. (2020). Energy and economic analysis of a 5 MW photovoltaic system in northern Jordan. *Case Studies in Thermal Engineering*, *21*, 100722. <https://doi.org/10.1016/j.csite.2020.100722>
- AlSkaif, T., Dev, S., Visser, L., Hossari, M., & van Sark, W. (2019). On the Interdependence and Importance of Meteorological Variables for Photovoltaic Output Power Estimation. *2019 IEEE 46th Photovoltaic Specialists Conference (PVSC)*, 2117–2120. <https://doi.org/10.1109/PVSC40753.2019.8981308>
- Arora, R., Arora, R., & Sridhara, S. N. (2022). Performance assessment of 186 kWp grid interactive solar photovoltaic plant in Northern India. *International Journal of Ambient Energy*, *43*(1), 128–141. <https://doi.org/10.1080/01430750.2019.1630312>
- Ashwini, K., Raj, A., & Gupta, M. (2016). Performance assessment and orientation optimization of 100 kWp grid connected solar PV system in Indian scenario. *2016 International Conference on Recent Advances and Innovations in Engineering (ICRAIE)*, 1–7. <https://doi.org/10.1109/ICRAIE.2016.7939505>



- Atsu, D., Seres, I., Aghaei, M., & Farkas, I. (2020). Analysis of long-term performance and reliability of PV modules under tropical climatic conditions in sub-Saharan. *Renewable Energy*, *162*, 285–295. <https://doi.org/10.1016/j.renene.2020.08.021>
- Ayadi, F., Colak, I., Genc, N., & Ibrahim Bulbul Halil. (2019). Impacts of wind speed and humidity on the performance of photovoltaic module. *8th International Conference on Renewable Energy Research and Applications*, 229–233.
- Babatunde, A. A., Abbasoglu, S., & Senol, M. (2018). Analysis of the impact of dust, tilt angle and orientation on performance of PV Plants. *Renewable and Sustainable Energy Reviews*, *90*, 1017–1026. <https://doi.org/10.1016/j.rser.2018.03.102>
- Banda, M. H., Nyeinga, K., & Okello, D. (2019). Performance evaluation of 830 kWp grid-connected photovoltaic power plant at Kamuzu International Airport-Malawi. *Energy for Sustainable Development*, *51*, 50–55. <https://doi.org/10.1016/j.esd.2019.05.005>
- Baschel, S., Koubli, E., Roy, J., & Gottschalg, R. (2018). Impact of Component Reliability on Large Scale Photovoltaic Systems' Performance. *Energies*, *11*(6), 1579. <https://doi.org/10.3390/en11061579>
- Behar, O., Sbarbaro, D., & Moran, L. (2021). Which is the most competitive solar power technology for integration into the existing copper mining plants: Photovoltaic (PV), Concentrating Solar Power (CSP), or hybrid PV-CSP? *Journal of Cleaner Production*, *287*, 125455. <https://doi.org/10.1016/j.jclepro.2020.125455>
- Bhattacharya, T., Chakraborty, A. K., & Pal, K. (2014). Effects of Ambient Temperature and Wind Speed on Performance of Monocrystalline Solar Photovoltaic Module in Tripura, India. *Journal of Solar Energy*, *2014*, 1–5. <https://doi.org/10.1155/2014/817078>
- Bouaichi, A., Merrouni, A. A., El Hassani, A., Naimi, Z., Ikken, B., Ghennioui, A., Benazzouz, A., El Amrani, A., & Messaoudi, C. (2017). Experimental evaluation of the discoloration effect on PV-modules performance drop. *Energy Procedia*, *119*, 818–827. <https://doi.org/10.1016/j.egypro.2017.07.107>
- Chawla, S., & Tikkiwal, V. A. (2021). Performance evaluation and degradation analysis of different photovoltaic technologies under arid conditions. *International Journal of Energy Research*, *45*(1), 786–798. <https://doi.org/10.1002/er.5901>
- Da Silva, I. P. (2017). *Towards a sustainable Strathmore University: 600 kW Grid Connected Solar Energy System* [Interview]. <https://strathmore.edu/news/towards-a-sustainable-strathmore-university-600-kw-grid-connected-solar-energy-system/>

- Daher, D. H., Gaillard, L., Amara, M., & Ménézo, C. (2018). Impact of tropical desert maritime climate on the performance of a PV grid-connected power plant. *Renewable Energy*, *125*, 729–737. <https://doi.org/10.1016/j.renene.2018.03.013>
- Dahlioui, D., Laarabi, B., & Barhdadi, A. (2019). Investigation of soiling impact on PV modules performance in semi-arid and hyper-arid climates in Morocco. *Energy for Sustainable Development*, *51*, 32–39. <https://doi.org/10.1016/j.esd.2019.05.001>
- El Hacen Jed, M., Ihaddadene, R., Ihaddadene, N., Elhadji Sidi, C. Elb., & EL Bah, M. (2020). Performance analysis of 954,809 kWp PV array of Sheikh Zayed solar power plant (Nouakchott, Mauritania). *Renewable Energy Focus*, *32*, 45–54. <https://doi.org/10.1016/j.ref.2019.11.002>
- Elhab, B. R., Sopian, K., Mat, S., Lim, C., Sulaiman, M. Y., Ruslan, M. H., & Saadatian, O. (n.d.). Optimizing tilt angles and orientations of solar panels for Kuala Lumpur, Malaysia. *Sci. Res. Essays*.
- EPRA. (2022). *Kenya tops East Africa in electricity access* (p. Nairobi, Kenya). <https://www.the-star.co.ke/business/2022-02-24-kenya-tops-east-africa-in-electricity-access/>
- Fernández-Solas, Á., Montes-Romero, J., Micheli, L., Almonacid, F., & Fernández, E. F. (2022). Estimation of soiling losses in photovoltaic modules of different technologies through analytical methods. *Energy*, *244*, 123173. <https://doi.org/10.1016/j.energy.2022.123173>
- Fraga, M. M., Campos, B. L. de O., Almeida, T. B. de, Fonseca, J. M. F. da, & Lins, V. de F. C. (2018). Analysis of the soiling effect on the performance of photovoltaic modules on a soccer stadium in Minas Gerais, Brazil. *Solar Energy*, *163*, 387–397. <https://doi.org/10.1016/j.solener.2018.02.025>
- Gakunga, M. (2021). *Kenya Lauded for Achieving 75% Electricity Access Rate*. <https://www.comesa.int/kenya-lauded-for-achieving-75-electricity-access-rate/>
- Ghosh A K. (2012). *Introduction to Measurements and Instrumentation*. PHI.
- Goel, S., & Sharma, R. (2021). Analysis of measured and simulated performance of a grid-connected PV system in eastern India. *Environment, Development and Sustainability*, *23*(1), 451–476. <https://doi.org/10.1007/s10668-020-00591-7>
- Gopi, A., Sudhakar, K., Keng, N. W., Krishnan, A. R., & Priya, S. S. (2021). Performance modeling of the weather impact on a utility-scale pv power plant in a tropical region. *International Journal of Photoenergy*, *2021*, 1–10. <https://doi.org/10.1155/2021/5551014>
- Hachicha, A. A., Al-Sawafta, I., & Said, Z. (2019). Impact of dust on the performance of solar photovoltaic (PV) systems under United Arab Emirates weather conditions. *Renewable Energy*, *141*, 287–297. <https://doi.org/10.1016/j.renene.2019.04.004>

- Hammad, B., Al-Abed, M., Al-Ghandoor, A., Al-Sardeah, A., & Al-Bashir, A. (2018). Modeling and analysis of dust and temperature effects on photovoltaic systems' performance and optimal cleaning frequency: Jordan case study. *Renewable and Sustainable Energy Reviews*, 82, 2218–2234. <https://doi.org/10.1016/j.rser.2017.08.070>
- IEC 61215-1-2-2021. (n.d.).
- IEC 61646-2008. (n.d.).
- IRENA. (2022). *Renewable Energy Statistics 2022* (p. 40). International Renewable Energy Agency. <https://irena.org/publications/2022/Jul/Renewable-Energy-Statistics-2022>
- Kagan, S., Giosa, E., Flottemesch, R., Andrews, R., Rand, J., Reed, M., Gostein, M., & Stueve, B. (2018). Impact of Non-Uniform Soiling on PV System Performance and Soiling Measurement. *2018 IEEE 7th World Conference on Photovoltaic Energy Conversion (WCPEC) (A Joint Conference of 45th IEEE PVSC, 28th PVSEC & 34th EU PVSEC)*, 3432–3435. <https://doi.org/10.1109/PVSC.2018.8547728>
- Kahoul, N., Houabes, M., & Sadok, M. (2014). Assessing the early degradation of photovoltaic modules performance in the Saharan region. *Energy Conversion and Management*, 82, 320–326. <https://doi.org/10.1016/j.enconman.2014.03.034>
- Kaundilya, S., Sastry, O. S., Bora, B., Rai, S., Bangar, M., Renu, Singh, R., Kumar, A., Yadav, K., Kumar, M., & Arun Prasath, R. (2018). Soiling Effect on Crystalline and Thin-film Technology PV Modules for Composite Climate Zone of India. *Materials Today: Proceedings*, 5(11), 23275–23280. <https://doi.org/10.1016/j.matpr.2018.11.060>
- Khalilnejad, A., Pour, M. M., Zarafshan, E., & Sarwat, A. (2016). Long term reliability analysis of components of photovoltaic system based on Markov process. *SoutheastCon 2016*, 1–5. <https://doi.org/10.1109/SECON.2016.7506762>
- KhareSaxena, A., Saxena, S., & Sudhakar, K. (2021). Energy performance and loss analysis of 100 kWp grid-connected rooftop solar photovoltaic system. *Building Services Engineering Research and Technology*, 42(4), 485–500. <https://doi.org/10.1177/0143624421994224>
- Khoo, Y. S., Nobre, A., Malhotra, R., Yang, D., Ruther, R., Reindl, T., & Aberle, A. G. (2014). Optimal Orientation and Tilt Angle for Maximizing in-Plane Solar Irradiation for PV Applications in Singapore. *IEEE Journal of Photovoltaics*, 4(2), 647–653. <https://doi.org/10.1109/JPHOTOV.2013.2292743>
- KNBS. (2022). *ECONOMIC SURVEY 2022* (p. 205). Kenya National Bureau of Statistics. <https://www.knbs.or.ke/download/economic-survey-2022/>

- Lillo-Bravo, I., González-Martínez, P., Larrañeta, M., & Guasumba-Codena, J. (2018). Impact of Energy Losses Due to Failures on Photovoltaic Plant Energy Balance. *Energies*, *11*(2), 363. <https://doi.org/10.3390/en11020363>
- Limmanee, A., Udomdachanut, N., Songtraï, S., Kaewniyompanit, S., Sato, Y., Nakaishi, M., Kittisontirak, S., Sriprapha, K., & Sakamoto, Y. (2016). Field performance and degradation rates of different types of photovoltaic modules: A case study in Thailand. *Renewable Energy*, *89*, 12–17. <https://doi.org/10.1016/j.renene.2015.11.088>
- Malvoni, M., Kumar, N. M., Chopra, S. S., & Hatziargyriou, N. (2020). Performance and degradation assessment of large-scale grid-connected solar photovoltaic power plant in tropical semi-arid environment of India. *Solar Energy*, *203*, 101–113. <https://doi.org/10.1016/j.solener.2020.04.011>
- Martín-Martínez, S., Cañas-Carretón, M., Honrubia-Escribano, A., & Gómez-Lázaro, E. (2019). Performance evaluation of large solar photovoltaic power plants in Spain. *Energy Conversion and Management*, *183*, 515–528. <https://doi.org/10.1016/j.enconman.2018.12.116>
- Menoufi, K. (2017). Dust Accumulation on the Surface of Photovoltaic Panels: Introducing the Photovoltaic Soiling Index (PVSI). *Sustainability*, *9*(6), 963. <https://doi.org/10.3390/su9060963>
- Menoufi, K., Farghal, H. F. M., Farghali, A. A., & Khedr, M. H. (2017). Dust accumulation on photovoltaic panels: A case study at the East Bank of the Nile (Beni-Suef, Egypt). *Energy Procedia*, *128*, 24–31. <https://doi.org/10.1016/j.egypro.2017.09.010>
- Mensah, L. D., Yamoah, J. O., & Adaramola, M. S. (2019). Performance evaluation of a utility-scale grid-tied solar photovoltaic (PV) installation in Ghana. *Energy for Sustainable Development*, *48*, 82–87. <https://doi.org/10.1016/j.esd.2018.11.003>
- Ministry of Energy, Kenya. (2012). *FEED-IN-TARIFFS POLICY ON WIND, BIOMASS, SMALL-HYDRO, GEOTHERMAL, BIOGAS AND SOLAR RESOURCE GENERATED ELECTRICITY*. GoK. <https://repository.kippra.or.ke/bitstream/handle/123456789/1016/Feed%20in%20Tariff%20Policy%202012.pdf?sequence=1>
- Mohammed, S., Boumediene, B., & Miloud, B. (2016). Assessment of PV Modules Degradation based on Performances and Visual Inspection in Algerian Sahara. *International Journal of Renewable Energy Research*, *v6i1*. <https://doi.org/10.20508/ijrer.v6i1.3155.g6765>
- Munene, L. N. (2019). Reducing Carbon Emissions: Strathmore University Contributions Towards Sustainable Development in Kenya. *African Journal of Business Ethics*, *13*(1). <https://doi.org/10.15249/13-1-173>

- Munoz, M. A., Alonso-García, M. C., Vela, N., & Chenlo, F. (2011). Early degradation of silicon PV modules and guaranty conditions. *Solar Energy*, 85(9), 2264–2274. <https://doi.org/10.1016/j.solener.2011.06.011>
- National Energy Policy, Kenya. (2018). *NATIONAL ENERGY POLICY*. GoK. [https://repository.kippra.or.ke/bitstream/handle/123456789/1947/BL4PdOqKtxFT\\_National%20Energy%20Policy%20October%20%202018.pdf?sequence=1&isAllowed=y](https://repository.kippra.or.ke/bitstream/handle/123456789/1947/BL4PdOqKtxFT_National%20Energy%20Policy%20October%20%202018.pdf?sequence=1&isAllowed=y)
- Ndiaye, A., Charki, A., Kobi, A., Kébé, C. M. F., Ndiaye, P. A., & Sambou, V. (2013). Degradations of silicon photovoltaic modules: A literature review. *Solar Energy*, 96, 140–151. <https://doi.org/10.1016/j.solener.2013.07.005>
- Ndiaye, A., Kébé, C. M. F., Charki, A., Ndiaye, P. A., Sambou, V., & Kobi, A. (2014). Degradation evaluation of crystalline-silicon photovoltaic modules after a few operation years in a tropical environment. *Solar Energy*, 103, 70–77. <https://doi.org/10.1016/j.solener.2014.02.006>
- Necaibia, A., Bouraiou, A., Ziane, A., Sahouane, N., Hassani, S., Mostefaoui, M., Dabou, R., & Mouhadjer, S. (2018). Analytical assessment of the outdoor performance and efficiency of grid-tied photovoltaic system under hot dry climate in the south of Algeria. *Energy Conversion and Management*, 171, 778–786. <https://doi.org/10.1016/j.enconman.2018.06.020>
- Ngre, S. M., Makokha, A. B., Ataro, E. O., & Adaramola, M. S. (2022). Degradation analysis of Solar photovoltaic module under warm semiarid and tropical savanna climatic conditions of East Africa. *International Journal of Energy and Environmental Engineering*, 13(2), 431–447. <https://doi.org/10.1007/s40095-021-00454-5>
- Njok, A. O., & Ogbulezie, J. C. (2019). The Effect of Relative Humidity and Temperature on Polycrystalline Solar Panels Installed Close to a River. *Physical Science International Journal*, 20(4), 1–11. <https://doi.org/10.9734/PSIJ/2018/44760>
- Nur'Aini, E., Budiarto, R., Setiawan, B., & Ma'arif, A. (2021). Reliability Analysis and Maintainability for the Design of Grid and Hybrid Solar Power Plant Systems in Wonogiri Regency. *ELKHA*, 13(1), 77. <https://doi.org/10.26418/elkha.v13i1.46011>
- Olivares, D., Ferrada, P., Bijman, J., Rodríguez, S., Trigo-González, M., Marzo, A., Rabanal-Arabach, J., Alonso-Montesinos, J., Batlles, F. J., & Fuentealba, E. (2020). Determination of the Soiling Impact on Photovoltaic Modules at the Coastal Area of the Atacama Desert. *Energies*, 13(15), 3819. <https://doi.org/10.3390/en13153819>
- Oloya, I. T., Gutu, T. J.L., & Adaramola, M. S. (2021). Techno-economic assessment of 10 MW centralised grid-tied solar photovoltaic system in Uganda. *Case Studies in Thermal Engineering*, 25, 100928. <https://doi.org/10.1016/j.csite.2021.100928>

- Omar, M. A., & Mahmoud, M. M. (2018). Grid connected PV- home systems in Palestine: A review on technical performance, effects and economic feasibility. *Renewable and Sustainable Energy Reviews*, 82, 2490–2497. <https://doi.org/10.1016/j.rser.2017.09.008>
- Oreški, G., Lang, R., & Wallner. (2009). *Evaluation of the aging behavior of ethylene copolymer flms for solar applications under accelerated weathering conditions*. [University of Leoben]. <https://pure.unileoben.ac.at/portal/files/1849857/AC07138315n01vt.pdf#page=89>
- Quansah, D. A., & Adaramola, M. S. (2018). Ageing and degradation in solar photovoltaic modules installed in northern Ghana. *Solar Energy*, 173, 834–847. <https://doi.org/10.1016/j.solener.2018.08.021>
- Quansah, D. A., Adaramola, M. S., Appiah, G. K., & Edwin, I. A. (2017). Performance analysis of different grid-connected solar photovoltaic (PV) system technologies with combined capacity of 20 kW located in humid tropical climate. *International Journal of Hydrogen Energy*, 42(7), 4626–4635. <https://doi.org/10.1016/j.ijhydene.2016.10.119>
- Quansah, D. A., Adaramola, M. S., & Takyi, G. (2020). Degradation and longevity of solar photovoltaic modules—An analysis of recent field studies in Ghana. *Energy Science & Engineering*, 8(6), 2116–2128. <https://doi.org/10.1002/ese3.651>
- Rajput, P., Tiwari, G. N., Sastry, O. S., Bora, B., & Sharma, V. (2016). Degradation of mono-crystalline photovoltaic modules after 22 years of outdoor exposure in the composite climate of India. *Solar Energy*, 135, 786–795. <https://doi.org/10.1016/j.solener.2016.06.047>
- Ramanan, P., Kalidasa, M. K., & Karthick, A. (2019). Performance analysis and energy metrics of grid-connected photovoltaic systems. *Energy for Sustainable Development*, 52, 104–115. <https://doi.org/10.1016/j.esd.2019.08.001>
- Ramli, M. A. M., Prasetyono, E., Wicaksana, R. W., Windarko, N. A., Sedraoui, K., & Al-Turki, Y. A. (2016). On the investigation of photovoltaic output power reduction due to dust accumulation and weather conditions. *Renewable Energy*, 99, 836–844. <https://doi.org/10.1016/j.renene.2016.07.063>
- Rao, A., Pillai, R., Mani, M., & Ramamurthy, P. (2014). Influence of Dust Deposition on Photovoltaic Panel Performance. *Energy Procedia*, 54, 690–700. <https://doi.org/10.1016/j.egypro.2014.07.310>
- Realini, A. (n.d.). *Mean Time Before Failure of Photovoltaic modules*. 58.
- Saad, B., Errattahi, R., Hannani, A. E., & Aqqal, A. (2022). The Impact of Forecasting Horizon and Resolution on PV Power Prediction using Artificial Neural Networks. *2022 11th International Symposium on Signal, Image, Video and Communications (ISIVC)*, 1–6. <https://doi.org/10.1109/ISIVC54825.2022.9800748>

- Sahouane, N., Dabou, R., Ziane, A., Neçaibia, A., Bouraiou, A., Rouabhia, A., & Mohammed, B. (2019a). Energy and economic efficiency performance assessment of a 28 kWp photovoltaic grid-connected system under desertic weather conditions in Algerian Sahara. *Renewable Energy*, *143*, 1318–1330. <https://doi.org/10.1016/j.renene.2019.05.086>
- Sahouane, N., Dabou, R., Ziane, A., Neçaibia, A., Bouraiou, A., Rouabhia, A., & Mohammed, B. (2019b). Energy and economic efficiency performance assessment of a 28 kWp photovoltaic grid-connected system under desertic weather conditions in Algerian Sahara. *Renewable Energy*, *143*, 1318–1330. <https://doi.org/10.1016/j.renene.2019.05.086>
- Saleem, E. A., & Rashid, E. F. (2016). *The Efficiency of Solar PV System*. 7.
- Salimi, H., Ahmadi Danesh Ashtiani, H., Mirabdollah Lavasani, A., & Fazaeli, R. (2020). Experimental analysis and modeling of weather condition effects on photovoltaic systems' performance: Tehran case study. *Energy Sources, Part A: Recovery, Utilization, and Environmental Effects*, 1–13. <https://doi.org/10.1080/15567036.2020.1765902>
- Saxena, A. K., Saxena, S., & Sudhakar, K. (2021). Energy, economic and environmental performance assessment of a grid-tied rooftop system in different cities of India based on 3E analysis. *Clean Energy*, *5*(2), 288–301. <https://doi.org/10.1093/ce/zkab008>
- Sayed, A., El-Shimy, M., El-Metwally, M., & Elshahed, M. (2019). Reliability, Availability and Maintainability Analysis for Grid-Connected Solar Photovoltaic Systems. *Energies*, *12*(7), 1213. <https://doi.org/10.3390/en12071213>
- Schill, C., Brachmann, S., & Koehl, M. (2015). Impact of soiling on IV-curves and efficiency of PV-modules. *Solar Energy*, *112*, 259–262. <https://doi.org/10.1016/j.solener.2014.12.003>
- Semaoui, S., Abdeladim, K., Taghezouit, B., Hadj Arab, A., Razagui, A., Bacha, S., Boulahchiche, S., Bouacha, S., & Gherbi, A. (2020). Experimental investigation of soiling impact on grid connected PV power. *Energy Reports*, *6*, 302–308. <https://doi.org/10.1016/j.egy.2019.08.060>
- Seme, S., Sredenšek, K., Štumberger, B., & Hadžiselimović, M. (2019). Analysis of the performance of photovoltaic systems in Slovenia. *Solar Energy*, *180*, 550–558. <https://doi.org/10.1016/j.solener.2019.01.062>
- Shahidirad, N., Niroomand, M., & Hooshmand, R.-A. (2018). Investigation of PV Power Plant Structures Based on Monte Carlo Reliability and Economic Analysis. *IEEE Journal of Photovoltaics*, 1–9. <https://doi.org/10.1109/JPHOTOV.2018.2814922>
- Sharma, P., Uppal, A., Kesari, D. J. P., & Singh, D. P. (2016). *Economic Analysis of Grid Connected 40 KW Solar Photovoltaic System at Administration Building, DTU*. 5.

- Sharma, V., & Chandel, S. S. (2013). Performance analysis of a 190 kWp grid interactive solar photovoltaic power plant in India. *Energy*, *55*, 476–485. <https://doi.org/10.1016/j.energy.2013.03.075>
- Sharma, V., Sastry, O. S., Kumar, A., Bora, B., & Chandel, S. S. (2014). Degradation analysis of a-Si, (HIT) hetero-junction intrinsic thin layer silicon and m-C-Si solar photovoltaic technologies under outdoor conditions. *Energy*, *72*, 536–546. <https://doi.org/10.1016/j.energy.2014.05.078>
- Shiva Kumar, B., & Sudhakar, K. (2015). Performance evaluation of 10 MW grid connected solar photovoltaic power plant in India. *Energy Reports*, *1*, 184–192. <https://doi.org/10.1016/j.egy.2015.10.001>
- Silva, A. M., Melo, F. C., Reis, J. H., & Freitas, L. C. G. (2019). The study and application of evaluation methods for photovoltaic modules under real operational conditions, in a region of the Brazilian Southeast. *Renewable Energy*, *138*, 1189–1204. <https://doi.org/10.1016/j.renene.2019.01.129>
- Silvestre, S., Kichou, S., Guglielminotti, L., Nofuentes, G., & Alonso-Abella, M. (2016). Degradation analysis of thin film photovoltaic modules under outdoor long term exposure in Spanish continental climate conditions. *Solar Energy*, *139*, 599–607. <https://doi.org/10.1016/j.solener.2016.10.030>
- Singh, S. S., & Fernandez, E. (2015). Reliability evaluation of a solar photovoltaic system with and without battery storage. *2015 Annual IEEE India Conference (INDICON)*, 1–6. <https://doi.org/10.1109/INDICON.2015.7443379>
- Sreenath, S., Sudhakar, K., & Af, Y. (2021). 7E analysis of a conceptual utility-scale land-based solar photovoltaic power plant. *Energy*, *219*, 119610. <https://doi.org/10.1016/j.energy.2020.119610>
- Sreenath, S., Sudhakar, K., & Yusop, A. F. (2022). Carbon mitigation potential of the airport-based solar PV plants in the Indian context. *International Journal of Ambient Energy*, *43*(1), 1311–1319. <https://doi.org/10.1080/01430750.2019.1696888>
- Takase, M., Kipkoech, R., & Essandoh, P. K. (2021). A comprehensive review of energy scenario and sustainable energy in Kenya. *Fuel Communications*, *7*, 100015. <https://doi.org/10.1016/j.jfueco.2021.100015>
- Thotakura, S. (2020). Operational performance of megawatt-scale grid integrated rooftop solar PV system in tropical wet and dry climates of India. *Case Studies in Thermal Engineering*, *11*.
- Tudisca, S., Di Trapani, A. M., Sgroi, F., Testa, R., & Squatrito, R. (2013). Economic analysis of PV systems on buildings in Sicilian farms. *Renewable and Sustainable Energy Reviews*, *28*, 691–701. <https://doi.org/10.1016/j.rser.2013.08.035>



- Ullah, A., Amin, A., Haider, T., Saleem, M., & Butt, N. Z. (2020). Investigation of soiling effects, dust chemistry and optimum cleaning schedule for PV modules in Lahore, Pakistan. *Renewable Energy*, *150*, 456–468. <https://doi.org/10.1016/j.renene.2019.12.090>
- Vidal, H., Rivera, M., Wheeler, P., & Vicencio, N. (2020). The Analysis Performance of a Grid-Connected 8.2 kWp Photovoltaic System in the Patagonia Region. *Sustainability*, *12*(21), 9227. <https://doi.org/10.3390/su12219227>
- Wohlgemuth, J. H., & Kurtz, S. (2011). Reliability testing beyond Qualification as a key component in photovoltaic's progress toward grid parity. *2011 International Reliability Physics Symposium*, 5E.3.1-5E.3.6. <https://doi.org/10.1109/IRPS.2011.5784534>
- Yadav, A., Pillai, S. R., Singh, N., Philip, S. A., & Mohanan, V. (2021). Preliminary investigation of dust deposition on solar cells. *Materials Today: Proceedings*, *46*, 6812–6815. <https://doi.org/10.1016/j.matpr.2021.04.361>
- Yadav, S. K., & Bajpai, U. (2018). Performance evaluation of a rooftop solar photovoltaic power plant in Northern India. *Energy for Sustainable Development*, *43*, 130–138. <https://doi.org/10.1016/j.esd.2018.01.006>
- Yan, W., Liu, W., & Kong, W. (2021). Reliability evaluation of PV modules based on exponential dispersion process. *Energy Reports*, *7*, 3023–3032. <https://doi.org/10.1016/j.egyr.2021.05.033>
- Yazdani, H., & Yaghoubi, M. (2021). Techno-economic study of photovoltaic systems performance in Shiraz, Iran. *Renewable Energy*, *172*, 251–262. <https://doi.org/10.1016/j.renene.2021.03.012>
- Yu, C., Khoo, Y., Chai, J., Han, S., & Yao, J. (2019). Optimal Orientation and Tilt Angle for Maximizing in-Plane Solar Irradiation for PV Applications in Japan. *Sustainability*, *11*(7), 2016. <https://doi.org/10.3390/su11072016>
- Yunus Khan, T. M., Soudagar, M. Elahi. M., Kanchan, M., Afzal, A., Banapurmath, Nagaraj. R., Akram, N., Mane, S. D., & Shahapurkar, K. (2020). Optimum location and influence of tilt angle on performance of solar PV panels. *Journal of Thermal Analysis and Calorimetry*, *141*(1), 511–532. <https://doi.org/10.1007/s10973-019-09089-5>
- Ziane, A., Necaibia, A., Sahouane, N., Dabou, R., Mostefaoui, M., Bouraiou, A., Khelifi, S., Rouabhia, A., & Blal, M. (2021). Photovoltaic output power performance assessment and forecasting: Impact of meteorological variables. *Solar Energy*, *220*, 745–757. <https://doi.org/10.1016/j.solener.2021.04.004>
- Zini, G., Mangeant, C., & Merten, J. (2011). Reliability of large-scale grid-connected photovoltaic systems. *Renewable Energy*, *36*(9), 2334–2340. <https://doi.org/10.1016/j.renene.2011.01.036>

## APPENDICES

### Appendix I: System 1 performance analysis (2015)

	GHI	AT	WS	kWh/m <sup>2</sup>	YR	Eac (Wh)	YF (kWh/kW)	Eac(kWh)	PR	CUF	$\eta$	days	hours	Pac(W)
1	537.97	21.75	3.88	6.50	6.50	3015762.30	4.86	3015.76	0.75	0.20	10.08	31	12.07	7100.63
2	602.55	22.38	4.79	7.27	7.27	2598736.80	4.64	2598.74	0.64	0.19	8.68	28	12.07	6851.15
3	603.94	21.94	5.82	7.37	7.37	2979227.77	4.81	2979.23	0.65	0.20	9.03	31	12.20	7139.61
4	498.62	20.59	2.72	5.93	5.93	2303998.30	3.84	2304.00	0.65	0.16	9.33	30	11.89	6092.64
5	426.16	19.96	1.76	4.93	4.93	1968375.90	3.17	1968.38	0.64	0.13	9.18	31	11.58	5123.74
6	361.81	18.77	0.98	4.11	4.11	1825363.95	3.04	1825.36	0.74	0.13	10.30	30	11.35	4877.92
7	439.59	18.40	1.42	5.12	5.12	1730342.16	2.79	1730.34	0.55	0.12	7.71	31	11.65	4439.26
8	415.51	18.79	2.06	4.85	4.85	1931978.20	3.12	1931.98	0.64	0.13	9.20	31	11.67	5007.12
9	475.47	20.56	1.67	5.71	5.71	2476354.08	4.13	2476.35	0.72	0.17	10.56	30	12.00	6572.39
10	477.78	21.00	4.32	5.93	5.93	2384113.24	3.85	2384.11	0.65	0.16	9.59	31	12.42	6001.00
11	324.08	19.76	3.87	3.98	3.98	1963008.47	3.27	1963.01	0.82	0.14	12.03	30	12.27	5103.47
12	384.73	20.65	4.00	4.81	4.81	2503764.02	4.04	2503.76	0.84	0.17	12.07	31	12.49	6081.96
AVG	462.35	20.38	3.11		5.54		3.80	27681.03	0.69	0.16	9.81			5865.91

### Appendix II: System 1 performance analysis (2016)

	GHI	AT	WS	kWh/m <sup>2</sup>	YR	Eac (Wh)	YF (kWh/kW)	Eac(kWh)	PR	CUF	$\eta$	days	hours	Pac(W)
1	499.08	21.64	5.90	6.03	6.03	2403185.29	3.88	2403.19	0.64	0.16	9.09	31	12.07	5942.15
2	544.68	21.79	5.99	6.57	6.57	2419283.82	4.17	2419.28	0.63	0.17	8.92	29	12.07	6364.69
3	605.48	22.65	6.23	7.39	7.39	2826250.31	4.56	2826.25	0.62	0.19	8.50	31	12.20	6737.57
4	374.77	20.65	4.39	4.45	4.45	1762234.75	2.94	1762.23	0.66	0.12	9.77	30	11.89	4792.21
5	386.35	19.63	2.13	4.47	4.47	1452930.19	2.34	1452.93	0.52	0.10	7.71	31	11.58	3902.67
6	321.99	18.50	1.92	3.65	3.65	1306300.94	2.18	1306.30	0.60	0.09	8.78	30	11.35	3702.52
7	353.01	18.27	0.61	4.11	4.11	1619848.90	2.61	1619.85	0.64	0.11	9.44	31	11.65	4364.25
8	413.43	18.53	0.84	4.82	4.82	1632864.52	2.63	1632.86	0.55	0.11	8.12	31	11.67	4396.23
9	458.11	19.63	0.53	5.50	5.50	2129849.06	3.55	2129.85	0.65	0.15	9.43	30	12.00	5656.22
10	459.26	21.39	2.87	5.70	5.70	2793284.11	4.51	2793.28	0.79	0.19	11.57	31	12.42	6960.43
11	354.86	20.14	4.67	4.35	4.35	2086440.16	3.48	2086.44	0.80	0.14	11.44	30	12.27	5315.01
12	393.98	20.66	6.37	4.92	4.92	2762459.78	4.46	2762.46	0.91	0.19	13.22	31	12.49	6822.64
AVG	430.42	20.29	3.54		5.17		3.44	25194.93	0.67	0.14	9.67			5413.05

**Key:** AT-Ambient temperature, WS-Wind speed. GHI- Global horizontal irradiance

**Appendix III: System 1 performance analysis (2017)**

	GHI	AT	WS	kWh/m <sup>2</sup>	YR	Eac (Wh)	YF (kWh/kW)	PR	Eac(kWh)	CUF	η	days	hours	Pac(W)
1	577.78	22.53	4.67	6.98	6.98	3176082.06	5.12	0.73	3176.08	0.21	9.65	31	12.07	7300.80
2	657.88	22.14	5.48	7.94	7.94	2744505.80	4.90	0.62	2744.51	0.20	8.47	28	12.07	7292.76
3	607.88	22.40	4.60	7.42	7.42	2938839.46	4.74	0.64	2938.84	0.20	8.77	31	12.20	6979.73
4	351.39	21.29	4.37	4.57	4.57	2306708.11	3.84	0.84	2306.71	0.16	13.10	30	11.89	6025.55
5	381.95	20.09	1.72	4.42	4.42	1388594.51	2.24	0.51	1388.59	0.09	9.85	31	11.58	4923.89
6	271.07	19.50	1.71	3.08	3.08	1126781.39	1.88	0.61	1126.78	0.08	12.93	30	11.35	4590.91
7	238.43	18.81	1.26	3.58	3.58	1867586.80	3.01	0.84	1867.59	0.13	15.87	31	11.65	4955.41
8	411.35	19.06	1.76	4.80	4.80	1633175.96	2.63	0.55	1633.18	0.11	8.03	31	11.67	4324.25
9	440.74	19.53	2.58	5.29	5.29	2112827.12	3.52	0.67	2112.83	0.15	9.63	30	12.00	5558.93
10	440.74	20.72	3.62	5.47	5.47	2578497.38	4.16	0.76	2578.50	0.17	11.15	31	12.42	6437.58
11	385.65	19.76	4.45	4.73	4.73	2123259.18	3.54	0.75	2123.26	0.15	10.94	30	12.27	5523.95
12	403.24	20.94	4.77	5.04	5.04	2689693.73	4.34	0.86	2689.69	0.18	12.35	31	12.49	6522.35
AVG	430.67	20.56	3.42		5.28		3.66	0.70	26686.55	0.15	10.89			5869.68

**Appendix IV: System 1 performance analysis (2018)**

	GHI	AT	WS	kWh/m <sup>2</sup>	YR	Eac (Wh)	YF (kWh/kW)	PR	Eac(kWh)	CUF	η	days	hours	Pac(W)
1	601.39	21.63	1.30	7.26	7.26	2237850.32	3.61	0.50	2237.85	0.15	7.37	31	12.07	5802.74
2	599.54	22.40	6.07	7.24	7.24	2623043.23	4.68	0.65	2623.04	0.20	9.55	28	12.07	7498.28
3	604.63	20.28	3.00	7.38	7.38	2024831.05	3.27	0.44	2024.83	0.14	6.53	31	12.20	5169.61
4	401.62	19.65	2.60	4.77	4.77	2055106.91	3.43	0.72	2055.11	0.14	10.55	30	11.89	5549.25
5	390.74	19.10	0.60	4.52	4.52	2024826.63	3.27	0.72	2024.83	0.14	10.07	31	11.58	5151.44
6	381.25	18.00	0.31	4.33	4.33	1497552.08	2.50	0.58	1497.55	0.10	8.24	30	11.35	4112.96
7	343.68	17.54	0.31	4.00	4.00	1454729.80	2.35	0.59	1454.73	0.10	8.62	31	11.65	3879.35
8	413.43	18.38	0.47	4.82	4.82	1666528.88	2.69	0.56	1666.53	0.11	8.01	31	11.67	4334.84
9	451.62	19.90	1.94	5.42	5.42	2292705.74	3.82	0.70	2292.71	0.16	10.30	30	12.00	6093.64
10	461.35	20.26	2.97	5.73	5.73	2257689.95	3.64	0.64	2257.69	0.15	9.30	31	12.42	5620.25
11	383.10	20.79	4.49	4.70	4.70	2361852.64	3.94	0.84	2361.85	0.16	12.00	30	12.27	6019.28
12	398.85	21.03	3.96	4.98	4.98	2445365.38	3.94	0.79	2445.37	0.16	11.68	31	12.49	6099.45
AVG	452.60	19.91	2.34		5.43		3.43	0.64	24942.08	0.14	9.35			5444.26

### Appendix V: System 1 performance analysis (2019)

	GHI	AT	WS	kWh/m <sup>2</sup>	YR	Eac (Wh)	YF (kWh/kW)	PR	Eac(kWh)	CUF	$\eta$	days	hours	Pac(W)
1	589.36	22.02	4.39	7.12	7.12	2879951.13	4.65	0.65	2879.95	0.19	9.04	31	12.07	6972.82
2	642.13	22.71	5.65	7.75	7.75	2649644.67	4.73	0.61	2649.64	0.20	8.43	28	12.07	7088.48
3	473.85	23.80	5.31	5.78	5.78	3033514.95	4.89	0.85	3033.51	0.20	11.80	31	12.20	7324.66
4	359.96	22.78	3.98	5.40	5.40	2510073.37	4.18	0.77	2510.07	0.17	13.76	30	11.89	6487.19
5	274.31	19.82	2.37	4.11	4.11	1932215.59	3.12	0.76	1932.22	0.13	13.83	31	11.58	4968.18
6	271.07	18.84	0.64	3.08	3.08	1509694.62	2.52	0.82	1509.69	0.10	11.65	30	11.35	4133.82
7	341.90	19.05	1.19	3.98	3.98	1694079.14	2.73	0.69	1694.08	0.11	10.12	31	11.65	4532.35
8	412.04	19.37	1.44	4.81	4.81	1893363.22	3.05	0.64	1893.36	0.13	9.18	31	11.67	4954.39
9	458.11	20.21	2.17	5.50	5.50	2160753.08	3.60	0.65	2160.75	0.15	9.33	30	12.00	5595.59
10	459.26	20.52	3.07	5.70	5.70	2119460.67	3.42	0.60	2119.46	0.14	8.73	31	12.42	5251.85
11	361.92	20.75	3.62	4.44	4.44	2285816.72	3.81	0.86	2285.82	0.16	12.49	30	12.27	5918.01
12	395.20	20.54	3.27	4.94	4.94	2151944.62	3.47	0.70	2151.94	0.14	10.53	31	12.49	5447.39
AVG	419.93	20.87	3.09		5.22		3.68	0.72	26820.51	0.15	10.74			5722.89

### Appendix VI: System 2 performance analysis (2015)

	GHI	AT	WS	kWh/m <sup>2</sup>	YR	Eac (Wh)	YF (kWh/kW)	PR	Eac(kWh)	CUF	$\eta$	days	hours	Pac(W)
1	537.97	21.75	3.88	6.50	6.50	2724988.13	4.40	0.68	2724.99	0.18	9.51	31	12.07	6702.61
2	602.55	22.38	4.79	7.27	7.27	2474839.13	4.42	0.61	2474.84	0.18	8.38	28	12.07	6614.49
3	603.94	21.94	5.82	7.37	7.37	2963666.58	4.78	0.65	2963.67	0.20	9.19	31	12.20	7267.41
4	498.62	20.59	2.72	5.93	5.93	2408240.16	4.01	0.68	2408.24	0.17	9.80	30	11.89	6395.94
5	426.16	19.96	1.76	4.93	4.93	2123612.67	3.43	0.69	2123.61	0.14	9.83	31	11.58	5483.20
6	361.81	18.77	0.98	4.11	4.11	1974655.18	3.29	0.80	1974.66	0.14	11.15	30	11.35	5282.24
7	439.59	18.40	1.42	5.12	5.12	1938398.74	3.13	0.61	1938.40	0.13	8.66	31	11.65	4982.31
8	415.51	18.79	2.06	4.85	4.85	2109740.30	3.40	0.70	2109.74	0.14	10.18	31	11.67	5540.76
9	475.47	20.56	1.67	5.71	5.71	2547717.17	4.25	0.74	2547.72	0.18	10.89	30	12.00	6783.04
10	477.78	21.00	4.32	5.93	5.93	2319731.30	3.74	0.63	2319.73	0.16	9.27	31	12.42	5801.75
11	324.08	19.76	3.87	3.98	3.98	1878902.67	3.13	0.79	1878.90	0.13	11.41	30	12.27	4843.53
12	384.73	20.65	4.00	4.81	4.81	2274927.21	3.67	0.76	2274.93	0.15	11.19	31	12.49	5637.01
AVG	462.35	20.38	3.11		5.54		3.80	0.70	27739.42	0.16	9.96			5944.52

**Appendix VII: System 2 performance analysis (2016)**

	GHI	AT	WS	kWh/m <sup>2</sup>	YR	Eac (Wh)	YF (kWh/kW)	PR	Eac(kWh)	CUF	η	days	hours	Pac(W)
1	499.08	21.64	5.90	6.03	6.03	2251118.49	3.63	0.60	2251.12	0.15	8.79	31	12.07	5745.02
2	544.68	21.79	5.99	6.57	6.57	2418150.42	4.17	0.63	2418.15	0.17	9.12	29	12.07	6503.96
3	605.48	22.65	6.23	7.39	7.39	2910695.30	4.69	0.64	2910.70	0.20	8.93	31	12.20	7081.72
4	374.77	20.65	4.39	4.45	4.45	1875206.52	3.13	0.70	1875.21	0.13	10.22	30	11.89	5017.12
5	386.35	19.63	2.13	4.47	4.47	1594720.91	2.57	0.58	1594.72	0.11	8.38	31	11.58	4240.55
6	321.99	18.50	1.92	3.65	3.65	1478193.49	2.46	0.67	1478.19	0.10	9.82	30	11.35	4141.64
7	353.01	18.27	0.61	4.11	4.11	1811845.85	2.92	0.71	1811.85	0.12	10.53	31	11.65	4868.12
8	413.43	18.53	0.84	4.82	4.82	1764846.48	2.85	0.59	1764.85	0.12	8.66	31	11.67	4688.14
9	458.11	19.63	0.53	5.50	5.50	2179895.09	3.63	0.66	2179.90	0.15	9.66	30	12.00	5793.34
10	459.26	21.39	2.87	5.70	5.70	2721413.35	4.39	0.77	2721.41	0.18	11.26	31	12.42	6771.93
11	354.86	20.14	4.67	4.35	4.35	2005171.00	3.34	0.77	2005.17	0.14	11.02	30	12.27	5121.91
12	393.98	20.66	6.37	4.92	4.92	2494502.41	4.02	0.82	2494.50	0.17	11.99	31	12.49	6184.31
AVG	430.42	20.29	3.54		5.17		3.48	0.68	25505.76	0.15	9.87			5513.15

**Appendix VIII: System 2 performance analysis (2017)**

	GHI	AT	WS	kWh/m <sup>2</sup>	YR	Eac (Wh)	YF (kWh/kW)	PR	Eac(kWh)	CUF	η	days	hours	Pac(W)
1	577.78	22.53	4.67	6.98	6.98	2820994.97	4.55	0.65	2820.99	0.19	9.13	31	12.07	6908.96
2	657.88	22.14	5.48	7.94	7.94	2602268.02	4.65	0.59	2602.27	0.19	8.19	28	12.07	7055.38
3	607.88	22.40	4.60	7.42	7.42	2942485.64	4.75	0.64	2942.49	0.20	8.93	31	12.20	7109.22
4	351.39	21.29	4.37	4.18	4.18	2425426.23	4.04	0.97	2425.43	0.17	13.53	30	11.89	6226.27
5	381.95	20.09	1.72	4.42	4.42	1475536.34	2.38	0.54	1475.54	0.10	10.44	31	11.58	5219.59
6	271.07	19.50	1.71	3.08	3.08	1212110.45	2.02	0.66	1212.11	0.08	14.02	30	11.35	4974.82
7	238.43	18.81	1.26	3.58	3.58	2017034.34	3.25	0.91	2017.03	0.14	17.06	31	11.65	5325.71
8	411.35	19.06	1.76	4.80	4.80	1726864.68	2.79	0.58	1726.86	0.12	8.47	31	11.67	4561.11
9	440.74	19.53	2.58	5.29	5.29	2148204.33	3.58	0.68	2148.20	0.15	9.77	30	12.00	5640.88
10	440.74	20.72	3.62	5.47	5.47	2499193.88	4.03	0.74	2499.19	0.17	10.72	31	12.42	6184.60
11	385.65	19.76	4.45	4.73	4.73	2039286.05	3.40	0.72	2039.29	0.14	10.39	30	12.27	5246.53
12	403.24	20.94	4.77	5.04	5.04	2401243.03	3.87	0.77	2401.24	0.16	11.34	31	12.49	5989.77
AVG	430.67	20.56	3.42		5.24		3.61	0.70	26310.65	0.15	11.00			5870.24

### Appendix IX: System 2 performance analysis (2018)

	GHI	AT	WS	kWh/m <sup>2</sup>	YR	Eac (Wh)	YF (kWh/kW)	PR	Eac(kWh)	CUF	η	days	hours	Pac(W)
1	601.39	21.63	1.30	7.26	7.26	2330169.55	3.76	0.52	2330.17	0.16	7.49	31	12.07	5898.25
2	599.54	22.40	6.07	7.24	7.24	2643446.79	4.72	0.65	2643.45	0.20	9.08	28	12.07	7131.15
3	604.63	20.28	3.00	7.38	7.38	2022277.80	3.26	0.44	2022.28	0.14	6.54	31	12.20	5174.14
4	401.62	19.65	2.60	4.77	4.77	2106409.67	3.51	0.74	2106.41	0.15	10.73	30	11.89	5644.71
5	390.74	19.10	0.60	4.52	4.52	2161305.69	3.49	0.77	2161.31	0.15	10.69	31	11.58	5469.31
6	381.25	18.00	0.31	4.33	4.33	1612528.48	2.69	0.62	1612.53	0.11	8.83	30	11.35	4409.43
7	343.68	17.54	0.31	4.00	4.00	1541641.09	2.49	0.62	1541.64	0.10	9.05	31	11.65	4073.95
8	413.43	18.38	0.47	4.82	4.82	1749141.58	2.82	0.58	1749.14	0.12	8.51	31	11.67	4607.81
9	451.62	19.90	1.94	5.42	5.42	2326305.80	3.88	0.72	2326.31	0.16	10.48	30	12.00	6197.58
10	461.35	20.26	2.97	5.73	5.73	2210353.34	3.57	0.62	2210.35	0.15	9.06	31	12.42	5474.87
11	383.10	20.79	4.49	4.70	4.70	2229229.37	3.72	0.79	2229.23	0.15	11.28	30	12.27	5660.21
12	398.85	21.03	3.96	4.98	4.98	2247489.89	3.62	0.73	2247.49	0.15	10.79	31	12.49	5635.98
AVG	452.60	19.91	2.34		5.43		3.46	0.65	25180.30	0.14	9.38			5448.12

### Appendix X: System 2 performance analysis (2019)

	GHI	AT	WS	kWh/m <sup>2</sup>	YR	Eac (Wh)	YF (kWh/kW)	PR	Eac(kWh)	CUF	η	days	hours	Pac(W)
1	589.36	22.02	4.39	7.12	7.12	2571208.46	4.15	0.58	2571.21	0.17	8.37	31	12.07	6458.31
2	642.13	22.71	5.65	7.75	7.75	2520899.97	4.50	0.58	2520.90	0.19	8.16	28	12.07	6860.37
3	473.85	23.80	5.31	5.78	5.78	3031290.30	4.89	0.85	3031.29	0.20	12.10	31	12.20	7509.06
4	359.96	22.78	3.98	5.40	5.40	2662172.40	4.44	0.82	2662.17	0.18	14.58	30	11.89	6871.04
5	274.31	19.82	2.37	4.11	4.11	2073503.45	3.34	0.81	2073.50	0.14	14.65	31	11.58	5261.93
6	271.07	18.84	0.64	3.08	3.08	1631107.91	2.72	0.88	1631.11	0.11	12.50	30	11.35	4437.94
7	341.90	19.05	1.19	3.98	3.98	1858079.49	3.00	0.75	1858.08	0.12	10.99	31	11.65	4921.16
8	412.04	19.37	1.44	4.81	4.81	1998402.70	3.22	0.67	1998.40	0.13	9.74	31	11.67	5255.22
9	458.11	20.21	2.17	5.50	5.50	2199663.88	3.67	0.67	2199.66	0.15	9.44	30	12.00	5663.63
10	459.26	20.52	3.07	5.70	5.70	2090921.97	3.37	0.59	2090.92	0.14	8.60	31	12.42	5171.05
11	361.92	20.75	3.62	4.44	4.44	2165387.96	3.61	0.81	2165.39	0.15	11.74	30	12.27	5563.51
12	395.20	20.54	3.27	4.94	4.94	1982376.59	3.20	0.65	1982.38	0.13	9.81	31	12.49	5077.02
AVG	419.93	20.87	3.09	5.22	5.22		3.68	0.72	26785.02	0.15	10.89			5754.19

**Appendix XI: System 3 performance analysis (2015)**

	GHI	AT	WS	kWh/m <sup>2</sup>	YR	Eac (Wh)	YF (kWh/kW)	PR	Eac(kWh)	CUF	$\eta$	days	hours	Pac(W)
1	537.97	21.75	3.88	6.50	6.50	3005388.36	4.85	0.75	3005.39	0.20	10.84	31	12.07	7634.41
2	602.55	22.38	4.79	7.27	7.27	2670909.01	4.77	0.66	2670.91	0.20	9.28	28	12.07	7322.56
3	603.94	21.94	5.82	7.37	7.37	2945608.93	4.75	0.64	2945.61	0.20	9.58	31	12.20	7578.03
4	498.62	20.59	2.72	5.93	5.93	2360032.83	3.93	0.66	2360.03	0.16	9.58	30	11.89	6251.93
5	426.16	19.96	1.76	4.93	4.93	2054835.13	3.31	0.67	2054.84	0.14	9.51	31	11.58	5306.87
6	361.81	18.77	0.98	4.11	4.11	1891165.79	3.15	0.77	1891.17	0.13	10.65	30	11.35	5043.48
7	439.59	18.40	1.42	5.12	5.12	1895999.41	3.06	0.60	1896.00	0.13	8.60	31	11.65	4948.34
8	415.51	18.79	2.06	4.85	4.85	2031858.88	3.28	0.68	2031.86	0.14	9.78	31	11.67	5322.03
9	475.47	20.56	1.67	5.71	5.71	2517266.00	4.20	0.74	2517.27	0.17	10.62	30	12.00	6613.45
10	477.78	21.00	4.32	5.93	5.93	2393223.86	3.86	0.65	2393.22	0.16	9.56	31	12.42	5978.13
11	324.08	19.76	3.87	3.98	3.98	1980218.50	3.30	0.83	1980.22	0.14	12.06	30	12.27	5118.30
12	384.73	20.65	4.00	4.81	4.81	2424814.23	3.91	0.81	2424.81	0.16	11.94	31	12.49	6012.89
AVG	462.35	20.38	3.11				3.86	0.70	28171.32	0.16	10.17			6094.20

**Appendix XII: System 3 performance analysis (2016)**

	GHI	AT	WS	kWh/m <sup>2</sup>	YR	Eac (Wh)	YF (kWh/kW)	PR	Eac(kWh)	CUF	$\eta$	days	hours	Pac(W)
1	499.08	21.64	5.90	6.03	6.03	2409398.75	3.89	0.64	2409.40	0.16	9.55	31	12.07	6240.38
2	544.68	21.79	5.99	6.57	6.57	2613344.99	4.51	0.69	2613.34	0.19	9.93	29	12.07	7080.65
3	605.48	22.65	6.23	7.39	7.39	2893324.17	4.67	0.63	2893.32	0.19	9.29	31	12.20	7364.32
4	374.77	20.65	4.39	4.45	4.45	1981001.59	3.30	0.74	1981.00	0.14	10.71	30	11.89	5254.75
5	386.35	19.63	2.13	4.47	4.47	1723828.61	2.78	0.62	1723.83	0.12	8.88	31	11.58	4493.11
6	321.99	18.50	1.92	3.65	3.65	1538191.57	2.56	0.70	1538.19	0.11	10.07	30	11.35	4247.52
7	353.01	18.27	0.61	4.11	4.11	1933054.71	3.12	0.76	1933.05	0.13	10.94	31	11.65	5058.38
8	413.43	18.53	0.84	4.82	4.82	1935780.53	3.12	0.65	1935.78	0.13	9.40	31	11.67	5087.69
9	458.11	19.63	0.53	5.50	5.50	2005016.56	3.34	0.61	2005.02	0.14	8.94	30	12.00	5363.24
10	459.26	21.39	2.87	5.70	5.70	2720943.06	4.39	0.77	2720.94	0.18	11.19	31	12.42	6730.53
11	354.86	20.14	4.67	4.35	4.35	2033512.86	3.39	0.78	2033.51	0.14	11.25	30	12.27	5227.56
12	393.98	20.66	6.37	4.92	4.92	2615260.43	4.22	0.86	2615.26	0.18	12.53	31	12.49	6466.65
AVG	430.42	20.29	3.54		5.17		3.61	0.70	26402.66	0.15	10.22			5717.90

**Appendix XIII: System 3 performance analysis (2017)**

	GHI	AT	WS	kWh/m <sup>2</sup>	YR	Eac (Wh)	YF (kWh/kW)	PR	Eac(kWh)	CUF	$\eta$	days	hours	Pac(W)
1	577.78	22.53	4.67	6.98	6.98	3014012.79	4.86	0.70	3014.01	0.20	10.16	31	12.07	7687.81
2	657.88	22.14	5.48	7.94	7.94	2647470.08	4.73	0.60	2647.47	0.20	8.65	28	12.07	7447.68
3	607.88	22.40	4.60	7.42	7.42	2855595.26	4.61	0.62	2855.60	0.19	9.13	31	12.20	7263.85
4	351.39	21.29	4.37	4.18	4.18	2292694.15	3.82	0.91	2292.69	0.16	13.12	30	11.89	6036.28
5	381.95	20.09	1.72	4.42	4.42	2016490.91	3.25	0.74	2016.49	0.14	10.22	31	11.58	5109.30
6	271.07	19.50	1.71	3.08	3.08	1809050.02	3.02	0.98	1809.05	0.13	13.90	30	11.35	4933.40
7	238.43	18.81	1.26	3.34	3.34	1841838.54	2.97	0.89	1841.84	0.12	15.79	31	11.65	4928.64
8	411.35	19.06	1.76	4.80	4.80	1476758.02	2.38	0.50	1476.76	0.10	7.24	31	11.67	3897.38
9	440.74	19.53	2.58	5.29	5.29	2056766.15	3.43	0.65	2056.77	0.14	9.38	30	12.00	5414.48
10	440.74	20.72	3.62	5.47	5.47	2512792.18	4.05	0.74	2512.79	0.17	10.85	31	12.42	6260.40
11	385.65	19.76	4.45	4.73	4.73	2066400.20	3.44	0.73	2066.40	0.14	10.54	30	12.27	5320.49
12	403.24	20.94	4.77	5.04	5.04	2530145.18	4.08	0.81	2530.15	0.17	11.95	31	12.49	6307.42
AVG	430.67	20.56	3.42		5.22		3.72	0.74	27120.01	0.16	10.91			5883.93

**Appendix XIV: System 3 performance analysis (2018)**

	GHI	AT	WS	kWh/m <sup>2</sup>	YR	Eac (Wh)	YF (kWh/kW)	PR	Eac(kWh)	CUF	$\eta$	days	hours	Pac(W)
1	601.39	21.63	1.30	7.26	7.26	2310812.29	3.73	0.51	2310.81	0.16	8.07	31	12.07	6355.40
2	599.54	22.40	6.07	7.24	7.24	2733521.07	4.88	0.67	2733.52	0.20	9.48	28	12.07	7440.98
3	604.63	20.28	3.00	7.38	7.38	1953747.25	3.15	0.43	1953.75	0.13	6.03	31	12.20	4772.45
4	401.62	19.65	2.60	4.77	4.77	2019678.44	3.37	0.71	2019.68	0.14	9.47	30	11.89	4981.08
5	390.74	19.10	0.60	4.52	4.52	1999260.12	3.22	0.71	1999.26	0.13	9.42	31	11.58	4822.29
6	381.25	18.00	0.31	4.33	4.33	1409545.14	2.35	0.54	1409.55	0.10	7.01	30	11.35	3499.36
7	343.68	17.54	0.31	4.00	4.00	1434152.60	2.31	0.58	1434.15	0.10	7.05	31	11.65	3172.84
8	413.43	18.38	0.47	4.82	4.82	1589361.56	2.56	0.53	1589.36	0.11	6.84	31	11.67	3704.46
9	451.62	19.90	1.94	5.42	5.42	2153916.08	3.59	0.66	2153.92	0.15	9.08	30	12.00	5371.55
10	461.35	20.26	2.97	5.73	5.73	2091665.30	3.37	0.59	2091.67	0.14	8.32	31	12.42	5024.82
11	383.10	20.79	4.49	4.70	4.70	2155578.44	3.59	0.76	2155.58	0.15	10.41	30	12.27	5223.92
12	398.85	21.03	3.96	4.98	4.98	2208306.42	3.56	0.71	2208.31	0.15	9.93	31	12.49	5184.33
AVG	452.60	19.91	2.34		5.43		3.31	0.62	24059.54	0.14	8.43			4962.79



**Appendix XV: System 3 performance analysis (2019)**

	GHI	AT	WS	kWh/m <sup>2</sup>	YR	Eac (Wh)	YF (kWh/kW)	PR	Eac(kWh)	CUF	η	days	hours	Pac(W)
1	589.36	22.02	4.39	7.12	7.12	2454437.85	3.96	0.56	2454.44	0.16	7.26	31	12.07	5601.08
2	642.13	22.71	5.65	7.75	7.75	2291523.96	4.09	0.53	2291.52	0.17	7.57	28	12.07	6365.34
3	473.85	23.80	5.31	5.78	5.78	2643397.99	4.26	0.74	2643.40	0.18	11.04	31	12.20	6848.18
4	359.96	22.78	3.98	4.28	4.28	2181305.84	3.64	0.85	2181.31	0.15	12.41	30	11.89	5848.00
5	274.31	19.82	2.37	3.18	3.18	1731523.38	2.79	0.88	1731.52	0.12	12.62	31	11.58	4532.78
6	271.07	18.84	0.64	3.08	3.08	1308287.79	2.18	0.71	1308.29	0.09	10.30	30	11.35	3654.44
7	341.90	19.05	1.19	3.98	3.98	1337462.86	2.16	0.54	1337.46	0.09	7.99	31	11.65	3576.10
8	412.04	19.37	1.44	4.81	4.81	1598695.69	2.58	0.54	1598.70	0.11	8.01	31	11.67	4320.80
9	458.11	20.21	2.17	5.50	5.50	1902198.77	3.17	0.58	1902.20	0.13	8.78	30	12.00	5269.25
10	459.26	20.52	3.07	5.70	5.70	1884788.82	3.04	0.53	1884.79	0.13	8.02	31	12.42	4820.43
11	361.92	20.75	3.62	4.44	4.44	2076504.47	3.46	0.78	2076.50	0.14	11.56	30	12.27	5478.90
12	395.20	20.54	3.27	4.94	4.94	1909656.19	3.08	0.62	1909.66	0.13	9.74	31	12.49	5038.67
AVG	419.93	20.87	3.09		5.05		3.20	0.65	23319.78	0.13	9.61			5112.83

**Appendix XVI: System 4 performance analysis (2015)**

	GHI	AT	WS	kWh/m <sup>2</sup>	YR	Eac (Wh)	YF (kWh/kW)	PR	Eac(kWh)	CUF	η	days	hours	Pac(W)
1	537.97	21.75	3.88	6.50	6.50	3028182.83	4.88	0.75	3028.18	0.20	10.44	31	12.07	7354.56
2	602.55	22.38	4.79	7.27	7.27	2652756.48	4.74	0.65	2652.76	0.20	9.07	28	12.07	7156.26
3	603.94	21.94	5.82	7.37	7.37	2230125.68	3.60	0.49	2230.13	0.15	7.16	31	12.20	5659.05
4	498.62	20.59	2.72	5.93	5.93	2123640.53	3.54	0.60	2123.64	0.15	8.80	30	11.89	5742.31
5	426.16	19.96	1.76	4.93	4.93	2132063.75	3.44	0.70	2132.06	0.14	9.38	31	11.58	5235.89
6	361.81	18.77	0.98	4.11	4.11	1765935.60	2.94	0.72	1765.94	0.12	9.98	30	11.35	4729.47
7	439.59	18.40	1.42	5.12	5.12	1821871.31	2.94	0.57	1821.87	0.12	8.24	31	11.65	4742.90
8	415.51	18.79	2.06	4.85	4.85	1944093.12	3.14	0.65	1944.09	0.13	9.27	31	11.67	5042.92
9	475.47	20.56	1.67	5.71	5.71	2358376.23	3.93	0.69	2358.38	0.16	10.00	30	12.00	6228.71
10	477.78	21.00	4.32	5.93	5.93	2125424.97	3.43	0.58	2125.42	0.14	8.55	31	12.42	5349.80
11	324.08	19.76	3.87	3.98	3.98	2005071.12	3.34	0.84	2005.07	0.14	12.08	30	12.27	5124.81
12	384.73	20.65	4.00	4.81	4.81	2377864.60	3.84	0.80	2377.86	0.16	11.46	31	12.49	5772.92
AVG	462.35	20.38	3.11		5.54		3.65	0.67	26565.41	0.15	9.54			5678.30

**Appendix XVII: System 4 performance analysis (2016)**

	GHI	AT	WS	kWh/m <sup>2</sup>	YR	Eac (Wh)	YF (kWh/kW)	PR	Eac(kWh)	CUF	η	days	hours	Pac(W)
1	499.08	21.64	5.90	6.03	6.03	2401923.64	3.87	0.64	2401.92	0.16	9.02	31	12.07	5894.62
2	544.68	21.79	5.99	6.57	6.57	2616838.09	4.51	0.69	2616.84	0.19	9.69	29	12.07	6913.93
3	605.48	22.65	6.23	7.39	7.39	2782518.31	4.49	0.61	2782.52	0.19	8.44	31	12.20	6694.39
4	374.77	20.65	4.39	4.45	4.45	1869205.63	3.12	0.70	1869.21	0.13	10.33	30	11.89	5070.78
5	386.35	19.63	2.13	4.47	4.47	1554561.16	2.51	0.56	1554.56	0.10	7.95	31	11.58	4023.50
6	321.99	18.50	1.92	3.65	3.65	1542929.16	2.57	0.70	1542.93	0.11	10.05	30	11.35	4235.90
7	353.01	18.27	0.61	4.11	4.11	1835804.08	2.96	0.72	1835.80	0.12	10.61	31	11.65	4906.56
8	413.43	18.53	0.84	4.82	4.82	1776760.58	2.87	0.59	1776.76	0.12	8.57	31	11.67	4639.18
9	458.11	19.63	0.53	5.50	5.50	1859857.20	3.10	0.56	1859.86	0.13	8.31	30	12.00	4983.91
10	459.26	21.39	2.87	5.70	5.70	2240839.58	3.61	0.63	2240.84	0.15	9.55	31	12.42	5740.54
11	354.86	20.14	4.67	4.35	4.35	1839373.67	3.07	0.70	1839.37	0.13	10.28	30	12.27	4775.49
12	370.84	20.66	6.37	4.63	4.63	2382380.21	3.84	0.83	2382.38	0.16	12.02	31	12.49	5834.93
AVG	428.49	20.29	3.54		5.14		3.38	0.66	24702.99	0.14	9.57			5309.48

**Appendix XVIII: System 4 performance analysis (2017)**

	GHI	AT	WS	kWh/m <sup>2</sup>	YR	Eac (Wh)	YF (kWh/kW)	PR	Eac(kWh)	CUF	η	days	hours	Pac(W)
1	577.78	22.53	4.67	6.98	6.98	2638317.58	4.26	0.61	2638.32	0.18	8.54	31	12.07	6463.80
2	657.88	22.14	5.48	7.94	7.94	2353808.37	4.20	0.53	2353.81	0.18	7.63	28	12.07	6575.95
3	607.88	22.40	4.60	7.42	7.42	2606078.69	4.20	0.57	2606.08	0.18	7.92	31	12.20	6306.83
4	351.39	21.29	4.37	4.18	4.18	1937220.04	3.23	0.77	1937.22	0.13	11.04	30	11.89	5079.38
5	381.95	20.09	1.72	4.42	4.42	1843406.44	2.97	0.67	1843.41	0.12	9.48	31	11.58	4742.82
6	271.07	19.50	1.71	3.08	3.08	1326498.99	2.21	0.72	1326.50	0.09	14.67	30	11.35	5208.74
7	238.43	18.81	1.26	2.78	2.78	1471297.47	2.37	0.85	1471.30	0.10	14.42	31	11.65	4503.10
8	411.35	19.06	1.76	4.80	4.80	1590895.70	2.57	0.53	1590.90	0.11	7.77	31	11.67	4184.16
9	440.74	19.53	2.58	5.29	5.29	2002609.25	3.34	0.63	2002.61	0.14	8.94	30	12.00	5161.27
10	440.74	20.72	3.62	5.47	5.47	2495775.91	4.03	0.74	2495.78	0.17	10.73	31	12.42	6194.07
11	385.65	19.76	4.45	4.73	4.73	2073757.10	3.46	0.73	2073.76	0.14	10.59	30	12.27	5349.33
12	356.95	20.94	4.77	4.46	4.46	2679235.03	4.32	0.97	2679.24	0.18	13.91	31	12.49	6501.82
AVG	426.82	20.56	3.42		5.13		3.43	0.69	25018.90	0.14	10.47			5522.61

**Appendix XIX: System 4 performance analysis (2018)**

	GHI	AT	WS	kWh/m <sup>2</sup>	YR	Eac (Wh)	YF (kWh/kW)	PR	Eac(kWh)	CUF	η	days	hours	Pac(W)
1	601.39	21.63	1.30	7.26	7.26	2569847.75	4.14	0.57	2569.85	0.17	8.13	31	12.07	6405.90
2	599.54	22.40	6.07	7.24	7.24	2698326.08	4.82	0.67	2698.33	0.20	9.35	28	12.07	7342.39
3	604.63	20.28	3.00	7.38	7.38	1953920.95	3.15	0.43	1953.92	0.13	5.93	31	12.20	4693.14
4	401.62	19.65	2.60	4.77	4.77	1944014.96	3.24	0.68	1944.01	0.14	10.08	30	11.89	5301.77
5	390.74	19.10	0.60	4.52	4.52	1722256.79	2.78	0.61	1722.26	0.12	8.84	31	11.58	4521.86
6	381.25	18.00	0.31	4.33	4.33	1529927.10	2.55	0.59	1529.93	0.11	8.76	30	11.35	4371.32
7	343.68	17.54	0.31	4.00	4.00	1722981.59	2.78	0.69	1722.98	0.12	9.38	31	11.65	4220.79
8	413.43	18.38	0.47	4.82	4.82	1635562.39	2.64	0.55	1635.56	0.11	7.96	31	11.67	4310.49
9	451.62	19.90	1.94	5.42	5.42	2253819.42	3.76	0.69	2253.82	0.16	10.12	30	12.00	5986.18
10	461.35	20.26	2.97	5.73	5.73	2201332.90	3.55	0.62	2201.33	0.15	9.15	31	12.42	5526.16
11	383.10	20.79	4.49	4.70	4.70	2309169.27	3.85	0.82	2309.17	0.16	11.74	30	12.27	5890.74
12	398.85	21.03	3.96	4.98	4.98	2285272.23	3.69	0.74	2285.27	0.15	10.66	31	12.49	5567.44
AVG	452.60	19.91	2.34		5.43		3.41	0.64	24826.43	0.14	9.18			5344.85

**Appendix XX: System 4 performance analysis (2019)**

	GHI	AT	WS	kWh/m <sup>2</sup>	YR	Eac (Wh)	YF (kWh/kW)	PR	Eac(kWh)	CUF	η	days	hours	Pac(W)
1	589.36	22.02	4.39	7.12	7.12	2671244.32	4.31	0.61	2671.24	0.18	8.60	31	12.07	6640.28
2	642.13	22.71	5.65	7.75	7.75	2444559.17	4.37	0.56	2444.56	0.18	7.93	28	12.07	6664.23
3	473.85	23.80	5.31	5.78	5.78	2685910.81	4.33	0.75	2685.91	0.18	10.87	31	12.20	6745.35
4	359.96	22.78	3.98	4.28	4.28	2337594.13	3.90	0.91	2337.59	0.16	12.95	30	11.89	6105.27
5	274.31	19.82	2.37	3.18	3.18	1815628.42	2.93	0.92	1815.63	0.12	12.98	31	11.58	4662.38
6	271.07	18.84	0.64	3.08	3.08	1432596.65	2.39	0.78	1432.60	0.10	11.02	30	11.35	3911.78
7	341.90	19.05	1.19	3.98	3.98	1599656.46	2.58	0.65	1599.66	0.11	9.55	31	11.65	4276.67
8	412.04	19.37	1.44	4.81	4.81	1771493.21	2.86	0.59	1771.49	0.12	8.59	31	11.67	4634.16
9	458.11	20.21	2.17	5.50	5.50	2010643.32	3.35	0.61	2010.64	0.14	8.88	30	12.00	5326.33
10	459.26	20.52	3.07	5.70	5.70	1974886.83	3.19	0.56	1974.89	0.13	8.33	31	12.42	5009.30
11	361.92	20.75	3.62	4.44	4.44	2180710.05	3.63	0.82	2180.71	0.15	11.85	30	12.27	5616.73
12	395.20	20.54	3.27	4.94	4.94	2109149.48	3.40	0.69	2109.15	0.14	10.26	31	12.49	5308.75
AVG	419.93	20.87	3.09		5.05		3.44	0.70	25034.07	0.14	10.15			5408.44

### Appendix XXI: Statistical performance analysis of PV modules

YR	Solar PV system						PR	Solar PV system 1 oriented south					
Year	YR	Mean(M)	(YR-M) ^2	((YR-M) ^2)/n	$\sigma$	COV	Year	PR	Mean(M)	(YR-M) ^2	((YR-M) ^2)/n	$\sigma$	COV
2015	5.54	5.280	0.068	0.034	0.18	3.48	2015	69	69.4	0.16	0.08	0.282843	0.407554
2016	5.16	5.280	0.014	0.007	0.08	1.61	2016	67	69.4	5.76	2.88	1.697056	2.445326
2017	5.18	5.280	0.010	0.005	0.07	1.34	2017	72	69.4	6.76	3.38	1.838478	2.649103
2018	5.43	5.280	0.022	0.011	0.11	2.01	2018	64	69.4	29.16	14.58	3.818377	5.501984
2019	5.09	5.280	0.036	0.018	0.13	2.54	2019	75	69.4	31.36	15.68	3.959798	5.705761
	5.28	5.280	0.03	0.015	0.12	2.20		69.4	69.4	14.64	7.32	2.31931	3.341946
YF	Solar PV system 1 oriented south						$\eta$	Solar PV system1 oriented south					
Year	YF	Mean(M)	(YR-M) ^2	((YR-M) ^2)/n	$\sigma$	COV	Year	$\eta$	Mean(M)	(YR-M) ^2	((YR-M) ^2)/n	$\sigma$	COV
2015	3.80	3.600	0.04	0.020	0.14	3.93	2015	9.81	10.102	0.085264	0.042632	0.206475	2.043904
2016	3.44	3.600	0.0256	0.013	0.11	3.14	2016	9.67	10.102	0.186624	0.093312	0.30547	3.023858
2017	3.66	3.600	0.0036	0.002	0.04	1.18	2017	10.89	10.102	0.620944	0.310472	0.5572	5.515741
2018	3.43	3.600	0.0289	0.014	0.12	3.34	2018	9.35	10.102	0.565504	0.282752	0.531744	5.263753
2019	3.68	3.600	0.0064	0.003	0.06	1.57	2019	10.79	10.102	0.473344	0.236672	0.486489	4.815774
	3.60	3.600	0.0209	0.010	0.09	2.63		10.102	10.102	0.386336	0.193168	0.417476	4.132606
YF	Solar PV system 4 oriented east-west						$\eta$	Solar PV system 4 oriented east-west					
Year	YF	Mean(M)	(YR-M) ^2	((YR-M) ^2)/n	$\sigma$	COV	Year	$\eta$	Mean(M)	(YR-M) ^2	((YR-M) ^2)/n	$\sigma$	COV
2015	3.65	3.460	0.0361	0.018	0.13	3.88	2015	9.54	9.782	0.058564	0.029282	0.17112	1.749334
2016	3.38	3.460	0.0064	0.003	0.06	1.63	2016	9.57	9.782	0.044944	0.022472	0.149907	1.532474
2017	3.43	3.460	0.0009	0.000	0.02	0.61	2017	10.47	9.782	0.473344	0.236672	0.486489	4.973313
2018	3.41	3.460	0.0025	0.001	0.04	1.02	2018	9.18	9.782	0.362404	0.181202	0.425678	4.351649
2019	3.44	3.460	0.0004	0.000	0.01	0.41	2019	10.15	9.782	0.135424	0.067712	0.260215	2.660144
	3.46	3.460	0.00926	0.005	0.05	1.51		9.782	9.782	0.214936	0.107468	0.298682	3.053383

### Appendix XXII: Statistical performance analysis of PV modules

Eac	Solar PV system 1 oriented south						CUF	Solar PV system 1 oriented south					
Year	Eac	Mean(M)	(YR-M) ^2	((YR-M) ^2)/n	$\sigma$	COV	Year	CUF	Mean(M)	(YR-M) ^2	((YR-M) ^2)/n	$\sigma$	COV
2015	27.74	26.310	2.0449	1.022	1.01	3.84	2015	0.16	0.148	0.000144	7.2E-05	0.008485	5.733298
2016	25.51	26.310	0.64	0.320	0.57	2.15	2016	0.14	0.148	6.4E-05	3.2E-05	0.005657	3.822199
2017	26.31	26.310	0	0.000	0.00	0.00	2017	0.15	0.148	4E-06	0.000002	0.001414	0.95555
2018	25.18	26.310	1.2769	0.638	0.80	3.04	2018	0.14	0.148	6.4E-05	3.2E-05	0.005657	3.822199
2019	26.79	26.310	0.2304	0.115	0.34	1.29	2019	0.15	0.148	4E-06	0.000002	0.001414	0.95555
	26.31	26.310	0.83844	0.419	0.54	2.06		0.148	0.148	5.6E-05	0.000028	0.004525	3.057759
Eac	Solar PV system 4 oriented east-west						CUF	Solar PV system 4 oriented east-west					
Year	Eac	Mean(M)	(YR-M) ^2	((YR-M) ^2)/n	$\sigma$	COV	Year	CUF	Mean(M)	(YR-M) ^2	((YR-M) ^2)/n	$\sigma$	COV
2015	26.57	25.230	1.7956	0.898	0.95	3.76	2015	0.15	0.142	6.4E-05	3.2E-05	0.005657	3.9837
2016	24.70	25.230	0.2809	0.140	0.37	1.49	2016	0.14	0.142	4E-06	2E-06	0.001414	0.995925
2017	25.02	25.230	0.0441	0.022	0.15	0.59	2017	0.14	0.142	4E-06	2E-06	0.001414	0.995925
2018	24.83	25.230	0.16	0.080	0.28	1.12	2018	0.14	0.142	4E-06	2E-06	0.001414	0.995925
2019	25.03	25.230	0.04	0.020	0.14	0.56	2019	0.14	0.142	4E-06	2E-06	0.001414	0.995925
	25.23	25.230	0.46412	0.232	0.38	1.50		0.142	0.142	1.6E-05	8E-06	0.002263	1.59348
Solar PV system 4 oriented east-west													
Year	PR	Mean(M)	(YR-M) ^2	((YR-M) ^2)/n	$\sigma$	COV							
2015	67.00	67.2	0.04	0.02	0.141	0.21							
2016	66.00	67.2	1.44	0.72	0.849	1.26							
2017	69.00	67.2	3.24	1.62	1.273	1.89							
2018	64.00	67.2	10.24	5.12	2.263	3.37							
2019	70.00	67.2	7.84	3.92	1.980	2.95							
	67.20	67.2	4.56	2.28	1.301	1.94							

### Appendix XXIII: Statistical performance analysis of PV modules

Solar PV system 2 oriented south, tilt angle 18°						Solar PV system 3 oriented south, tilt angle 11°						
PR	Mean(M)	(YR-M) ^2	((YR-M) ^2)/n	$\sigma$	COV	Year	PR	Mean(M)	(YR-M) ^2	((YR-M) ^2)/n	$\sigma$	COV
70.00	69.4	0.360	0.180	0.424	0.61	2015	70.00	68.20	3.2400	1.6200	1.273	1.87
68.00	69.4	1.960	0.980	0.990	1.43	2016	70.00	68.20	3.2400	1.6200	1.273	1.87
72.00	69.4	6.760	3.380	1.838	2.65	2017	74.00	68.20	33.6400	16.8200	4.101	6.01
65.00	69.4	19.360	9.680	3.111	4.48	2018	62.00	68.20	38.4400	19.2200	4.384	6.43
72.00	69.4	6.760	3.380	1.838	2.65	2019	65.00	68.20	10.2400	5.1200	2.263	3.32
69.40	69.4	7.040	3.520	1.640	2.36		68.20	68.20	17.7600	8.8800	2.659	3.90
Solar PV system 2 oriented south, tilt angle 18°						Solar PV system 2 oriented south, tilt angle 18°						
YF	Mean(M)	(YR-M) ^2	((YR-M) ^2)/n	$\sigma$	COV	Year	$\eta$	Mean(M)	(YR-M) ^2	((YR-M) ^2)/n	$\sigma$	COV
3.80	3.606	0.038	0.019	0.137	3.80	2015	9.96	10.22	0.0676	0.0338	0.184	1.80
3.48	3.606	0.016	0.008	0.089	2.47	2016	9.87	10.22	0.1225	0.0613	0.247	2.42
3.61	3.606	0.000	0.000	0.003	0.08	2017	11.00	10.22	0.6084	0.3042	0.552	5.40
3.46	3.606	0.021	0.011	0.103	2.86	2018	9.38	10.22	0.7056	0.3528	0.594	5.81
3.68	3.606	0.005	0.003	0.052	1.45	2019	10.89	10.22	0.4489	0.2245	0.474	4.64
3.61	3.606	0.016	0.008	0.077	2.13		10.22	10.22	0.3906	0.1953	0.410	4.01
Solar PV system 3 oriented south, tilt angle 11°						Solar PV system 3 oriented south, tilt angle 11°						
YF	Mean(M)	(YR-M) ^2	((YR-M) ^2)/n	$\sigma$	COV	Year	$\eta$	Mean(M)	(YR-M) ^2	((YR-M) ^2)/n	$\sigma$	COV
3.86	3.54	0.102	0.051	0.226	6.39	2015	10.17	9.87	0.0912	0.0456	0.214	2.16
3.61	3.54	0.005	0.002	0.049	1.40	2016	10.22	9.87	0.1239	0.0620	0.249	2.52
3.72	3.54	0.032	0.016	0.127	3.60	2017	10.91	9.87	1.0858	0.5429	0.737	7.47
3.31	3.54	0.053	0.026	0.163	4.59	2018	8.43	9.87	2.0678	1.0339	1.017	10.30
3.20	3.54	0.116	0.058	0.240	6.79	2019	9.61	9.87	0.0666	0.0333	0.182	1.85
3.54	3.54	0.062	0.031	0.161	4.55		9.87	9.87	0.6871	0.3435	0.480	4.86

### Appendix XXIV: Statistical performance analysis of PV modules

Solar PV system 2 oriented south, tilt angle 18°							Solar PV system 2 oriented south, tilt angle 18°						
Year	Eac	Mean(M)	(YR-M) ^2	((YR-M) ^2)/n	$\sigma$	COV	Year	CUF	Mean(M)	(YR-M) ^2	((YR-M) ^2)/n	$\sigma$	COV
2015	27.68	26.266	1.999	1.000	1.000	3.81	2015	0.16	0.15	0.0001	0.0001	0.007	4.71
2016	25.20	26.266	1.136	0.568	0.754	2.87	2016	0.15	0.15	0.0000	0.0000	0.000	0.00
2017	26.69	26.266	0.180	0.090	0.300	1.14	2017	0.15	0.15	0.0000	0.0000	0.000	0.00
2018	24.94	26.266	1.758	0.879	0.938	3.57	2018	0.14	0.15	0.0001	0.0000	0.007	4.71
2019	26.82	26.266	0.307	0.153	0.392	1.49	2019	0.15	0.15	0.0000	0.0000	0.000	0.00
	26.27	26.266	1.076	0.538	0.677	2.58		0.15	0.15	0.0000	0.0000	0.003	1.89
Solar PV system 3 oriented south, tilt angle 11°							Solar PV system 3 oriented south, tilt angle 11°						
Year	Eac	Mean(M)	(YR-M) ^2	((YR-M) ^2)/n	$\sigma$	COV	Year	CUF	Mean(M)	(YR-M) ^2	((YR-M) ^2)/n	$\sigma$	COV
2015	28.17	25.906	5.126	2.563	1.601	6.18	2015	0.16	0.15	0.0001	0.0001	0.008	5.73
2016	26.40	25.906	0.244	0.122	0.349	1.35	2016	0.15	0.15	0.0000	0.0000	0.001	0.96
2017	27.12	25.906	1.474	0.737	0.858	3.31	2017	0.16	0.15	0.0001	0.0001	0.008	5.73
2018	24.07	25.906	3.371	1.685	1.298	5.01	2018	0.14	0.15	0.0001	0.0000	0.006	3.82
2019	23.77	25.906	4.562	2.281	1.510	5.83	2019	0.13	0.15	0.0003	0.0002	0.013	8.60
	25.91	25.906	2.955	1.478	1.123	4.34		0.15	0.15	0.0001	0.0001	0.007	4.97

### Appendix XXV: Economic analysis of solar PV power plant

Years	Avg. kWh	Saving (80%)	grid (20%)	cost	FIT	saving	FiT2	TOT	Ot	C	Ct nor 7	Ct IRR 7		IRR 7	DPP7	SPP
0	4000000									-4608882	-4608882	-4608882			-4608882	-4000000
1	28085	22468	5617	26	12.00	584168	67404	651572	180000	471572	458038	443391	0.97	0.9402	-4150844	-3528428
2	27539	22031	5508	26	12.12	572811	66755	639566	180000	459566	433565	406280	0.94	0.8841	-3717279	-3068862
3	25452	20362	5090	26	12.24	529402	62306	591708	180000	411708	377268	342220	0.92	0.8312	-3340011	-2657154
4	26284	21027	5257	26	12.36	546707	64974	611681	180000	431681	384217	337379	0.89	0.7815	-2955794	-2225473
5	24752	19802	4950	26	12.48	514842	61781	576623	180000	396623	342882	291455	0.86	0.7348	-2612912	-1828850
6	26422	21138	5284	26	12.60	549578	66583	616161	180000	436161	366241	301356	0.84	0.6909	-2246671	-1392689
7	26118	20895	5224	26	12.72	543257	66445	609702	180000	429702	350462	279151	0.82	0.6496	-1896209	-962987
8	25818	20654	5164	26	12.84	537010	66300	603310	180000	423310	335340	258564	0.79	0.6108	-1560869	-539677
9	25521	20417	5104	26	12.96	530834	66150	596985	180000	416985	320849	239480	0.77	0.5743	-1240020	-122693
10	25227	20182	5045	26	13.08	524730	65995	590725	180000	410725	306962	221788	0.75	0.5400	-933058	288032
11	24937	19950	4987	26	13.20	518695	65834	584530	180000	404530	293655	205389	0.73	0.5077	-639403	692562
12	24650	19720	4930	26	13.32	512730	65669	578399	180000	398399	280905	190188	0.71	0.4774	-358498	1090961
13	24367	19494	4873	26	13.44	506834	65499	572333	180000	392333	268688	176099	0.68	0.4489	-89810	1483294
14	24087	19269	4817	26	13.56	501005	65323	566329	180000	386329	256983	163042	0.67	0.4220	167173	1869622
15	23810	19048	4762	26	13.68	495244	65144	560387	180000	380387	245769	150941	0.65	0.3968	412942	2250010
16	23536	18829	4707	26	13.80	489549	64959	554508	180000	374508	235026	139727	0.63	0.3731	647968	2624518
17	23265	18612	4653	26	13.92	483919	64771	548689	180000	368689	224734	129336	0.61	0.3508	872702	2993207
18	22998	18398	4600	26	14.04	478354	64578	542931	180000	362931	214875	119708	0.59	0.3298	1087577	3356139
19	22733	18187	4547	26	14.16	472853	64381	537233	180000	357233	205431	110787	0.58	0.3101	1293008	3713372
20	22472	17977	4494	26	14.28	467415	64180	531594	180000	351594	196386	102522	0.56	0.2916	1489393	4064966
	498074					10359936	1305030	11664966	3600000	NPV	1489393	-82		-82		
	(1+i)^84	(1+i)^120							7600000							
	1.33214	1.50637	0.00456	0.00515		LCOE 7	16.48		TLCC 7	TLCC 7					IRR	0.000
			0.33214	0.50637		LCOE 10	17.03		CRF	0.014		0.010				
									EMI	54867		40696				
									TLC	4608822		4883527				



**Appendix XXVI: Silicon Amorphous thin technology data of the clean module**

	<b>Isc</b>	<b>Isc<sub>STC</sub></b>	<b>Voc</b>	<b>Imp</b>	<b>Imp<sub>STC</sub></b>	<b>Vmp</b>	<b>P</b>	<b>P<sub>STC</sub></b>	<b>FF</b>	<b>T</b>	<b>G</b>	<b>η</b>	<b>Inc</b>
1	4.146	3.57	40	3.31	2.85	28.33	93.9	80.74	0.57	45.4	1175	0.0519	12
2	4.109	3.53	39.8	3.21	2.76	28.69	92.2	79.30	0.56	45.4	1158	0.0517	12
3	4.059	3.49	39.7	3.19	2.74	28.71	91.6	78.76	0.57	45.4	1151	0.0517	12
4	4.109	3.53	39.8	3.21	2.76	28.69	92.2	79.30	0.56	45.4	1158	0.0517	12
5	4.059	3.49	39.7	3.19	2.74	28.71	91.6	78.76	0.57	45.4	1151	0.0517	12
6	4.146	3.57	40.00	3.31	2.85	28.33	93.9	80.74	0.57	45.4	1175	0.0519	12
7	4.059	3.49	39.65	3.19	2.74	28.71	91.6	78.76	0.57	45.4	1151	0.0517	12
8	4.109	3.53	39.8	3.21	2.76	28.69	92.2	79.30	0.56	45.4	1158	0.0517	12
9	4.146	3.57	40	3.31	2.85	28.33	93.9	80.74	0.57	45.4	1175	0.0519	12
10	4.059	3.49	39.7	3.19	2.74	28.71	91.6	78.76	0.57	45.4	1151	0.0517	12
11	4.109	3.53	39.8	3.21	2.76	28.69	92.2	79.30	0.56	45.4	1158	0.0517	12
12	4.146	3.57	40	3.31	2.85	28.33	93.9	80.74	0.57	45.4	1175	0.0519	12
13	4.109	3.53	39.8	3.21	2.76	28.69	92.2	79.30	0.56	45.4	1158	0.0517	12
14	4.059	3.49	39.7	3.19	2.74	28.71	91.6	78.76	0.57	45.4	1151	0.0517	12
15	4.146	3.57	40	3.31	2.85	28.33	93.9	80.74	0.57	45.4	1175	0.0519	12
16	4.146	3.57	40	3.31	2.85	28.33	93.9	80.74	0.57	45.4	1175	0.0519	12
17	4.109	3.53	39.8	3.21	2.76	28.69	92.2	79.30	0.56	45.4	1158	0.0517	12
18	4.059	3.49	39.7	3.19	2.74	28.71	91.6	78.76	0.57	45.4	1151	0.0517	12
19	4.146	3.57	40	3.31	2.85	28.33	93.9	80.74	0.57	45.4	1175	0.0519	12
20	4.109	3.53	39.8	3.21	2.76	28.69	92.2	79.30	0.56	45.4	1158	0.0517	12
21	4.059	3.49	39.7	3.19	2.74	28.71	91.6	78.76	0.57	45.4	1151	0.0517	12
22	4.109	3.53	39.8	3.21	2.76	28.69	92.2	79.30	0.56	45.4	1158	0.0517	12
23	4.059	3.49	39.7	3.19	2.74	28.71	91.6	78.76	0.57	45.4	1151	0.0517	12
24	4.146	3.57	40	3.31	2.85	28.33	93.9	80.74	0.57	45.4	1175	0.0519	12
25	4.059	3.49	39.7	3.19	2.74	28.71	91.6	78.76	0.57	45.4	1151	0.0517	12
26	4.109	3.53	39.8	3.21	2.76	28.69	92.2	79.30	0.56	45.4	1158	0.0517	12
27	4.146	3.57	40	3.31	2.85	28.33	93.9	80.74	0.57	45.4	1175	0.0519	12
28	4.059	3.49	39.7	3.19	2.74	28.71	91.6	78.76	0.57	45.4	1151	0.0517	12
29	4.109	3.53	39.8	3.21	2.76	28.69	92.2	79.30	0.56	45.4	1158	0.0517	12
30	4.146	3.57	40	3.31	2.85	28.33	93.9	80.74	0.57	45.4	1175	0.0519	12
<b>AVG</b>	<b>4.10</b>	<b>3.53</b>	<b>39.81</b>	<b>3.24</b>	<b>2.79</b>	<b>28.58</b>	<b>92.57</b>	<b>79.60</b>	<b>0.57</b>	<b>45.40</b>	<b>1161.33</b>	<b>0.052</b>	

**Appendix XXVII: Silicon Amorphous thin technology data of the unclean module**

	Isc	Isc <sub>STC</sub>	Voc	Imp	Imp <sub>STC</sub>	Vmp	P	Pmax	FF	T	G	η	Inc
1	3.35	3.21	40.45	2.64	2.53	29.7	78.5	75.14	0.58	39.6	943	0.052	9
2	3.37	3.23	40.38	2.67	2.57	29.4	78.6	75.41	0.58	39.6	948	0.052	9
3	3.38	3.24	40.32	2.65	2.55	29.7	78.7	75.54	0.58	39.6	949	0.052	9
4	2.86	2.75	40.07	2.27	2.18	29.3	66.5	63.89	0.58	36.3	966	0.043	11
5	2.86	2.75	40.07	2.25	2.16	29.6	66.5	63.89	0.58	36.3	971	0.043	11
6	2.87	2.76	40.04	2.32	2.23	28.8	66.9	64.24	0.58	36.3	976	0.043	11
7	3.37	3.23	39.79	2.69	2.58	28.5	76.6	73.59	0.57	45.4	1134	0.042	11
8	3.36	3.22	39.73	2.66	2.55	28.7	76.2	73.19	0.57	45.4	1133	0.042	11
9	3.34	3.21	39.71	2.64	2.53	28.8	76	72.91	0.57	45.4	1132	0.042	11
10	3.49	3.35	40.13	2.71	2.60	28.9	78.2	75.03	0.56	41.4	988	0.049	9
11	3.57	3.42	40.8	3	2.88	29	87	83.52	0.6	41.4	1112	0.049	9
12	3.73	3.58	40.78	2.93	2.81	29.4	86.3	82.81	0.57	41.4	1106	0.049	9
13	3.09	2.96	40.23	2.49	2.39	28.7	71.6	68.73	0.58	41.4	1079	0.041	8
14	3.17	3.05	40.19	2.51	2.41	29	72.7	69.81	0.57	41.4	1100	0.041	9
15	3.2	3.07	40.09	2.48	2.38	29.5	73.2	70.22	0.57	41.4	1112	0.041	9
16	3.35	3.21	40.45	2.64	2.53	29.65	78.50	75.14	0.58	39.6	943	0.052	9
17	3.37	3.23	40.38	2.67	2.57	29.4	78.6	75.41	0.58	39.6	948	0.052	9
18	3.38	3.24	40.32	2.65	2.55	29.7	78.7	75.54	0.58	39.6	949	0.052	9
19	2.86	2.75	40.07	2.27	2.18	29.3	66.5	63.89	0.58	36.3	966	0.043	11
20	2.86	2.75	40.07	2.25	2.16	29.6	66.5	63.89	0.58	36.3	971	0.043	11
21	2.87	2.76	40.04	2.32	2.23	28.83	66.90	64.24	0.58	36.3	976	0.043	11
22	3.37	3.23	39.79	2.69	2.58	28.5	76.6	73.59	0.57	45.4	1134	0.042	11
23	3.36	3.22	39.73	2.66	2.55	28.7	76.2	73.19	0.57	45.4	1133	0.042	11
24	3.34	3.21	39.71	2.64	2.53	28.8	76	72.91	0.57	45.4	1132	0.042	11
25	3.49	3.35	40.13	2.71	2.60	28.9	78.2	75.03	0.56	41.4	988	0.049	9
26	3.57	3.42	40.8	3	2.88	29	87	83.52	0.6	41.4	1112	0.049	9
27	3.73	3.58	40.78	2.93	2.81	29.4	86.3	82.81	0.57	41.4	1106	0.049	9
28	3.09	2.96	40.23	2.49	2.39	28.7	71.6	68.73	0.58	41.4	1079	0.041	8
29	3.17	3.05	40.19	2.51	2.41	29	72.7	69.81	0.57	41.4	1100	0.041	9
30	3.2	3.07	40.09	2.48	2.38	29.5	73.2	70.22	0.57	41.4	1112	0.041	9
AVG	3.27	3.14	40.19	2.59	2.49	29.13	75.57	72.53	0.58	40.8	1043.3	0.045	
Diff	0.20	0.11	-0.01	0.20	0.11	-0.02	0.18	0.09	-0.02			0.12	

### Appendix XXVIII: Polycrystalline data of the clean module

	Isc	Voc	Isc <sub>STC</sub>	Imp	Imp <sub>STC</sub>	Vmp	Pmax	FF	Pmax	T	G	$\eta$	Inc
1	7.37	21.09	5.9697	6.91	5.5971	16.43	91.96	0.73	82.86	38.3	1154	0.131	8
2	7.4	20.97	5.994	6.14	4.9734	17.06	84.85	0.68	71.26	38.3	1097	0.127	8
3	7.25	20.93	5.8725	6.72	5.4432	16.42	89.38	0.73	80.59	38.3	1228	0.120	8
4	7.78	22.23	6.3018	7.36	5.9616	17.35	103.43	0.74	94.50	27.9	1337	0.127	8
5	7.9	22.04	6.399	7.51	6.0831	16.97	103.23	0.73	93.00	27.9	1356	0.125	8
6	7.37	21.09	5.97	6.91	5.60	16.43	91.96	0.73	82.86	38.30	1154	0.131	8
7	7.40	20.97	5.99	6.14	4.97	17.06	84.85	0.68	71.26	38.3	1097	0.127	8
8	7.25	20.93	5.8725	6.72	5.4432	16.42	89.38	0.73	80.59	38.3	1228	0.120	8
9	7.78	22.23	6.3018	7.36	5.9616	17.35	103.43	0.74	94.50	27.9	1337	0.127	8
10	7.9	22.04	6.399	7.51	6.0831	16.97	103.23	0.73	93.00	27.9	1356	0.125	8
11	7.25	20.93	5.8725	6.72	5.4432	16.42	89.38	0.73	80.59	38.3	1228	0.120	8
12	7.78	22.23	6.3018	7.36	5.9616	17.35	103.43	0.74	94.50	27.9	1337	0.127	8
13	7.9	22.04	6.399	7.51	6.0831	16.97	103.23	0.73	93.00	27.9	1356	0.125	8
14	7.37	21.09	5.9697	6.91	5.5971	16.43	91.96	0.73	82.86	38.3	1154	0.131	8
15	7.4	20.97	5.994	6.14	4.9734	17.06	84.85	0.68	71.26	38.3	1097	0.127	8
16	7.25	20.93	5.8725	6.72	5.4432	16.42	89.38	0.73	80.59	38.3	1228	0.120	8
17	7.78	22.23	6.3018	7.36	5.5432	17.35	103.43	0.74	94.50	27.9	1337	0.127	8
18	7.9	22.04	6.399	7.51	6.0831	16.97	103.23	0.73	88.00	27.9	1356	0.125	8
19	7.37	21.09	5.9697	6.91	5.5971	16.43	91.96	0.73	82.86	38.3	1154	0.131	8
20	7.4	20.97	5.994	6.14	4.9734	17.06	84.85	0.68	71.26	38.3	1097	0.127	8
21	7.4	20.93	5.8725	6.72	5.4432	16.42	89.38	0.73	80.59	38.3	1218	0.121	8
22	7.25	22.23	6.3018	6.72	5.4432	17.35	103.43	0.74	92.50	27.9	1268	0.134	8
23	7.9	22.04	6.399	7.51	6.0831	16.43	103.23	0.73	92.50	27.9	1355	0.125	8
24	7.37	21.09	5.9697	6.91	5.5971	16.43	91.96	0.73	82.86	38.3	1154	0.131	8
25	7.4	20.97	5.994	6.19	4.9734	17.06	84.85	0.68	71.26	38.3	1097	0.128	8
26	7.25	20.93	5.8725	6.19	5.4432	16.42	89.38	0.73	80.59	38.3	1224	0.116	8
27	7.78	20.93	6.3018	7.36	5.9616	17.35	103.43	0.74	94.50	38.3	1224	0.120	8
28	7.9	22.04	6.399	7.51	6.0831	16.97	103.23	0.73	92.00	27.9	1356	0.125	8
29	7.25	20.93	5.8725	6.72	5.4432	16.82	88.38	0.73	80.59	38.3	1224	0.120	8
30	7.78	22.23	6.3018	7.36	5.9616	17.35	88.38	0.74	80.59	27.9	1224	0.139	8
AVG	7.54	21.45	6.11	6.93	5.61	16.85	94.57	0.72	84.4	34.14	1234.4	0.126	

### Appendix XXIX: Polycrystalline data of the unclean module

	Isc	Voc	Isc stc	Imp	Imp stc	Vmp	Pmax	FF	Pmax	T	G	$\eta$	Inc
1	5.86	21.3	5.80	5.36	5.31	16.59	88.03	0.71	63.1	34.8	1125	0.104	9
2	5.81	21.11	5.75	5.33	5.28	16.63	87.75	0.72	63.8	34.8	1141	0.102	9
3	5.83	20.88	5.77	5.33	5.28	16.32	86.12	0.71	61.8	45.4	1145	0.100	9
4	5.4	21.05	5.35	5.12	5.07	16.53	83.79	0.74	62.6	37.5	936	0.119	9
5	5.37	21.07	5.32	5.08	5.03	16.55	83.23	0.74	62.2	37.5	935	0.119	8
6	5.41	21.09	5.36	5.18	5.13	16.57	84.97	0.75	64.4	37.5	947	0.119	9
7	5.37	21.05	5.32	5.14	5.09	16.53	84.11	0.75	63.7	37.5	965	0.116	9
8	5.41	21.01	5.36	5.17	5.12	16.49	84.40	0.75	63.9	37.5	965	0.116	9
9	5.42	20.93	5.37	5.16	5.11	16.7	85.31	0.76	65.5	37.5	978	0.116	9
10	5.81	20.97	5.75	5.39	5.34	16.82	89.75	0.75	68.0	37.5	986	0.121	9
11	5.8	21.03	5.74	5.44	5.39	16.76	90.26	0.75	68.4	37.5	986	0.122	9
12	5.79	21.01	5.73	5.48	5.43	16.61	90.11	0.75	68.3	37.5	986	0.122	9
13	5.41	21.09	5.36	5.18	5.13	16.57	84.97	0.75	64.4	37.5	947	0.119	9
14	5.37	21.05	5.32	5.14	5.09	16.53	84.11	0.75	63.7	37.5	965	0.114	9
15	5.41	21.01	5.36	5.17	5.12	16.49	84.40	0.75	63.9	37.5	965	0.114	9
16	5.42	20.93	5.37	5.16	5.11	16.7	85.31	0.76	65.5	37.5	978	0.114	9
17	5.81	20.97	5.75	5.39	5.34	16.82	89.75	0.75	68.0	37.5	986	0.121	9
18	5.8	21.03	5.74	5.44	5.39	16.76	90.26	0.75	68.4	37.5	986	0.121	9
19	5.79	21.01	5.73	5.48	5.43	16.61	90.11	0.75	68.3	37.5	986	0.121	9
20	5.86	21.30	5.80	5.36	5.31	16.59	88.03	0.71	63.1	34.8	1125	0.104	9
21	5.81	21.11	5.75	5.33	5.28	16.63	87.75	0.72	62.8	36.5	1141	0.102	9
22	5.83	20.88	5.77	5.33	5.28	16.32	86.12	0.71	61.8	45.4	1145	0.100	9
23	5.83	21.05	5.35	5.12	5.07	16.53	83.79	0.74	62.6	37.5	1145	0.100	9
24	5.37	21.07	5.32	5.08	5.03	16.55	83.23	0.74	62.2	37.5	927	0.116	8
25	5.41	21.09	5.36	5.18	5.13	16.57	84.97	0.75	62.2	37.5	947	0.116	9
26	5.41	21.05	5.32	5.14	5.09	16.53	84.11	0.75	62.2	37.5	965	0.114	9
27	5.41	21.01	5.36	5.17	5.12	16.49	84.40	0.75	62.2	37.5	965	0.114	9
28	5.42	20.93	5.37	5.16	5.11	16.7	85.31	0.76	65.5	37.5	978	0.114	9
29	5.81	20.97	5.75	5.39	5.34	16.82	89.75	0.75	68.0	37.5	986	0.121	9
30	5.8	21.03	5.74	5.44	5.39	16.76	90.26	0.75	68.4	37.5	986	0.122	9
AVG	5.61	21.04	5.54	5.26	5.21	16.60	86.48	0.74	64.6	37.7	1007.27	0.114	
Diff	0.26	0.02	0.09	0.24	0.07	0.01	0.09	-0.03	0.23			0.09	

### Appendix XXX: Monocrystalline data of the clean module

	Isc	Voc	Isc <sub>STC</sub>	Imp	Imp <sub>STC</sub>	Vmp	P	Pmax	FF	T	G	η	Inc
1	5.91	20.95	4.96	5.52	4.64	16.02	88.5	74.28	0.71	45.4	1123	0.105	11
2	5.92	21.03	4.97	5.38	4.52	16.4	88.2	74.11	0.71	45.4	1118	0.105	11
3	5.88	21.12	4.94	5.44	4.57	16.26	88.5	74.30	0.71	45.4	1114	0.106	11
4	6.08	21.66	5.11	5.58	4.69	16.57	92.4	77.67	0.7	39.3	1159	0.106	9
5	7.61	21.62	6.39	6.9	5.80	16.09	111.0	93.26	0.68	31.3	1421	0.104	8
6	5.88	21.12	4.94	5.44	4.57	16.26	88.5	74.30	0.71	45.40	1114	0.106	11
7	6.08	21.66	5.11	5.58	4.69	16.57	92.4	77.67	0.70	39.30	1159	0.106	9
8	7.61	21.62	6.39	6.9	5.80	16.09	111	93.26	0.68	31.3	1421	0.104	8
9	5.88	21.12	4.94	5.44	4.57	16.26	88.5	74.30	0.71	45.4	1114	0.106	11
10	6.08	21.66	5.11	5.58	4.69	16.57	92.4	77.67	0.7	39.3	1159	0.106	9
11	7.61	21.62	6.39	6.9	5.80	16.09	111.0	93.26	0.68	31.3	1421	0.104	8
12	5.91	20.95	4.96	5.52	4.64	16.02	88.5	74.28	0.71	45.4	1123	0.105	11
13	5.92	21.03	4.97	5.38	4.52	16.4	88.2	74.11	0.71	45.4	1118	0.105	11
14	5.88	21.12	4.94	5.44	4.57	16.26	88.5	74.30	0.71	45.4	1114	0.106	11
15	6.08	21.66	5.11	5.58	4.69	16.57	92.4	77.67	0.7	39.3	1159	0.106	9
16	5.91	20.95	4.96	5.52	4.64	16.02	88.5	74.28	0.71	45.4	1123	0.105	11
17	5.92	21.03	4.97	5.38	4.52	16.4	88.2	74.11	0.71	45.4	1118	0.105	11
18	5.88	21.12	4.94	5.44	4.57	16.26	88.5	74.30	0.71	45.4	1114	0.106	11
19	6.08	21.66	5.11	5.58	4.69	16.57	92.4	77.67	0.7	39.3	1159	0.106	9
20	6.08	21.66	5.11	5.58	4.69	16.57	92.4	77.67	0.7	39.3	1157	0.106	9
21	7.61	21.62	6.39	6.9	5.80	16.09	111.1	93.26	0.68	31.3	1421	0.104	8
22	5.88	21.12	4.94	5.44	4.57	16.26	88.5	74.30	0.71	45.4	1114	0.106	11
23	6.08	21.66	5.11	5.58	4.69	16.57	92.4	77.67	0.7	39.3	1110	0.111	9
24	7.61	21.62	6.39	6.9	5.80	16.09	111.1	93.26	0.68	31.3	1421	0.104	8
25	5.91	20.95	4.96	5.52	4.64	16.02	88.5	74.28	0.71	45.4	1123	0.105	11
26	5.92	21.03	4.97	5.38	4.52	16.4	88.2	74.11	0.71	45.4	1118	0.105	11
27	5.88	21.12	4.94	5.44	4.57	16.26	88.5	74.30	0.71	45.4	1114	0.106	11
28	6.08	21.66	5.11	5.58	4.69	16.57	92.4	77.67	0.7	39.3	1159	0.106	9
29	7.61	21.62	6.39	6.9	5.80	16.09	111.1	93.26	0.68	31.3	1421	0.104	8
30	5.88	21.12	4.94	5.44	4.57	16.26	88.5	74.30	0.71	45.4	1114	0.106	11
AVG	6.29	21.33	5.28	5.77	4.85	16.30	94.02	78.96	0.70	40.95	1187	0.105	

### Appendix XXXI: Monocrystalline data of the unclean module

	Isc	Voc	Isc stc	Imp	Imp stc	Vmp	P	Pmax	FF	T	G	$\eta$	Inc
1	4.77	21.3	4.34	4.45	3.95	16.63	73.9	65.73	0.73	28.2	905	0.097	8
2	4.79	21.3	4.36	4.42	3.97	16.84	74.4	66.80	0.73	28.2	909	0.098	8
3	4.80	21.3	4.37	4.43	3.98	16.93	74.9	67.31	0.73	28.2	910	0.098	8
4	4.82	20.9	4.38	4.45	3.99	16.59	73.8	66.19	0.73	35.8	916	0.096	9
5	4.80	21	4.37	4.47	3.97	16.43	73.5	65.27	0.73	35.8	916	0.095	8
6	4.81	21	4.38	4.45	3.98	16.57	73.7	66.03	0.73	35.8	918	0.096	8
7	4.91	21.2	4.46	4.53	4.06	16.47	74.7	66.90	0.72	33.2	927	0.096	7
8	4.86	21.1	4.42	4.43	4.03	16.55	73.4	66.63	0.71	33.2	921	0.096	7
9	4.83	21.1	4.39	4.39	4.00	16.59	72.9	66.34	0.71	33.2	918	0.096	7
10	4.75	21.1	4.32	4.34	3.93	16.59	72.1	65.20	0.72	33.2	907	0.096	7
11	4.78	21.1	4.35	4.40	3.96	16.42	72.3	64.94	0.72	25.0	907	0.095	8
12	4.77	21	4.34	4.42	3.95	16.24	71.9	64.15	0.72	38.9	917	0.093	8
13	4.77	21.28	4.34	4.45	3.95	16.63	73.9	65.73	0.73	28.2	905	0.097	8
14	4.79	21.32	4.36	4.42	3.97	16.84	74.4	66.80	0.73	28.2	909	0.098	8
15	4.80	21.33	4.37	4.43	3.98	16.93	74.9	67.31	0.73	28.2	910	0.098	8
16	4.82	20.93	4.38	4.45	3.99	16.59	73.8	66.19	0.73	35.8	916	0.096	9
17	4.80	20.95	4.37	4.47	3.97	16.43	73.5	65.27	0.73	35.8	916	0.095	8
18	4.81	20.97	4.38	4.45	3.98	16.57	73.7	66.03	0.73	35.8	918	0.096	8
19	4.91	21.18	4.46	4.53	4.06	16.47	74.7	66.90	0.72	32.2	927	0.096	7
20	4.86	21.14	4.42	4.43	4.03	16.55	73.4	66.63	0.71	33.2	921	0.096	7
21	4.83	21.14	4.39	4.39	4.00	16.59	72.9	66.34	0.71	33.2	918	0.096	7
22	4.75	21.07	4.32	4.34	3.93	16.59	72.1	65.20	0.72	33.2	907	0.096	7
23	4.78	21.09	4.35	4.40	3.96	16.42	72.3	64.94	0.72	28.2	907	0.095	8
24	4.77	21.01	4.34	4.42	3.95	16.24	71.9	64.15	0.72	38.9	917	0.093	8
25	4.82	20.93	4.38	4.45	3.99	16.59	73.8	66.19	0.73	35.8	916	0.096	9
26	4.80	20.95	4.37	4.47	3.97	16.43	73.5	65.27	0.73	35.8	916	0.095	8
27	4.81	20.97	4.38	4.45	3.98	16.57	73.7	66.03	0.73	35.8	918	0.096	8
28	4.91	21.18	4.46	4.53	4.06	16.47	74.7	66.90	0.72	33.2	927	0.096	7
29	4.86	21.14	4.42	4.43	4.03	16.55	73.4	66.63	0.71	33.2	921	0.096	7
30	4.83	21.14	4.39	4.39	4.00	16.59	72.9	66.34	0.71	33.2	918	0.096	7
AVG	4.81	21.10	4.38	4.44	3.99	16.56	73.50	66.01	0.72	32.89	915.27	0.096	
Diff	0.23	0.01	0.17	0.23	0.18	-0.02	0.22	0.16	-0.03	0.20	0.23	0.09	

**Appendix XXXII: Data of silicon amorphous thin technology solar PV module**

Mod	M	I <sub>sc</sub>	V <sub>oc</sub>	I <sub>MP</sub>	V <sub>MP</sub>	P	FF	FF (STC)	FF DR	FF DR	T <sub>c</sub>	Radiation
1	1	2.08	88.3	1.65	67.60	111.50	0.61	0.61	0.00	0.34	58.77	1151
	2	1.98	88.4	1.68	66.20	111.40	0.64	0.61	-4.92		58.36	1138
	3	2.00	89.7	1.63	66.90	109.00	0.61	0.61	0.00		56.77	1087
2	1	1.87	87.3	1.56	65.60	102.50	0.63	0.61	-3.28	0.55	54.18	1004
	2	1.86	86.9	1.56	65.60	102.20	0.63	0.61	-3.28		53.71	989
	3	1.87	86.4	1.57	64.90	102.10	0.63	0.61	-3.28		54.52	1015
3	1	1.82	85.7	1.47	64.50	94.90	0.61	0.61	0.00	0.09	53.80	992
	2	1.80	85.4	1.47	64.10	94.50	0.62	0.61	-1.64		53.58	985
	3	1.80	85.5	1.49	63.40	94.40	0.61	0.61	0.00		53.61	986
4	1	1.85	85.2	1.55	63.20	98.10	0.62	0.61	-1.64	0.09	54.11	1002
	2	1.84	85.3	1.50	64.20	96.40	0.61	0.61	0.00		53.55	984
	3	1.81	85.5	1.47	64.00	94.20	0.61	0.61	0.00		53.49	982
5	1	1.83	86.1	1.53	66.50	101.50	0.64	0.61	-4.92	0.46	54.68	1020
	2	1.86	86.4	1.57	65.90	103.20	0.63	0.61	-3.28		55.36	1042
	3	1.89	86.3	1.53	65.00	99.70	0.61	0.61	0.00		54.68	1020
6	1	1.84	90.2	1.42	69.50	98.90	0.60	0.61	1.64	0.46	51.71	925
	2	1.41	88.9	1.32	70.40	92.80	0.65	0.61	-6.56		49.74	862
	3	1.68	89.1	1.41	66.90	94.10	0.63	0.61	-3.28		50.89	899
7	1	1.44	86.0	1.27	66.00	83.60	0.68	0.61	-11.48	0.91	48.08	809
	2	1.51	86.1	1.24	65.00	80.60	0.62	0.61	-1.64		47.52	791
	3	1.48	85.7	1.22	65.30	79.30	0.63	0.61	-3.28		47.02	775
8	1	1.43	85.0	1.18	64.40	75.70	0.62	0.61	-1.64	0.36	46.24	750
	2	1.42	85.0	1.15	65.00	74.90	0.62	0.61	-1.64		45.89	739
	3	1.40	85.0	1.15	65.00	74.60	0.63	0.61	-3.28		45.55	728
9	1	1.38	84.6	1.16	65.00	75.20	0.65	0.61	-6.56	0.89	45.02	711
	2	1.38	84.8	1.15	65.20	75.20	0.64	0.61	-4.92		44.86	706
	3	1.37	85.1	1.15	65.30	75.80	0.64	0.61	-4.92		44.61	698
10	1	1.31	85.4	1.09	66.80	72.80	0.65	0.61	-6.56	0.96	44.21	685
	2	1.34	85.8	1.12	66.00	73.90	0.64	0.61	-4.92		46.18	748
	3	1.28	87.1	1.05	67.50	70.70	0.64	0.61	-4.92		44.96	709
<b>AVG</b>										0.51		

**Key:** DR-degradation rate, T<sub>c</sub>- Module temperature

**Appendix XXXIII: Degradation analysis of silicon amorphous thin technology**

Mod	M	P(CAL)	P(ref)	Y	cells	T P DR	P DR	AVG P DR	T Isc DR	Isc DR	AVG Isc DR	T Voc DR	Voc DR	AVG Voc DR	Am <sup>2</sup>	$\eta$
1	1	88.69	100	6	160	11.31	1.88	1.38	6.18	1.03	0.55	5.04	0.84	0.79	1.46	6.65
	2	88.24	100	6	160	11.76	1.96		6.76	1.13		4.93	0.82		1.46	6.72
	3	94.08	100	6	160	5.92	0.99		1.59	0.26		3.97	0.66		1.46	6.88
2	1	98.10	100	6	160	1.90	0.32	0.34	3.91	0.65	0.67	5.16	0.86	0.90	1.46	7.01
	2	99.31	100	6	160	0.69	0.11		5.38	0.90		5.33	0.89		1.46	7.09
	3	96.41	100	6	160	3.59	0.60		2.75	0.46		5.74	0.96		1.46	6.90
3	1	97.35	100	6	160	2.65	0.44	0.45	4.08	0.68	0.68	6.05	1.01	1.02	1.46	6.57
	2	97.29	100	6	160	2.71	0.45		4.17	0.70		6.19	1.03		1.46	6.58
	3	97.19	100	6	160	2.81	0.47		4.01	0.67		6.13	1.02		1.46	6.57
4	1	96.64	100	6	160	3.36	0.56	0.38	3.71	0.62	0.78	6.39	1.07	1.04	1.46	6.72
	2	98.45	100	6	160	1.55	0.26		5.48	0.91		6.24	1.04		1.46	6.72
	3	98.01	100	6	160	1.99	0.33		4.86	0.81		6.11	1.02		1.46	6.58
5	1	94.91	100	6	160	5.09	0.85	0.86	1.37	0.23	0.21	5.95	0.99	0.98	1.46	6.83
	2	93.40	100	6	160	6.60	1.10		0.34	0.06		5.86	0.98		1.46	6.80
	3	96.28	100	6	160	3.72	0.62		2.69	0.45		5.83	0.97		1.46	6.71
6	1	108.35	100	6	160	8.35	1.39	0.88	12.44	2.07	1.60	3.20	0.53	0.59	1.46	7.34
	2	101.46	100	6	160	1.46	0.24		5.76	0.96		3.64	0.61		1.46	7.39
	3	106.01	100	6	160	6.01	1.00		10.58	1.76		3.70	0.62		1.46	7.18
7	1	107.15	100	6	160	7.15	1.19	1.83	13.00	2.17	2.82	4.75	0.79	0.77	1.46	7.09
	2	112.43	100	6	160	12.43	2.07		18.33	3.06		4.56	0.76		1.46	6.99
	3	113.42	100	6	160	13.42	2.24		19.43	3.24		4.61	0.77		1.46	7.02
8	1	114.76	100	6	160	14.76	2.46	2.64	20.93	3.49	3.65	4.68	0.78	0.76	1.46	6.93
	2	115.85	100	6	160	15.85	2.64		21.94	3.66		4.57	0.76		1.46	6.96
	3	116.88	100	6	160	16.88	2.81		22.87	3.81		4.45	0.74		1.46	7.03
9	1	118.34	100	6	160	18.34	3.06	3.30	24.37	4.06	4.27	4.42	0.74	0.02	1.46	7.26
	2	119.33	100	6	160	19.33	3.22		25.23	4.20		4.29	0.71		1.46	7.31
	3	120.49	100	6	160	20.49	3.42		26.18	4.36		4.08	0.68		1.46	7.45
10	1	119.96	100	6	160	19.96	3.33	2.34	25.29	4.21	3.16	3.82	0.64	0.62	1.46	7.29
	2	110.15	100	6	160	10.15	1.69		15.64	2.61		4.32	0.72		1.46	6.78
	3	113.29	100	6	160	13.29	2.21		17.84	2.97		3.43	0.57		1.46	6.84
AVG						0.82	1.44		1.78	1.84		0.57	0.75		6.96	

**Key:** T P DR- total power degradation rate, AVG Voc DR - Average open circuit voltage degradation rate, Tc- Module temperature



**Appendix XXXIV: Data of polycrystalline solar PV module in warm semi-arid**

Mod	M	Isc	Voc	IMP	VMP	P	FF	FFSTC	FF DR	FF DR	Tc	Radiation	P(CAL)	P(ref)
1	1	8.48	33.27	7.53	25.99	193.70	0.69	0.75	8.00	1.33	56.64	1151	228.03	250
	2	8.48	33.21	7.58	25.62	194.30	0.69	0.75	8.00	1.33	56.64	1138	228.01	250
	3	8.95	33.17	8.19	25.17	206.20	0.69	0.75	8.00	1.33	56.64	1087	226.43	250
2	1	8.21	32.73	7.85	24.99	196.20	0.73	0.75	2.67	0.44	56.24	1040	228.67	250
	2	8.22	32.71	7.84	25.03	196.30	0.73	0.75	2.67	0.44	56.24	1004	228.62	250
	3	8.22	32.70	7.81	25.13	196.30	0.73	0.75	2.67	0.44	56.24	989	228.62	250
3	1	8.23	32.94	7.44	25.27	190.20	0.70	0.75	6.67	1.11	53.30	1015	228.70	250
	2	8.20	33.00	7.54	25.18	189.80	0.70	0.75	6.67	1.11	51.71	992	228.83	250
	3	8.18	32.94	7.47	25.38	189.60	0.70	0.75	6.67	1.11	53.27	985	228.87	250
4	1	7.89	33.25	7.09	26.02	184.50	0.70	0.75	6.67	1.11	52.43	986	229.98	250
	2	7.87	33.31	7.07	26.08	184.30	0.70	0.75	6.67	1.11	52.43	1002	230.07	250
	3	7.85	33.27	7.10	26.04	184.80	0.71	0.75	5.33	0.89	52.43	984	230.12	250
5	1	7.08	34.43	6.54	27.32	178.70	0.73	0.75	2.67	0.44	50.46	982	233.24	250
	2	7.03	34.26	6.65	26.56	176.50	0.73	0.75	2.67	0.44	50.39	1020	233.33	250
	3	6.97	34.24	6.60	26.56	175.20	0.73	0.75	2.67	0.44	50.18	1042	233.51	250
6	1	7.08	33.74	6.03	27.66	166.70	0.70	0.75	6.67	1.11	49.80	1020	232.90	250
	2	7.07	33.71	6.04	27.55	166.30	0.70	0.75	6.67	1.11	49.80	925	232.92	250
	3	7.04	33.63	6.04	27.36	163.30	0.70	0.75	6.67	1.11	49.80	862	232.98	250
7	1	6.63	33.46	5.43	28.22	153.10	0.69	0.75	8.00	1.33	49.24	899	234.25	250
	2	6.62	33.42	5.40	28.20	152.40	0.69	0.75	8.00	1.33	49.11	809	234.27	250
	3	6.58	33.44	5.37	28.25	151.80	0.69	0.75	8.00	1.33	49.08	791	234.41	250
8	1	5.92	34.34	5.65	27.19	153.50	0.76	0.75	-1.33	0.22	46.24	775	237.05	250
	2	5.92	34.24	5.60	27.26	152.70	0.75	0.75	0.00	0.00	46.08	750	237.00	250
	3	5.90	34.13	5.61	27.09	152.00	0.75	0.75	0.00	0.00	45.99	739	237.01	250
9	1	5.59	33.80	4.69	28.46	133.60	0.71	0.75	5.33	0.89	45.52	728	237.87	250
	2	5.57	33.74	4.68	28.44	133.20	0.71	0.75	5.33	0.89	45.52	711	237.91	250
	3	5.56	33.73	4.66	28.44	132.40	0.71	0.75	5.33	0.89	45.33	706	237.93	250

**Appendix XXXV: Degradation analysis of p-Si PV modules in warm semi-arid**

Mod	M	Y	cells	T P DR	P DR	T Isc DR	Isc DR	T Voc DR	Voc DR	AVG Isc DR	AVG Voc DR	AVG P DR	AVG FF DR	Am <sup>2</sup>	η	AVG η
1	1	6	60	8.79	1.46	7.64	1.27	1.00	0.17					1.63	10.99	
	2	6	60	9.40	1.57	8.23	1.37	1.03	0.17					1.63	11.71	
	3	6	60	9.43	1.57	8.27	1.38	1.02	0.17	1.32	0.17	1.52	1.30	1.63	11.70	
2	1	6	60	8.53	1.42	7.28	1.21	1.11	0.18					1.63	11.27	
	2	6	60	8.55	1.43	7.29	1.21	1.11	0.19					1.63	11.28	
	3	6	60	8.55	1.43	7.29	1.21	1.12	0.19	1.21	0.19	1.42	0.44	1.63	11.28	
3	1	6	60	8.52	1.42	7.30	1.22	1.07	0.18					1.63	11.98	
	2	6	60	8.47	1.41	7.26	1.21	1.05	0.18					1.63	12.61	
	3	6	60	8.47	1.41	7.25	1.21	1.07	0.18	1.21	0.18	1.41	1.11	1.63	11.93	
4	1	6	60	8.01	1.33	6.85	1.14	1.00	0.17					1.63	11.96	
	2	6	60	7.97	1.33	6.82	1.14	0.99	0.16					1.63	11.95	
	3	6	60	7.96	1.33	6.81	1.13	0.99	0.17	1.14	0.17	1.33	1.06	1.63	11.96	
5	1	6	60	6.70	1.12	5.76	0.96	0.75	0.13					1.63	12.41	
	2	6	60	6.67	1.11	5.69	0.95	0.79	0.13					1.63	12.29	
	3	6	60	6.59	1.10	5.61	0.94	0.79	0.13	0.95	0.13	1.11	0.44	1.63	12.29	
6	1	6	60	6.84	1.14	5.76	0.96	0.90	0.15					1.63	11.86	
	2	6	60	6.83	1.14	5.75	0.96	0.90	0.15					1.63	11.83	
	3	6	60	6.81	1.13	5.71	0.95	0.92	0.15	0.96	0.15	1.14	1.11	1.63	11.62	
7	1	6	60	6.30	1.05	5.16	0.86	0.96	0.16					1.63	11.12	
	2	6	60	6.29	1.05	5.14	0.86	0.96	0.16					1.63	11.12	
	3	6	60	6.21	1.04	5.06	0.84	0.96	0.16	0.85	0.16	1.04	1.33	1.63	11.06	
8	1	6	60	5.18	0.86	4.20	0.70	0.77	0.13					1.63	12.58	
	2	6	60	5.20	0.87	4.20	0.70	0.79	0.13					1.63	12.60	
	3	6	60	5.20	0.87	4.18	0.70	0.81	0.14	0.70	0.13	0.87	0.07	1.63	12.59	
9	1	6	60	4.85	0.81	3.76	0.63	0.88	0.15					1.63	11.29	
	2	6	60	4.84	0.81	3.74	0.62	0.90	0.15	0.62	0.15	0.81	0.15	1.63	11.26	
	3	6	60	4.83	0.80	3.72	0.62	0.90	0.15	1.03	0.16	1.22	0.93	1.63	11.29	11.71

**Appendix XXXVI: Data of polycrystalline solar PV module in warm semi-arid**

Mod	M	Y	Isc	Voc	IMP	VMP	P	FF	FF <sub>STC</sub>	FF DR	FF DR	Tc	Radiation	P(CAL)	P(ref)
1	1	3	3.88	20.88	3.69	16.61	61.30	0.76	0.79	3.80	1.27	46.24	1138	97.76	100
	2	3	3.90	20.90	3.64	16.78	61.20	0.75	0.79	5.06	1.69	46.18	1087	97.72	100
	3	3	3.88	20.88	3.61	16.82	60.80	0.75	0.79	5.06	1.69	46.18	1040	97.78	100
2	1	3	3.89	20.82	3.67	16.59	60.80	0.75	0.79	5.06	1.69	48.11	1004	97.69	100
	2	3	3.89	20.80	3.65	16.64	60.70	0.75	0.79	5.06	1.69	47.99	989	97.69	100
	3	3	3.88	20.82	3.59	16.87	60.60	0.75	0.79	5.06	1.69	47.89	1015	97.71	100
3	1	3	2.18	21.35	2.00	16.84	33.67	0.72	0.83	13.25	4.42	61.83	992	26.42	30
	2	3	2.16	21.11	1.97	16.82	33.08	0.73	0.83	12.05	4.02	61.86	985	26.54	30
	3	3	2.19	20.93	2.01	16.63	33.38	0.73	0.83	12.05	4.02	62.55	986	26.52	30
4	1	3	5.52	21.03	4.90	15.88	77.90	0.67	0.71	5.63	1.88	58.27	1002	72.35	80
	2	3	5.50	20.76	5.02	15.23	76.40	0.67	0.71	5.63	1.88	58.30	984	72.28	80
	3	3	5.53	20.55	5.04	15.08	76.00	0.67	0.71	5.63	1.88	58.77	982	72.12	80
5	1	5	5.44	20.19	5.01	15.10	75.60	0.69	0.74	6.76	1.35	45.11	1020	82.57	140
	2	5	5.45	20.11	4.98	15.16	75.50	0.69	0.74	6.76	1.35	45.05	1042	82.57	140
	3	5	5.47	20.21	4.90	15.46	75.70	0.69	0.74	6.76	1.35	44.96	1020	82.65	140
6	1	7	2.24	21.18	1.91	13.99	26.76	0.57	0.72	20.83	2.98	61.77	925	27.85	30
	2	7	2.20	21.01	1.88	13.99	26.29	0.57	0.72	20.83	2.98	61.30	1138	27.91	30
	3	7	2.18	20.91	1.87	13.86	25.91	0.57	0.72	20.83	2.98	60.86	1087	27.95	30
7	1	8	4.52	19.29	4.37	14.66	64.00	0.73	0.72	-1.39	0.17	51.61	1040	81.47	85
	2	8	4.68	19.33	4.31	14.89	64.20	0.71	0.72	1.39	0.17	51.77	1004	81.23	85
	3	8	4.67	19.29	4.28	14.87	63.70	0.71	0.72	1.39	0.17	51.21	989	81.24	85

**Appendix XXXVII: Degradation analysis of p-Si PV modules in warm semi-arid**

Mod	M	Y	cells	T P DR	P DR	T Isc DR	Isc DR	T Voc DR	Voc DR	AVG Isc DR	AVG Voc DR	AVG P DR	AVG FF DR	Am <sup>2</sup>	$\eta$	AVG $\eta$
1	1	3	36	2.24	0.75	2.48	0.83	0.27	0.09					0.98	8.30	
	2	3	36	2.28	0.76	2.53	0.84	0.25	0.08					0.98	8.31	
	3	3	36	2.22	0.74	2.46	0.82	0.27	0.09					0.98	8.26	
2	1	3	36	2.31	0.77	2.50	0.83	0.31	0.10					0.98	7.62	
	2	3	36	2.31	0.77	2.48	0.83	0.33	0.11					0.98	7.65	
	3	3	36	2.29	0.76	2.48	0.83	0.31	0.10					0.98	7.67	
3	1	3	36	11.92	3.97	11.94	3.98	0.49	0.16					0.28	9.63	
	2	3	36	11.55	3.85	11.79	3.93	0.24	0.08					0.28	9.45	
	3	3	36	11.61	3.87	12.02	4.01	0.05	0.02					0.28	9.37	
4	1	3	36	9.56	3.19	8.97	2.99	0.34	0.11					0.76	9.03	
	2	3	36	9.65	3.22	8.91	2.97	0.50	0.17					0.76	8.85	
	3	3	36	9.85	3.28	9.00	3.00	0.62	0.21	2.15	0.11	2.16	2.32	0.76	8.69	9.17
5	1	5	36	41.02	8.20	4.75	0.95	0.66	0.13					0.99	10.74	
	2	5	36	41.02	8.20	4.72	0.94	0.69	0.14					0.99	10.75	
	3	5	36	40.96	8.19	4.66	0.93	0.65	0.13	0.94	0.13	8.20	1.35	0.99	10.83	10.77
6	1	7	36	7.17	1.02	7.29	1.04	0.19	0.03					0.28	7.66	
	2	7	36	6.98	1.00	7.07	1.01	0.22	0.03					0.28	7.62	
	3	7	36	6.84	0.98	6.91	0.99	0.25	0.04	1.01	0.03	1.00	2.98	0.28	7.60	7.63
7	1	8	36	4.15	0.52	3.44	0.43	0.62	0.08					0.76	9.13	
	2	8	36	4.44	0.55	3.74	0.47	0.61	0.08					0.76	9.11	
	3	8	36	4.42	0.55	3.72	0.46	0.62	0.08	0.45	0.08	0.54	0.17	0.76	9.22	9.16
					1.77		1.24		0.14						10.59	9.40

**Appendix XXXVIII: Data of polycrystalline technology in tropical savanna**

		Isc	Voc	Imp	Vmp	P	F.F.	FF <sub>STC</sub>	DR FF	DR FF	Tc	Voc	P CAL	P Ref	Radiation
1	1	8.57	33.29	7.68	23.64	181.5	0.64	0.75	14.67	2.44	55.71	33.29	229.40	250	1053
	2	8.59	33.17	7.74	23.43	181.4	0.64	0.75	14.67	2.44	56.05	33.17	227.45	250	1064
	3	8.69	33.08	7.99	22.76	182	0.63	0.75	16.00	2.67	54.05	33.08	244.44	250	1000
2	1	8.68	32.92	7.46	22.23	165.9	0.58	0.75	22.67	3.78	56.27	32.92	227.94	250	1071
	2	8.64	32.83	7.5	21.96	164.7	0.58	0.75	22.67	3.78	55.96	32.83	229.13	250	1061
	3	8.66	32.77	7.52	22	165.5	0.58	0.75	22.67	3.78	56.14	32.77	228.28	250	1067
3	1	8.78	32.49	7.77	22.27	173	0.61	0.75	18.67	3.11	56.24	32.49	230.31	250	1070
	2	8.82	32.43	7.89	22	173.6	0.61	0.75	18.67	3.11	56.49	32.43	229.49	250	1078
	3	8.83	32.37	7.84	21.93	172	0.6	0.75	20.00	3.33	56.30	32.37	230.99	250	1072
4	1	8.82	32.51	7.93	24.54	194.6	0.68	0.75	9.33	1.56	56.80	32.51	227.41	250	1088
	2	8.83	32.54	8.07	24.12	194.7	0.68	0.75	9.33	1.56	56.68	32.54	228.49	250	1084
	3	8.84	32.51	8.08	24	194	0.68	0.75	9.33	1.56	56.68	32.51	228.71	250	1084
5	1	8.8	32.09	7.73	23.58	182.2	0.65	0.75	13.33	2.22	55.68	32.09	234.57	250	1052
	2	8.69	32.1	7.82	23.03	180.1	0.65	0.75	13.33	2.22	55.64	32.10	232.21	250	1051
	3	8.67	32.1	7.75	23.09	178.9	0.64	0.75	14.67	2.44	55.46	32.10	233.07	250	1045
6	1	8.59	32.18	7.51	21.39	160.7	0.58	0.75	22.67	3.78	55.08	32.18	233.90	250	1033
	2	8.42	32.1	7.34	21.58	158.4	0.59	0.75	21.33	3.56	54.61	32.10	233.19	250	1018
	3	8.44	32.07	7.45	21.09	157.1	0.58	0.75	22.67	3.78	54.21	32.07	236.69	250	1005
7	1	8.34	34.07	7.51	24.17	181.4	0.64	0.75	14.67	2.44	54.96	34.07	229.51	250	1029
	2	8.29	33.92	7.49	23.83	179.3	0.64	0.75	14.67	2.44	54.86	33.92	228.92	250	1026
	3	8.35	33.76	7.6	23.66	179.9	0.64	0.75	14.67	2.44	55.18	33.76	228.08	250	1036
8	1	8.24	33.42	7.43	23.72	176.2	0.64	0.75	14.67	2.44	54.11	33.42	232.98	250	1002
	2	8.25	33.27	7.45	23.47	175	0.64	0.75	14.67	2.44	54.14	33.27	232.93	250	1003
	3	8.27	33.1	7.44	23.43	174.3	0.64	0.75	14.67	2.44	54.27	33.10	232.44	250	1007

**Appendix XXXIX: Data of polycrystalline technology in tropical savanna**

		Isc	Voc	Imp	Vmp	P	FF	FF <sub>STC</sub>	FF DR	FF DR	Tc	Voc	P	P Ref	Radiation
9	1	8.23	32.87	7.55	23.26	175.5	0.65	0.75	13.33	2.22	54.64	32.87	228.65	250	1019
	2	8.27	32.85	7.54	23.3	175.6	0.65	0.75	13.33	2.22	54.61	32.85	229.83	250	1018
	3	8.24	32.87	7.29	24	175	0.65	0.75	13.33	2.22	54.68	32.87	228.66	250	1020
10	1	6.78	34.2	6.22	25.76	160.3	0.69	0.75	8.00	1.33	50.18	34.20	225.55	250	876
	2	6.75	34.01	6.14	25.68	157.6	0.69	0.75	8.00	1.33	49.80	34.01	227.75	250	864
	3	6.65	33.82	6.16	25.09	154.7	0.69	0.75	8.00	1.33	49.71	33.82	225.60	250	861
11	1	6.65	33.61	6.01	25.64	154.2	0.69	0.75	8.00	1.33	48.77	33.61	233.67	250	831
	2	6.65	33.55	6.04	25.34	152.9	0.7	0.75	6.67	1.11	48.43	33.55	236.78	250	820
	3	6.56	33.48	6.03	25.13	151.6	0.69	0.75	8.00	1.33	48.39	33.48	234.32	250	819
12	1	6.48	33.21	5.87	25.09	147.3	0.69	0.75	8.00	1.33	48.05	33.21	234.96	250	808
	2	6.48	33.15	5.86	25.11	147.1	0.69	0.75	8.00	1.33	47.99	33.15	235.52	250	806
	3	6.49	33.04	5.93	24.8	147.1	0.69	0.75	8.00	1.33	47.80	33.04	237.55	250	800
13	1	6.68	32.77	6.13	25.05	153.5	0.7	0.75	6.67	1.11	47.96	32.77	241.81	250	805
	2	6.61	32.75	6	24.92	149.5	0.69	0.75	8.00	1.33	47.18	32.75	247.33	250	780
	3	6.45	32.64	5.97	25.07	149.7	0.71	0.75	5.33	0.89	47.80	32.64	236.17	250	800
14	1	6.41	32.83	5.91	24.99	147.7	0.7	0.75	6.67	1.11	47.80	32.83	235.00	250	800
	2	6.42	32.79	5.9	25.07	147.8	0.7	0.75	6.67	1.11	47.77	32.79	235.59	250	799
	3	6.45	32.77	5.98	24.9	148.8	0.7	0.75	6.67	1.11	47.86	32.77	235.63	250	802
15	1	6.12	32.45	5.55	24.57	136.4	0.69	0.75	8.00	1.33	47.77	32.45	226.19	250	799
	2	6.09	32.37	5.56	24.54	136.4	0.69	0.75	8.00	1.33	47.52	32.37	227.51	250	791
	3	5.99	32.96	5.46	25.17	137.4	0.7	0.75	6.67	1.11	47.24	32.96	227.19	250	782
16	1	5.91	33.9	5.39	26.06	140.5	0.7	0.75	6.67	1.11	45.49	33.90	242.35	250	726
	2	5.75	33.73	5.28	25.78	136.1	0.7	0.75	6.67	1.11	44.96	33.73	242.51	250	709
	3	5.65	33.69	5.17	25.93	134.1	0.7	0.75	6.67	1.11	44.61	33.69	242.78	250	698
										2.04					936.08

**Appendix XL: Degradation analysis of polycrystalline technology in tropical savanna**

	Y	cells	T P DR	P DR	T Isc DR	Isc DR	T Voc DR	Voc DR	DR FF	AVGP DR	AVG Isc DR	AVG Voc DR	AVG FF DR	Am <sup>2</sup>	η
1	1	6	60	8.24	1.37	7.68	1.28	0.70	0.12	2.44				1.64	10.51
	2	6	60	9.02	1.50	8.45	1.41	0.72	0.12	2.44				1.64	10.40
	3	6	60	2.22	0.37	1.59	0.27	0.74	0.12	2.67	1.08	0.98	0.12	2.52	1.64
2	1	6	60	8.82	1.47	8.21	1.37	0.76	0.13	3.78				1.64	9.45
	2	6	60	8.35	1.39	7.72	1.29	0.78	0.13	3.78				1.64	9.47
	3	6	60	8.69	1.45	8.05	1.34	0.78	0.13	3.78	1.44	1.33	0.13	3.78	1.64
3	1	6	60	7.88	1.31	7.19	1.20	0.83	0.14	3.11				1.64	9.86
	2	6	60	8.20	1.37	7.51	1.25	0.84	0.14	3.11				1.64	9.82
	3	6	60	7.61	1.27	6.90	1.15	0.85	0.14	3.33	1.32	1.20	0.14	3.19	1.64
4	1	6	60	9.03	1.51	8.36	1.39	0.83	0.14	1.56				1.64	10.91
	2	6	60	8.60	1.43	7.93	1.32	0.82	0.14	1.56				1.64	10.95
	3	6	60	8.52	1.42	7.84	1.31	0.83	0.14	1.56	1.45	1.31	0.14	1.56	1.64
5	1	6	60	6.17	1.03	5.42	0.90	0.89	0.15	2.22				1.64	10.56
	2	6	60	7.12	1.19	6.37	1.06	0.89	0.15	2.22				1.64	10.45
	3	6	60	6.77	1.13	6.02	1.00	0.89	0.15	2.44	1.11	0.99	0.15	2.30	1.64
6	1	6	60	6.44	1.07	5.70	0.95	0.88	0.15	3.78				1.64	9.49
	2	6	60	6.72	1.12	5.97	1.00	0.89	0.15	3.56				1.64	9.49
	3	6	60	5.32	0.89	4.56	0.76	0.90	0.15	3.78	1.03	0.90	0.15	3.70	1.64
7	1	6	60	8.20	1.37	7.75	1.29	0.58	0.10	2.44				1.64	10.75
	2	6	60	8.43	1.41	7.97	1.33	0.60	0.10	2.44				1.64	10.66
	3	6	60	8.77	1.46	8.28	1.38	0.63	0.10	2.44	1.41	1.33	0.10	2.44	1.64
8	1	6	60	6.81	1.13	6.26	1.04	0.68	0.11	2.44				1.64	10.72
	2	6	60	6.83	1.14	6.25	1.04	0.71	0.12	2.44				1.64	10.64
	3	6	60	7.03	1.17	6.43	1.07	0.73	0.12	2.44	1.15	1.05	0.12	2.44	1.64

**Appendix XLI: Data of polycrystalline technology in tropical savanna**

	Y	Cells	T P DR	P DR	T Isc DR	Isc DR	T Voc DR	Voc DR	FF DR	AVG P DR	AVG Isc DR	AVG Voc DR	AVG FF DR	Am <sup>2</sup>	$\eta$
9	1	6	60	8.54	1.42	7.92	1.32	0.77	0.13	2.22				1.64	10.50
	2	6	60	8.07	1.34	7.44	1.24	0.77	0.13	2.22				1.64	10.52
	3	6	60	8.53	1.42	7.91	1.32	0.77	0.13	2.22	1.40	1.29	0.13	2.22	1.64
10	1	6	60	9.78	1.63	9.36	1.56	0.56	0.09	1.33				1.64	11.16
	2	6	60	8.90	1.48	8.45	1.41	0.59	0.10	1.33				1.64	11.12
	3	6	60	9.76	1.63	9.28	1.55	0.62	0.10	1.33	1.58	1.51	0.10	1.33	1.64
11	1	6	60	6.53	1.09	6.01	1.00	0.65	0.11	1.33				1.64	11.31
	2	6	60	5.29	0.88	4.75	0.79	0.66	0.11	1.11				1.64	11.37
	3	6	60	6.27	1.05	5.73	0.95	0.67	0.11	1.33	1.01	0.92	0.11	1.26	1.64
12	1	6	60	6.02	1.00	5.43	0.90	0.71	0.12	1.33				1.64	11.12
	2	6	60	5.79	0.97	5.19	0.87	0.72	0.12	1.33				1.64	11.13
	3	6	60	4.98	0.83	4.36	0.73	0.74	0.12	1.33	0.93	0.83	0.12	1.33	1.64
13	1	6	60	3.28	0.55	2.60	0.43	0.78	0.13	1.11				1.64	11.63
	2	6	60	1.07	0.18	0.37	0.06	0.79	0.13	1.33				1.64	11.69
	3	6	60	5.53	0.92	4.86	0.81	0.81	0.13	0.89	0.55	0.44	0.13	1.11	1.64
14	1	6	60	6.00	1.00	5.35	0.89	0.78	0.13	1.11				1.64	11.26
	2	6	60	5.76	0.96	5.11	0.85	0.78	0.13	1.11				1.64	11.28
	3	6	60	5.75	0.96	5.09	0.85	0.78	0.13	1.11	0.97	0.86	0.13	1.11	1.64
15	1	6	60	9.52	1.59	8.85	1.47	0.84	0.14	1.33				1.64	10.41
	2	6	60	8.99	1.50	8.30	1.38	0.85	0.14	1.33				1.64	10.51
	3	6	60	9.12	1.52	8.52	1.42	0.75	0.13	1.11	1.54	1.43	0.14	1.26	1.64
16	1	6	60	3.06	0.51	2.56	0.43	0.60	0.10	1.11				1.64	11.80
	2	6	60	2.99	0.50	2.47	0.41	0.63	0.11	1.11				1.64	11.70
	3	6	60	2.89	0.48	2.36	0.39	0.64	0.11	1.11	0.50	0.41	0.10	1.11	1.64
				1.15		1.05		0.13	2.04	1.15					10.71



**Appendix XLII: Data of monocrystalline technology in tropical savanna**

Mod	M	Isc	Voc	IMP	VMP	P	FF	FF <sub>STC</sub>	T FF DR	FF DR	Tc	Voc	Radiation	Inc.
1	1	5.02	42.82	4.52	34.43	155.7	0.72	0.77	6.49	0.98	50.49	42.82	886	22
	2	4.77	42.36	4.40	33.73	148.3	0.73	0.77	5.19	0.87	49.11	42.36	842	22
	3	4.70	42.27	4.37	33.61	146.8	0.74	0.77	3.90	0.65	48.99	42.27	838	25
2	1	4.68	41.75	4.34	33.31	144.7	0.74	0.77	3.90	0.65	48.89	41.75	835	25
	2	4.69	41.67	4.34	33.31	144.6	0.74	0.77	3.90	0.65	48.96	41.67	837	25
	3	4.91	41.98	4.62	33.88	156.7	0.76	0.77	1.30	0.22	54.05	41.98	1000	5
3	1	5.28	42.49	4.84	33.92	164.3	0.73	0.77	5.19	0.87	52.30	42.49	944	6
	2	5.41	42.88	4.89	33.93	165.8	0.71	0.77	7.79	1.3	52.27	42.88	943	6
	3	5.18	41.98	4.90	33.23	162.9	0.75	0.77	2.60	0.43	54.05	41.98	1000	4
4	1	5.48	41.81	5.05	32.79	165.7	0.72	0.77	6.49	0.98	54.05	41.81	1000	4
	2	5.45	41.54	5.01	32.54	163	0.72	0.77	6.49	0.98	54.05	41.54	1000	4
	3	5.45	41.37	5.01	32.33	161.9	0.72	0.77	6.49	0.98	54.05	41.37	1000	6
5	1	5.50	41.18	5.20	32.12	166.9	0.74	0.77	3.90	0.65	54.05	41.18	1000	9
	2	5.39	41.67	4.98	33.02	164.5	0.73	0.77	5.19	0.87	54.21	41.67	1005	9
	3	4.99	42.02	4.74	33.21	157.3	0.75	0.77	2.60	0.43	52.36	42.02	946	9
6	1	5.36	41.46	4.93	33.08	163.2	0.73	0.77	5.19	0.87	54.08	41.46	1001	9
	2	5.18	41.16	4.81	32.73	157.4	0.74	0.77	3.90	0.65	53.21	41.16	973	9
	3	5.26	40.97	4.81	32.47	156.3	0.72	0.77	6.49	0.98	53.18	40.97	972	10
AVG									0.76					

**Appendix XLIII: Data of monocrystalline technology in tropical savanna**

Mod	M	P(CAL)	P(ref)	Y	cell	T P DR	P DR	T Isc DR	Isc DR	T Voc DR	Voc DR	Average DR				Am <sup>2</sup>	$\eta$
												P	Isc	Voc	FF		
1	1	176.50	190	6	36	7.11	1.18	6.83	1.14	0.32	0.05					1.31	13.41
	2	168.30	190	6	36	11.42	1.90	11.10	1.85	0.38	0.06					1.31	13.44
	3	165.94	190	6	36	12.66	2.11	12.34	2.06	0.39	0.06	1.70	1.65	0.06	0.81	1.31	13.37
2	1	165.01	190	6	36	13.15	2.19	12.77	2.13	0.46	0.08					1.31	13.23
	2	165.41	190	6	36	12.94	2.16	12.54	2.09	0.47	0.08					1.31	13.19
	3	172.81	190	6	36	9.05	1.51	8.67	1.44	0.43	0.07	1.81	1.81	0.07	0.56	1.31	11.96
3	1	184.89	190	6	36	2.69	0.45	2.35	0.39	0.36	0.06					1.31	13.29
	2	189.23	190	6	36	0.41	0.07	0.11	0.02	0.31	0.05					1.31	13.42
	3	181.51	190	6	18	4.47	0.74	4.07	0.68	0.43	0.07	0.51	0.51	0.06	0.81	1.31	12.44
4	1	191.24	190	6	18	0.65	0.11	1.09	0.18	0.45	0.08					1.31	12.65
	2	190.19	190	6	18	0.10	0.02	0.58	0.10	0.49	0.08					1.31	12.44
	3	172.72	190	6	12	9.09	1.52	8.55	1.42	0.61	0.10	0.40	0.40	0.09	1.16	1.31	12.12
5	1	191.73	190	6	60	0.91	0.15	1.44	0.24	0.53	0.09					1.31	12.74
	2	171.17	190	6	60	9.91	1.65	9.62	1.60	0.34	0.06					1.31	13.02
	3	175.17	190	6	60	7.81	1.30	7.43	1.24	0.42	0.07	1.21	1.21	0.01	0.87	1.31	12.69
6	1	187.24	190	6	60	1.45	0.24	0.97	0.16	0.50	0.08					1.31	12.45
	2	181.31	190	6	60	4.57	0.76	4.07	0.68	0.54	0.09					1.31	12.35
	3	183.87	190	6	60	3.23	0.54	2.70	0.45	0.56	0.09	0.51	0.51	0.09	0.87	1.31	12.27
												0.99	1.02	0.06	0.85		12.70

### Appendix XLIV: Reliability analysis of PV module installation configurations

Year	SDU Mod	SPU Mod	SGT Mod	SGT Mod	SGT Inverter	SGT TR	SPG Mod	SPG Inverter	SPG TX	SPG MTX	SPG TR
1	0.98	0.92	0.86	1.00	0.98	0.98	1.00	1.00	1.00	0.97	0.97
2	0.97	0.84	0.64	1.00	0.97	0.97	1.00	1.00	1.00	0.94	0.94
3	0.95	0.77	0.44	1.00	0.95	0.95	1.00	1.00	1.00	0.92	0.92
4	0.93	0.71	0.29	1.00	0.93	0.93	1.00	1.00	1.00	0.89	0.89
5	0.92	0.65	0.19	1.00	0.92	0.91	1.00	1.00	1.00	0.87	0.87
6	0.90	0.60	0.12	0.98	0.90	0.88	1.00	1.00	1.00	0.84	0.84
7	0.89	0.55	0.08	0.91	0.88	0.81	1.00	1.00	1.00	0.82	0.82
8	0.88	0.50	0.05	0.78	0.87	0.68	1.00	1.00	1.00	0.80	0.80
9	0.86	0.46	0.03	0.62	0.85	0.53	1.00	1.00	1.00	0.77	0.77
10	0.85	0.42	0.02	0.45	0.84	0.38	0.99	1.00	1.00	0.75	0.75
11	0.84	0.39	0.01	0.32	0.82	0.26	0.99	1.00	1.00	0.73	0.72
12	0.82	0.36	0.01	0.21	0.81	0.17	0.98	1.00	1.00	0.71	0.70
13	0.81	0.33	0.01	0.14	0.79	0.11	0.97	1.00	1.00	0.69	0.67
14	0.80	0.30	0.00	0.09	0.78	0.07	0.96	1.00	1.00	0.67	0.65
15	0.79	0.28	0.00	0.06	0.77	0.04	0.95	1.00	1.00	0.65	0.62
16	0.78	0.26	0.00	0.04	0.75	0.03	0.94	1.00	1.00	0.64	0.60
17	0.77	0.24	0.00	0.02	0.74	0.02	0.92	1.00	1.00	0.62	0.57
18	0.76	0.22	0.00	0.01	0.73	0.01	0.90	1.00	1.00	0.60	0.54
19	0.75	0.20	0.00	0.01	0.71	0.01	0.88	1.00	1.00	0.58	0.51
20	0.74	0.18	0.00	0.01	0.70	0.00	0.86	1.00	1.00	0.57	0.49
21	0.73	0.17	0.00	0.00	0.69	0.00	0.83	1.00	1.00	0.55	0.46
22	0.72	0.16	0.00	0.00	0.68	0.00	0.80	1.00	1.00	0.54	0.43
23	0.71	0.14	0.00	0.00	0.67	0.00	0.78	1.00	1.00	0.52	0.40
24	0.70	0.13	0.00	0.00	0.65	0.00	0.75	1.00	1.00	0.51	0.38
25	0.69	0.12	0.00	0.00	0.64	0.00	0.72	1.00	1.00	0.49	0.35
AVG	0.82	0.40	0.11	0.39	0.80	0.35	0.93	1.00	1.00	0.71	0.67

**Key:** SDU-solar for domestic use, SPU-solar system for pumping water, SGT-solar system for grid-tie, SPG- solar system for electrical generation

### Appendix XLV: Solar PV system checklist

CHECKLIST: Used Module Label			Defect Present?			
COMPONENT	DEFECT		No	Yes	If yes, Score	Safety issue?
<b>1. Label</b>						
<b>2. Module</b>	2.2	Technology				
	2.3	Estimated deployment date				
	2.4	Certified				
<b>SUMMARY</b> Indicate if any defects and safety issues are present and sum score						
<b>CHECKLIST: Used Module</b>			<b>Back sheet</b>			
<b>Defect Present?</b>			<b>YES</b>		<b>NO</b>	
<b>1. Appearance</b>	Burn marks	Minor discoloration				
<b>2. Texture</b>						
<b>3. Material quality</b>						
<b>4. Damage</b>						
<b>2. Back sheet</b>	DEFECT		No	Yes	If yes, Score	Safety issue?
	2.1	Burn marks				
	2.2	Bubbles				
	2.3	Delamination				
	2.4	Cracks/scratches				
<b>SUMMARY</b> Indicate if any defects and safety issues are present and sum score						

<b>CHECKLIST: Used Module</b>			<b>Defect Present?</b>			
<b>COMPONENT</b>	<b>DEFECT</b>		<b>No</b>	<b>Yes</b>	<b>If yes, Score</b>	<b>Safety issue?</b>
<b>1. Label</b>	1.1	Missing				
	1.2	Poorly attached				
	1.3	Information is missing				
	1.4	Incorrect spelling				
<b>2. Junction Box</b>	3.1	Faulty electrical connection				
	3.2	Cracks/breaks/gaps in housing				
	3.3	Sealant failure				
	3.4	Electrical polarity not indicated				
<b>3. Wiring</b>	4.1	Wire(s) missing or poorly attached				
	4.2	Too short and/or too thin				
<b>4. Frame</b>	5.1	Damaged				
	5.2	Adhesive/sealant failure				
<b>5. Front Glass</b>	6.1	Cracking				
	6.2	Scratches				
<b>6. Encapsulation</b>	7.1	Delamination				
	7.2	Discolouration				
<b>7. Cells</b>	8.1	Fake				
	8.2	Dummy pieces disguising missing material				
	8.3	Cracks				
	8.4	Partially covered				
	8.5	Scratches				
	8.6	Differently sized				
	8.7	Edge chips				
	8.8	All cells very shiny				
	9.1	Fingers not connected to busbar				

<b>8. Cell Metallization</b>	9.2	Not the same pattern on all cells				
	9.3	Fingers off of edge of corner of cells				
<b>9. Cell Interconnection</b>	10.1	Interconnection is discontinuous				
	10.2	Cells connected in parallel (counterfeit)				
	10.3	Poorly aligned and/or soldered				
	10.4	Cells connected in parallel (real cells)				
Defects are present suggesting module is used rather than new						
<b>SUMMARY</b> Indicate if any defects and safety issues are present and sum score						
<b>CHECKLIST: Used Module</b>			<b>Rear-side glass</b>			
<b>Defect Present?</b>			<b>YES</b>		<b>NO</b>	
<b>Applicable</b>			<b>Non-applicable</b>			
<b>Damage</b>	No damage		Small, localized		Extensive	
<b>Defect</b>	<b>DEFECT</b>		<b>No</b>	<b>Yes</b>	<b>If yes, Score</b>	<b>Safety issue?</b>
	2.1	Crazing				
	2.2	Shattered (tempered)				
	2.3	Shattered (non-tempered)				
	2.4	Cracked				
	2.5	Chipped				
<b>SUMMARY</b> Indicate if any defects and safety issues are present and sum score						
<b>CHECKLIST:</b>			<b>Inverter</b>			
<b>Number</b>						
<b>Connected in series</b>						
<b>Connected in parallel</b>						
<b>Number of strings</b>						


<b>Defect Present?</b>		<b>YES</b>		<b>NO</b>	
<b>Damage</b>					
<b>Defect</b> 2.4	<b>DEFECT</b>	<b>No</b>	<b>Yes</b>	<b>If yes, Score</b>	<b>Safety issue?</b>
	2.1	Number of repairs			
	2.2	Time taken to repair			
	2.3	Number of replacements			
	2.4	warranty			
<b>SUMMARY</b> Indicate if any defects and safety issues are present and sum score					
<b>CHECKLIST:</b>		<b>Charge controller</b>			
<b>Defect Present?</b>		<b>YES</b>		<b>NO</b>	
<b>Damage</b>					
<b>Defect</b> 2.4	<b>DEFECT</b>	<b>No</b>	<b>Yes</b>	<b>If yes, Score</b>	<b>Safety issue?</b>
	2.1	Number of repairs			
	2.2	Time taken to repair			
	2.3	Number of replacements			
	2.4	warranty			
<b>SUMMARY</b> Indicate if any defects and safety issues are present and sum score					
<b>CHECKLIST:</b>		<b>Battery</b>			
<b>Rating</b>					
<b>Number</b>					
<b>Number of strings</b>					
<b>Connected in series</b>					
<b>Connected in parallel</b>					
<b>Defect Present?</b>		<b>YES</b>		<b>NO</b>	
<b>Damage</b>					

<b>Defect</b> 2.4	<b>DEFECT</b>		<b>No</b>	<b>Yes</b>	<b>If yes, Score</b>	<b>Safety issue?</b>
	2.1	Number of repairs				
	2.2	Time taken to repair				
	2.3	Number of replacements				
	2.4	warranty				
<b>SUMMARY</b> Indicate if any defects and safety issues are present and sum score						
<b>CHECKLIST:</b>			<b>Transformer</b>			
<b>Rating</b>						
<b>Number</b>						
<b>Connected in series</b>						
<b>Connected in parallel</b>						
<b>Defect Present?</b>			<b>YES</b>		<b>NO</b>	
<b>Damage</b>						
<b>Defect</b> 2.4	<b>DEFECT</b>		<b>No</b>	<b>Yes</b>	<b>If yes, Score</b>	<b>Safety issue?</b>
	2.1	Number of repairs				
	2.2	Time taken to repair				
	2.3	Number of replacements				
	2.4	warranty				
<b>SUMMARY</b> Indicate if any defects and safety issues are present and sum score						



## Appendix XLVI: Turnitin Originality Report

Turnitin Originality Report https://www.turnitin.com/newreport\_printview.asp?eq=1&eb=1&es...

 **Turnitin Originality Report**  
**PhD Thesis** by Samuel Maina Ngiure  
 From Ngiure PhD Thesis (Masters and PhD)

Processed on 03-Dec-2022 00:28 EAT  
 ID: 1969585046  
 Word Count: 52583

<b>Similarity Index</b> <span style="font-size: 24pt; font-weight: bold;">14%</span>	<b>Similarity by Source</b> Internet Sources: 9% Publications: 1% Student Papers: 2%
---	---

**sources:**

- 1 < 1% match (Internet from 24-Feb-2020)  
<https://www.mdpi.com/1996-1073/12/7/1213/html>
- 2 < 1% match (Internet from 03-Nov-2019)  
<https://www.mdpi.com/2071-1050/11/17/4697/html>
- 3 < 1% match (Internet from 29-Dec-2019)  
<https://www.mdpi.com/1996-1073/11/2/363/html>
- 4 < 1% match (Internet from 12-Nov-2020)  
<https://www.mdpi.com/2071-1050/12/21/9227/html>
- 5 < 1% match (Internet from 30-Oct-2020)  
<https://www.mdpi.com/2071-1050/9/6/963/html>
- 6 < 1% match (Internet from 16-Nov-2022)  
<https://www.mdpi.com/1996-1073/15/20/7595/html>
- 7 < 1% match (Internet from 10-Oct-2022)  
<https://WWW.MDPI.COM/1996-1073/14/14/4278/html>
- 8 < 1% match (Internet from 28-Jul-2020)  
<https://www.mdpi.com/1996-1073/13/15/3819/html>
- 9 < 1% match (Internet from 05-Feb-2021)  
<https://www.mdpi.com/1996-1073/13/5/1178/html>
- 10 < 1% match (Internet from 01-Oct-2022)  
<https://www.engineeringforchange.org/wp-content/uploads/2017/09/Solar-PV-Product-Visual-Inspection-Guide.pdf>

1 of 181
12/3/2022, 12:39 AM

Turnitin Originality Report https://www.turnitin.com/newreport\_printview.asp?eq=1&eb=1&es...